IntechOpen

Air Traffic Control

Edited by Max Mulder

Air Traffic Control

edited by
Max Mulder

Air Traffic Control
http://dx.doi.org/10.5772/268
Edited by Max Mulder

Notice

Statements and opinions expressed in the chapters are these of the individual contributors and not necessarily those of the editors or publisher. No responsibility is accepted for the accuracy of information contained in the published chapters. The publisher assumes no responsibility for any damage or injury to persons or property arising out of the use of any materials, instructions, methods or ideas contained in the book.

First published in Croatia, 2010 by INTECH d.o.o.
eBook (PDF) Published by IN TECH d.o.o.
Place and year of publication of eBook (PDF): Rijeka, 2019.
IntechOpen is the global imprint of IN TECH d.o.o.
Printed in Croatia

Legal deposit, Croatia: National and University Library in Zagreb

Additional hard and PDF copies can be obtained from orders@intechopen.com

Air Traffic Control
Edited by Max Mulder

p. cm.

ISBN 978-953-307-103-9

eBook (PDF) ISBN 978-953-51-5944-5

Meet the editor

Professor Max Mulder is a Full Professor of Aerospace Human-Machine Systems and Head of the Control and Simulation section of the Faculty of Aerospace Engineering, Delft University of Technology. Max received his MSc and PhD (cum laude) in Aerospace Engineering from the Delft University of Technology in 1992 and 1999, respectively, for his work on the cybernetics of perspective tunnel-in-the-sky displays. His research interests are twofold. He studies manual control cybernetics and its use in modelling pilot perception and performance, in particular the modelling of pilot self-motion perception and neuromuscular system characteristics. Secondly, he investigates cognitive systems engineering and its application in the design of ecological human-machine systems for pilots and air traffic controllers. Max teaches several graduate courses on stochastic signal analysis and stochastic control systems, avionics, human-machine systems and air traffic management. He (co-)authored more than 350 academic publications.

Contents

Preface

Improving air traffic control and air traffic management is currently one of the top priorities of the global research and development agenda. Massive, multi-billion euro programs like SESAR (Single European Sky ATM Research) in Europe and NextGen (Next Generation Air Transportation System) in the United States are on their way to create an air transportation system that meets the demands of the future.

Air traffic control is a multi-disciplinary field that attracts the attention of many researchers, ranging from pure mathematicians to human factors specialists, and even in the legal and financial domains the optimization and control of air transport is extensively studied. This book, by no means intended to be a basic, formal introduction to the field, for which other textbooks are available, includes nine chapters that demonstrate the multi-disciplinary character of the air traffic control domain.

The first three chapters in the book concern the more fundamental, mathematical approaches to some of the main air transportation problems. First, the dynamic management of airspace, including air traffic flow management constitutes a formidable challenge from a computational perspective. Second, in creating a safe and efficient, possibly even autonomous system, stochastic, hybrid approaches to airborne or ground-based conflict detection and resolution are discussed. And third, the consequences of conducting the exchange of information between the ground and air-based elements by other means than using voice are discussed.
The following four chapters discuss elements of what may be the most important challenge of all when improving the current air transportation system: the development of more advanced automation and the support of the human operators involved in the process. Balancing the increase in the use of automated tools, both in the air as well as on the ground, with the identified need for human decision-makers to be involved and, ultimately, in charge, touches upon the existential problem of human versus automated control. Here, the first two chapters discuss in detail the development of advanced ground-based and airborne planning and control algorithms, designed to support time-based operations, increase the autonomy of aircraft, reduce fuel burn and emissions, and ultimately the increase of capacity while safeguarding safety. Then, the book contains two chapters that discuss examples of some of the more advanced human-machine interfaces that are currently under development. Whereas the first interface aims at the presentation of weather constraints to air traffic controllers, the second interface aims to support controllers to supervise and control streams of aircraft that all conduct continuous descent approaches.

The book ends with two chapters that further illustrate the broadness of the air traffic control problem. It is argued in the first chapter that the advent of air traffic management tools that require satellite-based navigation could have dramatic effects on the current ways in which legal issues are being resolved. That is, in the event of incidents or even accidents that (partly)

have their origins in imperfect satellite navigation, who bears the responsibility? In the second chapter, the last chapter in the book, it is discussed that even the current drive towards wind-based energy generation systems could have a large effect on the use of radar, one of the key components of the air traffic control system. Pragmatic solutions are discussed that allow the safe and concurrent developments in two of the world's most challenging problems: sustainable energy generation, and a more safe and more efficient air traffic management system.

I hope you like the book. In any case, I would like to thank all authors for their efforts and assistance in completing the book. Special thanks to the SCIYO team for their help, the great editing job, and for making this book possible in the first place.

Editor

Max Mulder

1

Dynamic Airspace Management - Models and Algorithms

Peng Cheng and Rui Geng
Department of Automation, Tsinghua University
P. R. China
chengp@tsinghua.edu.cn
gengrui@tsinghua.edu.cn

1. Introduction

Global air transport has been growing for decades and is expected to continue increasing in the future. The development of the air transport system has significantly increased the demands on airspace system resources. During the past several years, the operational concept of Dynamic Airspace Management has been developed to balance the mushrooming demands and limited airspace resources.

The Dynamic Airspace Management is an important approach to extend limited airspace resources by using them more efficiently and more flexibly. Under the Dynamic Airspace Management paradigm, the national airspace is administrated as a unified resource with temporary utilization clearances assigned to various airspace users on demand and reclaimed at the end of the utilization period. The structure of airspace can be changed as well if needed.

The airspace system typically has civil users and military users. In China, for example, most of the airspace is administrated by the military except for a few air routes reserved for civil aviation, that resemble a lot of tubes through the airspace. The air transport system is restricted not only by insufficient airport capacities (as in the United States) and sector capacities (as in Europe), but also by the structure and the management policy of air route networks. When there is a temporary increase of the air traffic demands or a decrease of airspace capacities, the civil air traffic controllers usually have to apply for additional routes from the military.

In the last two decades, the models and algorithms for Air Traffic Flow Management (ATFM) have been developed to provide better utilization of airspace resources to reduce flight delays(Vossen & Michael, 2006). Early ATFM models only considered airport capacity limitations(Richetta & Odoni, 1993; 1994). Bertsimas and Patterson(Bertsimas & Patterson, 1998; 2000), Lulli and Odoni(Lulli & Odoni, 2007) included airport capacity limitation and sector capacity limitation together. Cheng et al.(Cheng et al., 2001) and Ma et al.(Ma et al., 2004) investigated the ATFM problem in China and added air route capacity constraints into their models. In all these models, the airspace structure was treated as deterministic and unchangeable. These models follow the similar way that makes optimal schedules for a given set of flights passing through the airspace network by dynamically adjusting flight plans via airborne holding, rerouting, or ground holding to adapt to the possible decreases of the network capacity while minimizing the delays and costs.

Few studies have focused on how to reconstruct an efficient air traffic network and how to adjust the current network in a dynamic environment. In this chapter we discuss three problems of dynamically adjust air space resources including air routes and air traffic control sectors.
Firstly, an integer program model named Dynamic Air Route Open-Close Problem (DROP) is presented to facilitate the utilization of air routes. This model has a cost-based objective function and takes into account the constraints such as the shortest occupancy time of routes, which have not been considered in the past ATFM studies. The aim of the Dynamic Air Route Open-Close Problem is to determine what routes will be open for a certain user during a given time period. Considered as a simplified implementation of air traffic network reconstruction, it is the first step towards realizing the Dynamic Airspace Management.
Secondly, as a core procedure in Dynamic Airspace Management, the Dynamic Air Route Adjustment Problem is discussed. The model and algorithm of Dynamic Air Route Adjustment Problem is about making dynamic decisions on when and how to adjust the current air route network with the minimum cost. This model extends the formulation of the ATFM problem by integrating the consideration of dynamic opening and closing of air route segments and introducing several new constraints, such as the shortest occupancy time. The sensitivities of important coefficients of the model are analyzed to determine their proper values.
Thirdly, we discuss a set-partitioning-based model on the dynamic adjustment to air traffic control sectors to balance the workload of controllers and to increase the airspace capacity. By solving the optimization model, we get not only the optimal number of opened sectors but also the specific forms of sector combinations. To obtain the input parameters of the set-partitioning model, we also apply a method to evaluate controllers' workload through massive statistical analysis of historical radar data.
Several computational examples are also presented in this chapter to test the models and algorithms. All scenarios and data are extracted from Beijing Regional Air Traffic Control Center, which controls one of the most challenging airspaces of the world, in terms of either air traffic or airspace structure.

2. Dynamic Air Route Open-Close Problem

There are typically civil users and military users in the airspace system. When there is a temporal increase in air traffic demand or a decrease in airspace capacity, civil aviation user has to apply for additional routes from the military. The military may also "borrow" some air routes from the civil aviation system for training or combat. The Dynamic Air Route Open-Close Problem determines when additional routes should be opened or closed to the civil aviation system, and when the civilian routes can be used by the military. In this problem all air routes are considered to be independent. There is a special constraint named the Shortest Usage Time constraint. Since the airspace system does not allow air routes to be opened or closed arbitrarily, it has to be used for a shortest usage time once a route has been used.

2.1 Model Formulation

Consider a set of time intervals, $t \in \{1, ..., T\}$, a set of routes, $i \in \{1, ..., I\}$, and two users (civil aviation and military aviation), $k \in \{1, 2\}$. The notations for the problem are as follows.

$a_k(t)$ Cost coefficient for one unit of resource shortage of user k in time interval t
$b_{i,k}(t)$ Cost of user k using route i during time interval t
$o_{i,k}(t)$ Opening fee of user k borrowing route i from the other user in time interval t. If user k uses his own route, this coefficient will be zero
$C_{i,k}(t)$ Number of flights that can enter route i in time interval t when user k use this route
$P_k(t)$ Resource demand of user k in time interval t
$U_{i,k}$ Shortest occupancy time that user k uses a borrowed route i. If user k uses his own route, this coefficient will be zero
$d_k(t)$ Amount of resource shortage of user k in time interval t

The decision variables are defined as follows,

$$x_{i,k}(t) = \begin{cases} 1 & \text{if the route } i \text{ is occupied by the user } k \text{ in time interval } t. \\ 0 & \text{Otherwise.} \end{cases}$$

$$z_{i,k}(t) = \begin{cases} 1 & \text{if the route } i \text{ is opened to the user } k \text{ in time interval } t. \\ 0 & \text{Otherwise.} \end{cases}$$

The objective function can be written as

$$Min \sum_{k,t} a_k(t) d_k(t) + \sum_{i,k,t} o_{i,k}(t) z_{i,k}(t) + \sum_{i,k,t} b_{i,k}(t) x_{i,k}(t) \tag{1}$$

In Equation 1, the first term represents the cost of resource shortage which may cause flight delay or cancellation. The second term represents the cost of opening a route to users except the owner, since many things such as resource allocations, communications, and authorizations have to be done before the route can be opened to other users. The third term represents the cost of using another user's routes.
The constraints are given as below.

$$d_k(t) = max(0, P_k(t) - \sum_i C_{i,k}(t) x_{i,k}(t)) \qquad \forall t, k \tag{2}$$

$$\sum_k x_{i,k}(t) = 1 \qquad \forall i, t \tag{3}$$

$$z_{i,k}(t) = 0 \qquad \text{If } 1 \leq \sum_{\tau \in (t - U_{i,k}, t)} x_{i,k}(\tau) \leq U_{i,k} \qquad \forall i, k, t \tag{4}$$

$$x_{i,k}(t) - x_{i,k}(t-1) \leq z_{i,k}(t) \qquad \forall i, k, t \tag{5}$$

$$x_{i,k}(t) \in \{0,1\}, \quad z_{i,k}(t) \in \{0,1\}, \quad d_k(t) \in \mathbb{Z}^+ \qquad \forall i, k, t \tag{6}$$

Constraint 2 gives the resource shortages $d_k(t)$. Constraint 3 shows that each route i is occupied by one specific user whether the route is actually used (there are flights using it) or not. Constraint 4 is the shortest occupancy time constraint. Any request to borrow a route for a planned occupancy time less than $U_{i,k}$ will be refused. This constraint ensures sufficient time for route switching between users. Constraint 5 describes the relationship between $x_{i,k}(t)$ and $z_{i,k}(t)$. Constraint 6 is the standard non-negativity and integral constraint.
Considering the model has nonlinear terms, which are usually difficult to handle, the formulation can be rewritten as follows.

$$P_k(t) - \sum_i C_{i,k}(t)x_{i,k}(t) \leq d_k(t) \qquad \forall t,k \tag{7}$$

$$\sum_k x_{i,k}(t) = 1 \qquad \forall i,t \tag{8}$$

$$U_{i,k}(z_{i,k}(t) - (x_{i,k}(t) - x_{i,k}(t-1))) \leq \sum_{\tau \in (t-U_{i,k},t)} x_{i,k}(\tau) \qquad \forall i,k,t \tag{9}$$

$$x_{i,k}(t) - x_{i,k}(t-1) \leq z_{i,k}(t) \qquad \forall i,k,t \tag{10}$$

$$x_{i,k}(t) \in \{0,1\}, \quad z_{i,k}(t) \in \{0,1\}, \quad d_k(t) \in \mathbb{Z}^+ \qquad \forall i,k,t \tag{11}$$

Constraint 7 is derived from constraint 2. When $P_k(t) - \sum_i C_{i,k}(t)x_{i,k}(t) \leq 0$, then $d_k(t) = 0$ according to constraint 11. When $P_k(t) - \sum_i C_{i,k}(t)x_{i,k}(t) \geq 0$, since the objective function has the term $\sum_{k,t} a_k(t)d_k(t)$, $d_k(t)$ will be equal to the minimum under constraint 7, and $d_k(t) = P_k(t) - \sum_i C_{i,k}(tx_{i,k}(t)$. Therefore, constraint 7 is equal to constraint 2 when combined with the objective function and constraint 11.
For the same reason, the relationship between $x_{i,k}(t)$ and $z_{i,k}(t)$ can be described as the combination of the object function and constraints 5 and 11. Figure 1 illustrates the relationship between $x_{i,k}(t)$ and $z_{i,k}(t)$.

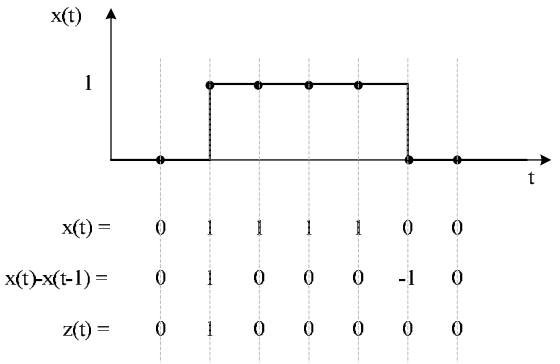

Fig. 1. Typical relationship between $x_{i,k}(t)$ and $z_{i,k}(t)$

2.2 Simulations

Figure 2 shows an area with three civilian routes and a military training area through which an additional route can be opened to civilian users. All of these routes have different capacities, opening costs, usage costs. The military may borrow route 3 from the civil aviation authority when an additional area is needed.
Figure 3 shows the solution of a realistic instance of the Dynamic Air Route Open-Close Problem. In this case, the time horizon from 8:00 am to 11:00 pm is divided into many 15-minute time periods. The opening cost and the usage cost of route are set to be twice the cost of one unit of resource shortage. The shortest occupancy time is set to be 4 time intervals. The

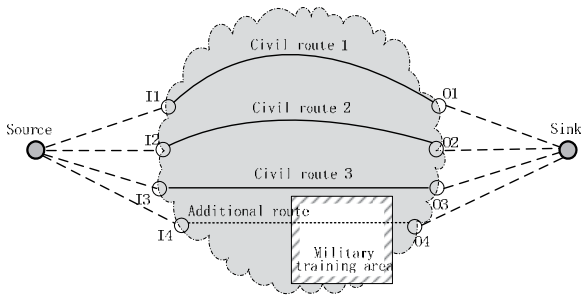

Fig. 2. Area with temporary additional routes

capacity of all three civilian routes, the capacity of the military area, and the demands of all users are shown in Figure 3(a). Note the capacity decrease of the civilian routes that lasts 6 time intervals, which is usually caused by severe weather.
Figure 3(b) to (e) show the value of $x_{i,k}(t)$ for the various routes. Routes 1 and 2 are exclusively used by the civilian users. Route 3 and the additional route (military training area) are opened or closed according to the total cost of all users' resource shortages, route opening, route usage, and the constraint of the shortest occupancy time.
The ratio of the resource shortage cost, route opening cost, and route usage cost significantly affects the result. If the cost of using an additional route is much higher than the cost of the resource shortage, for example due to a very complex route application procedure, the user may accept the shortage and change their flight plans.
Using the air space resources flexibly, the Dynamic Air Route Open-Close Problem is the first step towards the Dynamic Airspace Management. In this model all air routes are considered to be independent. But in more common situation, air routes are usually dependent. In next section we will focus our investigation onto the network of air routes and present the Dynamic Air Route Adjustment Problem.

3. Dynamic Air Route Adjustment Problem

Given an air traffic network composed of airports, way points, and routes, and a set of flights that are planned to fly through the network, the Dynamic Air Route Adjustment Problem makes dynamic decisions on when and how to adjust the current air traffic route network by applying for additional temporary air route segments (or arcs) to minimize the overall cost including opening cost, the usage cost for temporary arcs, and the flight and delay costs to all flights. The development of this model is partially motivated by the characteristics of the air route structure and the management policy in China.

3.1 Model Formulation

The model of the Dynamic Air Route Adjustment Problem is defined on a network, $\mathcal{G}$, having the node set $\mathcal{N}$ and the arc set $\mathcal{A}$. In $\mathcal{G}(\mathcal{N}, \mathcal{A})$, the nodes represent the airports and the way points while the arcs represent air route segments including the reserved routes for civil users as well as the dynamic routes, which can be temporarily used by civil users. The model can be

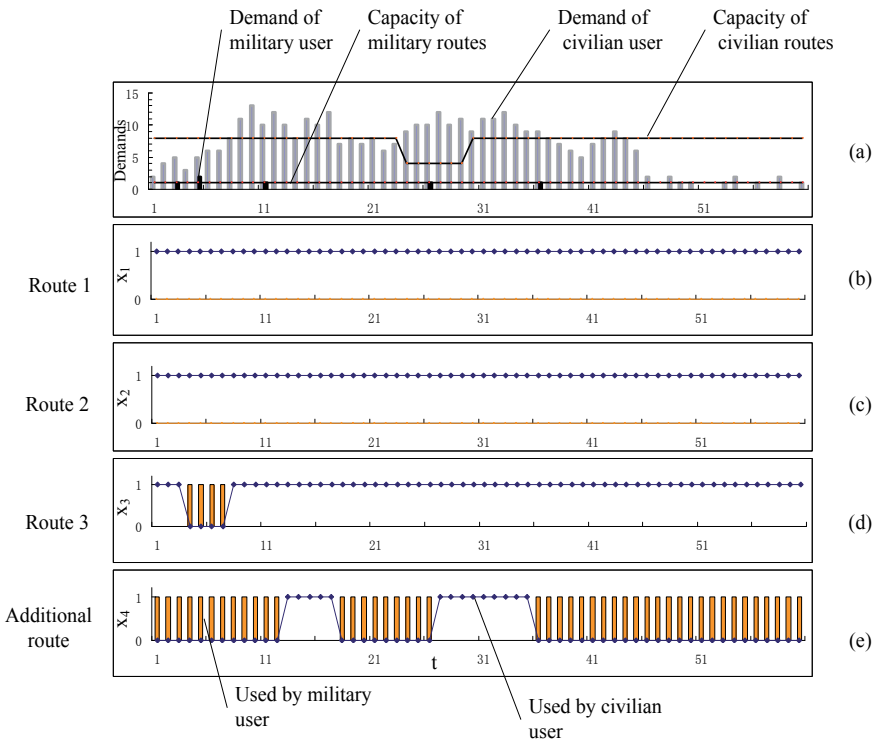

Fig. 3. A realistic instance of the Dynamic Air Route Open-Close Problem

described as a multi-commodity network flow model, where all flights with the same origin and destination belong to one commodity.
The model is based on the following assumptions.

1. Since the quantity of each commodity is the number of flights, it must be a nonnegative integer.
2. All flights must land at their destination nodes eventually.
3. The time period T is sampled into discrete time slots with equal intervals.
4. All flights have identical mechanical characteristics and fly at the same speed. So the travel time through one arc is identical for every flight. But it may differ at different instances.
5. The arc capacities are known and given in this model but they may differ at different times.
6. All flights have the same fuel consumption rate and the same delay fees, which are constants in this model.

7. If a temporary arc opens, it should be kept open for at least the shortest occupancy time so that the air traffic controllers have enough time to switch access to the arc between different users.

The notations for the model are as follows.

$\mathcal{A}$	set of arcs
$\mathcal{A}_{tmp}$	set of arcs that can be temporarily opened, $\mathcal{A}_{tmp} \subset \mathcal{A}$,
$\mathcal{K}$	set of flight commodities
$\mathcal{N}$	set of nodes
$\mathcal{N}_{orig}$	set of origin nodes, $\mathcal{N}_{orig} \subset \mathcal{N}$,
$\mathcal{N}_{dest}$	set of destination nodes, $\mathcal{N}_{dest} \subset \mathcal{N}$;
$\mathcal{N}_{mid}$	set of nodes other than origin and destination nodes, $\mathcal{N}_{mid} \subset \mathcal{N}$
i	node index, $i \in \mathcal{N}$
(i,j)	arc index, $(i,j) \in \mathcal{A}$
t	time interval index, $t \in \mathcal{T}$
k	flight commodity index
$dis_{i,j}$	Length of arc (i,j)
$a_{i,j}$	Travel time along arc (i,j)
$c_{i,j}(t)$	Maximum number of flights that can enter arc (i,j) during time interval t
$U_{i,j}$	The shortest occupancy time of arc (i,j)
$P_i^k(t)$	Number of commodity k flights scheduled to take off from origin node i during time interval t
$w_{in}(i)$	The maximum indegree of node i
$w_{out}(i)$	The maximum outdegree of node i
r	Cost of flying one kilometer
$d_i(t)$	Cost of holding a flight at origin node i during time interval t
$o_{i,j}(t)$	Opening fee of temporary arc (i,j) during time interval t
$m_{i,j}(t)$	Usage cost of temporary arc (i,j) during time interval t

The decision variables are defined as follows.

$$x_{i,j}(t) = \begin{cases} 1 & \text{if the arc } (i,j) \text{ is in use during time interval } t. \\ 0 & \text{Otherwise.} \end{cases}$$

$$z_{i,j}(t) = \begin{cases} 1 & \text{if the arc } (i,j) \text{ is opened during time interval } t. \\ 0 & \text{Otherwise.} \end{cases}$$

$f_{i,j}^k(t)$ is the number of flights of commodity k entering arc(i,j) during time interval t.
The objective function can be written as

$$\begin{aligned} minZ \quad = \quad & \sum_{t,k,i \in \mathcal{N}_{orig}} d_i(t) \cdot f_{i,i}^k(t) + \sum_{t,k,(i,j) \in \mathcal{A}} r \cdot dis_{i,j} \cdot f_{i,j}^k(t) \\ & + \sum_{t,(i,j) \in \mathcal{A}_s} o_{i,j}(t) \cdot z_{i,j}(t) \\ & + \sum_{t,(i,j) \in \mathcal{A}_s} m_{i,j}(t) \cdot x_{i,j}(t) \end{aligned} \tag{12}$$

The first term represents the cost of flight delay at origin nodes. Here, $\sum_k f_{i,i}^k(t)$ is the number of all kinds of flights on the self-loop arc (i,i) at time t. The arc (i,i) begins and ends at the same origin node i, which has a travel time equal to 1 and a length equal to 0. The flight on arc (i,i) is delayed and waiting on node i. The second term represents the flight costs bases on the flying distance. Since the lengths of self-loop arcs are 0, their flying distance is zero. The third term represents the cost of opening all temporary arcs. The last term represents the cost of using the temporary arcs.
The constraints are given as below.

$$\sum_{j:(i,j)\in\mathcal{A}} f_{i,j}^k(t) - \sum_{j:(j,i)\in\mathcal{A}} f_{j,i}^k(t-a_{j,i}) = P_i^k(t) \qquad \forall i \in \mathcal{N}_{orig},\ t \in \mathcal{T},\ k \in \mathcal{K} \tag{13}$$

$$\sum_{j:(i,j)\in\mathcal{A}} f_{i,j}^k(t) - \sum_{j:(j,i)\in\mathcal{A}} f_{j,i}^k(t-a_{j,i}) = 0 \qquad \forall i \in \mathcal{N}_{mid},\ t \in \mathcal{T},\ k \in \mathcal{K} \tag{14}$$

$$\sum_{t,j:(j,i)\in\mathcal{A}} f_{j,i}^k(t) - \sum_{t,q\in\mathcal{N}_{orig}} P_q^k(t) = 0 \qquad \forall i \in \mathcal{N}_{dest},\ k \in \mathcal{K} \tag{15}$$

$$\sum_{k\in\mathcal{K}} f_{i,j}^k(t) \le c_{i,j}(t)\cdot x_{i,j}(t) \qquad \forall (i,j) \in \mathcal{A},\ t \in \mathcal{T} \tag{16}$$

$$U_{i,j}[z_{i,j}(t) - (x_{i,j}(t) - x_{i,j}(t-1))] \le \sum_{\tau\in(t-U_{i,j},t)} x_{i,j}(\tau) \qquad \forall (i,j) \in \mathcal{A}_s,\ t \in \mathcal{T} \tag{17}$$

$$x_{i,j}(t) - x_{i,j}(t-1) \le z_{i,j}(t) \quad \forall (i,j) \in \mathcal{A}_s,\ t \in \mathcal{T} \tag{18}$$

$$\sum_j x_{j,i}(t) \le w_{in}(i) \quad \forall i \in \mathcal{N}_{mid},\ t \in \mathcal{T} \tag{19}$$

$$\sum_j x_{i,j}(t) \le w_{out}(i) \quad \forall i \in \mathcal{N}_{mid}, t \in \mathcal{T} \tag{20}$$

$$x_{i,j}(t) \in \{0,1\}, \quad z_{i,j}(t) \in \{0,1\}, \quad f_{i,j}^k(t) \in Z^+ \qquad \forall t \in \mathcal{T},\ k \in \mathcal{K},\ (i,j) \in \mathcal{A} \tag{21}$$

Constraints 13 to 15 are flow-conservation constraints. Constraint 13 shows that all flights departing from an origin node in time interval t are either flights scheduled to take off from this node in time interval t or flights which were delayed and waiting at this node. Constraint 15 states that all flights taking off from origin nodes must land at destination nodes. Constraint 16 is the capacity constraint. Constraint 17 is the shortest occupancy time constraint. Constraint 18 describes the relationship between $x_{i,j}(t)$ and $z_{i,j}(t)$. This constraint combined with the objective function ensures that $z_{i,j}(t)$ is equal to 1 when $x_{i,j}(t)$ changes from 0 to 1. Constraint 19 and 20 limit the number of arcs entering or leaving a node so that the situation will not be too complex to be handled by the air traffic controllers. Constraint 21 is the standard non-negativity and integrality constraint.

3.2 Analysis and Evaluation

This section gives several examples of the Dynamic Air Route Adjustment Problem. These examples model possible scenarios in the southern part of the Beijing ATC Region, one of the busiest air traffic control regions in China. Figure 4 shows the air-route network model for this region with 5 origin nodes, 1 destination node, 17 reserved arcs, and 26 temporary arcs. The time horizon from 8:00 am to 11:00 pm is divided into 90 time slots with the flight plans

of 473 flights generated based on real air traffic in this region. The solution uses $r = 0.0025$, $d_i(t) = 1$, $o_{i,j}(t) = 5.5$, and $m_{i,j}(t) = 0.3$.

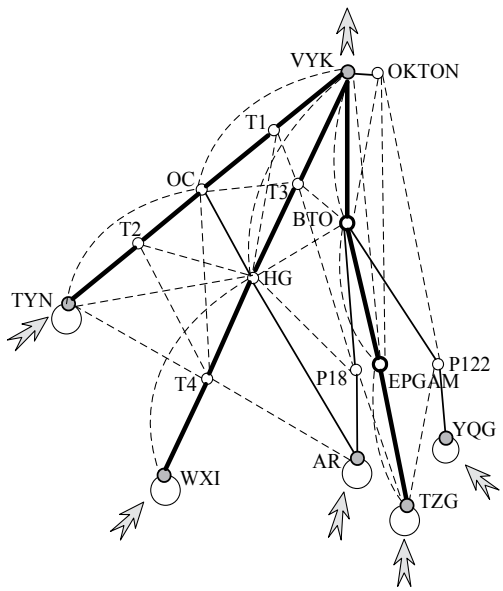

Fig. 4. Network with temporary additional route segments

Table 1 lists six scenarios with different arc capacities to simulate capacity decreases caused by severe weather or other incidents. Scenario I has normal conditions with the normal capacity of arc "EPGAM-BTO" as 4. This capacity decreases from 4 to 3 in scenario II, to 2 in III, to 1 in IV, and to 0 in V. In scenario VI, the capacity of arc "EPGAM-BTO" decreases to 2 only between 9:00 am to 11:00 am.
Figure 5 shows some details of the result for scenario VI which shows the demands of flights entering from TZG. The normal condition (scenario I) does not experience delays. In scenario VI, if no temporary arcs can be used, flights will be delayed for 125 slots. If the temporary arcs can be used, the temporary arc 5 will open and only 3 slots delays will occur in total. Figure 5 also shows the number of delays on TZG and the opening and closing schedule of the temporary arc "EPGAM-VYK."

3.3 Sensitivity Analysis

In the model, the opening fee, $o_{i,j}(t)$, and the usage fee, $m_{i,j}(t)$, of temporary arc (i, j) at time t significantly affect the opening and closing schedules of the temporary arcs and the flight arrangements. This section describes several analyses to show the sensitivity of $o_{i,j}(t)$ and $m_{i,j}(t)$.
The flight delay cost has been estimated from the experience of air traffic management experts and the statistical data from the FAA, Eurocontrol, and various airlines (Eurocontrol, 2008), (Dubai, 2008) to be €72 per minute in Europe and $123.08 per minute in the Unite States. The fuel consumption of a flight is related to its type, load, and route. According to Shenzhen

Table 1. Computational Results of Dynamic Air Route Adjustment Problem

Scenario	Without temporary arcs		With temporary arcs			
	Total costs	Delay time (slots)	Total costs	Delay time (slots)	Temporary arcs used	Usage time (slots)
I	392.4	0	392.4	0	0	0
II	412.3	24	403.3	8	1	6
III	1290.2	903	412.5	0	1	66
IV	5517.5	5131	429.0	6	2	79
V	10172.5	9786	447.2	0	2	155
VI	513.3	125	400.6	3	2	10

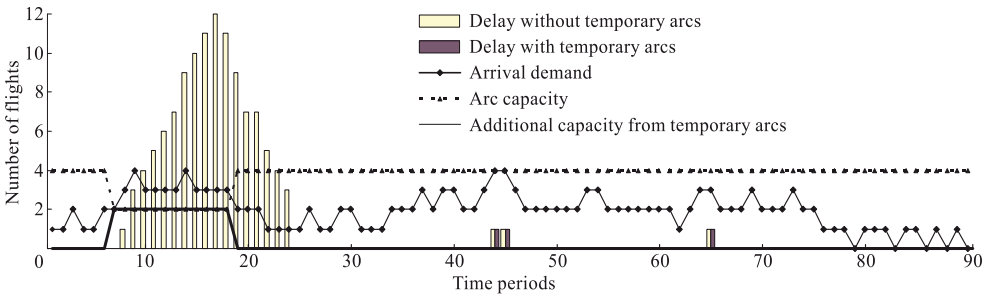

Fig. 5. Solution of scenario VI with and without temporary arcs

Airline's operational data for 2006, the fuel consumption per thousand kilometers for their aircraft is 3.7 to 3.8 tons on average and the price of aviation fuel is about $900 per ton. Therefore, $r : d_i(t)$ is about 1:400, and the scenarios assume $r = 0.0025$ and $d_i(t) = 1$.

Four scenarios were considered to test the effect of changing $o_{i,j}(t)$ and $m_{i,j}(t)$. Scenario 1 simulates operations with little overload. In scenario 2, the capacities of arcs EPGAM-BTO and BTO-VYK are reduced to half of their normal level. In scenario 3, arcs EPGAM-BTO and BTO-VYK are closed for two hours because of severe weather. In scenario 4, EPGAM-BTO and BTO-VYK are closed throughout the simulation time.

In these comparisons, $o_{i,j}(t) \in [1, 10]$ and is increased from 1 with step size 0.5, $m_{i,j}(t) \in [0.1, 1.4]$ and is increased from 0.1 with step size 0.1.

Figures 6(a) to 6(f) show the relationships between the number of opened arcs, the occupancy time for all the temporary arcs, the total delay and the opening fee, $o_{i,j}(t)$, or the usage fee, $m_{i,j}(t)$. The symbols are the calculated results with the curves drawn to connect the average values of the results for same opening fee or usage fee. Each curve shows one scenario's result and the curve noted by "S1" shows the result of scenario 1.

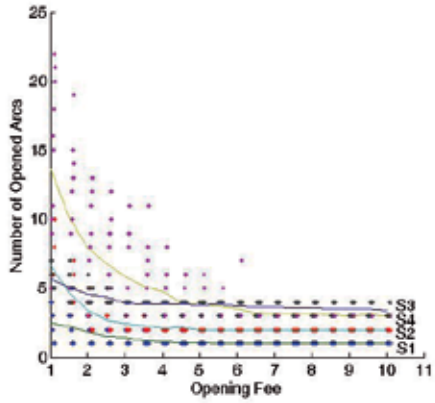

(a) Opening fee and no. of opened arcs

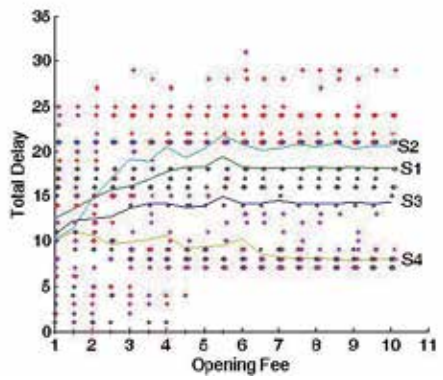

(b) Opening fee and total delay

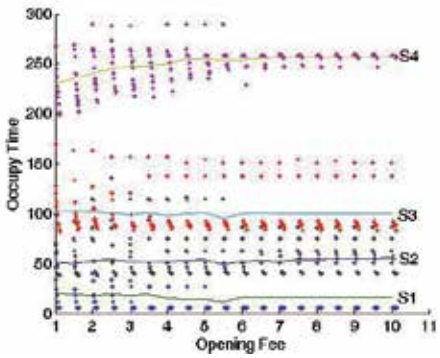

(c) Opening fee and occupying time

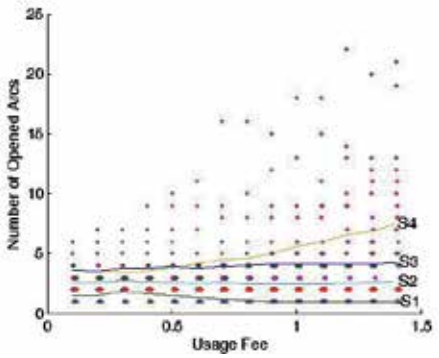

(d) Using fee and no. of opened arcs

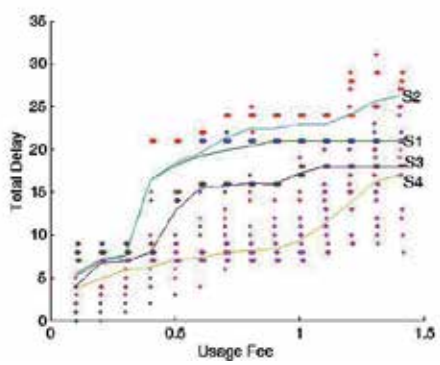

(e) Using fee and total Delay

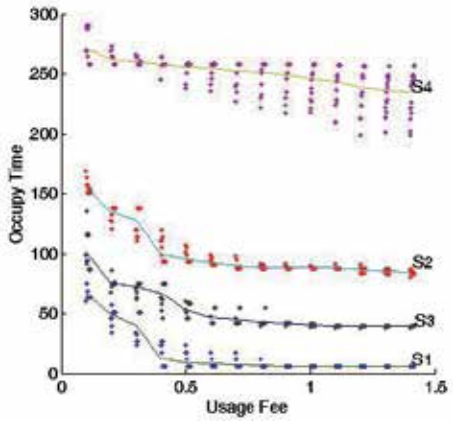

(f) Using fee and occupying Time

Fig. 6. Sensitivity analysis of factors

Figures 6(a) shows that the number of opened temporary arcs decreases as the opening fee, $o_{i,j}(t)$, increases. When the opening fee is larger than 5, the number does not change much. As in Figure 6(c), when the opening fee increases, the occupancy times remain steady because the temporary arcs are well used so they will not be opened and closed frequently. They will keep open after they are opened so that the opening fee has little effect on the occupancy time. Figure 6(b) shows that in scenario I to III, the total delays increase as $o_{i,j}(t)$ increases until $o_{i,j}(t) = 6$ and keep steady after that. The curve in scenario 4 is a little different since the occupancy time for temporary arcs is very large which means more temporary arcs are used. Figure 6(f) and 6(e) show that as the usage fee, $m_{i,j}(t)$, increases, the occupancy times for all the scenarios decrease and the total delays increase. Figure 6(d) shows that in scenario I to III, the number of opened arcs almost keeps steady. In scenario IV, it decreases a little for $m_{i,j}(t) < 0.5$ and then increases from then on. Two arcs were closed during this scenario, so some temporary arcs have to remain open no matter how expensive the usage fee is to prevent severe delays.
The values of $o_{i,j}(t)$ and $m_{i,j}(t)$ balance the military and civil users. These results provide a good reference for pricing the temporary arcs to balance these two needs.

4. Dynamic Sector Adjustment Problem

It is critical to explore how to utilize limited airspace resource via more flexible approaches in order to meet the increasing demand of air traffic. Since 1990 United States has planned the future National Airspace System (NAS) and introduced the concept of Free Flight, the object of which is using emerging technology, procedures, and concept to implement the transition from the modernization of NAS to air flight freerization, and then to satisfy the requirement of users and service providers of National Airspace System(Bai, 2006). In 1992, Europe presented a new concept of Flexible Use of Airspace (FUA), the main content of which is to abandon the method of simply partitioning airspace into two fixed types - civil airspace and military airspace, and to investigate and establish a new method of airspace use, i.e. flexibly using airspace on demand based on coordination between civil users and military users. Recently China has also started the attempt of developing new airspace planning method and technology considering the characteristics of its airspace structure and the features of its air traffic.
Dynamic adjustment to air traffic control sectors is to make reasonable sector configurations to meet all of following criteria: 1) satisfying the requirement of air traffic control service; 2) keeping the controller's workload not beyond a bearable range; and 3) taking up the least resource of air traffic control.

4.1 Dynamic Adjustment to Air Traffic Control Sectors

An aircraft is usually under the control of several different control units, including the tower control, the terminal control and the en-route control during the whole flight process(Wang et al., 2004). Considering the air traffic control is one kind of heavy brainwork, the workload of on-duty air traffic controllers is kept under a limited level to ensure the flight safety. A controlled airspace is usually divided into several sectors, each of which is under the control of an air traffic control seat, usually consisting of a group of two air traffic controllers. Air traffic controllers are responsible for surveilling flight activity, commanding aircrafts to avoid conflicts, and communicating with neighbor sectors for control handover according to flight plan.

Daily fluctuation of air traffic flow causes the unbalance of controller's workload in different hours or between different sectors. During peak hours more sectors are required to open to increase the airspace capacity and to ensure the flight safety. But when air traffic flow is low some sectors are allowed to merge to avoid unnecessary waste of resources of air traffic control.
One of the difficulties of dynamic sector adjustment is how to evaluate the controller's workload of each sector. The aim of sector adjustment is, on one side, to open enough control sectors to satisfy the air traffic requirement, and on the other side, to open as few as possible control sectors to avoid unnecessary waste of control resources. Therefore the control workload is the direct basis to implement dynamic sector adjustment and the criterion of evaluating the sector adjustment results as well.
Another difficulty of dynamic sector adjustment is how to choose the best scheme of sector configurations, i.e. how to assign n sectors to $k(1 \leq k \leq n)$ air traffic control seats reasonably. The complexity of the problem consists in too many possible assignments of n sectors. Suppose the number of possible assignments of n sectors to k control seats is $P(n,k)$. The computation rule is shown in equation 22. Also suppose the total number of means of grouping n sector is $P(n)$. The computation rule is shown in equation 23(Gianazza & Alliot, 2002). For example, if the number of total sectors is 13, there exists 27,644,437 possible means of assignments and the computation of searching optimal scheme of sector configurations by traversing will be enormous.

$$P(n,1) = 1, \quad P(n,n) = 1$$
$$P(n,k) = kP(n-1,k) + P(n-1,k-1) \tag{22}$$
$$P(n) = \sum_{k=1}^{n} P(n,k) \tag{23}$$

4.2 Evaluation of Controller's Workload

The workload of an air traffic controller refers to the objective requirement of tasks assigned to him(or her), his objective efforts to fulfill the requirements, his working performance, his physiological and psychological states, and his subjective perception to the efforts he ever made.
Many studies have been done on the evaluation of controller's workload and a lot of models and algorithms have been presented. Meckiff et al.(Meckiff et al., 1998) introduced the concept of air traffic complexity in order to evaluate controller's workload. Air traffic complexity refers to the level of complexity of air traffic controller's work caused by a certain air traffic situation. It doesn't consider the difference of control procedures of different airspace, nor the difference of of controller's responses to the same traffic situation. Therefore the air traffic complexity is easier to evaluate than the controller's workload(Schaefer et al., 2001). But no matter what the definition of air traffic complexity or the definition of controller's workload is, it is important to distinguish the degree of requirement of air traffic control under different traffic situations. It seems it is a better way to combine these two concept together, i.e. , to compute the air traffic complexity using the classification of controller's workload, and to quantify controller's workload using air traffic complexity.
The factors that influence the air traffic complexity and the controller's workload include the space structure of sectors, the features of in-sector flight activities, and the types and numbers of conflicts occurred inside the sector. Different sectors have different traffic demands

due to their specific geographic locations. The sectors near an airport, usually spanning the climbing or descending phase of flight, have more workloads of adjusting headings, altitudes and speeds. Furthermore, the more percentage of climbing and descending flights there is, the more possibly the flight conflicts could happen, and the more controller's workloads there are. Also, the more complex the airspace structure is, the more complex the fight activities are. The types and numbers of in-sector conflicts largely depend on the complexity of flight activities inside. The more complex the flight activities are, the more probably the conflicts could occur.
In order to objectively quantify the evaluation of controller's workload, we build an evaluation model based on the features of flight activities. Table 2 lists all feature variables of flight activities. We count 22,000 flights in 15 days and analyze the features of these flights' activities inside each sector in each hour. According to this we evaluate the controller's workload of each sector in different hours.

Table 2. Feature Variables of Flight Activities in the Airspace

Feature Variables	Meanings
$\bar{T}$	average service time
α_{al_up}	percentage of climbing flights
α_{al_down}	percentage of descending flights
α_{al_keep}	percentage of traversing flights
α_{sp_up}	percentage of accelerating flights
α_{sp_down}	percentage of decelerating flights
α_{sp_keep}	percentage of flights with constant speed
α_{hd}	percentage of flights changing their headings
N_{al_up}	average time of climbs for the climbing flights
N_{al_down}	average time of descents for the descending flights
N_{sp_up}	average time of accelerations for the accelerating flights
N_{sp_down}	average time of decelerations for the decelerating flights
N_{hd}	average time of changes for the heading-changing flights

Normally the controller's workload can be classified into three types: 1) surveillance workload, i.e., the workload of inspecting each aircraft's trajectory and its flight state inside the sector; 2) conflict-resolution workload, i.e., the workload of any actions for resolving flight conflicts inside the sector; 3) coordination workload, i.e., the workload of information exchange between pilots and air traffic controllers, or between air traffic controllers of different sectors when aircrafts fly across the border of sectors.
We build an evaluation model of controller's workload by analyzing all kinds of influence factors, as shown in Equation 24. The meanings of variables and parameters are shown in Table 3. In Equation 24, λ, γ, β represent respectively the influence factors related to each feature of flight activities and a, b, c are coordination factors among three kinds of controller's workload.

$$
\begin{aligned}
W_{total} &= CI \times F \\
&= W_{mo} + W_{cf} + W_{co} \\
&= F \times \{a\bar{T}(\lambda_{al}\partial_{al} + \lambda_{sp}\partial_{sp} + \lambda_{hd}\partial_{hd} + \lambda_{al\_keep}\partial_{al\_keep}) \\
&\quad + b\bar{T}\left[\frac{\min(\alpha_{al\_up}, \alpha_{al\_down}, \alpha_{al\_keep})}{\max(\alpha_{al\_up}, \alpha_{al\_down}, \alpha_{al\_keep})} + \frac{\min(\alpha_{sp\_up}, \alpha_{sp\_down}, \alpha_{sp\_keep})}{\max(\alpha_{sp\_up}, \alpha_{sp\_down}, \alpha_{sp\_keep})}\right] \\
&\quad \cdot(\gamma_{al}\partial_{al} + \gamma_{sp}\partial_{sp} + \gamma_{hd}\partial_{hd} + \gamma_{al\_keep}\partial_{al\_keep}) + c \cdot 2\beta\}
\end{aligned} \tag{24}
$$

where

$$
\begin{aligned}
\partial_{al} &= \alpha_{al\_up}N_{al\_up} + \alpha_{al\_down}N_{al\_down} \\
\partial_{sp} &= \alpha_{sp\_up}N_{sp\_up} + \alpha_{sp\_down}N_{sp\_down} \\
\partial_{hd} &= \alpha_{hd}N_{hd}
\end{aligned}
$$

Table 3. Feature Variables in the Evaluation Model of Controller's Workload

Feature Variables	Meanings
W_{total}	controller's workload
F	traffic flow
CI	coefficient of air traffic complexity
W_{mo}	surveillance workload
W_{cf}	conflict-resolution workload
W_{co}	coordination workload

Considering the Beijing Air Traffic Control Region as our investigation object, the sector division scheme is shown in Figure 7. Figure 8 shows the percentage of climbing flights in each hour. The 15 curves in the upper part of Figure 8 show the daily changes of percentage of climbing flight since Jan 1, 2008 to Jan 15, 2008. The lower part of Figure 8 presents the average value of percentage of climbing flights in each hour. We can see the variation tendencies of daily percentage of climbing flight are basically identical, that shows the daily in-sector flight activities have some regularity.

We input the feature variables of flight activities into Equation 24 and obtain the variation tendencies of air traffic complexity in each hour as shown in Figure 11(a). It is perceptible that the no.1, no.3, and no.13 sector, which are the nearest ones to Beijing Terminal Control Area, have the largest air traffic complexity, above 1.2 during peak hours. The no.4, no. 6, no.9, and no.10 sector also have fairly large air traffic complexity, above 1.0 during peak hours, because the structure of air route networks in no.9 and no.10 sector are comparatively complex while no.4 and no.6 sector are quite close to Beijing Terminal. Those that are far from Beijing Terminal, such as no.5, no.7, no.8, no.11, and no.12 sector, have relatively small air traffic complexity, basically around 0.8. The computational results tally with the analysis of influence factors to air traffic complexity and show the validity of the evaluation model of controller's workload.

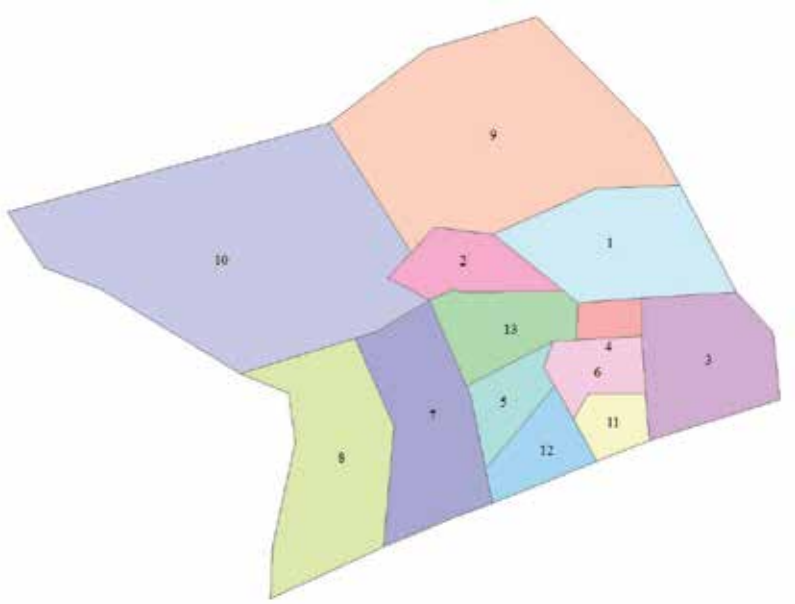

Fig. 7. The Current sector configuration of Beijing Regional ATC Center

4.3 Set-Partitioning Based Model

As what we have discussed, if we seek optimal sector configuration scheme by traversing directly, the amount of calculation will be enormous because many sector combinations dissatisfy the constraint of sector structure features. Therefore we firstly determine all feasible sector combinations and then search optimal sector configuration scheme from the feasible sector combinations using an optimization model based on set partitioning.

4.3.1 Finding Feasible Sector Combinations

We define a sector combination as the mergence of several sectors. Only those sector combinations that satisfy the constraints of sector structure features are feasible sector combinations. A feasible sector combination can be assigned to an air traffic control seat.

The constraints of sector structure features include the continuity constraint and the convexity constraint(Trandac et al., 2003) (Han & Zhang, 2004). According to the principle of air traffic control, a controller's working airspace should be inside a comparatively concentrated airspace for favoring the smoothness of the control work. Otherwise the controller's attention could be distracted due to the dispersion of controlled airspace(Han & Zhang, 2004). Therefore any feasible sector combination must be a continuous airspace. The convexity constraint of sector combination's shape is for avoiding the same aircraft flying across the sector borders twice when executing a flight plan. In fact it is difficult to ensure every sector's shape to be absolutely convex. So we consider a sector combination to satisfy the convexity constraint if the situation that an aircraft flies across the sector borders twice during a single flight activity will not happen.

To obtain all feasible sector combinations, we firstly find out all interconnected sector combinations by setting the prerequisite of interconnection of all participated sectors. Secondly,

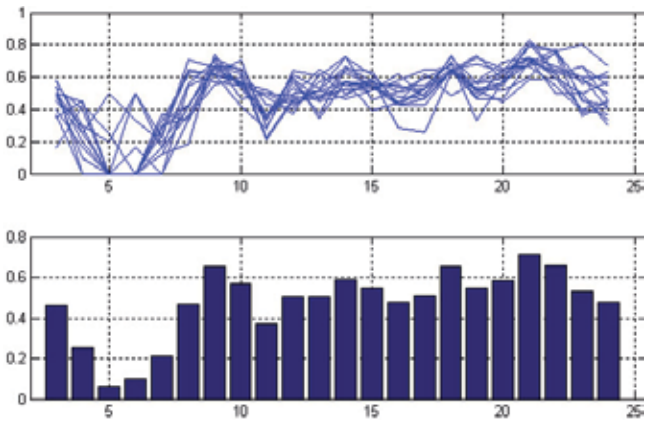

Fig. 8. Hourly percentage variations of climbing flights

we find out all sector combinations that are in accord with the convexity constraint of sector's shape.

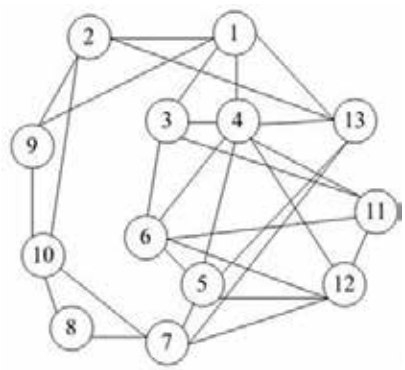

Fig. 9. The Neighborhood Network of Beijing Regional ATC Center

There are 13 sectors in total among the Beijing Regional ATC Center as shown in Figure 7 .So there are $2^{13} = 8192$ possible sector combinations in all. We firstly filter all these sector combinations according to interconnection. Figure 9 is the neighborhood network of each sector of the Beijing ATC Region. Filtering out the sector combinations satisfying the interconnection feature is equal to finding out all interconnected subnets from the network. According to the computation, we know that there are 1368 interconnected sector combinations in all within this network structure.

Basically we have two ways to filter out the sector combinations that satisfy the convexity constraint. One way is by analyzing historical flight data. After screening historical radar data to count the times of each flight flying in or out the sector, we can get all flights passing each sector combinations. If a flight occurs several times and the adjacent two occurring times are discontinuous, it is can be determined that the current sector combination fails to satisfy the convexity constraint. The other way is by human experiences. It is can be distinguished

whether the sector combination satisfies the convexity constraint through analyzing the detailed shape of each sector combination and the spacial distribution of historical radar trace points. Finally 438 feasible sector combinations are determined by the above two ways.

4.3.2 Model's Formulation

Suppose that the set of sectors is S, the set of all feasible sector combinations is R, and the set of sampling points in time period t is I. The optimal sector configuration problem can be described as shown in Equation 25, 26, 27, and 28, where c_r represents the cost efficient of choosing sector combination r and decision variable x_r represents whether to choose the sector combination r. The objective function is to minimize the total costs of choosing opened sector combinations. a_{sr} represents the mapping coefficient of sector combination r and sector s. If sector s is contained by sector combination r, $a_{sr} = 1$; otherwise $a_{ar} = 0$. The constraint 26 shows that each sector must be attached to one and only one opened sector combination. The constraint 27 shows that the instantaneous traffic flow at each sampling point inside the chosen sector combination at time t must be within the limited range.

$$\min \quad \sum_{r \in R} c_r x_r \tag{25}$$

$$s.t. \quad \sum_{r \in R} a_{sr} x_r = 1 \quad \forall s \in S \tag{26}$$

$$f_{ri} x_r \leq f_0 \qquad \forall r \in R, \forall i \in I \tag{27}$$

$$x_r \in \{0, 1\} \qquad \forall r \in R \tag{28}$$

where $a_{sr} = 1$ when $s \in r$ or $a_{sr} = 0$ otherwise. As shown in equation 29, the instantaneous traffic flow within the sector combination r is equal to the sum of the instantaneous traffic flow of all sectors constructing the sector combination.

$$f_{ri} = \sum_{s \in S} a_{sr} f_{si} \tag{29}$$

$$\begin{aligned} c_r &= a \cdot C_r^{++} + b \cdot C_r^{--} + c \cdot (C_r^{+} + C_r^{-}) \\ &= a \cdot (\Delta W_r^{++})^2 + b \cdot (\Delta W_r^{--})^2 + c \cdot (\Delta W_r^{+} + \Delta W_r^{-}) \end{aligned} \tag{30}$$

$$\Delta W_r = W_r - W_0 \tag{31}$$

$$\Delta W_r^{+} = \begin{cases} \Delta W_r & 0 \leq \Delta W_r \leq u \\ 0 & otherwise \end{cases} \tag{32}$$

$$\Delta W_r^{++} = \begin{cases} \Delta W_r & \Delta W_r > u \\ 0 & otherwise \end{cases} \tag{33}$$

$$\Delta W_r^{-} = \begin{cases} |\Delta W_r| & l \leq \Delta W_r \leq 0 \\ 0 & otherwise \end{cases} \tag{34}$$

$$\Delta W_r^{--} = \begin{cases} |\Delta W_r| & \Delta W_r \leq l \\ 0 & otherwise \end{cases} \tag{35}$$

Referring to the research result by Gianazza et al.(Gianazza & Alliot, 2002), we define the opening cost of sector combination r as shown in Equation 30 and Equation 31, 32, 33, 34, and

35 where ΔW_r represents the difference of controller's workload W_r and the average workload W_0. The purpose of defining such cost function is to make the controller's workload of opened sector combination r as close as possible to the average working ability.

$$CI_r = \frac{\sum_{s \in S} a_{sr} \cdot F_s \cdot CI_s}{\sum_{s \in S} a_{sr} \cdot F_s} \tag{36}$$

As shown in Equation 36, the air traffic complexity of sector combination r is derived from the weighted sum of the air traffic complexity of the constituent sectors. The weighted coefficient is the current traffic flow inside the sector.

4.4 Computational Example

We calculate the hourly optimal sector configuration schemes of Beijing Regional ATC Center in a typical day - Jan 4, 2008. The curves of the hourly variations of air traffic complexity of each sector are shown in Figure 11(a). The curves of the hourly variations of controller's workload are shown in Figure 11(b). Figure 10 shows the optimal sector configuration scheme during the time period from 8:00am to 9:00am. Eight sector combinations are chosen to open for the whole ATC region. Figure 11(c) shows the optimal sector configuration in each hour, each grid of which represents an opened sector combination. The first number in a grid indicates the serial number of opened sector combination and the second number represents the controller's workload of the sector combination during current time period. It shows that the controller's workloads are kept balanced, i.e. basically around 25, among all opened sector combinations after adjustment.

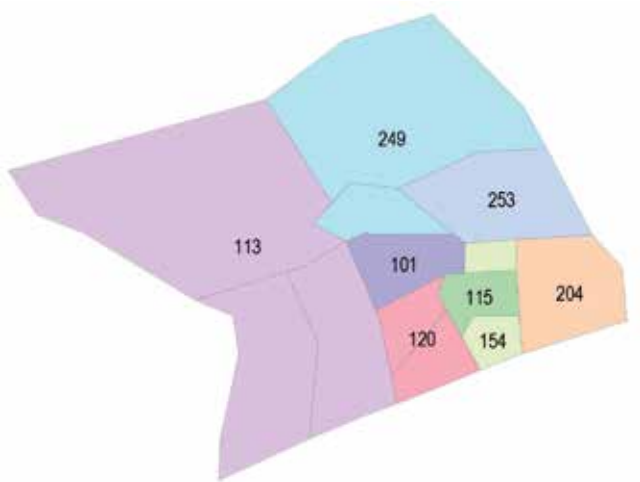

Fig. 10. Optimal Sector Configuration of Beijing ATC Region (8:00-9:00 Jan 4, 2008)

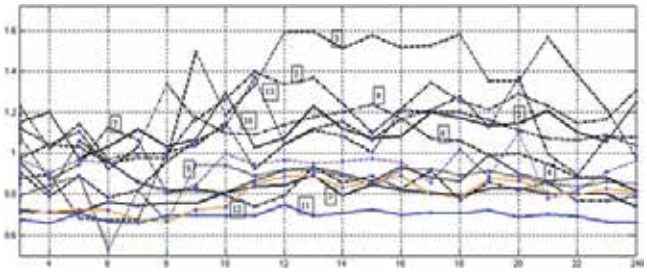

(a) Hourly Variations of Air Traffic Complexity of Each Sector

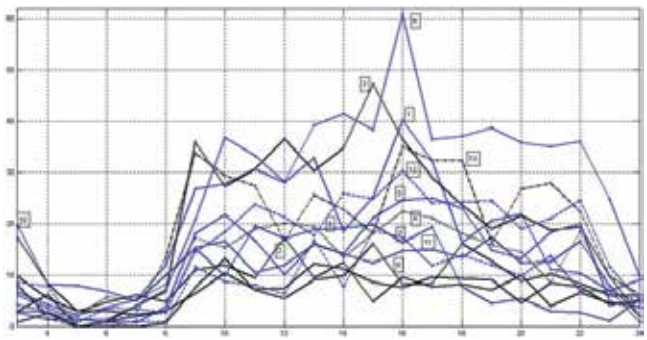

(b) Hourly Variations of Controller's Workload of Each Sector

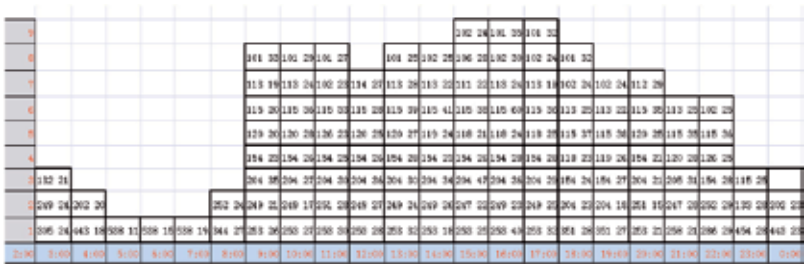

(c) Hourly Optimal Sector Configurations

Fig. 11. Computational Results (Jan 4, 2008)

5. Conclusion

This chapter investigates the models and algorithms for implementing the concept of Dynamic Airspace Management. Three models are discussed. First two models are about how to use or adjust air route dynamically in order to speed up air traffic flow and reduce delay. The third model gives a way to dynamically generate the optimal sector configuration for an air traffic control center to both balance the controller's workload and save control resources. The first model, called the Dynamic Air Route Open-Close Problem, is the first step toward the realization of Dynamic Airspace Management. It designs a pricing mechanism for civil users and military users once they need to use each other's resources and decides what routes will be open and for how long the routes keep open for a certain user during a given time period. The second model, called the Dynamic Air Route Adjustment Problem, provides a new approach to optimize air traffic flow with the option to adjust or reconstruct the air route

network. This model extends the formulation of the ATFM problem by integrating the consideration of dynamic opening and closing of air route segments and introducing several new constraints, such as the shortest occupancy time constraint and the indegree and outdegree constraints, which have not been considered in previous research. The algorithm provides management insight for improving the current airspace management strategy from static to dynamic, from restricted to flexible, and from policy-based to market-based. The sensitivity analysis provides useful reference for pricing temporary arcs in the new flexible market-based airspace management system. The third model, called the Dynamic Sector Adjustment Problem, tries to dynamically utilize airspace resources from another viewpoint. Dynamic adjustment to air traffic control sectors according to the traffic demand is an important means of increasing the efficiency of airspace utilization. We present an empirical model of evaluating controller's workload and build a set-partitioning based mixed integer programming model searching optimal sector configurations. Several examples are solved based on the data from Beijing Regional Air Traffic Control Center. The computational results show that our models on Dynamic Airspace Management are suitable to solve actual-sized problems quickly using current optimization software tools. The work of model validations and implementations are to be completed in the future.

6. References

Bai, Y. (2006). Future national airspace system plan of u.s.a (in chinese), *Air Traffic Management* **8**: 37–39.

Bertsimas, D. & Patterson, S. S. (1998). The air traffic flow management problem with enroute capacities, *Operations Research* **46**(3): 406–422.

Bertsimas, D. & Patterson, S. S. (2000). The traffic flow management rerouting problem in air traffic control: a dynamic network flow approach, *Transportation Science* **34**(3): 239–255.

Cheng, P., Cui, D. & Wu, C. (2001). Optimization based model for short-term air traffic flow management (in chinese), *Journal of Tsinghua University* **41**(4/5): 163–166.

Dubai, A. (2008). The costs of delays and cancellations - analysis and means for cost reductions.
URL: *http://www.agifors.org/document.go?documentId=1579*

Eurocontrol (2008). Cost of delay.
URL: *http://www.eurocontrol.int/ecosoc/gallery/content/public/documents/CBAdelay.pdf*

Gianazza, D. & Alliot, J.-M. (2002). Optimization of air traffic control sector configurations using tree search methods and genetic algorithms, *Digital Avionics Systems Conference, 2002. Proceedings. The 21st*, Vol. 1, pp. 2A5–1–2A5–8 vol.1.

Han, S.-C. & Zhang, M. (2004). The optimization method of the sector partition based on metamorphic voronoi polygon, *Chinese Journal of Aeronautics* **17**(1): 7–12.

Lulli, G. & Odoni, A. R. (2007). The european air traffic flow management problem, *Transportation Science* **41**(4): 431–443.

Ma, Z., Cui, D. & Cheng, P. (2004). Dynamic network flow model for short-term air traffic flow management, *IEEE Transactions on System, Man and Cybernetics, Part A: Systems and Humans* **34**(3): 351–358.

Meckiff, C., Chone, R. & Nicolaon, J.-P. (1998). The tactical load smoother for multi-sector planning, *2nd USA/Europe Air Traffic Management R&D Seminar*, Orlando.

Richetta, O. & Odoni, A. R. (1993). Solving optimally the static ground-holding policy problem in air traffic control, *Transportation Science* **27**(3): 228–238.

Richetta, O. & Odoni, A. R. (1994). Dynamic solution to the ground-holding problem in air traffic control, *Transportation Science* **28**(3): 167–185.

Schaefer, D., Meckiff, C., Magill, A., Pirard, B. & Aligne, F. (2001). Air traffic complexity as a key concept for multi-sector planning, *Digital Avionics Systems, 2001. DASC. The 20th Conference*, Vol. 2, pp. 7E5/1–7E5/12 vol.2.

Trandac, H., Baptiste, P. & Duong, V. (2003). Optimized sectorization of airspace with constraints, *5th USA/Europe Air Traffic Management R&D Seminar*, Budapest, Hungary.

Vossen, T. & Michael, B. (2006). Optimization and mediated bartering models for ground delay programs, *Naval Research Logistics* **53**(1): 75–90.

Wang, L., Zhang, Z. & Yang, X. (2004). The model and algorithm of automatically sectoring airspace (in chinese), *Aeronautical Computer Technique* **34**(3): 46–49.

2

Stability of switched stochastic nonlinear systems

Vojislav Filipovic and Novak Nedic
Mechanical Engineering Kraljevo
Serbia

1. Introduction

Hybrid systems are digital real-time systems which are embedded in analog environment. Analog part of the hybrid system is described with differential equations and discrete part of the hybrid systems is an event driven dynamics which can be described using concept from discrete event systems (Cassandras & Lafortune, 2008) and (Tabuada, 2009). In this paper we will consider the switched systems which can be viewed as higher-level abstraction of hybrid systems (Liberzon, 2003) and (Sun & Ge, 2005).We model each subsystem of a switched system by differential equation.

There are two ways for analysis of stability of switched deterministic systems. The first one is a construction of common Lyapunov function. Find the common Lyapunov functions is a difficult task (Narendra & Balakrishnan, 1994). The second one utilizes multiple Lyapunov functions for analysis of switched systems (Branicky, 1998). In this paper we will consider a stability of switched stochastic systems. We assume that (i) there is no jump in the state at switching instants and (ii) there is no Zeno behaviour, i.e. there is finite number of switches on every bounded interval of time. The situation with jump in the state of x at the switching instants is considered in (Guan et. al., 2005) and (Li et al., 2005).

In recent years the stochastic hybrid systems become hot research topic. There are a few approaches to the problem. In the stochastic setting we have jump diffusion as the solution of stochastic differential equation driven by Levy process which is a linear combination of time, Brownian motion and pure jump process (Oksendal & Sulem, 2005). Close to deterministic hybrid systems is the concept of Piecewise deterministic Markov processes (Davis, 1993) and Stochastic hybrid systems (Hu et al., 2000). The most important difference among the models lies in where the randomness is introduced (Pola et al., 2001). Recently a few monographs are appeared which are devoted to Markov jump systems (Costa et al., 2005) and (Boukas, 2006). The monographs describe the processes that are subject to uncertain changes in their dynamics. Such kinds of systems can be described with Markov jump processes.

In this paper we will deal with stochastic stability of switched systems. Such problem for the systems in usual sense is covered in (Kozin, 1969), (Kushner, 1967) and (Hasminskii, 1980).

In the area of stochastic switched systems the important result is presented in (Chatterjee & Liberzon, 2004). In this paper is considered switched systems perturbed by a Wiener

process. Using multiple Lyapunov like functions the global asymptotic stability in probability is proved. In (Battilotti & De Santis, 2005) the novel notion of stochastic stability is introduced which guarantees a given probability that the trajectories of the system hit some target set in finite time and remain thereinafter.
In this paper we find a set of conditions under which the stochastic switching system is exponentially m-stable. We use multiple Lyapunov function approach. The finite set of models is nonlinear stochastic systems. It is important to mention that the exponentially stable equilibrium is relevant for practice. Namely, such systems are robust to perturbations. After the main result, using Holder and generalized Chebyshev inequalities, it is proved, as a consequences of our result, that stochastic switched system is exponentially m_1-stable for $\forall m_1 \in (0, m)$ and, also, is stable in probability.

2. Practical stochastic hybrid systems

The switching stochastic hybrid control is important tool for large class of real problems. We will briefly describe a few of such problems.
In (Hespanaha, 2005) is proposed the model for stochastic systems where transition between discrete models are triggered by stochastic events like transitions between states a continuous-time Markov chains. The rate at which transitions occur is allowed to depend bouth on the continuous and the discrete states of stochastic hybrid systems. Theory is applied for construction of stochastic models for on-off transmission control protocol (TCP) flows that considers both the congestion avoidance and slow-start modes.
In (Oh & Sastry, 2007) the algorithm for estimating states of a distributed networked system (DNCS) is described. A DCNS is extension of networking control systems (NCS) to model a distributed multi-agent system such as the Vicsek model where multiple agents communicate over a lassy communication channel. The best examples of such system include ad hoc wireless sensor networks and the network of mobile agents. The discrete time linear dynamic model of the DNCS with lossy links is the stochastic hybrid model.
Reference (Glower & Ligeros, 2004) describes the model for multiple flights from the point of view of an air traffic controller. The proposed model is multi-agent, hybrid and stochastic. It consists of many instances of flights, each with different aircraft dynamics, flight plan and flight management system. The different flights are canpled trough the effect of the mind which is modeled as a random field.
Hybrid control, also, has the application in industrial processes. Namely, in the design of PID control systems there is often a choice between fast controllers giving a large overshoot. With hybrid controller very fast step response could be combined with good steady state regulation. The controller consists of a PID controller, a time-optimal controller and a selector. The stochastic hybrid control is need for basic weight regulation in pulp and paper processes (Astrom, 2006)
The solar energy plant (Costa et al., 2005) is another example of stochastic hybrid systems. It consists of a set of adjustable mirrors, capable of focusing sunlight on a tower that contains a boiler, trough which flows water. The power transferred to the boiler depends on the atmospheric conditions. Namely, whether it is sunny or cloudy day. With clear skies the boiler receives more solar energy and the water flow is greater than on cloudy conditions. It means that process dynamics is different for each of these conditions.

In (Filipovic, 2007) the problem of robust control of constrained linear dynamic system in the presence of a communication network with queues is considered. The communication network is between the process output and controller. It is assumed that the queue is at the sensor. The closed-loop system may face the problem of induced random delays caused by the communication network and that delay would deteriorate the system performance as well as stability. The described system is modeled as discrete – time jump linear systems with transition jumps being modeled as finite state Markov chains. Reference (Filipovic, 2008) describes the robustness of picewise linear LQ control with prescribed degree of stability by using switching, low-and-high gain and over-saturation. It is shown that a robust controller with allowed over-saturation can exponentially to stabilize linear uncertain system with prescribed exponential rate.

3. Models for hybrid systems and their importance

In this part of the chapter we will review some fundamental definitions for hybrid systems. First we will define deterministic hybrid systems (Abate, 2007).

Definition 1. A deterministic hybrid system is a collection

$$N^* = (Q, E, D, \Gamma, A, R)$$

where

(i) $Q = \{q_1, q_2, ...q_m\}$ is a finite set of discrete modes.

(ii) $E = \{e_{i,j}, (i,j) \in Q\} \subseteq Q \times Q$ is a set of edges, each of which is indexed by a pair of modes. In the edge $e_{i,j}, i = s(e)$ is its source and $j = t(e)$ its target.

(iii) $D = \{D_1, D_2, ...D_m\}$ is a set of domains each of which is associated with a mode. Suppose that $D_q \subseteq R^n$, $n, < \infty$, $\forall q \in Q$. The hybrid state space is

(iv) $S = \underset{q \in Q}{\cup} q \times D_q$

(v) $A = \{a_q, q \in Q\}$, $a_q : Q \times D \to D$ is the set of the vector fields which are assumed to be Lipschitz. Each vector field characterizes the continuous dynamics in the corresponding domain.

(vi) $\Gamma = \{\gamma_{i,j} \subset D_i\} \subset S$, $j \neq i \in Q$ is the guards set. They represent boundary conditions and are associated with an edge

(vii) $\forall i, j \in Q : \gamma_{i,j} \in \Gamma, \exists e_{i,j} \in E$

(viii) $R : Q \times Q \times D \to D$ is a reset function associated with each element in Γ. With the point $s = (i, x) \in \gamma_{i,j}$ is associated a reset function $R(j,(i,x))$

The initial conditions will be taken from the set of hybrid values $Init \subseteq S$ ▪

Hybrid systems have a problem known as the Zeno dynamics. Such behaviours happen when, in finite time interval, the hybrid trajectory jumps between specific domains infinitely many times. A hybrid system N* is Zeno if for some execution

$$s(t), t \in \tau : \tau \to S \tag{1}$$

of N* there exists a finite constant t_∞ such that

$$\lim_{i \to \infty} t_i = \sum_{i=0}^{\infty} (t_{i+1} - t_i) = t_\infty \tag{2}$$

We can distinguish two qualitatively different types of Zeno behaviour. For an execution $s(t), t \in \tau$ that is Zeno, $s(t), t \in \tau$ is

(i) chattering Zeno (if there exists a finite constant C such that $t_{i+1} - t_i = 0$ for $\forall i \geq C$)

(ii) genuinely Zeno $(if \ \ \forall i \in N \ , \ \exists k > 0 : t_{i+k+1} - t_{i+k} > 0)$

It is very important to make difference between the hybrid systems and switching systems (this kind of systems will be considered in this paper). The hybrid systems specify possible event conditions in terms of the variable of the model by introducing a guard set. The event times are then specified on the single trajectory and the sequence of these times varies depending on the single initial condition. The switching systems are characterized by event conditions that are a priori defined trough a sequence of jumping times $\{t_k\}_{k \in N}$.

The hybrid models are more complicated then switched models.

To prove properties of a hybrid system which is a simulation of it and contains all of its behaviors. Properties of hybrid systems are then proved on the simulation and translated back to the original hybrid model.

Our final target is introduction of stochastic hybrid systems (SHS). In deterministic model N* we will introduce probabilistic terms. An important work which has influenced the theory development for SHS is (Davis, 1993). In that reference the piecewise deterministic Markov processes are introduced.

The work (Gosh et al., 1997) has considered the optimal control for switching diffusions. This model describes the evolution of a process depending on a set of stochastic differential equations among which the process jumps according to state – dependent transitions intensities. The detailed treatment of hybrid switching diffusions is published recently (Yin & Zhu, 2010). Control of linear discrete-time stochastic systems subject both to multiplicative while noise and to Markovian jumping is considered in (Dragan et al., 2010).

Engineering applications include communication, fault detection and isolation, stochastic filtering, finance and so on.
Now we will introduce the general stochastic hybrid model according with reference (Bujorianu & Lygeros, 2006)

Definition 2: A general stochastic hybrid model is a collection

$$S_{SH} = \left(Q, n, A, B, W, \Lambda, \Gamma, R^{A}, R^{\Gamma}\right)$$

where

(i) $Q = \{q_1, q_2, ...q_m\}$, $m \in N$ is a set of discrete modes.

(ii) $n : Q \to N$ is the dimension of the domain associated with each mode. For $q \in Q$ the domain D_q is the Euclidean space $R^{n(q)}$. The hybrid state space is

$$S = \underset{q \in Q}{\cup} \{q\} \times D_q$$

(iii) The drift term in the continuous dynamics is

$$A = \{a_q, q \in Q\} \ , \ a_q : D_q \to D_q$$

(iv) The $n(q)$ - dimensional diffusion term in the continuous dynamics is

$$B = \{b_q, q \in Q\} \ , \ b_q : D_q \to D_q \times D_q$$

(v) The $n(q)$ - dimensional standard Wiener process is

$$W = \{w_q, q \in Q\}$$

(vi) The transition intensity function is

$$\Lambda : S \times Q \to R^{+}$$

$$j \neq i \in Q \ , \ \lambda\left(s = (i, x), j\right) = \lambda_{i,j}(x)$$

(vii) The reset stochastic kernel is

$$R^{\Lambda} : B\left(R^{n(\cdot)}\right) \times Q \times S \to [0,1]$$

(viii) The closed guard set of the each of the domain is

$$\Gamma = \left\{ \bigcup_{\substack{j \neq i \\ (i,j) \in Q}} \gamma_{ij} \subset D_i \right\} \subset S$$

where γ_{ij} describes the jump events.

(ix) The reset stochastic kernel associated with point $s = (i, x) \in \gamma_{i,j}$ is

$$R^{\Gamma} : B\left(R^{n(\cdot)}\right) \times Q \times S \to [0,1]$$

The γ_{ij} describes the reset probabilities associated with the elements in Γ.

The initial condition for the stochastic solution of the general stochastic hybrid model can be given from an initial probability distribution

$$\tilde{u} : B(S) \to [0,1] \quad \blacksquare$$

The important result (Brockett, 1983) shows that, even local asymptotic stabilization by continuous feedback, is impossible for some systems.

Result 1 (Brockett, 1983). Consider the following continuous system

$$\dot{x} = f(x,u) \quad , \quad x \in R^n \quad , \quad u \in R^m$$

and supposed that there exists a continuous feedback law

$$u = k(x) \quad , \quad k(0) = 0$$

which makes the origin a locally asymptotically stable equilibrium of the closed-loop system

$$\dot{x} = f(x, k(x))$$

Then the image of every neighborhood of $(0,0)$ in $R^n \times R^m$ under the map

$$(x,u) \to f(x,u)$$

contains some neighborhood of zero in R^n $\blacksquare$

Above result provides a necessary condition for asymptotic stabilizability by continuous feedback. It means that, starting near zero and applying small controls, we must be able to move in all directions.

Let us consider the class of nonholonomnic systems

$$\dot{x} = \sum_{i=1}^{m} g_i(x)u_i = G(x)u \tag{3}$$

where

$$x \in R^n \quad , \quad u \in R^m \quad \text{and} \quad G \in R^{n\times m} \tag{4}$$

Nonholonomy means that the system is subject to constrains involving both the state x (position) and its derivative $\dot{x}$ (velocity). Under the assumption that

$$rank\, G(0) = m < n \tag{5}$$

the above nonholonomnic system violates Brockett condition. For that case we have following result (Liberzon, 2003).

Result 2. The nonholonomic system (3), for which is satisfied condition (5), cannot be asymptotically stabilized by a continuous feedback law ▪

In the singular case, when $G(x)$ drops rank at 0, the Result 2 does not hold. The full-rank assumption imposed on G is essential. Nonholinomic system satisfying this assumption are nonsingular systems.

The good example of superiority of hybrid system is the problem of parameter estimation of option pricing in quantitative finance. The Black-Scholes model

$$\frac{\partial c(t)}{\partial t} + rS(t)\frac{\partial c(t)}{\partial S(t)} + \frac{1}{2}\sigma^2 S\ (t)\frac{\partial^2 c(t)}{\partial S^2(t)} = rc(t) \tag{6}$$

where $c(t)$ is call option, σ is volatility, r is interest rate and $S(t)$ is price of the stock at time t. Traditionally, a geometric Brownian motion (GBM) is used to capture the dynamics of the stock market by using a stochastic differential equation with deterministic expected returns and nonstochastic volatilities. It does give a reasonable good desciption of the market in the short time period. But, in the long run, it fails to describe the behaviors of stock price owing the nonsensitivity to random parameters changes. Because, the modification of the model is need. According with those observations the price of the stock will be described by the following stochastic hybrid model.

$$dS(t) = \mu S(t)dt + \sigma S(t)dw(t) \tag{7}$$

where $\mu(\cdot)$ and $\sigma(\cdot)$ represent the expected rate of return and volatility of the stock price and $w(\cdot)$ is a standard one-dimensional Brownian motion. The $\alpha(\cdot) = \{\alpha(t) : t \geq 0\}$ is a finite-state Markov chain which is independent of the Brownian motion.

We will find the optimal value of σ by using stochastic optimization. For that we shall use stochastic approximation when the noise is non Gaussian (Filipovic, 2009)

$$\sigma_{n+1} = \prod[\sigma_n - \gamma_n c_\sigma(\sigma_n)\psi(c(\sigma_n) - c_n)] \tag{8}$$

where $\psi(\cdot)$ ise Huber function

$$\psi(x) = \min(|x|, k)\operatorname{sgn} x \quad , \quad 1 < k < 3 \tag{9}$$

and given by minimization of the following function

$$H(x) = -log\ p^*(x) \tag{10}$$

where $p^*(\cdot)$ is the least favorable density for apriori known class of distribution to which stochastic noise belongs.

In relation (12) $c_\sigma(\cdot)$ denotes the derivative of $c(\cdot)$ and $\Pi = \Pi_{[0,M]}$, $M > 0$ is a projection operator given by

$$\prod(\sigma) = \begin{cases} 0, & \text{if} \quad \sigma < 0 \\ M, & \text{if} \quad \sigma > M \\ \sigma, & \text{if} \quad \text{otherwise} \end{cases} \tag{11}$$

The $\{\gamma_n\}$ is a sequence which satisfies following conditions

$$\lim_{n\to\infty} \gamma_n = 0 \quad , \quad \sum_{n=1}^{\infty} \gamma_n = \infty \quad , \quad \sum_{n=1}^{\infty} \gamma_n^2 < \infty \tag{12}$$

The above scheme (hybrid stochastic model + stochastic approximation) predicts more accurate option price then traditional Black-Scholes model does.

4. Application of switched stochastic nonlinear systems in air traffic management

Switched systems have been studied dominantly in the deterministic frame. On the other hand the stochastic switched systems are rather young. We have many possibilities to introduce randomness into the traditional switching systems framework. The one way is to assume that the dynamics is governed by stochastic differential equations. Another one is to make the discrete jumps random according to a Markov transitions matrix whereby the continuous dynamics is deterministic. If the transition matrix is independent of the state we have setting similar to that of Markov jump linear systems.

Here we will consider situation when the continuous part of the system is described with stochastic differential equations. Such model describes much real situations: communication networks, distributed network systems, solar energy plant, cardiac stimulators, encephalogram analyzers and air traffic control system. In the sequel we will shortly describe last kind of systems.

In the current organization of Air Traffic Management the centralized Air Traffic Control (ATC) is a complete control of the air traffic and responsible for safety (Prandini et al., 2000). The main objective of ATC is to maintain safe separation whereby minimum safe separation can vary with the density of the traffic and the region of airspace. To improve performance of ATC owing the increasing levels of traffic, research has been devoted to create tools for Conflict Detection and Conflict Resolution. In Conflict Detection one has to evaluate the possibility in the future position of aircraft while they follow their flight plans. As the model for prediction of the future position of aircraft can be used stochastic differential equations (Glower & Lygeros, 2004). On the basis of the prediction one can evaluate matrices related to safety (for example, conflict probability over a certain time horizon). For Conflict Resolution it is need to calculate suitable maneuvers to avoid a predicted conflict. A framework for such problem can be Monte Carlo Markov Chains which is based on Bayesian statistics.
Here we will consider the stochastic model in the form of family of stochastic differential equations (stochastic switched systems). The switched systems are nonlinear. It is assumed that there is no jump in the state of switching instants and there is no Zero behavior, i.e. there is finite number of switches on energy bounded interval. For such system we will find a set of conditions under which the stochastic switching system is exponentially m-stable. The exponentially stable equilibrium is relevant for practice because such systems are robust in perturbation.

5. Formulation of the main problem

Let us suppose that S_1 and S_2 are subset of Euclidean space, $C[S_1, S_2]$ denotes the space of all continuous functions $f : S_1 \to S_2$ and $C^2[S_1, S_2]$ is a space functions which are twice continuously differentiable. We now introduce some functions according with (Isidori, 1999). A continuous function $\alpha : [0, a) \to [0, \infty)$ is said to belong to class K if it is strictly increasing and $\alpha(0) = 0$. If $a = \infty$ and $\alpha(r) \to \infty$ for $r \to \infty$ the function is said to belongs to class K_∞. A continuous function $\beta : [0, a) \times [0, \infty) \to [0, \infty)$ belongs to class KL if, for each s the mapping $\beta(r, s)$ belongs to class K with respect to r and, for each fixed r, the mapping $\beta(r, s)$ is decreasing with respect to s and $\beta(r, s) \to 0$ as $t \to \infty$.
Let (Ω, F, P) is a complete probability space. We define a family of stochastic differential equations as (Oksendal, 2000)

$$dx(t) = f_p(x(t))dt + G_p(x(t))dw(t) \tag{13}$$

where $x \in R^n$ is a state of system, w is an s-dimensional normalized Wiener process defined on probability space Ω, dx is a stochastic differential of x, P is an index set, $f_p : R^n \to R^n$ and $G_p : R^n \to R^{nxs}$ are corresponding functions. The quantities in the relation (1) ensure existence and uniqueness of stochastic differential equations (Oksendal, 2000).
For definition of switched system generated by the family (1) we will introduce a switching signal. This is a piecewise constant function.

$$\sigma : [0,\infty) \to P^S \tag{14}$$

Such a function has a finite number of discontinuities on every bounded time interval and takes constant values on every interval between two consecutive switching times. The σ is a continuous from the right everywhere

$$\sigma(t) = \lim_{\tau \to t^+} \sigma(t) \quad , \quad \forall \tau > 0 \tag{15}$$

The switched system for the family (1) generated by σ is

$$dx(t) = f_{\sigma(t)}(x(t))dt + G_{\sigma(t)}(x(t))dw(t) \tag{16}$$

For the system (16) we denote the switching instants with t_i , $i = 1,2..,$ $t_0 = 0$ and the sequence $\{t_i\}_{i \geq 0}$ is strictly increasing

The infinitesimal generator for every system from family (13) is (Oksendal, 2000)

$$L_p = f_p'(x)\frac{\partial}{\partial x} + \frac{1}{2}T_r G_p(x) G_p^T(x)\frac{\partial^2}{\partial x^2} \tag{17}$$

where T_r is trace of square matrix.

We now will introduce the concept of stochastic m-stability (Afanasev et al., 1989).

Definition 1. Trivial solution of equation (1) is exponentially m-stable if for some constants $(k_1, k_2) > 0$ is valid.

$$E\left[\|x(t)\|^m\right] \leq k_1 \|x(t_0)\|^m \exp\{-k_2(t - t_0)\} \quad , \quad \exists m > 0$$

where $E[\cdot]$ is mathematical expectation.

For the every $p \in \mathrm{P}$ also is valid next result (Afanasev et al., 1989)

Lemma 1. Let us consider the system from family (1) with index p. Suppose that exists function $V_p \in C^2\left[R^n, R_{\geq 0}\right]$ and constants *a, b, c, m > 0.* For function V_p is a valid next assumption

1° $\quad a\|x\|^m \leq V_p(x) \leq b\|x\|^m$

2° $\quad L_p V_p(x) \leq -c\|x\|^m$

Then, for fixed p, the stochastic system (1) is exponentially m-stable▪

6. Exponential stability of switched systems

Now we will formulate the main result of this paper.

Theorem 1. Let us suppose that for system (4) is satisfied

1° $x(0)$ is deterministic quantity

2° index set P^S is finite, i.e.

$$P^S = \{1,2,...,N\}$$

3° function $V_p \in C^2\left[R^n, R_{\geq 0}\right]$ for $\forall p \in P^S$

4° function $U \in KL$ where functions in *KL* has the form $kre^{-\gamma s}$, $k > 0$, $\gamma > 0$

5° for $\forall x \in R^n$, $\forall m \in (0,\infty)$, $\forall p \in P^S$ and a, b>0

$$a\|x(t)\|^m \leq V_p(x(t)) \leq b\|x(t)\|^m$$

6° for $\forall x \in R^n$, $\forall m \in (0,\infty)$, $\forall p \in P^S$ and $c > 0$

$$L_p V_p(x(t)) \leq -c\|x(t)\|^m$$

7° for $\forall p \in P^S$ and pair of switching instants

$$\sigma(t_i) = \sigma(t_j) = p \ , \ \forall (t_i, t_j) \ , \ i < j \text{ and}$$

$$\sigma(t_n) \neq p \text{ for } i < k < j$$

the inequality

$$E\left[V_p\left(x\left(t_j\right)\right)\right] - E\left[V_p\left(x\left(t_i\right)\right)\right] \leq -E\left[U\left(\left\|x\left(t_i\right)\right\|\right)\right]$$

is satisfied.

Then the system (4) is exponentially *m*-stable ▪

Proof: Let us consider subsystem (13) for fixed *p*. From probabilistic interpretation of infinitesimal generator we have

$$E\left[V_p(x(t)) - V_p\left(x\left(t_0\right)\right)\right] = E\int_{t_0}^{t} L_p V_p(x(\tau))d\tau \tag{18}$$

By differentiation of both sides of relation (18) and using conditions 5^0 and 6° of theorem, we have

$$\frac{d}{dt}E\left[V_p(x(t))\right]=E\left[L_pV_p(x(t))\right]\le -c\|x(t)\|^m\le -\frac{c}{b}E\left[V_p(x(t))\right] \tag{19}$$

From last relation we have

$$E\left[V_p(x(t))\right]\le E\left[V_p(x(t_0))\right]\exp\left\{-\frac{c}{b}(t-t_0)\right\} \tag{20}$$

Using conditions 1° and 5° of theorem follows

$$E\left[V_p(x(t))\right]\le b\|x(t_0)\|^m\exp\left\{-\frac{c}{b}(t-t_0)\right\} \tag{21}$$

Let is, now, consider the interval $[t_0,t_1[$. From relation (21) and assumption 5° and 6° of theorem one can get

$$E\left[V_{\sigma(t_0)}(x(t_1))\right]\le E\left[V_{\sigma(t_0)}(x(t_0))\right]\exp\left\{-\frac{c}{b}(t_1-t_0)\right\}\le b\|x(t_0)\|^m\exp\left\{-\frac{c}{b}(t_1-t_0)\right\} \tag{22}$$

But, over the same interval, for $p\ne\sigma(t_0)$ using assumption 5° of theorem, the estimate

$$E\left[V_p(x(t_1))\right]\le E\left[b\|x(t_1)\|^m\right]=\frac{b}{a}E\left[a\|x(t_1)\|^m\right]\le\frac{b}{a}E\left[V_p(x(t_1))\right] \tag{23}$$

holds true. Using last two equations follows

$$E\left[V_p(x(t_1))\right]\le b\left(\frac{b}{a}\right)\|x(t_0)\|^m\exp\left\{-\frac{c}{b}(t_1-t_0)\right\} \tag{24}$$

Now, consider the interval $[t_1,t_2[$. From (20) and (24) we have

$$\begin{aligned}E\left[V_{\sigma(t_1)}(x(t_2))\right]&\le E\left[V_{\sigma(t_1)}(x(t_1))\right]\exp\left\{-\frac{c}{b}(t_2-t_1)\right\}\le\\ b\left(\frac{b}{a}\right)\|x(t_0)\|^m\exp\left\{-\frac{c}{b}(t_1-t_0)\right\}&\cdot\exp\left\{-\frac{c}{b}(t_2-t_1)\right\}=\\ =b\left(\frac{b}{a}\right)\|x(t_0)\|^m&\exp\left\{-\frac{c}{b}(t_2-t_0)\right\}\end{aligned} \tag{25}$$

Over the same interval $p \neq \sigma(t_1)$ we have

$$E\left[V_p(x(t_2))\right] \leq E\left[b\|x(t_2)\|^m\right] = \frac{b}{a} E\left[a\|x(t_2)\|^m\right] \leq \frac{b}{a} E\left[V_{\sigma(t_1)}(x(t_2))\right] \tag{26}$$

From (25) and (26) follows

$$E\left[V_p(x(t_2))\right] \leq b\left(\frac{b}{a}\right)^2 \|x(t_0)\|^m \exp\left\{-\frac{c}{b}(t_2 - t_0)\right\} \tag{27}$$

The maximum possible value of the function V_σ occurs when the switching signal σ takes the every element from finite set P^S. Let us suppose that t_j^* is the first switching instant after all subsystems have become active at least once since initialization at t_0.
From the above analysis follows

$$E\left[V_p\left(x\left(t_j^*\right)\right)\right] \leq b\left(\frac{b}{a}\right)^{N-1} \|x(t_0)\|^m \exp\left\{-\frac{c}{b}\left(t_j^* - t_0\right)\right\} \tag{28}$$

Let us define the

$$\begin{gathered} \gamma = \max\left(b, b\left(\frac{b}{a}\right)\exp\left\{-\frac{c}{b}(t_1 - t_0)\right\}\right), \ \ldots, \\ \ldots\ b\left(\frac{b}{a}\right)^{N-1} \exp\left\{-\frac{c}{b}\left(t_j^* - t_0\right)\right\} \end{gathered} \tag{29}$$

From condition 7° of theorem it is possible to conclude

$$E\left[V_{\sigma(t)}(x(t))\right] \leq \gamma \|x(t_0)\|^m \exp\left\{-\frac{c}{b}(t - t_0)\right\} \tag{30}$$

If a σ become constant at same index (the case of switching stops in finite times) the switched system, according with condition 5° and 6° of theorem and Lemma 1, is exponentially m-stable.
The second situation is that exists at least one index $p \in P^S$ such that positive subsequence

$$E\left[V_{\sigma(t_i)}(x(t_i))\right], \quad i \geq 0, \ \ \sigma(t_i) = p \tag{31}$$

is infinite in length and exponentially fast decreasing according with hypothesis 7° of theorem.

From (30) and (31) it is possible to conclude that for $\exists p \in P^S$

$$E\left[V_p(x(t))\right] \le \gamma \|x(t_0)\|^m \exp\left\{-\frac{c}{b}(t-t_0)\right\} \tag{32}$$

Using condition 5° of theorem we, finally, have

$$E\left[\|x(t)\|^m\right] \le \frac{\gamma}{a}\|x(t_0)\|^m \exp\left\{-\frac{c}{b}(t-t_0)\right\} \tag{33}$$

Theorem is proved ▪

Corollary 1. If solution of system (4) is exponentially m-stable then for $\forall m_1,\ m_1 \in (0, m)$ the solution is m_1-stable ▪

Proof: Using Holder inequality we have

$$E\left[\|x(t)\|^{m_1}\right] \le \left[E\left[\|x(t)\|^m\right]\right]^{\frac{m_1}{m}} \tag{34}$$

From (33) and (34) follows

$$E\left[\|x(t)\|^{m_1}\right] \le \gamma^{\frac{m_1}{m}}\|x(t_0)\|^{m_1} \exp\left\{-\frac{cm_1}{bm}(t-t_0)\right\} \tag{35}$$

Corollary is proved ▪

Now we will show that from results of Theorem 1 follows stability in probability. For that to us need generalized Chebyshev's inequality (Gihman et al., 1988).

Generalized Chebyshev's inequality: Let us suppose that $g(x)$ nonnegative and nondecreasing function on set of random variables ξ and $E[g(\xi)]$ exists. Then for $\forall \varepsilon > 0$

$$P[\xi > \varepsilon] < \frac{E[g(\xi)]}{g(\varepsilon)} \quad ▪$$

Corollary 2. If solution of (4) is exponentially m-stable then, also, is stable in probability ▪

Proof: From generalized Chebyshev's inequality follows that for function $g(x) = \|x\|^m \ \ (m > 0)$

$$P\left[\|x(t)\| > \varepsilon\right] \le \frac{E\left[\|x(t)\|^m\right]}{\varepsilon^m} \tag{36}$$

Using (33) and (36) we have

$$P\left[\|x(t)\| > \varepsilon\right] \le \frac{\gamma}{\varepsilon^m a}\|x(t_0)\|^m \exp\left\{-\frac{c}{b}(t-t_0)\right\} \tag{37}$$

From last inequality we have

$$\lim_{\|x(t_0)\|\to 0} P\left[\|x(t)\| > \varepsilon\right] = 0 \tag{38}$$

Corollary is proved ▪

7. Conclusion

In this chapter the exponential m-stability of stochastic switched system is proved. The models, in a set of models, are nonlinear stochastic autonomous systems. For stability analysis it is used a multiple Lyapunov functions. The further possibility of investigations is consideration of stochastic switched system with control input.

8. References

Abate, A. (2007). Probabilistic reachability for stochastic hybrid systems: Theory, computations and applications, *PhD University of California,* Berkeley, USA

Afanasev, V. N., Kolmanovskij, V. B and Nosov, V. P. (1989). *Mathematical Theory for Control Systems Design*, Vishaja Skola, Moskva

Astrom, J.K.(2006). *Introduction to Stochastic Control Theory*, Dover Publications, New York

Battilotti, S. and De Santis, A. (2005). Dwell-time controllers for systems with switching Markov chain. *Automatica* 41, 923-934

Boukas, El-K. (2006). Stochastic *Switching Systems. Analysis and Design*, Birkhauser, Boston

Branicky, M. S. (1998). Multiple Lyapunov function and other analysis tools for switched and hybrid systems. *IEEE Trans. Automatic Control* 43, 475-482

Brockett, R.N. (1983). Asymptotic stability and feedback stabilization, In: *Differential Geometric Control Theory*, Brockett, R.W., Millman, R.S. and Sussmann, H.J. (Ed), 181-191, Birkhauser, Boston

Bujorianu, M.L. & Lygeros (2006). Toward a general theory of stochastic hybrid systems, In H.A.P. Blom & Ligeros (Eds) (2006). *Stochasic Hybrid Systems,* pp. 3-30, Springer, Berlin

Cassandras, C. G. and Lafortune S. (2008). *Introduction to Discrete Event Systems*, Springer, Berlin

Chatterjee, D. and Liberzon, D. (2004). On stability of stochastic switched systems. *Proceedings of CDC* 4, pp. 4125-4127

Costa, O. I. V., Fragoso, M. D. and Marques, R. P. (2005). *Discrete-Time Markov Jump Linear Systems*, Springer, Berlin

Davis, M. H. A. (1993) *Markov Processes and Optimization*, Chapman and Hall, London

Dragan, V., Morozan, & Stoica, A.M. (2010). *Mathematical Methods in Robust Control of Discrete – Time Linear Stochastic Systems,* Springer, Berlin

Filipovic, V. Z. (2007). Robust control of constrained systems over a communication network with queues. *International Conference on Control Systems and Computer Sciences,* Buchurest, Romania

Filipovic, V. Z. (2008). Switching control in the presence of constraints and unmodeled dynamics, In: *New Approaches in Automation and Robotics*, Aschemann, H. (Ed), 227-238, I-TECH, Vienna

Filipovic, V. Z. (2009). Applications of robust stochastic approximation in quanitative finance, *Proc. of HIPNE*F, pp. 87-91, Serbia

Gihman, I. I., Skorohod, A. V. and Jadrenko, M. I. (1988). *Probabilty Theory and Mathematical Statistics*, Visha Skola, Moskva

Glower, W. and Lygeros, J. (2004). A stochastic hybrid model for air traffic control simulation. In: *Hybrid Systems: Computation and Control.* Eds. Alur, R. and Pappas, G., Springer , Berlin

Guan, Z. H, Hill, D. J. and Shen, X. (2005). On hybrid impulsive and switching systems and applications to nonlinear control. *IEEE Trans. Automatic Control* 50, 1058-1062

Hasminskii, R. Z. (1980). *Stochastic Stability of Differential Equations*, Sijthoff and Noordhoff, The Netherlands

Hespanaha, J.P. (2005). A model for stochastic hybrid systems with application to communication networks. *Nonlinear Analysis* 62, 1353-1389

Hu, J., Lygeros, J. and Sastry, S. (2000). Towrds a theory of stochastic hybrid systems. *In Hybrid Systems: Computation and Control, Eds. Lynch, N. and Krogh, B. H.*, 79-95, Springer, Berlin

Isidori, A. (1999). *Nonlinear Control Systems II*, Springer, Berlin

Kozin, F. (1969). A survey of stability of stochastic systems. *Automatica* 5, 95-112

Kushner, H. J. (1967). *Stochastic Stability and Control*, Academic Press, New York

Li, Z., Soh, Y. and Wen, C. (2005). *Switched and Impulsive Systems. Analysis, Design and Applications*, Springer, Berlin

Liberzon, D. (2003). *Switching in Systems and Control*, Birkhauser, Boston

Narendra, K. S. and Balakrishnan, J. (1994). A Common lyapunov function for stable LTI systems with computing A-matrices. *IEEE Trans. Automatic Control* 39, 2469-2471

Oksendal, B. (2000). *Stochastic Differential Equations. An Introduction with Applications, Fifth edition*, Springer, Berlin

Oh, S. and Sastry, S. (2007). Approximate estimation of distributed networked control systems. *Proceedings of American Control Conference*, pp. 987-1002

Oksendal, B. and Sulem, A. (2005). *Applied Stochastic Control of Jump Diffusions*, Springer, Berlin

Pola, G., Bujorianu, M. L., Ligeros, J. and Benedetto, M. D. D. (2003). Stochastic hybryd models. An overview. *IFAC Conference on Analysis and Design of Hybrid Systems,* Saint Malo Brittany, France

Prandini, M., Hu, J., Lygeros, J. & Sastry, S.(2000). A probabilistic approach to aircraft conflict detection. *IEEE Trans. Intelligent Transportation Systems* 1, 199-220

Sun, Z. and Ge, S.S. (2005). *Switched Linear Systems. Control and Design*, Springer Verlag

Tabuda, P. (2009). *Verification and Control of Hybrid Systems. A Simbolic Approach,* Springer, Berlin

Yin, G.G. & Zhu, C. (2010). *Hybrid Switching Diffusions. Properties and Applications*, Springer, Berlin

3

Link Capacity Dimensioning Model of ATS Ground Voice Network

Štefica Mrvelj, Miro Cvitković and Ivan Markežić
Faculty of Transport and Traffic Sciences
Croatia Control Ltd
Faculty of Transport and Traffic Sciences
Croatia

1. Introduction

Apart from a number of new technologies which are currently implemented in air traffic control for the exchange of messages the ground/ground (G/G) voice communication is still very significant and is currently irreplaceable. The problem regarding introduction of new technologies that would replace voice communication lies in insufficient development and linking of very expensive ATM (*Air Traffic Management*) systems that have been already in implementation for a number of years. The best indicator showing this is the implementation of MFC (*Multi Frequency Coding*) standard which is still being implemented in the majority of Eurocontrol member countries.
The introduction of advanced automatic message exchange system in ATM will result in the reduction of voice communication in coordination. It will not be possible, however, to perform the implementation of the new systems that will enable exchange of data essential for the coordination, integrally for all the ATM users, so that voice communication will continue to be implemented either as a basic service or as a *backup* service.
In order to realize the planning and dimensioning of the telecommunication network for G/G voice communication which is to be the basic task of this paper, it is necessary to have all the data on the relevant network parameters that may affect the very operation process in air traffic control system. The most important parameter used for this purpose is the telecommunication traffic which is generated among the network nodes and the intensity of which has to be adequately forecast. It will obviously depend on the number of flights between two network nodes during the peak hour and the type of flight which will affect the duration of communication between two working positions in G/G Voice network.
The problem that always occurs is due to the telecommunication network which is designed on the basis of forecast values of several different parameters. The forecast errors are always present in the network design process. They occur either through overestimation or underestimation of the future traffic requirements in the network. In order to correct these errors, eliminate them, or at least alleviate them, the routing design procedure and introduction of dynamic routing in the network are used.

The advances in the technology of modern telecommunication systems have brought to significant interest in the development of schemes that can dynamically manage the calls in the network. The purpose of developing such dynamic routing schemes is the harmonization of the routing pattern in accordance with the variations of the supplied traffic that are not deterministic, in order to better use the network capacity and to enable additional flexibility and robustness that will be able to react to the errors and overloads.
Dynamic routing is nothing new, and the dynamic routing phenomenon is considered apart from the circuit switched networks also in the packet switched networks. There is a number of categories of dynamic routing in the telecommunication networks, both operative ones and many others, recommended through various criteria, such as network planning efficiency, price and complexity of implementation, performances, etc. Up to now a large number of dynamic routing methods have been proposed, and some of them have been partially implemented in the networks of some countries.
One may observe two basic approaches that have attracted significant attention. In the USA, AT&T has implemented the scheme called Dynamic Non-Hierarchical Routing (DNHR) (Ash et al., 1981), which used traffic forecasts for different periods during the day in order to pre-determine the routing patterns. In Canada, Bell-Northern Research presented a scheme called Dynamically Controlled Routing (DCR) based on the controllers receiving information on the current condition for links in the network in regular time intervals (Cameron & Hurtubise, 1986).
Apart from the basic approaches, also the approach which features the advantages for certain network formations is used and it refers to the scheme that is implemented in the British Telecom main network (Stacey & Songhurst, 1987), (Gibbens et al., 1988) and (Key & Whitehead, 1988). This scheme does not use the central controllers, but the information related to the planning of routing pattern is exchanged among the nodes. It has been primarily designed for use in the fully connected networks or nearly full connected networks and employs random search techniques in order to find the beneficial routing pattern.
Since the problems of considering the dynamic routing increase with the number of possible network structures and they vary with the set limitations, the attention will be focused here on special network structure which is not fully connected, and it is imposed by the arrangement of sectors and organization of airspace. This network structure will be used to study the dependence between the efficiency, robustness, simplicity and planning.
This chapter has been organized in the following manner. The second section analyzes the existing and expected communication needs of the G/G Voice network users in order to design the supply of services, forecast the traffic and plan the network capacities. It discusses the specific characteristics of communication needs and requirements in ATM. The technical and technological specification of the telecommunication services has been expressed in a set of specified parameters necessary for further analysis.
The third section studies the specified parameters and the set constraints within which their measures need to be realized.
The chapter presents the adapted version of the dynamic routing method for voice traffic, and therefore the ICAO recommendations for call routing i.e. traffic in the G/G Voice network are considered in the fourth section of the chapter. These have been used as the criterion to define the alternative routes in the analyzed network.

The fifth section describes the used dynamic routing scheme, using the defined conditions to derive a routing table for the analyzed network structure. The relations for determining the route usage probability for all the node pairs in the network have been derived. On their basis and based on the expected traffic among the nodes obtained by measuring of the call duration in aircraft coordination the link capacities between individual network nodes have been determined.
Since in recent years there has been an increasing demand for shifting to new technologies like as migrating to IP (Internet Protocol) transport networks (Markežić et al., 2009), the sixth section analyse bandwidth requirements for the voice transmission over an IP based network between individual nodes.

2. Specification of users' communication needs and requirements

2.1 Current and expected communication needs

Today's European Air Traffic Service Ground Voice Network (AGVN) is composed of many nodes, and each of them contains Voice Communication Systems (VCS). They represent the node entities that contain the functions for automatic switching management in order to provide the telecommunication services. The majority of networks of the Eurocontrol member countries use analogue signalization, whereas the countries with larger traffic have changed to digital signalization. Connecting of such different networks represents a problem that is currently solved by gateway within VCS (Eurocontrol (a), 2005), (Eurocontrol (b), 2005).
It often happens that the network configurations are also distinguished on international links which leads to difficulties in the interworking between VCSs of different Aeronautical Service Providers (ANSP). Sometimes these problems of interoperability can be solved by special border agreements, but this type of solution is not suitable for the realization of the concept of seamless Trans-European network for voice transmission between the ATM services.
Eurocontrol has recognized the need to prepare and define the documents that would provide guidelines for ANSPs for the configuration of their VCSs that will be included in the Trans-European ATS Ground Voice Network. The first goal of these recommendations is to ensure the advice in the configuration of a large number of parameters of Voice Communication Systems (VCS). Another goal is to define in which way such a network should be planned and implemented, in relation to the services and functions, with the aim of smooth achievement of network operations. The introduction of unique standards and network technologies sets the basics for the service quality improvement and the possibility of introducing new functions in VCSs.

2.2 Technical and technological specification of services

In order to design the supply of services, forecast the traffic and plan the network capacities it is necessary to study the existing and expected communication needs of the G/G Voice network users. Well defined users requirements need to be related with the technical and technological specifications of the telecommunication services and networks, which means that a number of parameters need to be specified out of which the following are crucial for further analysis:

- *bandwidth;*
- *call setup time;*
- *delay;*
- *blocking.*

2.3 Specific characteristics communication needs and requirements in ATM

In order to enable coordination among sectors, the ATM has to provide message exchange either by means of data exchange or by voice. In individual airspace communication links are necessary among those participants who are involved in coordination in ATM. In case of increased density of air traffic new sectors may be opened within the already existing sector or in case of a reduction in air traffic density several sectors may merge into one. This change dynamics in number of sectors also affects the G/G and A/G (air/ground) communication needs.

Regarding the organization of airspace both in the Upper Space (ACC- Area Control Centre) and in the Lower space (TMA - Terminal Manoeuvring Area, APP - Approach Control, TWR - Tower Control) there is need for several users to access the communication resources at any moment. The ATM needs for coordination, dynamics of sectors opening and organization of airspace may render the design of such systems a very complex task. The complexity is additionally increased if the category of priority is introduced into the G/G communication systems.

3. Specification of requests for G/G Voice communication affecting AGVN planning

3.1 Access method in the G/G Voice network

Since the call setup time represents an important factor in air traffic safety, the access method will be described here briefly. The required time values of call setup affect the number of nodes through which the call in the network may be set up. According to (Eurocontrol (c), 2005) the following access methods are distinguished:

- *Instantaneous Access (IA)*: This access type is most frequently used for coordination between APP and TWR services when no action by the called user to set up the connection is necessary. The call has to be set up within 1s or less in 99% of the time, (ICAO, 2002). The interval starts from initiating the call from the A side until voice link is established. According to EUROCONTROL recommendations the IA call has to be set up within 100ms.
- *Direct Access (DA)*: This call is usually used between sectors, both in case of a routed link or in case of a point to point link whose characteristics will be presented in Chapter 5 of this paper. The call has to be set up within 2s in 99% of the time, (ICAO, 2002). The interval starts from initializing the call by A side to the moment of obtaining indication of incoming call at the B side.
- *Indirect Access (IDA)*: This method is most often used for coordination with other ATM users that have not been defined in the previously mentioned access types or in accessing the public and closed private networks. The call in this case has to be set up within 15s or less in 99% of the time, (ICAO, 2002). The interval starts from initiating the call by A side to the moment of obtaining an indication of the incoming call at B side.

3.2 Bandwidth requirements for voice transmission in G/G Voice network

The analogue G/G networks use the 300 – 3400Hz bandwidth which is necessary for smooth operation of MFC signalization methods. This bandwidth has to be secured in order to provide high-quality transmission of voice and signalization throughout the network.
The implementation of digital communication systems has enabled better usage of bandwidth so that with the implementation of ATS-QSIG methods and standards for compression per single channel of 64kbps capacity, three voice channels and one signalization channel can be transmitted. The implementation of the methods of voice compression and coding affects also the increase in delay compared to the analogue transmission due to additional voice processing.

3.3 Voice delay in G/G Voice network

Voice delay understands the time necessary to perform voice transmission from end to end between a speaker and a listener. The delay occurs already in A/D (analogue/digital) conversion and depends on the applied method of voice compression. Thus, e.g. for PCM A law (G.711) compression it amounts to 0.75ms whereas for ADPCM (G.726) compression it amounts to 1ms.
Voice delay in transmission through the telecommunication network is defined according to ITU-T G.114 recommendation, which defines 150ms as acceptable end-to-end delay. Detailed analysis of delay components in G/G network is presented in (Markežić et al. 2007).

3.4 Call Blocking

Voice communication systems (VCS) are designed as non-blocking systems, which means that the communication resources have to be availability at any moment at any working position. This property also has to be transferred to the transmission network where the implementation of signalization methods, standards and recommendations for network design ensures minimal call blocking through the network and increase in the system availability. According to recommendations in (ICAO, 2002) for the dimensioning transmission links of G/G Voice network the GoS (Grade of Service) value is 0.001. GoS is defined as the probability that a call is lost during the peak hour due to the lack of transmission links (capacities). Based on this criterion the capacities of the communication links between VCSs will be dimensioned which will be presented in Section 5.

4. Traffic and technological characteristics of G/G voice communication

The previously presented requests for the specified parameters affect the call routing strategy through AGVN; therefore, this section will present the recommendations defined according to (Eurocontrol, 2006), which are used to form the call routing table (Subsection 5.2).

4.1 Recommendations and network routing strategy in G/G Voice network

The basic routing strategy is done according to the following steps (Figure 1):

1. VCS should always try to route a call to the *Direct Point-to-Point Route* or *Direct Network Route.*
2. In case the route is out of service or congested, VCS should try to route the call to another *Direct Point-to-Point Route* or *Direct Network Route* of another network operator (presented by dash line in Figure 1), if such a one is configured.
3. In case all the defined *Direct Routes* are not available, VCS should then try to route the call via *Detour Route*. If multi-*Detour Routes* have been configured in the preferred routing tables, then VCS should have an order of selecting *Detour Routes* with respect to the call establishment time.
4. In case of congestion of the *Direct Point-to-Point Route* or *Direct Network Route*, VCS should attempt to route the call to another *Direct Point-to-Point Route* or *Direct Network Route* (of a different network operator), if such a one is configured.
5. In case all the planned routes are congested, VCS should determine whether there is a call that has priority. In that case the procedures need to be followed to realize the priority call.

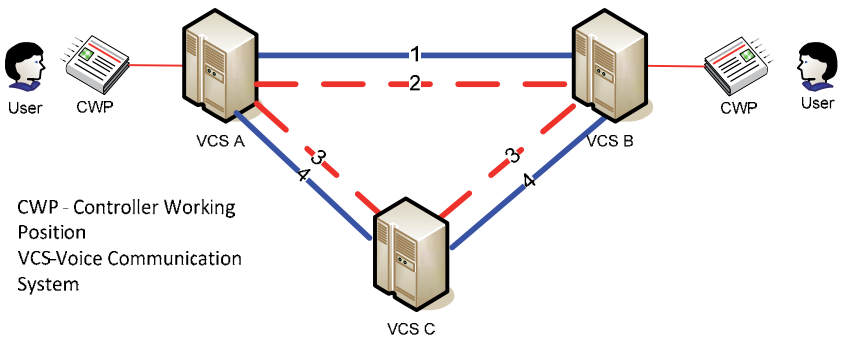

Fig. 1. Call routing strategy with two network operators

4.2 Topology and design of G/G Voice network

Figure 2 presents an example of the network topology for which transmission capacities analysis in this paper is to be carried out. The network consists of five nodes (VCS) that can be of national or international character.

Each node can contain several working positions that can be ACC sectors, TWA or APP working positions. The network design has to allow communication among all sectors at any moment regardless of the air traffic density in a sector. The network also has to be flexible in order to be able to respond to the requests for dynamic changes in the number of sectors and the size of sectors. G/G network for voice transmission has to have the possibility: call routing, priority call, call diversion as well as call waiting.

As can be seen in Figure 2 all VCSs do not have to be in direct connection with everyone, and the call setup time as well as voice delay for the analyzed network with special purpose, impose the need of defining the set of routes (direct and alternative ones) that will satisfy the required criteria. The following chapters tend to present the characteristics of single routes as defined in (Eurocontrol (c), 2005).

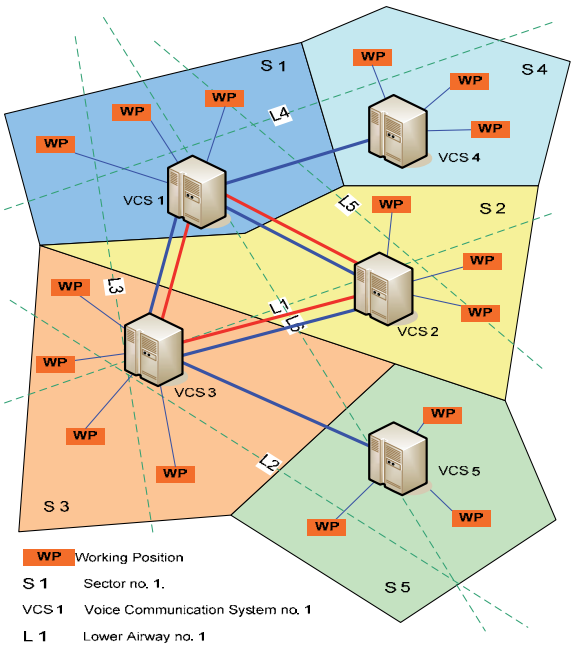

Fig. 2. Sectors and VCS nodes

4.2.1 Direct Point-to-Point Route

The most direct path from the originating to terminating VCS is called *Direct Point-to-Point Route* (Figure 3). In order to respect the time limitations for the IA calls determined in (ICAO, 2002) it is recommended that it be a physical circuit or inter-VCS link that does not pass through the transit/gateway VCS and is not switched by network.

Fig. 3. Direct Point-to-Point Route

Such route cannot consist of more than two nodes and there is no call routing. This is the most frequent communication between the positions within one node or between two adjacent nodes or even direct communication between two VCSs without routing through the network. DA access is used for this type of communication.

4.2.2 Direct Network Route

Direct Network Route can be defined as fixed and pre-established path through the network, between the originating and terminating VCS. This path can comprise of successive physical circuit or inter-VCS link passing through transit or *gateway* VCSs as presented in Figure 4. Owing to shorter call setup times achieved by the usage of digital signalization methods,

ICAO recommendations for ATS Ground-Ground Voice Switching and Signalling allow that maximally three inter-VCS links are used on the *Direct Network Route* among the ATS units (i.e. two transit VCSs) for calls with direct access, under the condition that the network is fully digital and that the criterion for call realization with direct access of 2s can be satisfied.

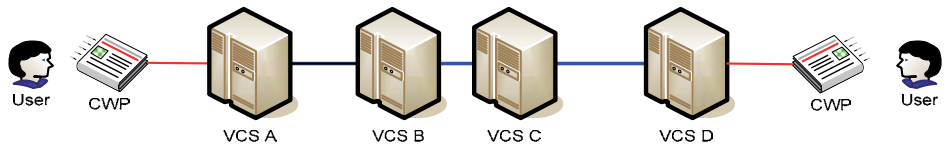

Fig. 4. *Direct Network Route* with maximum number of VCSs

4.2.3 Detour Route

The characteristics of *Detour Routes* are distinguished regarding of whether the network is an analogue or a digital one. Regarding analogue network, the *Detour Route* is an indirect physical path between the originating and terminating VCS through transit VCSs. VCS selects this path when the defined direct routes (*Point to Point or Network Route*) between two points and are not available (do to congestion or failure). The maximum number of inter-VCS links is two for DA calls in analogue networks.

Owing to the shorter call setup time realized by using the digital signalization method, a larger number of inter-VCS links is allowed. Thus, for calls with direct access up to three links on *Detour Route* between ATS units is allowed (Eurocontrol (c), 2005). An example of *Detour Route* with maximally allowed number of links is presented in Figure 5.

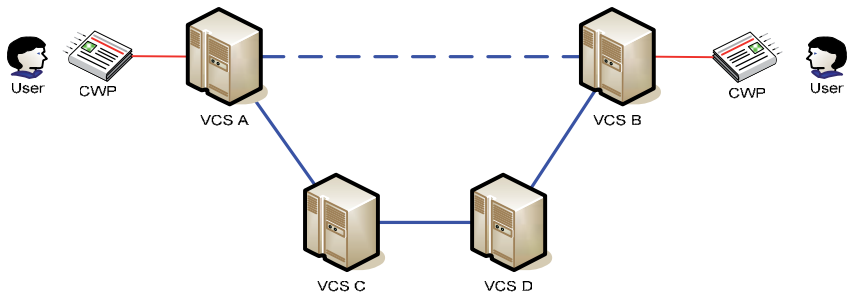

Fig. 5. *Detour Route* in digital network

In case of a stricter criterion that call setup has to be maximum 1s, planned for calls with instantaneous access, it is recommended that these calls (IA calls) are not routed via *Detour Routes*. If there is still need for this, the *Detour Route* in digital network should not contain more than two inter-VCS links.

4.3 Line diversification strategy for G/G Voice network

It is recommended that even for minimal traffic at least two leased lines are available on the inter-VCS link and leased by two network operators. ANSP should check that the network operators have carried out the line separation (i.e. that the leased lines occupy different physical paths in the network) so that a single point of failure would not cause complete

disruption in customer service provision. The recommendation is to configure the VCSs so that they separate traffic into two routes of different operators.
It is extremely important to make it possible for the routing tables for calls on detour routes to be correctly applied for every VCS within AGVN in order to avoid long delays. Badly configured routing table can lead to a closed loop in network routing and for this reason the network can become congested. It causes network degradation due to activation of all resources and a drop in service level experienced by users. With correct call routing and routing table definition it is important in fact to limit the number of transit VCSs through which the call can pass within the network.
Consequently, one may conclude that the maximal number of nodes that a call can pass is four.

5. Traffic capacity analysis of G/G voice network

5.1 Presentation of dynamic alternative routing scheme

The routes in routing tables can contain a group of direct routes and a group of alternative routes that are defined in compliance with the requirements given in Chapters 3 and 4, taking into consideration the network instability that can be caused by dynamic call routing. This understands the avoidance of a closed loop and tromboning, (Eurocontrol (c), 2005). It should be noted that the majority of papers that refer to the dynamic routing problems in the network are based on fully connected network formations and limit the set of alternative routes only to those with two links, which is not the case in this paper.
Next, in forming the routing table the nodes capabilities are respected (i.e. their intelligence). This refers to the possibility that a node can recognize which is the originating node for the call that has entered it, and that it has information on the state of all the links that come out of it (whether they are available or not). Consequently, the routing is done in a way that is known in literature as the call-by-call.
A method is analyzed, according to which, the table of alternative routes is formed with the order which has been determined according to the pre-adopted criterion, and call-by-call routing is carried out in the following way. The selection of an alternative route from the routing table is done according to the order of route in the table, i.e. sequentially. This means that always first the alternative route is selected (of course after the *Direct Network Route*), which is on the first place in the table. If the call cannot be routed along this alternative route, it is directed to the next route in the table, etc. Which means that the call will use one of the alternative routes not completely randomly, but rather conditioned by the occupancy of the previous routes defined by the routing table.
Since a single VCS has information only about links availability to the first next node, it may happen that some of the links further on the stipulated route are not available, and therefore the attempt of setting up the call is returned to the node that offered the alternative routes for a certain observed call. Thus, the analytical procedure of determining the probability that the call will use one of the supplied routes corresponds to the sub-method of alternative routing known as "originating node management with possibility to move management options to other nodes", (Sinković, 1994). In case all the defined routes are occupied after one checking, the call will be rejected, unlike the similar method described in (Kostić-Ljubisavljević et al., 2000) where the attempt will be made to set up the call on a set of pre-defined routes until a given time has passed for the call setup. The authors call this method

sequential routing (i.e. dynamic automatic alternative routing) since the selection of alternative routes follows the order determined by some in-advance adopted criterion (route length, delay, capacity).
The criterion for the definition of the set of routes and their order in selection is exclusively the route length that it is derived from the conditions presented through previous sections.

5.2 Defining the routing tables

The routing strategy can be completely described by the routing table and call management rule. For the presented network (Figure 2) the routing is described by Table 1 (Mrvelj et al., 2009). In order to describe the routing a "typical routing table" can't be used because when a call reaches a certain node, it's further routing depends on the originating node. Therefore, the routing rule will be defined by a three-dimensional field (*i,j,k*), where *i* denotes the node in which the call is currently positioned, *j* is the originating node, and *k* is the terminating node of the respective call.
The *n*-tuple in a certain table cell has the following meaning. If you look at the *n*-tuple in the table cell (1,4,3), (1st row, 4th sub-column of the 3rd column) which is (3,2), it means that the call that is in node 1 whose terminating node is 3, and which originated from node 4, will be routed in two ways according to the order of priority into node 3, and if the link towards it is occupied then to node 2.

		Node k																								
		1					**2**					**3**					**4**					**5**				
		Node j					***Node j***					***Node j***					***Node j***					***Node j***				
		1	***2***	***3***	***4***	***5***	***1***	***2***	***3***	***4***	***5***	***1***	***2***	***3***	***4***	***5***	***1***	***2***	***3***	***4***	***5***	***1***	***2***	***3***	***4***	***5***
Node i	**1**	x	x	x	x	x	2.3	x	2	2.3	2	3.2	3	x	3.2	x	4	4	4	x	4	3.2	3	x	3	x
	2	x	1.3	1	x	1	x	x	x	x	x	3	3.1	x	3	x	x	1.3	1	x	x	3	3.1	x	x	x
	3	x	1	1.2	x	1.2	2	x	2.1	2	2.1	x	x	x	x	x	x	1	1.2	x	1	5	5	5	5	x
	4	x	x	x	1	x	x	x	x	1	x	x	x	x	1	x	x	X	x	x	x	x	x	x	1	x
	5	x	x	x	x	3	x	x	x	x	3	x	x	x	x	3	x	X	x	x	3	x	x	x	x	x

Table 1. Routing table

It will depend on the following condition which route the call will use. If link 1-3 is free, it means that the call on this route has reached its destination. If link towards 3 was blocked, and link 1-2 available, new $i = 2$ (j and k remain unchanged), and then the table cell (2,4,3) is considered. This means that the call that has reached node 2 whose origin is 4, and terminating node is 3, will be made on this route if link 2-3 is available (*n*-tuple in table cell is 3). If the call is not set up on the last in the series of pre-defined routes, it will be rejected.

5.3 Traffic analysis in G/G Voice network

5.3.1 Analysis of ATM users communication time

For the dimensioning of the telecommunication network transmission capacity it is necessary, apart from the requirements previously presented, that are required from a specific telecommunication network to know also the traffic volume between individual location areas, i.e. switch nodes. In order to determine the traffic volume between the nodes measurements were carried out for the purpose of paper (Mrvelj et al., 2009), measuring the duration of calls for various working positions. The measurement results are presented in Table 2.

In the observed peak hour there were 16 aircraft in the coordination of which node 1 and 2 participate. The number of calls and their duration per working positions for that aircraft number are presented in the table (3rd and 4th column). Based on the measured values of the link occupancy times the average values of the call duration per aircraft were obtained (column 5). Current communication which is used to obtain the measured values is performed on the point-to-point principle between working positions of the same category, which facilitated obtaining of realistic picture on the link occupancy for a certain working position.

Apart from measuring traffic on the links i.e. link occupancy duration, the call duration analysis per single working position was carried out also by measuring the time of certain working procedures that refer to communication between the working positions. For the purpose of the analysis of the technological processes the UML diagrams were used, and the sequence diagram is given in Figure 6.

Working position	Aircraft number	Call number	Results obtained by measuring link occupancy			Results obtained by analysis using UML formalism		
			Duration of a single call [second]	Duration of call per aircraft [second]	Total duration of all calls [second]	Duration of a single call [second]	Duration of call per aircraft [second]	Total duration of all calls [second]
1	2	3	4	5	6	7	8	9
1	16	9	20	11.2	180	20	11.2	180
2		6	16	6	95	20	6	95
3		14	37	32.3	518	50	43.7	700
4		4	24	6	96	23	5.7	62
Total/ *average*	**16**	**33**	*24.5*	**55.5**	**889**	*28.2*	**64.8**	**1037**

Table 2. Call duration in aircraft coordination between two nodes (VCS)

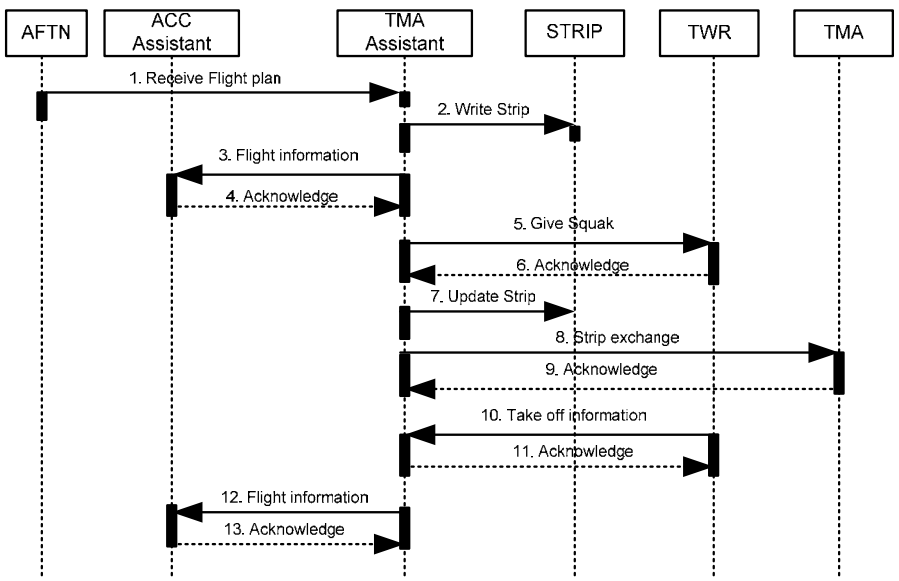

Fig. 5. UML sequence diagram

It may be observed that there are certain differences in the call duration between the data obtained in these two ways, and the reason is that the increase in air traffic often results in the reduction of the coordination time. Thus, e.g. for working position 3 the call duration per single aircraft is longer than according to the measured link occupancy. Regarding working position 4, it is of shorter call duration per aircraft in the analysis using UML formalism than the call duration obtained on the basis of link occupancy. The reason may also be the shorter call duration due to increased traffic.

5.3.2 Traffic matrix

Based on the obtained data on the duration of individual types of calls and data on the number of aircraft in the unit of time the expected values of telecommunication traffic between individual nodes can be determined. It should be noted also, that there is no high uncertainty regarding the volume of the telecommunication traffic such as present in public telecommunication networks. The reason is that the number of aircraft handling is limited by the capacities of single airports.

For the purpose of the analysis, a period of one hour was taken, as usual in the analysis of telephone telecommunication network, and the total traffic between two nodes can be expressed by the following formula

$$A_{jk}=N_{zr}\cdot\sum_{i=1}^{n}\frac{n_{zr_i}\cdot T_{s_i}}{3600} \tag{1}$$

where:

A_{jk}- traffic between nodes *j* and *k*
N_{zr}- number of aircraft between nodes *j* and *k*
n_{zr_i}- number of calls from the working position *i* per aircraft
T_{s_i}- average call duration characteristic for working position *i*
n- number of working positions.

Applying formula 1 and data from Table 2, one can obtain the traffic matrix as presented in Table 3, for the forecast number of aircraft between single nodes.

		Traffic towards node ' k' [Erl]				
		VCS1	VCS2	VCS3	VCS4	VCS5
Traffic from node'j' [Erl]	VCS1	A_{11}=0	A_{12}=0.1	A_{13}=0.2	A_{14}=0.05	A_{15}=0.06
	VCS 2	A_{21}=0.1	A_{22}=0	A_{23}=0.15	A_{24}=0.15	A_{25}=0.05
	VCS 3	A_{31}=0.14	A_{32}=0.34	A_{33}=0	A_{34}=0.14	A_{35}=0.1
	VCS 4	A_{41}=0.2	A_{42}=0.1	A_{43}=0.1	A_{44}=0	A_{45}=0.08
	VCS 5	A_{51}=0.15	A_{52}=0.08	A_{53}=0.08	A_{54}=0.06	A_{55}=0

Table 3. Traffic matrix

5.3.3 Probability of route usage

After having described for the considered network presented in Figure 2, the traffic routing using the routing table (Table 1), and after having determined the expected traffic between the nodes (Table 3), for further analysis it is necessary to determine the probability of the usage of individual route. Before this it is necessary to develop the expanded routing trees

and based on them using the expression which represents the recursive formula for determining the probability of using a certain route (expression 2) according to (Sinković, 1994) determine the probability of using the defined routes for every origin-destination pair. Examples of expanded routing trees are presented in Figure 6, where Li shows nodes where a call could be blocked.

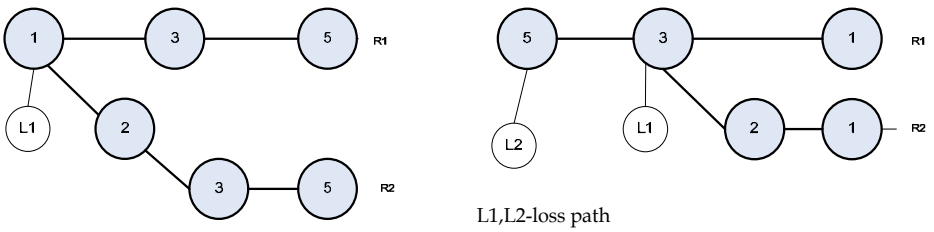

Fig. 6. Expanded routing trees for origin destination pair 1-5 and 5-3

The recursive formula is

$$P(R_i \text{ used}) = \left(\prod_{C_k \in R_i} x_k \right) \cdot \left(1 - \sum_{j=1}^{i-1} P\{R_{j(i)} \text{ used}\} \right) \quad (2)$$

where:

- R_i- analyzed route from the defined set of routes
- x_k- probability that link *k* in route is available (the link availability understands that at least one voice channel is free between two nodes)
- $R_{j(i)}$- set of links as result of the difference of two routes and not a route in itself
- C_k- link *k* which is element of the observed route *i*.

Since the number of recursive calculations depends on index *i*, and on the number of node pairs (originating node and terminating node of call) here the expressions will be developed only for node pair 1-5. Based on the routing table it may be read that the routes according to search order for this pair of nodes are as follows: R_1(1-3-5), R_2(1-2-3-5). The probabilities of using a route are:

$$P(R_1 \text{ used}) = x_{13} \cdot x_{35} \quad (3)$$

$$P(R_2 \text{ used}) = x_{12} \cdot x_{23} \cdot x_{35} \cdot (1 - x_{13}). \quad (4)$$

As seen in formulas 3 and 4 the probabilities of using a route will depend on the probability of the link availability on the route. In calculating the probability of using a route for every call origin – destination pair the probabilities of link availability between nodes have been used in the amount of 0.999 as recommended by ICAO.

VCSs have the possibility of assigning priorities to certain calls, and they are not included in the calculation of the usage probability of a certain route since this would additionally complicate the calculation (increase in the number of conditions in the formula). Therefore,

the probability of link availability can be reduced since the calls with higher priority can interrupt the call with lower priority. The Quality of Service expressed by the probability of path availability between two nodes will be realized anyway, since all calls do not have to be guaranteed the same probability of path availability.
Table 4 presents the probabilities of route usage for different values of link availability probability x_k for those pairs of nodes to which node 1 is the originating one and those to which node 2 is the origin, (Mrvelj et al., 2009).

Origin–destination pair	**route**	**Probability of using route for $x_k = 0{,}999$**	**Probability of using route for $x_k = 0{,}99$**	**Origin–destination pair**	**Probability of using route for $x_k = 0{,}999$**	**Probability of using route for $x_k = 0{,}99$**
1-2	**direct**	0,999	0,99	**2-1**	0,999	0,99
	alternative	*0,000998001*	*0,009801*		*0,000998*	*0,009801*
1-3	**direct**	0,999	0,990000	**2-3**	0,999	0,99
	alternative	*0,000998001*	*0,009801*		*0,000998*	*0,009801*
1-4	**direct**	0,999	0,990000	**2-4**	0,998001	0,9801
	alternative	*0*	*0*		*0,000997*	*0,009703*
1-5	**direct**	0,998001	0,980100	**2-5**	0,998001	0,9801
	alternative	*0,000997003*	*0,009703*		*0,000997*	*0,009703*

Table 4. Probabilities of route usage

The probabilities of connection realization for a pairs of nodes (origin - destination) are obtained by summing up the probabilities of usage of all routes between pair of nodes. That is, the measure for the assessment of the quality of network communication properties entitled *node-to-node Grade of service* (NNGoS) can be presented by the following expression:

$$\text{NNGoS}=1 - \sum_{i=1}^{\text{number of rutes}} P\{R_i \text{ used}\} \tag{5}$$

5.4 Dimensioning of link capacities between VCSs

The basic goal of this chapter is to determine the link capacities between individual nodes whose arrangement depends on the airport location. Using all the previously introduced restrictions on the route length, on avoiding of closed loops and tromboning, and knowing the traffic requirements between individual nodes, using expression 2 the values of the expected traffic on a link have been obtained. The obtained values are presented in Table 5, and they have been achieved by summing up traffic that is expected to be on that link of direct routes and of all the alternative routes in which this link is included.
For determining the capacities between the nodes the Erlang B-formula is used as well as all its assumptions defined in (Akimaru & Kawashima, 1993). The obtained values are presented in Table 5 for different Grades of Service (GoS) expressed by the blocking probability (Mrvelj et al., 2009).

Link between two adjacent nodes	Expected traffic in *[Erl]* on the link with $x_k = 0{,}999$	Number of channels for expected traffic and permitted blocking probability $p_b = 0{,}001$	Expected traffic in *[Erl]* on the link with $x_k = 0{,}99$	Number of channels for expected traffic and permitted blocking probability $p_b = 0{,}01$
1-2	0.330997	4	0.339661	3
1-3	0.929339	6	0.923257	5
1-4	0.75896	5	0.749569	4
2-3	0.670267	5	0.672438	4
3-5	0.70901	5	0.700065	4
Total		25		20

Table 5. Expected traffic on link and necessary number of channels with defined quality

It may be observed from the table that there is significant saving in reducing the link availability even on such a small network. By setting priorities for a certain group of calls satisfactory quality can be achieved that will guarantee air traffic safety. In (Eurocontrol (b), 2005) it has been suggested that the number of links between VCSs be determined based on adding redundancy to links between VCSs depending on the number of routes defined between the pair of nodes (call origin - destination). However, this redundancy is equal also for the expected traffic on a link of 0.33***[Erl]*** and for the traffic of 0.99***[Erl],*** since it is only indicated that the number of links has to exceed the sum of the expected traffic between two VCSs.

6. Bandwidth requirements for voice transmission over IP based network

As voice services in G/G voice network have stricter requirements regarding call set-up time, blocking probability and voice latency than voice services in public network, it is essential to get into account those requirements for the network design. Analysis capacity of transport link for IP (Internet Protocol) based G/G voice network is based on the research carried in previous section regarding the number of offered calls per hour and call duration.

6.1 Impact factor for bandwidth calculation

There are many factors involved when calculating the bandwidth required through a network. This section of chapter aims to explain these factors, and to offer a simple means of making such calculations. The designer of any network solution that includes voice will need to decide upon which coding algorithm to use. Detailed consideration of each coding method is beyond the scope of this section, but it should be understood that the various coding methods vary in the levels of complexity, delay characteristics and quality. The CODECs which are used for bandwidth calculation in this section are G.728 (ITU-T, 1992), whereas the same CODEC is used in ATS QSIG, and G.711 (ITU-T, 2000).

There are many ways to reduce the bandwidth requirements, and these can be particularly important in the specific network like AGVN. These include silence suppression, RTP (Real-time Transport Protocol**)** header compression and RTP multiplexing.

In common with many communications systems, the protocols involved in Voice over IP (VoIP) follow a layered hierarchy which can be compared with the theoretical model developed by the International Standards Organisation (*OSI seven layer model*). Standard method of transporting voice samples through an IP based network required the addition of

three headers; one for each layer. These headers are IP, UDP (User Datagram Protocol) and RTP. An IPv4 header is 20 octets; a UDP header is 8 octets and an RTP header is 12 octets. The total length of this header information is 40 octets (bytes), or 320 bits, and these headers are sent each time a packet containing voice samples is transmitted. The additional bandwidth occupied by this header information is determined by the number if packets which are sent each second. The effect of each layer's contribution the communication process is an additional header preceding the information being transmitted.
This section does not discuss header compression schemes and include them in calculation of bandwidth requirements. Furthermore, this section only considers IPv4 and does not discuss layer 2 protocols which increase overall bandwidth requirements, depending on type of protocol.
The selection of payload duration is a compromise between bandwidth requirements and quality. Smaller payloads demand higher bandwidth per channel band, because the header length remains at forty octets. However, if payloads are increased, the overall delay of the system will increase, and the system will be more susceptible to the loss of individual packets by the network.
It is known that there are not recommendations concerning packet duration. Although codecs vary in their quality and delay characteristics and there is not yet an agreed standard, there are only the most common codecs used for voice transmission over IP. Similarly, there is no recommendation on the packet duration to use in the different environments, but it is considered that 20ms is a good choice for normal Internet conversation with acceptable bandwidth. For office environments where there is almost no bandwidth restriction, G.711 at 20ms packet duration is recommended. In RFC 1889, the Internet Engineering Task Force includes an example where the duration is 20ms, but they do not suggest this as a recommended value. The Table 6 shows bandwidth requirement depending on packet duration for G. 711 (PCM) and G.728 (LD-CELP) which is used for bandwidth calculation in this in this section.

Codec	Packet duration	Bandwidth [kbps]
G.728 (LD-CELP) 16kbps compression	30 milliseconds (48 samples)	27
G.711 (PCM) 64kbps uncompressed	20 milliseconds (32 samples)	80

Table 6. Bandwidth requirements for G.711 and G.728 at different packet duration

There is no absolute answer to this question, but for the purpose of this section, it will be assumed that voice samples representing 30ms and 20ms are sent in each packet, respectively.

6.2. Comparative analysis of the bandwidth requirements for the transmission of voice

Respecting all the assumptions and restrictions introduced in previous sections regarding the route length, avoiding of closed loops and tromboning and knowing the values of the expected traffic on a link, the capacities between the nodes have been obtained.
The results of bandwidth calculation for the transmission of voice over an IP based network have been presented in table 7 (Markežić et al., 2009) for the same number of voice channel which is planned for circuit switch network considered in section 5 and shown in Figure 2.

Link between two adjacent nodes	Expected traffic in *[Erl]* on the link with $x_k = 0{,}999$	Number of ATS QSIG channels for expected traffic and permitted blocking probability $p_b = 0{,}001$	Link capacity requirements for the transmission voice over ATS QSIG based network	Bandwidth requirements for the transmission of voice over an IP based network (CODEC G.711: RTP/UDP/IP, RTCP, packet duration 20ms)	Bandwidth requirements for the transmission of voice over an IP based network (CODEC G.728: RTP/UDP/IP, RTCP, packet duration 30ms)
1	2	3	4	5	6
1-2	0,330997	4 x 16k	2 x 64 **[kbps]**	4 (336,8 **[kbps]**)	4 (112,2 **[kbps]**)
1-3	0,929339	6 x 16k	2 x 64 **[kbps]**	6 (505,2 **[kbps]**)	6 (168,4**[kbps]**)
1-4	0,75896	5 x 16k	2 x 64 **[kbps]**	5 (421 **[kbps]**)	5 (140,3**[kbps]**)
2-3	0,670267	5 x 16k	2 x 64 **[kbps]**	5 (421 **[kbps]**)	5 (140,3**[kbps]**)
3-5	0,70901	5 x 16k	2 x 64 **[kbps]**	5 (421 **[kbps]**)	5 (140,3**[kbps]**)
Total		***25x16k (400*kbps)**	***640* kbps**	***2105* kbps**	***561,2* kbps**

Table 7. Bandwidth calculations for different type of links

The values in columns 5 and 6 are obtained respecting all previously introduced in section 6.1 and for two types of codecs: G.711 (column 5) and G.728 (column 6). Furthermore, obtained values are presented in Table 7 (column 5 and 6) have been achieved without the impact factors regarding layer 2 protocols.
The data in Table 7 show that in all cases a part of the bandwidth remains unused with respect to calculated capacities. Implementation of ATS QSIG link requires the G.703 physical interfaces that allow data transmission speed of 64 kbps. Such a physical link allows a maximum of three voice transmission channels and one common signaling channel.

7. Conclusion

Modern communication networks have to be capable of responding to random fluctuations of requests and errors in different ways. One of them is traffic routing i.e. resource allocation. The designing of such networks (intelligent ones) and their management represent a challenge in mathematical, engineering and economic manner. This chapter describes the scheme of dynamic routing and the derived and presented model which is useful for dimensioning of initial link capacities as well as in the analysis of network stability. Emphasis is on the telephone network for G/G communication in ATM, for which the user's requirements have been described together with the technical requirements that are necessary to support them.
For the design of AGVN the usual methods of determining the telecommunication traffic are used. It should be emphasised, however, that there is a difference in relation to public telephone networks in that the calls in ATM are shorter and the recommended GoS value is lower (0.001). The chapter presents the necessary capacities for GoS value that is used in public networks and for the recommended GoS value for AGVN. The results show substantial savings in the number of channels. Since VCSs can distinguish the type of call and allocate priorities, for the dimensioning of the transmission link capacities a higher GoS value can be used, realizing at the same time a satisfactory Quality of Services for certain calls.

The improvement of dimensioning models of the transmission capacities requires a detailed analysis of traffic flow characteristics in AGVN, as well as inclusion of priorities for a certain group of calls in the model that represents the goal of further research.

8. References

Akimaru, H. & Kawashima K. (1993). *Teletraffic - Theory and Applications*, Springer Verlag, Berlin

Ash, G.R.; Cardwell, R.H. & Murray R.P. (1981). Design and Optimization of Networks with Dynamic Routing, *Bell system Technical Journal*, Vol. 60, No. 8, pp. 1787-1820

Cameron, H.& Hurtubise, S. (1986). Dynamically Controlled Routing, *Telesis*, Vol. 1, No. 1, pp. 33-37

Eurocontrol (a). (2005). Inter-working between ATS-QSIG and ATS R2 signalling system, *Edition 1.0*; February 2005, EATM Infocentre Ref 05/01/12-05

Eurocontrol (b). (2005). Inter-working between ATS-QSIG and ATS No.5 signalling system'' *Edition 1.0*; February 2005, EATM Infocentre Ref.: 05/01/12-06

Eurocontrol (c). (2005). ATS Voice Network Implementation and Planning Guidelines- *Edition 1.0*, February 2005, EATM Infocentre Ref 05/01/12-02

Gibbens, R.J.; Kelly, F.P. & Key P.B. (1988). Dynamic Alternative Routing: Modelling and Behaviour, *Proceedings of 12th International Teletraffic Congress*, Turin, Italy

ICAO (2002). Manual of Air Trafic Services (ATS) Ground-Ground Voice Switching and Signaling, (Doc 9804 AN/762)

ITU-T (1992). G.728 - Coding of speech at 16 kbit/s using low-delay code excited linear prediction (09/92)

ITU-T (2000). G.711: Appendix II: A comfort noise payload definition for ITU-T G.711 use in packet-based multimedia communication systems (02/00)

Key, P.B. & Whitehead M.J. (1988). Cost-effective use of networks employing Dynamic Alternative Routing", *Proceedings of 12th International Teletraffic Congress*, Turin, Italy

Kostić-Ljubisavljević, A.; Aćimović-Raspopović, V. & Bakmaz, M. (2000). Sekvencijalno dinamičko rutiranje: poređenje nekih metoda, *TELFOR* 2000, *on-line* (www.telfor.rs/telfor2000/spisak.html)

Markežić, I.; Mrvelj, Š. & Cvitković, M. (2007). Air-Ground Voice Communication in ATM, *Proceedings of the 18th International Conference on Information and Intelligent Systems*, pp. 377-381, Varaždin, Croatia

Markežić, I.; Cvitković, M. & Mrvelj, Š. (2009). Possibilities of Migration to the G/G VoIP Network for Voice Communication in the Air Traffic Management, *Proceedings of the 20th Central European Conference on Information and Intelligent Systems* pp. 311-317, Varaždin, Croatia

Mrvelj, Š.; Cvitković, M. & Markežić, I. (2009). Link Capacity Dimensioning Model of ATS Ground Voice Network, *PROMET - Traffic&Transportation Scientific Journal on Traffic and Transportation Research*. pp. 73-84, 21 (2009.)

Sinković, V. (1994). *Informacijske mreže*, Školska knjiga, 953-0-30632-6, Zagreb

Stacey, R.R. & Songhurst, D.J.(1987). Dynamic Alternative Routing in the British Telecom Trunk Network, *Proceedings* of *ISS '87*, March, Phoenix, Arizona

4

The potential of some of the innovative operational procedures for increasing the airport landing capacity

Milan Janic
Senior Researcher
OTB Research institute
Delft University of Technology
Jaffalaan 9
2628 BX Delft
The Netherlands
Phone: + 31(0) 15 278 78 99
Fax: + 31 (0) 15 278 34 50
Email: M.Janic@tudelft.nl

Abstract
The ATC (Air Traffic Control) system is established over some designated airspace in order to enable safe, efficient and effective aircraft movements between their origin and destination airports. The main operational performance of these airports has been their airside and landside capacity. In particular, the airport airside capacity includes the capacity of the runway system and surrounding (close) airspace, and the capacities of of taxiways and apron/gate complex. Different concepts of the airport runway system capacity can exist. The first is the concept of the "ultimate" capacity expressed by the maximum number of air transport movements (atms), carried out during a given period of time (usually one hour) under conditions of constant demand for service (atm is either one landing or take-off). The other is the concept of "practical" capacity expressed by the maximum number of atms carried out during a given period of time guaranteeing the average delay per atm within the prescribed limits. Both capacities are calculated respecting the given operational procedures and supportive technologies.
This chapter describes modeling of a potential of some of the innovative operational procedures for safe increasing the "ultimate" runway landing capacity. These are: i) the ATC time-based separation rules applied to landings on a single runway; and ii) the steeper approach procedures applied tp landings on the closely-spaced parallel runways. The modeling implies developing a methodology consisting of the dedicated analytical models for estimating the runway "ultimate" landing capacity under given conditions, which are applied to the selected airports according to the "what-if" traffic scenario approach.

Key words: airport, runway landing capacity, innovative operational procedures, the ATC time-based separation rules, the steeper approach procedures, closely-spaced parallel runways.

1. Introduction

Despite continuous efforts by the air transport system operators, regulators, and researchers (academic and consultants), the problem of providing sufficient airport runway capacity to match continuously growing demand safely, efficiently, and effectively has had rather limited success. A[art from growing demand, the specific environmental (mainly noise) constraints at many large airports both in US and Europe have prevented the full utilization of the designed runway capacity. The sharp concentration of atms (air transport movements) (one atm corresponds to one landing or one take off) within the rather short time periods at the hub airports due to operating the hub-and-spoke networks has created sharp peaks causing further already existing imbalance between demand and the available runway capacity. At some other airports one of which is, for example New York La Guardia airport (US), a high demand/capacity imbalance has been created simply because of their attractiveness and not primarily due the type of airline scheduling practice. In addition, specifically in the US, the operation of airports under IMC (Instrument Meteorological Conditions) and VMC (Visual Meteorological Conditions) and the corresponding difference in the ATC (Air Traffic Control) minimum landing distance-based separation rules (IFR – Instrument Flight Rules, and VFR – Visual Flight Rules, respectively) have inherently created instability of the airports' declared runway landing capacities and consequently their rather high vulnerability to weather conditions. In Europe, such capacity instability caused by weather has also been relatively high, even though the aircraft landings have been carried out exclusively by applying IFR under both IMC and VMC. As well, the shortage of land for expanding the airport runway capacity at many airports has also contributed to the above-mentioned demand/capacity imbalance there in the long-term. In all cases, this imbalance has created congestion, delays and related airline and air passenger costs.

Under such circumstances, the different ultimately short-term measures for mitigating the demand/capacity imbalance by influencing both demand and capacity have been considered. On the demand side, these have generally been demand management by the slot regulation, auction and trading-off of slots, and eventually congestion charging. On the capacity side in addition to building new runways as the long-term measure, these have mainly included introducing the innovative operational procedures supported by the existing and/or innovative technologies. In general, these latter measures have expected to contribute to reducing the ATC separation minimums between landing aircraft and consequently provide the landing capacity gains within the existing airspace and airport infrastructures (Czerny et al., 2008; Janic, 2008, 2008a; CRS, 2008). The ATC separation minimums have mainly been based on the horizontal distances between landing aircraft, which have been modified respecting the impact of the wake-vortices generated behind the large (heavy) aircraft. The landing aircraft have followed the standardized GS (Glide Slope) angle of 3^0 of the ILS (Instrument Landing System). Such rather inflexible but safe operational pattern has provided the runway landing capacity with the above-mentioned characteristics – insufficient and vulnerable to weather. Consequently, the question is whether some innovative operational procedures supported by the existing and/or new technologies could safely increase the airport runway landing capacity and diminish its vulnerability to weather. Some of these considered are the ATC time-based instead of the current ATC distance–based separation rules between landings on a single runway, and the steeper approach procedures to the closely-spaced parallel runways. Both would be supported by the various ATC (Air Traffic Control) decision-support tools at both tactical and operational level. Specifically, in the US, some of these have included Ground Holding Program (GHP),

Airspace Flow Program (AFP), Flight Schedule Monitor (FSM), Flight Schedule Analyzer (FSA), and Traffic Management Advisor (TMA) (CRS, 2008).
In addition to this introductory section, this Chapter consists of five other sections. Section 2 describes the above-mentioned innovative operational procedures for increasing and stabilizing the airport runway landing capacity. Section 3 develops a methodology consisting of the dedicated models for estimating the potential contribution of particular innovative procedures to increasing the runway landing capacity. Section 4 presents application of particular models. The final section (5) summarizes some conclusions.

2. The innovative operational procedures for increasing the runway landing capacity

2.1 Background

The innovative operational procedures for increasing (and stabilizing) the airport runway capacity include the ATC time-based instead of the currently used distance-based separation rules between landings on a single runway and the steeper approach procedures to the closely-spaced parallel runways (Janic, 2008; 2008a).

2.2. The ATC time-based separation rules for landing aircraft

2.2.1 Background

At oresent, at the US airports, depending on weather, the aircraft landings are carried out either under IMC or VMC. Both types of conditions are specified by two parameters - ceiling and visibility - as shown in Figure 1 (FAA, 2004).

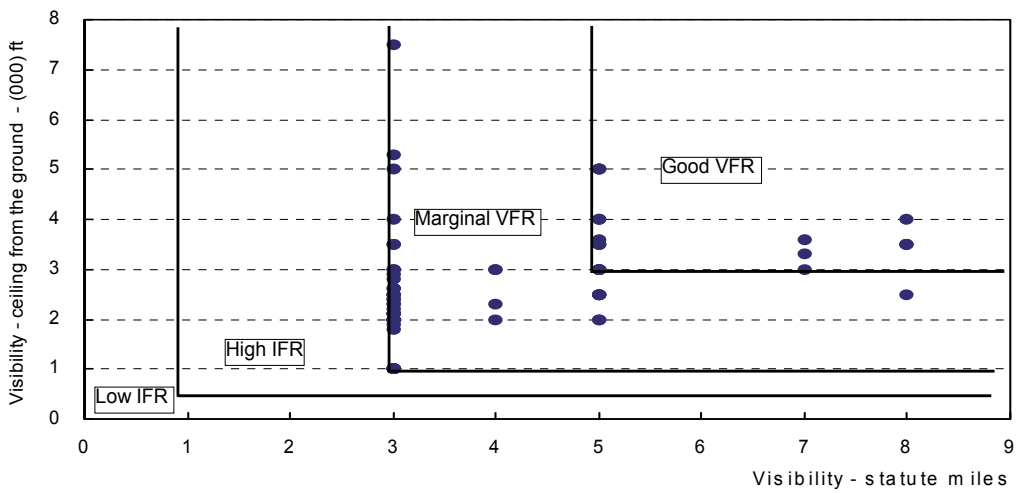

Fig. 1. Characteristics of the meteorological boundary conditions at the 75 selected US airports (Compiled from (FAA, 2004; NASA, 2001)

As can be seen, the critical ceiling is the most diverse when the horizontal visibility is 3 and 5 (statute) miles and relatively homogenous when this visibility is 4, 7 and 8 miles. In addition, most airports operate at the margin between the "high IFR" and the "marginal VFR" (FAA,

2004; NASA, 2001). Depending on the above-mentioned weather conditions (IMC or VMC), the ATC applies the VFR and IFR corresponding minimum separation rules between landing aircraft given in Table 1 (FAA, 2004).

IFR				
i/j	**Small**	**Large**	**B757**	**Heavy**
Small	2.5(3)	2.5(3)	2,5(3)	2.5(3)
Large	4.0	2.5(3)	2.5(3)	2,5(3)
B757	5.0	4.0	4.0	4.0
Heavy	6.0	5.0	5.0	4.0
VFR				
i/j	**Small**	**Large**	**B757**	**Heavy**
Small	1.9	1.9	1.9	1.9
Large	2.7	1.9	1.9	1.9
B757	3.5	3.0	3.0	2.7
Heavy	4.5	3.6	3.6	2.7

Table 1. The FAA (ICAO) minimum separation rules between landing aircraft (nm)
Compiled from: (FAA, 2004; NASA, 1999, 2001)

As can be seen, the current IFR separations applied under IMC are for about 40 per cent stricter than the VFR separations applied under VMC. Both separation rules generally eliminate the impact of the wake vortices of the leading aircraft on the trailing aircraft in particular combinations of landing sequences on the same runway. Under an assumption that the potential exposure of the trailing aircraft to the wakes generated by the leading aircraft in a given landing sequence is nearly the same for both types of separations, the question is: "Why is such a distinction between the VFR and the IFR separations?". The possible answer could be that under VMC, the trailing aircraft fly on the principle "see and be seen" by keeping just a sufficient distance to avoid the wake vortex hazard from the leading aircraft. Under IMC, in addition to the basic separation rules required to avoid the wake vortices, the ATC introduces the additional "buffers" to compensate the cumulative system error in estimating the aircraft position(s). These positions are visualized for the ATC controllers thanks to the sophisticated radar systems. The influence of the two categories of separation rules on the landing capacities, i.e arrival rates, at the selected US airports are shown in Figure 2.

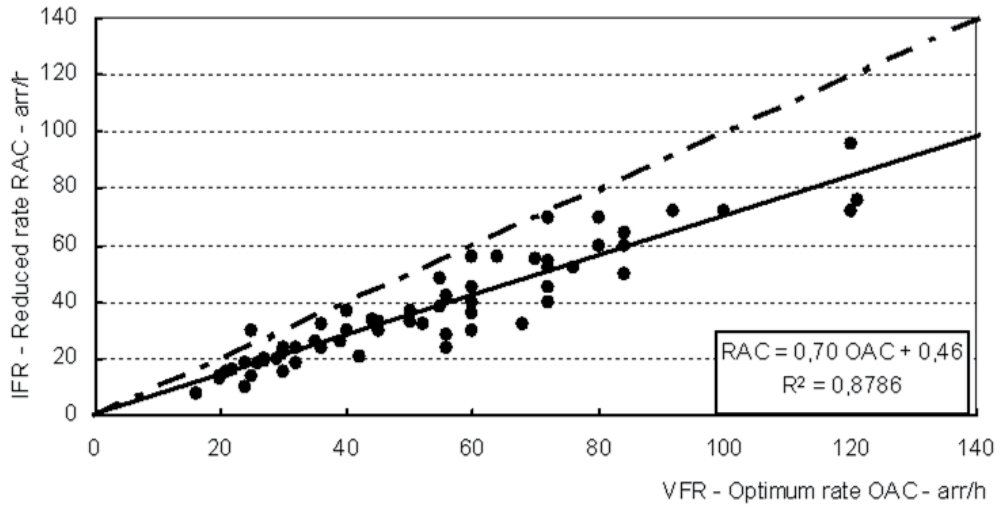

Fig. 2. Relationship between the IFR and VFR landing capacity at the selected US airports (Compiled from: FAA, 2004; NASA, 2001)

As can be seen, a rather strong linear relationship between the IFR and VFR landing capacities (arrival rates), with an average difference of about 30 per cent exists, i.e. the IFR landing capacities generally amount up to about 70 per cent of the corresponding VFR landing capacities. In Europe, independently of the weather conditions, the landings are carried out exclusively according to the IFR separations in Table 1 (EEC, 2005). Consequently, the question is if it is possible to set up the time-based separation rules, which would be standardised respecting the true (dynamic) behaviour of the wake vortices under all weather conditions. In general, these separation rules are expected to provide the shorter minimum time-distance intervals between successive landing aircraft and consequently increase the current distance-dependent runway landing capacity while maintaining it rather stable subject to weather changes. This could be possible if more precise monitoring of the true behaviour of the wake vortices behind particular aircraft would be enabled to pilots, ATC, and/or both.

2.2.2 The "wake reference airspace"

Monitoring the true behaviour of the wake vortices, i.e. dynamically, requires defining the "wake reference airspace" used for the final approach and landing on a given runway. In general, this space consists of two parts: i) the "wake vortex corridor", i.e. the airspace of shape of a horizontal prism, which spreads along the extended centreline of the runway; and ii) the SHA (Simplified Hazard Area) in which the wake vorteuces generated by a given aircraft remains until they decay and/or vacate the "wake reference airspace" (Janic, 2008; ONERA/DOTA, 2005). The "wake vortex corridor" begins at FAG (Final Approach Gate), which is usually defined as the waypoint or by the radio-navigational aid (VOR/DME). Ur ends at the runway touchdown area. Figure 3 shows the simplified three-dimensional scheme of the "wake reference airspace".

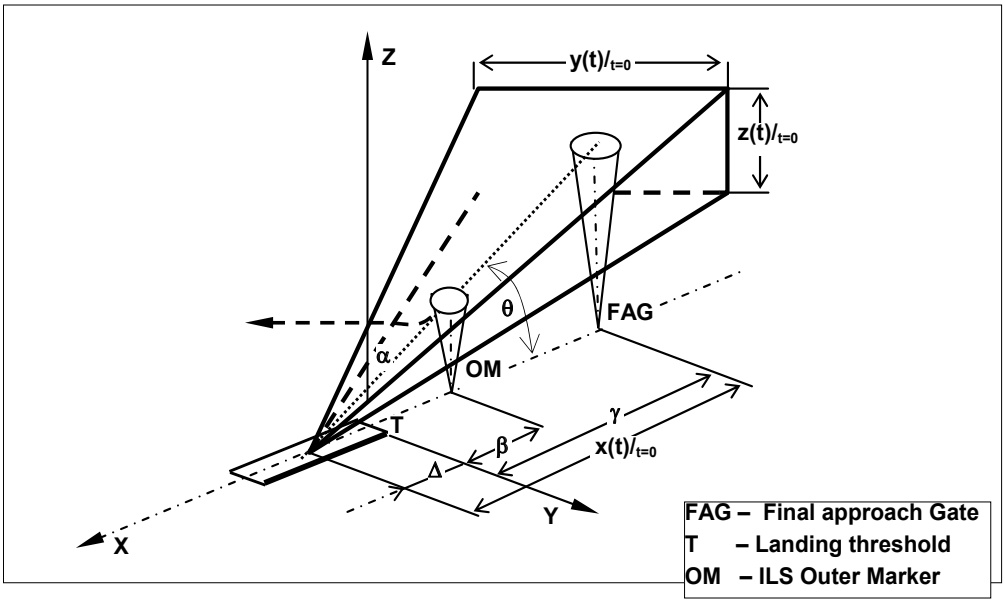

Fig. 3. Three-dimensional scheme of the "wake reference airspace" (Compiled from (Janic, 2008)

where γ is the length of the "wake vortex corridor"; Δ is the horizontal distance between the FAG (Final Approach Gate) at the beginning of the "wake vortex corridor", and the runway landing threshold T; OM and MM are Outer and Middle marker, respectively, of ILS (Instrument Landing System); $x(t)$, $y(t)$, and $z(t)$ are longitudinal, horizontal, and vertical coordinates, respectively, of the "wake reference airspace", depending on time (t); β is the horizontal distance between the location of the OM and the runway-landing threshold T α is the angle between the axis of the "wake vortex airspace" and one of its sides in the horizontal plane; and θ is the nominal angle (ILS Glide Slope) of the aircraft approach path in the "wake vortex airspace".

As mentioned above, ILS provides the approaching and landing aircraft with primary navigation. In the future, the Cockpit Display Traffic Information (CDTI) system on-board the aircraft supported by the ADS-B device will be used for easier self-managing the arrival procedure individually and relative to other close traffic. The ATC usually uses the highly sophisticated radar system for monitoring the arriving traffic. For example, the Precision Radar Monitoring (PRM) system is one of them. In addition, monitoring and prediction of the wake vortex behavior in the "wake reference airspace" is and will be carried out by the current and forthcoming technologies and systems both on the ground and on board the aircraft (Choroba, 2003; Wilkenmans and Desenfans, 2006). The most well-known current system on the ground is Aircraft Vortex Spacing System (AVOSS) currently operating at Dallas Fort Worth airport (US). The system provides the dynamic spacing criteria between aircraft approaching the single runway along a pre-defined corridor based on the prediction of the wake vortex position and strength dependent on the current weather conditions. The wake attribute, which first clears the corridor at a certain ("reference") profile, defines the distance separation criterion for a given aircraft. The standardization and operationalization of such ATC distance-based into the ATC time-based separation rules will likely require the full development of the active (dynamic) forthcoming wake vortex advisory systems such as ATC WAKE, WAKEVAS, and WVWS The particular components of these systems both onboard the aircraft and at the ATC working desk

will enable monitoring and predicting the wake vortex behavior within the entire "wake reference airspace" and exchanging the information between pilots and controllers online, i.e. automatically via data link. The information on the wake vortex of the preceding aircraft would be presented to the crew either on the Navigational or Primary Flight Display containing the wake's strength and prospective behavior (movement) within the "wake reference airspace". Under such circumstances enabling pilots to monitor the wake vortex of the aircraft they follow on the cockpit screen instead of looking at the aircraft itself, which they cannot see under IMC, the separation between the landing aircraft could become purely the dynamic time-based separation, and, in terms of the distances, closer to the today's VFR minimum distance-based separation intervals mainly applied to the US airports (Choroba, 2003; Wilkenmans and Desenfans, 2006).

2.3 The steeper approach procedures

2.3.1 Background

Different configurations of parallel runways are used at busy European and US airports. In Europe, the four busiest continental hubs operate parallel runways: Frankfurt-Main (Germany) a pair of closely-spaced (dependent), and London Heathrow (UK), Paris Charles de Gaulle (France), and Amsterdam Schiphol airport (The Netherlands) a pair, two pairs, and three pairs of the far-spaced (independent) parallel runways, respectively. Currently, at the U.S. the busiest hub airports operate 28 pairs of closely-spaced, 10 pairs of the intermediate-s[aced, and 28 pairs of the far-spaced parallel runways (NASA, 1998). In addition to the above-mentioned characteristics valid for a single runway, in case of parallel runways, the wakes can move from the "wake reference airspace" of one runway to this airspace of the adjacent runway(s) at the speed almost proportional to the speed of crosswind. If the wakes do not sufficiently decay before reaching the adjacent runway, they can create a hazard for the aircraft there, thus making operations on both runways dependent on each other (Burnham, 2002; FAA, 2004; Hammer, 2000; NASA, 2001). Under such circumstances, under VMC, the ATC applies the VFR to the approaches to the parallel runways spaced by 2500 ft (762m) and less by assuming that the wakes generated along the "wake reference airspace" of one runway will never reach this airspace of the adjacent (parallel) runway. This makes the two runways operationally independent on each other (FAA, 2004; Janic, 2008a; LMI, 2004). Under IMC, the ATC exclusively applies the IFR horizontal separation rules in Table 1 between the aircraft approaching to either of the closely-spaced parallel runways, thus making both runways to operate as dependent of each other, i.e. as a single runway. In such case, the CNAP (Conventional Approach Procedure) is performed (Janic, 2008a).

2.3.2 The characteristics of Steeper Approach Procedure (SEAP)

In order to mitigate the above-mentioned dependency of closely-spaced parallel runways the procedures for pairing the arriving aircraft under IMC similarly as under VMC have been considered in both Europe and US. In Europe this has been Staggered Approach Procedure (SGAP) with displaced landing threshold at one of the closely–spaced parallel runways at Frankfurt Mian airport (Germany) (Fraport, 2004). In the US these have been: Simultaneous Offset Instrument Approach/Precision Runway Monitoring (SOIA/PRM), and the most advanced but still under the conceptual development NASA/FAA TACEC (Terminal Area Capacity Enhancing Concept) (Burnham, 2002; Cotton et al., 2001; EEC, 2005), These and an additional innovative procedure called Steeper Approach Procedure (SEAP) use both ATC

horizontal and vertical separation rules simultaneously. Figure 4 (a, b) shows the principal difference between CNAP and SEAP performed under IMC (Janic, 2008a).

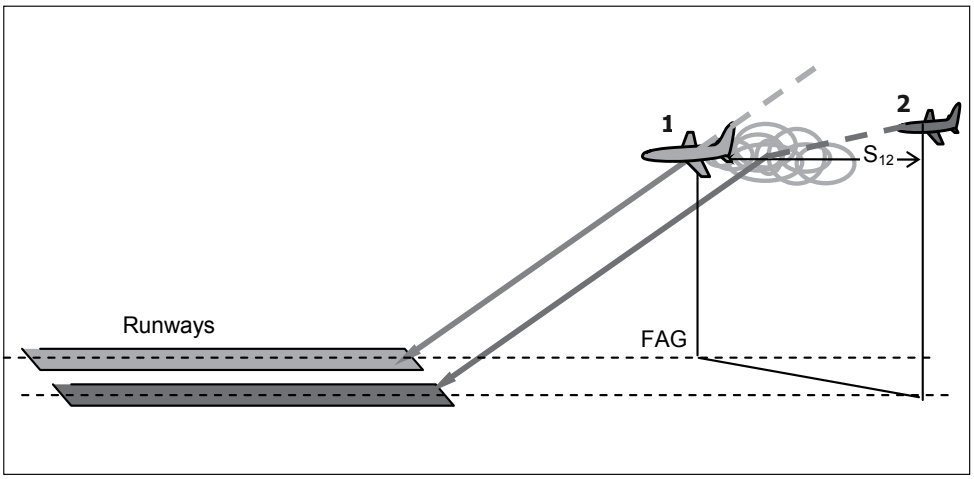

a) Conventional Approach Procedure (CNAP)

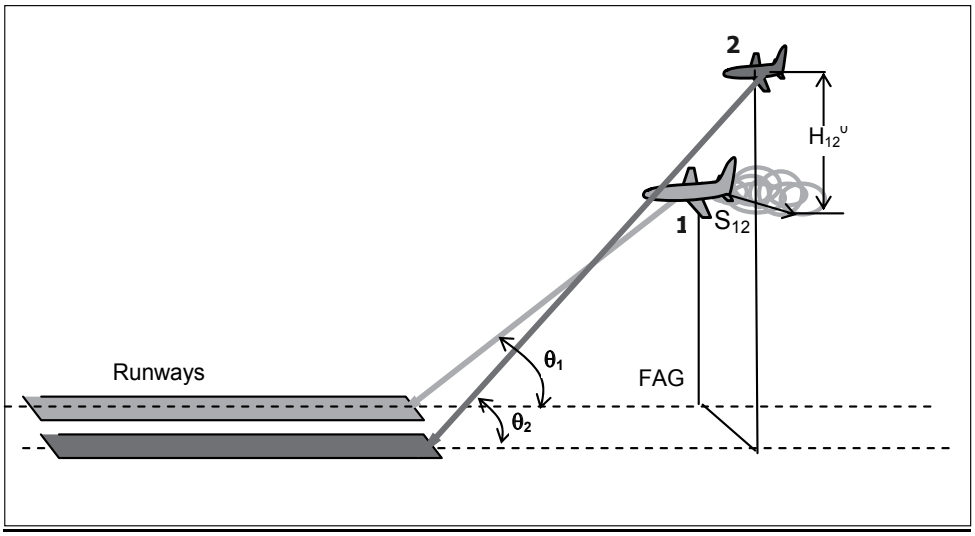

b) Steeper Approach Procedure (SEAP)

Fig. 4. The CNAP and SEAP to the closely spaced parallel runways under IMC (Compiled from: Janic, 2008a)

The Steeper Approach Procedure (SEAP) could be considered as the prospective approach procedure under IMC in cases when it is necessary to avoid obstacles in the final approach airspace, if it is not possible to displace the landing threshold of one of two (closely spaced) parallel runways, but if it is needed to eventually relatively substantively increase the runway system capacity. Currently, the SEAP is applied to some single runway regional airports (six in Europe) mainly for avoiding obstacles and/or eventually reducing the noise burden (EEC, 2005). This procedure has never been considered for application to the closely-spaced parallel

runways for any of the above-mentioned purposes and particularly not for eventual increasing of the runway system capacity under IMC. Even the above-mentioned future concept (TACEC) does not consider the final approaches at different (and steeper) GS angles than nowadays. Consequently, at this preliminary stage the SEAP is characterized as follows:

- Technologies

The SEAP applied to the closely-spaced parallel runways can be based on two pairs of ILSs (or GNSS supporting ADS-B in the future) each attached to one of the runways or a pair of MLSs each serving a single runway. For a given runway, one ILS provides the standard GS angle of 3^0 and the other the steeper GS angle of $5\text{-}7^0$. A single MLS provides simultaneously both GS angles within a given range: $3\text{-}7^0$ (This will also be possible when GNSS and ADS-B will be available) (Rossow, 2003;TC, 2004). The ILSs are preferably of the category IIIb or IIIc (i.e. with zero Decision Height (DH) and Runway Visual Range- (RVR) of 50ft or 0ft, respectively) thus enabling also the auto-landing under the worst visibility conditions (ICAO, 1996). Each ILS has different LLZ (Localizer) frequency coupled with the GP (Glide Path) frequency, which prevents interference between the ILSs serving the same runway. Thus, given aircraft can perform either the standard or the steeper approach and landing procedure independently, by using existing ILS avionics and Flight Management (FM) auto-landing system. MLS also enables the similar auto landing opportunities. In addition, the ATC can also use PRM for monitoring the arriving traffic. As well, other technologies improving the situational awareness both at aircraft and on the ground could be gradually implemented (EEC, 2005; ICAO, 1996; Janic, 2006, 2008a). Ub addition, the lighting system on each parallel runway must be appropriately calibrated respecting the different ILS or MLS GS angles. This might appear unfeasible causing the pilot confusion, and thus being considered as insufficiently safe. The auto-landing could mitigate or even eliminate this concern.

- Operations

The SEAP implies that the arriving aircraft can use either the standard or the steeper ILS GS angle while approaching to the closely-spaced parallel runways under IMC. In particular, if the aircraft pairing is made similarly as under VMC or the SOIA/PRM, the leading aircraft can be assigned the standard and the trailing aircraft the steeper GS angle. Figure 4b shows the simplified typical scheme when at the moment of pairing the heavy - leading *(1)* and small - trailing *(2)* aircraft approaching to the closely-spaced parallel runways. As can be seen, the leading aircraft *(1)* approaches to the right parallel runway at the standard GS angle θ_1; the trailing aircraft *(2)* approaches to the left runway at the steeper GS angle θ_2 ($\theta_1 < \theta_2$). The leading aircraft *(1)* and trailing aircraft *(2)* are appropriately vertically separated by the ATC vertical separation rules H_{12}^0 at the moment of pairing at FAG (Final Approach Gate) of aircraft *(1)*. This initial vertical separation does not exclude some horizontal separation S_{12}, which might be unnecessary. In addition, when the condition regarding the aircraft speeds and GS angles is fulfilled (i.e. $v_1 > v_2 \sin\theta_2 / \sin\theta_1$), the initial minimum vertical separation H_{12}^0 continuously increases - until the leading aircraft *(1)* lands. Under such circumstances the aircraft *(2)* will always stay above the aircraft *(1),* thus completely avoiding the hazard of its wakes staying all the time below its final approach trajectory. Nevertheless, the hazard from wakes along the same approach path still requires application of the ATC longitudinal (in-trail) separation rules.

- Traffic complexity

Performing the SEAP and CNAP simultaneously on the same runway(s) may increase the traffic complexity and consequently the workload of ATC controllers and pilots. However, the updated decision supporting tools such as CTAS (Centre/TRACON Automation System) and Integrated Arrival/Departure manager on the one hand, and CDTI on the other, may compensate such increased workload, respectively (Janic, 2006).

- Standardization

The SEAP is not the standardized ICAO procedure such as CNAP. Therefore, it needs approval from the local airport and national aviation.

- The aircraft certification

Specifically, the aircraft should be technically capable and consequently certified for SEAP similarly as they are currently certificated for CEAP. The certification could include only discrete but also the continuous GS angles within a given range. Since most Boeing and Airbus aircraft do not have such certification, the related costs of additional certification might be relatively high, of course if the aircraft are considered capable for being certified for the SEAP safely[1]. While following the steeper approach trajectory, the aircraft need higher descent speed, which in turn reduces the horizontal component of the resultant speed and thus seemingly increases the wake-vortex. In order to prevent the impact the resultant approach speed should be increased to compensate the higher vertical component authorities.

- Training the staff

The pilots and ATC controllers must be appropriately trained. One aspect of training of pilots is preparation of the aircraft full landing configuration in the SEAP earlier than in the CNAP, which includes intercepting the steeper GS angle, and stabilizing and keeping the constant approach speed at the lower thrust. Training of the ATC controllers implies familiarizing with application of different combinations of separation rules and eventually with a potential for handling an increased number of missed approaches.

- Passenger comfort

The vertical speed during CNAP of about 500-800ft/min currently appears comfortable for passengers. Under the same circumstances, increase in the vertical speed during SEAP for about 80% as compared to CNAP might be uncomfortable.

3. A methodology for estimating the potential of innovative procedures to increasing the runway landing capacity

3.1 Background

The methodology for estimating the potential contribution of the above-mentioned innovative procedures to the airport runway landing capacity consists of two dedicated models: i) the model when the ATC time-based separation rules are applied; and ii) the model when the SEAP

[1] The earliest, De Havilland DHC-6 and DHC-8 had been certified as the STOL (Short Take Off and Landing) aircraft. Later, the regional aircraft Cessna Citation, BAe RJ 85/100, Fokker 50, Dornier 328, Embraer ERJ 135/170, and recently the larger Airbus A318/319 have been certified for the SEAP (EEC, 2005; TC, 2004).

in addition to CNAP is applied to the closely-spaced parallel runways. The models have the analytical structure enabling carrying out the sensitivity analysis with respect to changes of the most influencing factors.

3.2 Previous research

Modelling of the airport ultimate (runway) capacity has occupied the airport, ATC, and airline operators, planners, analysts and academics for a long time. These efforts have resulted in developing the numerous analytical and simulation models, which could be classified into two broad classes for: i) calculating the (runway) capacity of individual airports and of the airport network(s) (Odoni and Bowman, 1997); and ii) optimization of utilization of the airport (runway) available capacity under changing influencing factors and conditions (Andreatta and Romanin-Jacur, 1987; Bianco and Bielli, 1993; Richetta and Odoni, 1993, 1994; Richetta, 1995; Terrab and Odoni, 1993; Vranas et al., 1994).

Specifically, the analytical models for calculation of the airport runway capacity have provided the two-value parameter – one for the arrival and another for the departure capacity (Blumstein, 1959; Donahue, 1999; Gilbo, 1993; Harris, 1972; Hockaday and Kanafani, 1974; Janic and Tosic, 1982; Janic, 2006; Newell, 1979; Swedish, 1981). Some other models such as the FAA Airport Capacity Model, LMI Runway Capacity Model, and DELAYS as 'Quasi-Analytical Models of Airport Capacity and Delay', developed mainly for the airport (runway) planning purposes and based on the analytical single-runway capacity model, have calculated the so-called "capacity coverage curve" including the associated aircraft delays (Gilbo, 1993; Newell, 1979). In parallel, separate models of the ultimate capacity of the airport apron/gate complex and the system of taxiways have been developed. Recently, these analytical models have been integrated into the 'airport integrated-strategic planning tool' (EEC, 2005). An additional integration has however been achieved by developing the computer-supported simulation models for calculating the airport capacity and delay at i) Low (HERMES and The Airport Machine), ii) Intermediate (NASPAC, FLOWSIM and TMAC), and iii) High Level of Detail (TAAM and SIMMOD) (Ignaccolo, 1993; Janic, 2001; Odoni and Bowman, 1997; Swedish, 1981; Wu and Caves, 2002). In comparison to the analytical models, these models have studied the airport airside operations in much greater details. In some cases, they have seemed to require relatively long time for familiarization, time-consuming preparation of input, consequently relatively high cost, and produced too detailed output, which paradoxically made the strategic planning choices more complex and time consuming than otherwise (Odoni and Bowman, 1997; Stamatopoulos et al., 2004). However, the efforts on further refining existing and developing new models offering estimation of the potential of some of the innovative operational procedures and technologies for increasing the airport runway landing capacity have been made. They have resulted in developing the analytical models for estimating the "ultimate" landing capacity for the cases elaborated in this Chapter, i.e. the ATC time-based separation rules and and the steeper approach procedures, both considered as elements of the current NextGen (US) and SESAR (Europe) programmes (http://vams.arc.nasa.gov/activities/tacec.html). (Janic, 2006, 2008, 2008a).

3.3 Objectives and assumptions

The objectives of the research described in this Chapter are to develop the methodology consisted of the dedicated analytical models, which will enable estimating the potential of the selected innovative operational procedures and technologies to increase the airport runway

landing capacity under given conditions. In addition, each model should enable carrying out the sensitivity analysis of the capacity with respect to changes of the most important influencing factors. Consequently, the methodology is based on the following assumptions (Janic, 2006, 2008; 2008a, 2009):

- The runway system consisting of a single and/or a pair of the closely-spaced parallel runways with the specified geometry used exclusively for landings is considered;
- The aircraft arrive at the specified locations of their prescribed arrival paths almost precisely when the ATC (controller) expects them, i.e. the system is considered as "the error free";
- The occurrence of particular aircraft categories in particular parts are mutually independent events;
- The arrival mix characterized by the weight (i.e. the wake-vortex category) and approach speed of particular aircraft categories is given;
- The aircraft approach speeds along particular segments of the "wake reference airspace" are constant.
- The influence of the weather conditions on the wake vortex behavior for a given landing sequence is constant during the aircraft staying in the "wake reference airspace";
- The ATC uses the radar-based longitudinal and horizontal-diagonal, and vertical separation rules between the arriving aircraft;
- Assignment of CNAP/SEAP depends on type of the arrival sequence(s) in terms of the aircraft wake-vortex category, approach speed, and capability to perform SEAP in the latter case;
- The successive arrival aircraft approaching to the closely-spaced parallel runways, are paired and alternated on each runway; and
- Monitoring of the current, and prediction of the prospective behavior of the wake vortices in the "wake reference airspace" is reliable thanks to the advanced technologies;

3.4 Basic structure of the models

The models developed possess a common basic structure, which implies determining the "ultimate" landing capacity of a given runway(s) as the reciprocal of the minimum average "inter-arrival" time of passing of all combinations of pairs of landing aircraft through a given "reference location" selected for their counting during a given period of time (Bluemstein, 1959). In the given context, the minimum average inter-arrival time enables maximization of the number of passes through the "reference location", which is usually the runway landing threshold. The period of time is ¼, ½, and/or most usually 1 hour.

Consequently, the basic structure of the model using the ATC time-based instead of the ATC distance-based separation rules between landing aircraft on a single runway is based on the traditional analytical model for calculating the "ultimate" runway landing capacity as follows(Blumstein, 1959; Janic, 2001):

$$\lambda_a = T / \sum_{ij} p_{i\,a} t_{ij\,\min} p_j \tag{1}$$

where

$_{a}t_{ijmin}$ is the minimum inter-arrival time of the aircraft pair *(i)* and *(j)* at the runway landing threshold selected as the "reference location" for counting the operations;

p_i, p_j is the proportion of aircraft types *(i)* and *(j)* in the landing mix, respectively;

T are the periods of time (usually one hour).

In the case of the SEAP on the closely-spaced parallel runways, let's assume yajy yjere are two aircraft landing sequences: i) the aircraft sequence *(ij)* is to land on RWY1; and ii) the aircraft sequence *(kl)* is to land on RWY2. Since the occurrences of particular aircraft categories are mutually independent events on both runways, the probability of occurrence of the "strings" of aircraft *(ikj)* and *(kjl)* can be determined as follows (Janic, 2006, 2008a):

$$p_{ij/k} = p_i p_k p_j \quad \text{and} \quad p_{kl/j} = p_k p_j p_l \tag{2}$$

where

p_i, p_k, p_j, p_l is the proportion of aircraft categories *(i)*, *(k)*, *(j)* and *(l)* in the mix, respectively.

Given the minimum inter-arrival time at the landing threshold of RWY1 and RWY2 as $_{a}t_{ij/k/min}$, and $_{a}t_{kl/j/min}$, respectively, and the probabilities $p_{ij/k}$ and $p_{kl/j}$ for all combinations of the aircraft sequences *(ikj)* and *(kjl)*, respectively, the average inter-arrival time at the threshold of RWY1 and RWY2 in Figure 4b as the "capacity calculating locations" can be computed as follows (Janic, 2006, 2008s):

$$\bar{t}_{a1} = \sum_{ikjk} {}_{a}t_{ij/k/\min} p_{ij/k} \quad \text{and} \quad \bar{t}_{a2} = \sum_{kjl} {}_{a}t_{kl/j/\min} p_{kl/j} \tag{3}$$

Then, the "ultimate" arrival capacity of a given pair of the closely-spaced parallel runways can be calculated separately for each runway as (Janic, 2006):

$$\lambda_{a1} = T / \bar{t}_{a1} \quad \text{and} \quad \lambda_{a2} = T / \bar{t}_{a2} \tag{4}$$

The total landing capacity for the runway system can be calculated as the sum of the individual capacities of each runway.

3.5 Determining the minimum interarrival time(s) at the "reference location"

3.5.1 The ATC time-based separation rules

The minimum time-based separation rules for the aircraft landing on a single runway are determined by modeling the wake-vortex behavior in the "wake reference airspace", setting up the dynamic time-based separation rules, and calculating the inter-arrival times of particular sequences of landing aircraft at the "reference location", i.e. the runway landing threshold *T* in Figure 3 (Janic, 2008).

3.5.1.1 The wake vortex behavior

The wake vortex appears as soon as the lift on the aircraft wings is created. The investigations so far have shown that the wakes behind the aircraft decay over time generally at more than proportional rate, while simultaneously descending below the aircraft trajectory at a certain descent speed. Without crosswind they also move from the aircraft trajectory at a self-induced speed of about 5kt (knots). Otherwise, they move according to the direction and speed of the crosswind (Shortle and Jeddi, 2007).
Modeling the wake-vortex behavior includes determining its strength, i.e. the root circulation, the "reference time", decaying pattern, decent speed, and the movement influenced by the ambient weather.

The wake strength – the root circulation at time (t). This can be estainated as follows:

$$\Gamma_0(t) = \frac{4Mg}{\rho v(t) B \pi} \tag{5a}$$

The wake reference time, i.e. the time for the wake to descend for one wing span at time (t). This can be estimated as follows:

$$t^*(t) = \frac{\pi^3 B^2}{8\Gamma_0(t)} = \frac{\rho \pi^4 B^3 v(t)}{32Mg} \tag{5b}$$

The wake-decaying pattern. This is estimated as follows:

$$\Gamma(t) = \Gamma_0(t)\left(1 - \frac{t}{kt^*(t)}\right) \tag{5c}$$

If the safe wake strength is Γ^*, the time the wake needs to decay to this level, $\tau_d(\Gamma^*)$ can be determined from expression (5c) as follows:

$$\tau_d(t, \Gamma^*) = kt^*(t)\left(1 - \frac{\Gamma^*(t)}{\Gamma_0(t)}\right) \tag{5d}$$

The wake's self-induced descent speed. This is determined as follows:

$$w(t) = \frac{2\Gamma(t)}{\pi^2 B} = \frac{2\Gamma_0(t)\left[1 - t/kt^*(t)\right]}{\pi^2 B} \tag{5e}$$

where

M is the aircraft (landing) mass (kg);

g is the gravitational acceleration (m/s^2);

ρ is the air density near the ground (kg/m^3);

$v(t)$ is the aircraft speed at time (t) (m/s);

B is the aircraft wingspan (m); and

k is the number of the reference time periods after the wakes decay to the level of the natural turbulence near the ground (70 m^2/s) (k = *8 - 9*).

The impact of ambient weather

The ambient weather is characterized by the ambient wind, which can influence the wake vortex behaviour in the "wake reference airspace". This wind is characterized by the crosswind and headwind components as follows.

- Crosswind:

The crosswind can be determined as follows:

$$V_{cw}(t) = V_w(t)\sin(\varphi_w - \varphi_a) \tag{5f}$$

The wake vacates the "reference profile" at almost the same speed as the crosswind.

- Headwind:

The headwind can be determined as follows:

$$V_{hw}(t) = V_w(t)\cos(\varphi_w - \varphi_a) \tag{5g}$$

where

$V_w(t)$ is the wind reported by the ATC at time (t);

φ_w is the course of the wind (^{U});

φ_a is the course of the aircraft (^{U}).

The headwind does not directly influence the wake descent speed (rate) but does move the wake from the ILS GS and thus increases its vertical distance from the path of the trailing aircraft. This vertical distance increases linearly over time and in proportion to the headwind as follows:

$$\Delta z_{hw}(t) = V_{hw}(t) * t * tg\,\theta \tag{5h}$$

where all symbols are as in the previous expressions.

3.5.1.2 The dynamic time-based separation rules

Let $\tau_{ij/min}(t)$ be the minimum time-based separation rules between the leading aircraft *(i)* and aircraft *(j)* in the landing sequence *(ij)* at time *(t)*. Currently, this time depends on the ATC distance-based separation rules (either IFR or VFR) implicitly including the characteristics of the wake vortex behavior, and the aircraft approach speeds (see Table 1). The main idea is to make these time separations explicitly based on the current and predicted characteristics and behavior of the wake vortex generated by the leading aircraft *(i)* in the given sequence *(ij)*. The characteristics and behavior of the wake vortex include its initial strength and time of decay to a reasonable (i.e. safe) level, and/or the time of clearing the given profile of the "wake reference airspace" either by the self-induced descend speed, headwind, self-induced lateral speed, and/or crosswind.

Let $\tau_{ij}(t)$, $\tau_{iy}(t)$ and $\tau_{iz}(t)$, respectively, be the time separation intervals between the aircraft *(i)* and *(j)* based on the current ATC distance-based separation rules in Table 1, and the predicted times of moving the wakes of the leading aircraft *(i)* either horizontally or vertically at time *(t)*, out of the "wake reference airspace" at a given location. In addition, let $\tau_{id/j}(t)$ be the predicted time of decay of the wake of the leading aircraft *(i)* to the level acceptable for the trailing aircraft *(j)* at time *(t)*. Refering to Figure 3, these times can be estimated as follows:

$$\begin{aligned}
&\tau_{ij}(t) = \delta_{ij}(t)/v(t) \\
&\tau_{iy}(t) = Y_i(t)/V_{cw}(t) \\
&\tau_{iz}(t) = \min[Z_i(t)/w_i(t); \Delta z_{ij/\min}(t)/V_{hw}(t)tg\theta] \\
&\tau_{id/j}(t,\Gamma^*) = kt_i^*(t)\left[1-\Gamma_j^*/\Gamma_{0i}(t)\right]
\end{aligned} \tag{6a}$$

where

$\delta_{ij}(t)$ is the minimum ATC distance-based separation rules applied to the landing sequence *(ij)* at time *(t)*;

$v_j(t)$ is the average approach speed of the trailing aircraft *(j)* at time *(t)*; and

$\Delta z_{ij/min}(t)$ is the minimum vertical separation rule between the aircraft *(i)* and *(j)* at time *(t)*.

Other symbols are analogous to those in the previous expressions. Expression (6a) indicates that the time the wakes of the leading aircraft *(i)* take to move out of the given "reference profile" does not depend on the type of trailing aircraft *(j)*. However, the decaying time of the wakes from the leading aircraft *(i)* depends on its strength, which has to be acceptable (i.e. safe) for the trailing aircraft *(i)*. Consequently, at time *(t)*, the trailing aircraft *(j)* can be separated from the leading aircraft *(i)* by the minimum time separation rules as follows:

$$\tau_{ij/\min}(t) = \min\left[\tau_{ij}(t); \tau_{iy}(t); \tau_{iz}(t); \tau_{id/j}(t,\Gamma^*)\right] \tag{6b}$$

- If $v_i \le v_j$, the minimum time separation rule $\tau_{ij/min}(t)$ should be established when the leading aircraft *(i)* is at the runway landing threshold *T* in Figure 3, i.e. at time $t = \gamma/v_i$. In

addition, the following condition must be fulfilled: $\tau_{ij/min}(t) \geq t_{ai}$, where t_{ai} is the runway occupancy time of the leading aircraft *(i)*.

- If $v_i > v_j$, the minimum time separation rule $\tau_{ij/min}(t)$ should be established when the leading aircraft *(i)* is just at FAG (Final Approach Gate) in Figure 3, i.e. at time $t = 0$. This is based on the fact that the faster leading aircraft *(i)* will continuously increase the distance from the slower trailing aircraft *(j)* during the time of approaching the runway.

3.5.1.3 The minimum inter-arrival times between landings

The minimum inter-arrival times for the aircraft sequences *(i)* and *(j)* at the landing threshold can be determined based on expression (6b) as follows:

$$ {}_a t_{ij/\min} = \begin{cases} \tau_{ij/\min}(t=0) + \gamma\left(1/v_j - 1/v_i\right) & \text{for} \quad v_i > v_j \\ \max\left[t_{ai};\ \tau_{ij/\min}(t = \gamma / v_i)\right] & \text{for} \quad v_i \leq v_j \end{cases} \qquad (6c) $$

where $\tau_{ij/min}(t)$ is determined according to expression 6(a, b).

At time $t = 0$, when the leading aircraft *(i)* is at FAG, the "wake reference profile" is as its greatest, which implies that the wakes need the longest time to vacate it by any means. At time $t = \gamma/v_i$, when the leading aircraft *(i)* is at the landing threshold, the "wake reference profile" is the smallest, which implies that the wakes need much shorter time to vacate it (see Figure 3).

3.5.2 The Steeper Approach Procedure (SEAP)

The minimum inter-arrival times between the aircraft landing on the closely-spaced parallel runways are estimated respecting the fact that they can perform both CNAP (Conventional Approach Procedures) and SEAP (Steeper Approach Procedures). At both, the ATC applies the longitudinal (i.e., in-trail) separation rules to the aircraft on the same and the horizontal-diagonal and/or the vertical separation rules to the aircraft on the different (parallel) approach trajectories.

3.2.2.1 Scenario for performing SEAP

Simultaneous performing of CNAP and SEAP at a given pair of the closely-spaced parallel runway is carried out according to the traffic scenario shown in Figure 5.

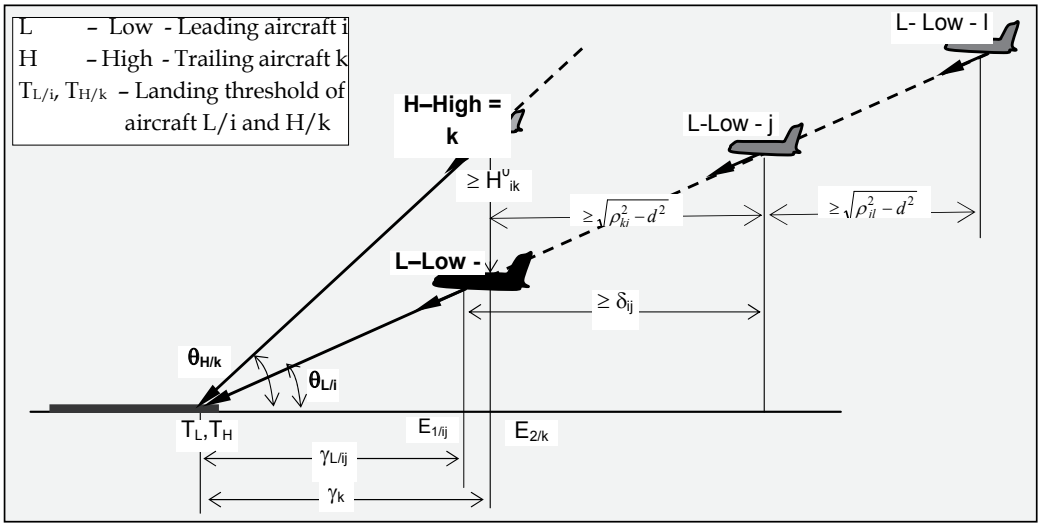

Fig. 5. The geometry of CNAP and SEAP in the vertical plane applied to the closely spaced parallel runways under IMC (Compiled from: Janic, 2008a)

As can be seen, as in Figure 4b, the aircraft *(i)*, as the leading one in the pair (*ik)* and the sequence (*ij*), approaches to the ultimate RWY1. The aircraft *(k)* as the trailing in the pair (*ik)* approaches to the ultimate RWY2 (Janic, 2006). Thus, the pair of aircraft *(ij)* is going to land on RWY1 and the aircraft (*k)* on RWY2. The order of landings on either runway is (*i*, *k*, *j*). This implies that the pair *(ij)* is influenced by the aircraft *(k)*. Another pair *(kl)* in Figure 5 is influenced by the aircraft *(j)*.

3.5.2.2 The minimum inter-arrival times at the "reference location(s)"

The inter-arrival times $_{a}t_{ij/k}$ for particular "strings" of landing aircraft (*ijk)* in Figure 5 are calculated under assumption that each aircraft category can perform both CNAP and SEAP (Janic, 2006, 2008b). Regarding the relative speeds along the final approach trajectories, the aircraft *(ikj)* can relate to each other as either "fast" *F* or "slow" *S*, which gives eight combinations. In the first four, the aircraft (*i)* and (*j)* are considered as either "slow" *S* or "fast" *F*; the aircraft (*k)* is considered as "slow" *S*. The possible combinations of sequences are: *S-S-S*, *S-S-F*, *F-S-S* and *F-S-F*. In other four combinations, the aircraft (*k)* is considered as "fast" *F*. The possible combinations of sequences are: *S-F-S, S-F-F, F-F-S* and *F-F-F*. After selecting the control variable *u*, the attributes "low" *L* and "high" *H* can be additionally attached to each aircraft in each of the above-mentioned landing sequences. One of the principles can be that in any sequence, the "slow" aircraft always performs SEAP (i.e. as "high" *H*) and the "fast" aircraft always performs CNAP (i.e. as "low" *L*). The same applies to the aircraft "string" *(kjl)*. In developing expressions for calculating the minimum inter-arrival times $_{a}t_{ij/k}$ the following notation is used:

$\gamma_{i/j/k}$ is length of the final approach path of the aircraft (*i)* and (*j)* landing on RWY1 and the aircraft (*k)* landing on RWY2, respectively;

d is spacing between centerlines of the closely-spaced parallel runways;

$v_{i/k/j}$ is the final approach speed of the aircraft (*i*), (*k*) and (*j*), respectively;

$\theta_{i/k/j}$ is the GS angle of trajectory of the aircraft (*i*), (*k*) and (*j*), respectively;

δ_{ij} is the ATC minimum longitudinal (in-trail) separation rules applied to the aircraft pair (*ij);*

.

$\rho_{ik/kj}$ is the ATC minimum horizontal-diagonal separation rules applied to the aircraft pairs (*ik)* and (*kj*), respectively;

$H^{0}_{i/k/j}$ is the ATC minimum vertical separation rules applied to the aircraft pairs (*ij*), (*ik)* and (*kj*), respectively;

$u_{ij,}$ $u_{ik,}$ u_{kj} is the control variable taking the value "0" if the ATC longitudinal (in-trail) separation rules between the aircraft pair *(ij)* and the ATC horizontal-diagonal separation rules between the aircraft pair *(ik)* and *(kj)* are applied, respectively, and the value "1", otherwise, i.e. if the ATC vertical separation rules between aircraft in given pairs are applied, respectively.

$u_{kj,}$ $u_{jl,}$ u_{kl} is the control variable taking the value "0" if the ATC longitudinal (in-trail) separation rules between the aircraft *(kl)* and the ATC horizontal-diagonal separation rules between the aircraft pairs *(kj)* and *(jl)* are applied, respectively, and the value "1", otherwise, i.e., if the ATC vertical separation rules between aircraft in given pairs are applied, respectively.

Respecting the approach procedures (CNAP and SEAP) and the associated ATC separation rules for different combinations of aircraft landing sequences, expressions for the minimum times ${}_{a}t_{ij/k}$ are developed as follows (Janic, 2009).

i) <u>*Sequences $v_i \le v_k \le v_j$; Aircraft speed/procedure combination*</u>: *S/H-S/H-S/H, S/H-S/H-F/L, S/H-F/L-F/L, F/L-F/L-F/L*

The aircraft (*i*), (*k*), (*j*) are separated by the ATC minimum separation rules at the moment when the aircraft (*i*) arrives at the landing threshold of RWY1. The inter arrival time ${}_{a}t_{ij/k}$ is determined as follows:

$$ {}_{a}t_{ij/k} = {}_{a}t_{ik} + {}_{a}t_{kj} = \max\left\{\begin{array}{l}(1-u_{ij})\delta_{ij}/v_j + u_{ij}H^{0}_{ij}/v_j \sin\theta_j; \\ \\ (1-u_{ik})(\sqrt{\rho^2_{ik}-d^2}/v_k) + u_{ik}(H^{0}_{ik}/v_k \sin\theta_k) + \\ (1-u_{kj})(\sqrt{\rho^2_{kj}-d^2}/v_j) + u_{kj}(H^{0}_{kj}/v_j \sin\theta_j)\end{array}\right\} \quad (7a) $$

In expression (7a), the aircraft (*i*) and (*k*) perform SEAP ($u_{ik} = 1$) and the aircraft *(j)* performs CNAP, i.e. $u_{ij} = u_{kj} = 0$; in addition $u_{jl} = 1$ if the aircraft (*l*) of the pair (*jl*) is *F/L*, and $u_{jl} = 0$ if it is *S/H*; consequently $u_{kl} = u_{kj} = 0$.

ii) Sequence: $v_i > v_k \geq v_j$: Aircraft speed/procedure combination: *F/L-S/H-S/H*

The aircraft (*ik*) and (*kj*) are separated by the ATC minimum separation rules at the moment when the leading aircraft (*i*) is at FAG of RWY1. The inter arrival time ${}_at_{ij/k}$ is determined as follows:

$$ {}_at_{ij/k} = {}_at_{ik} + {}_at_{kj} = \max \left\{ \begin{array}{l} (1-u_{ij})[\delta_{ij} / v_j + (\gamma_j / v_j - \gamma_i / v_i)] + \\ u_{ij}[H_{ij}^0 / v_j \sin\theta_j + \gamma_i \sin\theta_i (1 / v_j \sin\theta_j - 1 / v_i \sin\theta_i)]; \\ \\ (1-u_{ik})(\sqrt{\rho_{ik}^2 - d^2} / v_k + \gamma_k / v_k - \gamma_i / v_i) + \\ u_{ik}[H_{ik}^0 / v_k \sin\theta_k + \gamma_i \sin\theta_i (1 / v_k \sin\theta_k - 1 / v_i \sin\theta_i)] + \\ (1-u_{kj})(\sqrt{\rho_{kj}^2 - d^2} / v_j + \gamma_j / v_j - \gamma_k / v_k) + \\ u_{kj}[H_{kj}^0 / v_j \sin\theta_j + \gamma_k \sin\theta_k (1 / v_j \sin\theta_j - 1 / v_k \sin\theta_k)] \end{array} \right\} \quad (7b) $$

In expression (7b) the aircraft (*i*) performs CNAP and the aircraft (*k*) and (*j*) perform SEAP, i.e., $u_{ij} = u_{ik} = u_{kj} = 0$; in addition $u_{jl} = 1$ if the aircraft (*l*) is *F/L* and $u_{jl} = 0$ if it is *S/H;* consequently in both cases $u_{kl} = u_{kj}$.

iii) Sequence $v_i > v_k < v_j$: Aircraft speed/procedure combination: *F/L-S/H-F/L*

The aircraft (*ik*) are separated by the ATC minimum separation rules at the moment when the leading aircraft (*i*) is at FAG of RWY1. The aircraft in the pair (*kj*) are separated by the ATC minimum separation rules at the moment when the aircraft (*k*) arrives at the landing threshold of RWY2. The inter arrival time ${}_at_{ij/k}$ is determined as follows:

$$ {}_at_{ij/k} = {}_at_{ik} + {}_at_{kj} = \max \left\{ \begin{array}{l} (1-u_{ij})\delta_{ij} / v_j + u_{ij} H_{ij}^0 / v_j \sin\theta_j; \\ \\ (1-u_{ik})(\sqrt{\rho_{ik}^2 - d^2} / v_k + \gamma_k / v_k - \gamma_i / v_i) + \\ u_{ik}[H_{ik}^0 / v_k \sin\theta_k + \gamma_i \sin\theta_i (1 / v_k \sin\theta_k - 1 / v_i \sin\theta_i)] \\ +(1-u_{kj})(\sqrt{\rho_{kj}^2 - d^2} / v_j) + u_{kj} H_{kj}^0 / v_j \sin\theta_j + \end{array} \right\} \quad (7c) $$

In expression (7c), the aircraft (*i*) and (*j*) perform CNAP and the aircraft (*k*) performs SEAP, i.e., $u_{ij} = u_{kj} = 0$ and $u_{ik} = 1$; in addition $u_{jl} = 1$ if the aircraft (*l*) is *F/L* and $u_{jl} = 0$ if it is *S/H;* consequently in both cases $u_{kl} = u_{kj}$.

iv) Sequences $v_i = v_k > v_j$; Aircraft speed/procedure combination: *F/L-F/L-S/H*

The aircraft (*ik)* are separated by the ATC minimum separation rules at the moment when the aircraft (*i)* is at FAG and further when it arrives at the landing threshold of RWY1. The aircraft (*kj)* are separated by the ATC minimum separation rules at the moment when the aircraft (*k)* is at the final approach gate of RWY2. The inter arrival time ${}_at_{ij/k}$ is determined as follows:

$$ {}_at_{ij/k} = {}_at_{ik} + {}_at_{kj} = \max \begin{Bmatrix} (1-u_{ij})[\delta_{ij}/v_j + (\gamma_j/v_j - \gamma_i/v_i)] + \\ u_{ij}[H^0_{ij}/v_j \sin\theta_j + \gamma_i \sin\theta_i (1/v_j \sin\theta_j - \gamma_i/v_i \sin\theta_i)]; \\ \\ (1-u_{ik})(\sqrt{\rho^2_{ik} - d^2}/v_k) + u_{ik}(H^0_{ik}/v_k \sin\theta_k) + \\ (1-u_{kj})(\sqrt{\rho^2_{kj} - d^2}/v_j + \gamma_j/v_j - \gamma_k/v_k) + \\ u_{kj}[H^0_{kj}/v_j \sin\theta_j + \gamma_k \sin\theta_k (1/v_j \sin\theta_j - 1/v_i \sin\theta_k)] \end{Bmatrix} \quad (7d) $$

In expression (7d), the aircraft (*i)* and (*k)* perform CNAP and the aircraft (*j)* performs SEAP, i.e., $u_{ij} = u_{kj} = 1$ and $u_{ik} = 0$; in addition $u_{jl} = 1$ if the aircraft (*l)* is *F/L* and $u_{jl} = 0$ if it is *S/H;* consequently in both cases $u_{kl} = u_{kj}$.

v) Sequences $v_i < v_k > v_j$; Aircraft speed/procedure combination: *S/H-F/L-S/H*

The aircraft (*ik)* are separated by the ATC minimum separation rules at the moment when the aircraft (*i)* arrives at the landing threshold of RWY1. The aircraft (*kj)* are separated by the ATC minimum separation rules at the moment when the aircraft (*k)* is at the final approach gate of RWY2. The inter arrival time ${}_at_{ij/k}$ is determined as follows:

$$ {}_at_{ij/k} = {}_at_{ik} + {}_at_{kj} = \max \begin{Bmatrix} (1-u_{ij})\delta_{ij}/v_j + u_{ij}H^0_{ij}/v_j \sin\theta_j; \\ \\ (1-u_{ik})(\sqrt{\rho^2_{ik} - d^2}/v_k + u_{ik}(H^0_{ik}/v_k \sin\theta_k) + \\ (1-u_{kj})(\sqrt{\rho^2_{kj} - d^2}/v_j + \gamma_j/v_j - \gamma_k/v_k) + \\ u_{kj}[H^0_{kj}/v_j \sin\theta_j + \gamma_k \sin\theta_k (1/v_j \sin\theta_j - 1/v_i \sin\theta_k)] \end{Bmatrix} \quad (7e) $$

In expression (7e), the aircraft (*i)* and (*j)* perform SEAP and the aircraft (*k)* performs CNAP, i.e., $u_{ij} = u_{kj} = 1$ and $u_{ik} = 0$; in addition $u_{jl} = 1$ if the aircraft (*l)* is *F/L* and $u_{jl} = 0$ if it is *S/H;* consequently in both cases $u_{kl} = u_{kj}$.
Expression 7(a-e) can then be used in combination with expression (3) to calculate the landing capacity of a given pair of the closely-spaced parallel runways from expression (4).

4. An application of the methodology

4.1 Background

The application of the above-mentioned methodology for assessment of the potential of some innovative operational procedures to increasing the airport runway landing capacity is carried out by applying particular models to the generic and the specific airport runway case using the "what-if" scenario approach (Janic, 2006, 2008, 2008a, 2009).

4.2 The ATC time-based separation rules

The model of the "ultimate" capacity of a single runway using the ATC time-based instead of the ATC distance-based separation rules for landing aircraft is applied using the generic input. This relates to the size (i.e. geometry) of the "wake reference airspace", characteristics of the wake vortices of the landing aircraft fleet, behavior of the wake vortices within and around the "wake reference airspace" influenced by the external weather conditions, and the current ATC distance-based separation rules.

4.2.1 Input

4.2.1.1 The size of the "wake reference airspace"

The size of the "wake reference airspace" is determined by using the following input: The length of the common approach path between FAG and the runway landing threshold T in Figure 3 is taken to be similar to that at most airports, i.e. $\gamma = 6\ nm$. Since the aircraft use ILS, the distance from the threshold to the ultimate point of touchdown is assumed to be $\Delta = 0.16nm$, i.e. $300m$. This gives the total distance between FAG and the runway touchdown of $6.16\ nm$. The nominal ILS GS angle is $\theta = 3^0$ with the maximum deviations of about $\pm 0.5^0$. The angle between the axis and each side of the "wake reference airspace" in the horizontal plane is determined by the characteristics of the ILS LLZ (Localizer) and amounts to $\alpha = \pm 1.5^0$. The distance between the ILS Outer Marker (OM) and the landing threshold T is $\beta = 4nm$. Consequently, the "wake reference profiles" along the "wake reference airspace" are calculated depending on the distances and times from the landing threshold and given in Table 2.

Distance/time to the landing threshold (nm)/(s)[1)]	**The size of the profile**	
	y (ft)	**z** (ft)
6/0	2000	600
5/27	1600	500
4/54	1200	400
3/81	950	300
2/108	640	200
0/162	200	50

[1)]*Based on average aircraft speed of 135 kts.*

Table 2. The size of the "wake free profile" depending on distance and time to the landing threshold

4.2.1.2 Characteristics of the aircraft fleet

In this case, the aircraft types are categorized into four categories following Table 1. Their average characteristics, based on the specific values of particular parameters including the calculated wake vortex parameters of particular category, are given in Table 3.

Aircraft category	Mass **M** (10^3kg)	Wing span **B** (m)	Approach speed v (kts)[1)]	Circulation Γ_0 (m/s^2)[2)]	The wake reference time t^* (s)[2)]
Small	20	24	120/90	138/184	16/12
Large	55	30	140/120	260/303	13/12
B757	117	38	170/140	359/436	16/13
Heavy	206	65	170/140	370/449	44/36

[1)] The maximum and the minimum approach speed, respectively, at FAG and the landing threshold T,[2)] The values correspond to the maximum and the minimum approach speed, respectively. Compiled from (NASA 1999, 2001; Donohue and Rutishauser, 2001)

Table 3. Characteristics of the particular aircraft landing categories (the averages)

In addition, the initially generated wake vortices are assumed to decay to the observed typical atmospheric background circulation of $\Gamma^* = 70m^2/s$ over the period $k = 8t^*$ (Donohue and Rutishauser, 2001 Sarpkaya, 2000; Shortle and Jeddi, 2007). The proportion of particular aircraft categories in the aircraft fleet mix is varied parametrically.

4.2.1.3 The external conditions

The external conditions are specified by a constant crosswind of $V_{cw} = 5\ m/s$, which is above the conditions of "no wind" of $V_{cw} \leq 3m/s$. The influence of the headwind $V_{hw}(t)$ is not particularly considered since some preliminary calculations have shown that even a very strong headwind cannot increase the vertical distance between the wake vortex of the leading and the flight path of the trailing aircraft in a shorter time than that obtained by the current ATC distance-based separation rules.

4.2.1.4 The ATC separation rules

The ATC minimum distance-based separation rules in Table 1 are used as the basis for initial setting up the ATC time-based separation rules in combination with the average runway landing occupancy time of $t_{ai} = 60s$ for all aircraft categories.

4.2.2 Results

The results from the model application consist of the following components:

- The strength (i.e. circulation) of wake vortices to which the trailing aircraft are exposed in particular landing sequences if the ATC VFR and IFR in Table 1 are applied;

- The matrix of the standardized time-based separation rules for particular categories of the aircraft landing sequences; and
- The runway landing capacity calculated for the current ATC distance-based VFR and IFR separation rules, and the ATC tiem-based separation rules based on the wake vortex behavior influenced by weather (wind) conditions.

The strength (i.e. circulation) of the wake vortices to which the trailing aircraft in particular landing sequences are potentially exposed when the minimum ATC IFR and VFR are applied is given in Table 4.

ATC VFR				
i/j	**Small**	**Large**	**B757**	**Heavy**
Small	134	134	134	134
Large	207	231	231	231
B757	244	275	305	313
Heavy	317	333	379	379
ATC IFR				
i/j	**Small**	**Large**	**B757**	**Heavy**
Small	17	62	69	69
Large	0	87	101	101
B757	0	70	79	79
Heavy	181	234	261	197

Table 4. The potential circulation $\Gamma(t)$, which the trailing aircraft faces under the ATC VFR and IFR while flying at the given approach speeds (see Table 3)

As can be seen the potential wake vortex strength is higher under VFR than under IFR as could be intuitively expected. In addition, in both cases, for most sequences this circulation is significantly higher than the typical atmospheric circulation of $70 m^2/s$. Furthermore, it should be born in mind that the trailing aircraft of different types in the particular sequences are sensitive differently to the different strength of the wake vortices. Last but not least, the trailing aircraft are not actually exposed to such circulation because the wakes of the leading aircraft sink below their flight paths thanks to their self-induced descent speed simultaneously with their decaying. This again illustrates the fact that the landing aircraft could also be put closer to each other under IMC just as under the VMC without significant risk of the wake vortex hazard, but, of course, only if the corresponding technology for "see and be seen" was available under IMC. In such case, the separation rules under IMC and VMC would be unified as the ATC time-based separation rules. The basis for setting up these rules would be the existing ATC VFR (Table 1) and the typical aircraft approach speeds (Table 3). Table 5 gives an example of such standardized time-based separation rules.

i/j	Small	Large	B757	Heavy
Small	1.0	1.0	1.0	1.0
Large	1.5	1.0	1.0	1.0
B757	2.0	1.3	1.5	1.2
Heavy	2.5	1.5	1.5	1.2

Table 5. The standardized ATC time-based minimum VFR/IFR separation rules $\tau_{ij/min}$ for landing aircraft (min)

The particular values in Table 5 are rounded-up in order to be convenient for practical use. As can be seen, in some landing sequences, the runway landing occupancy times can be used as the minimum separation rule. In addition, as on case of the distance-based rules, these rules are applied depending on the landing sequence at the runway threshold ($v_i \leq v_j$) and, at FAG ($v_i > v_j$).

Using the above-mentioned inputs in Tables 3 and 5, the runway landing capacity is calculated for different cases. Figure 6 shows the dependence of this capacity on the proportion of Heavy aircraft in the fleet, the above-mentioned separation rules, and the wake vortex characteristics and behavior. The proportion of Small and B757 aircraft is kept constant, each of 5%.

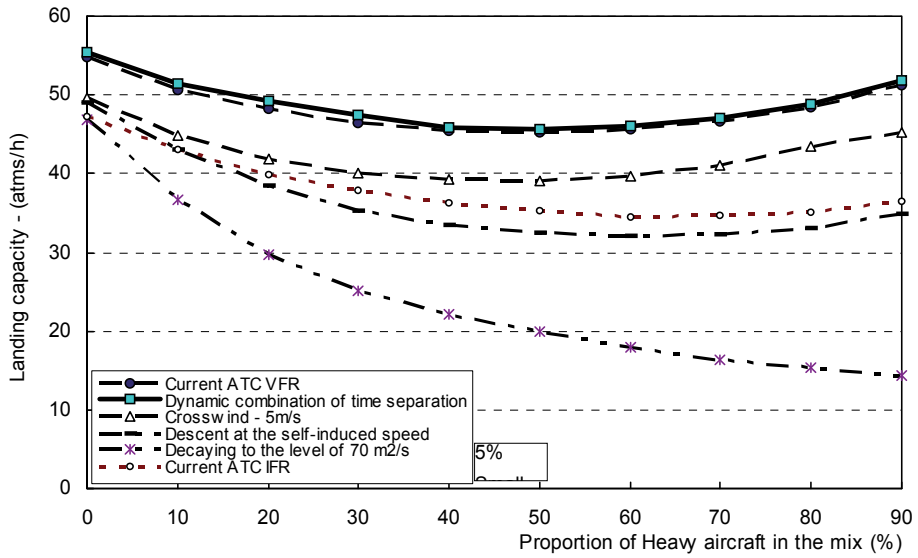

Fig. 6. Dependence of the runway landing capacity on the aircraft fleet mix, the ATC separation rules, and the wake vortex characteristics and behavior

As can be seen, in the case when the ATC time separation rules are based on the wake decaying to the typical atmospheric circulation of 70m²/s, the capacity is the lowest and continuously decreases with increasing the proportion of Heavy aircraft in the mix, as compared with the other cases. The latter is because the stronger wakes of the leading Heavy aircraft need a longer

time to decay to the safe level. In other cases the capacity decreases with increasing of the proportion of Heavy aircraft in the mix up to about 20%, and then increases again. In the former case, the impact of strong wakes behind Heavy aircraft prevails. In the latter case, the higher approach speeds of Heavy aircraft prevail.
In addition, the capacity for the nominal ATC VFR is higher than the capacity for the nominal ATC IFR by about 30% as shown in Figure 2. If the time-based separation rules were applied under the conditions of a crosswind of 5m/s, the capacity would be somewhere in between the current VFR and IFR capacity. This indicates that the capacity gains would be comparable to the IFR capacity if the influence of the crosswind on the wake vortex behavior was taken into account. When the time-based separation rules respecting the wake vortex descent time, were applied the corresponding capacity would be lower than the current IFR capacity. This implies that the current IFR seem to be based only partially on the descent time of the wake vortices below the flight path of the trailing aircraft and not on the time they need to completely move out of the "wake reference airspace".
The dynamically selected ATC time-based separation rules for particular landing sequences combining the current ATC VFR and the ambient factors influencing the wake vortex behavior seem to be able to produce the highest capacity. However, in the given example, this capacity would only be just slightly higher than the capacity obtained under the current ATC VFR. This again suggests that the current ATC VFR could be the basis for setting up the corresponding time-based separation rules, which would be also applicable under both VMC and IMC, thus stabilizing the runway landing capacity with respect to changes of weather.

4.3 The Steeper Approach Procedure (SEAP)

4.3.1 The case of San Francisco international Airport (U.S.)

4.3.1.1 Inputs

The model for estimating the landing capacity of the closely-spaced parallel runways when both CNAP and SEAP are used has been applied to the traffic scenario at San Francisco International Airport (SFO) (U.S.) shown in Figure 7 (Janic, 2008a).

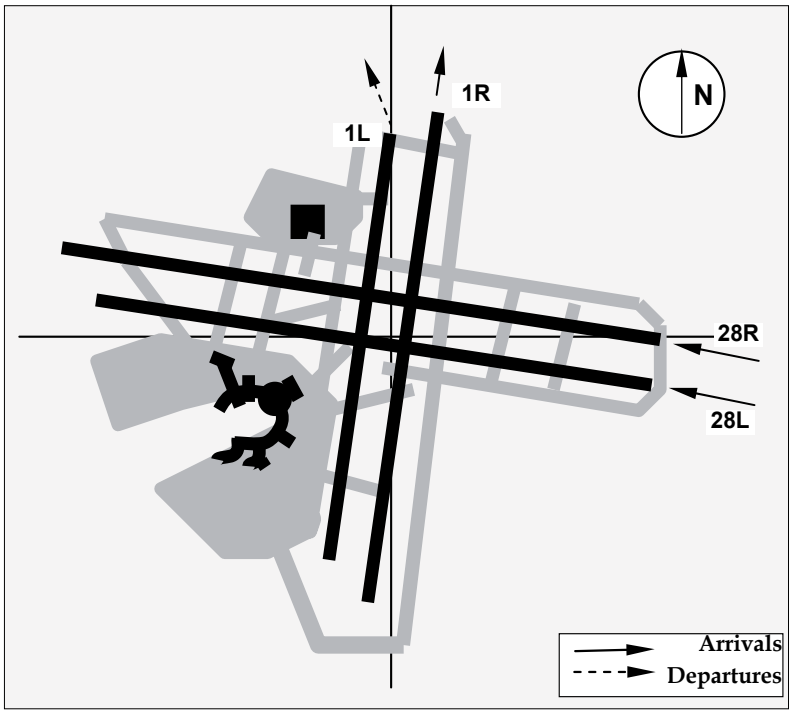

Fig. 7. Simplified layout of the runway system at San Francisco International Airport (SFO) (Compiled from Janic, 2008a)

Currently, the airport operates two pairs of the closely-spaced parallel runways - 1L/R and 28R/L. Dimensions of runways 1L/28R are 11879x200ft (3618x61m). Dimensions of the runways 1R/28L are 10602x200ft (3231x61m). Each pair of runways is spaced for 750 ft (i.e., 228.75m), which is sufficient for simultaneous arrivals and departures under VMC but not under IMC (FAA, 2006). Under preferable VMC the runways 28R/L are used for paired arrivals and the runways 1L/R for paired departures as shown in Figure 7. In dependence on the mixture of arrivals and departures, the paired departures can be realized between the successive pairs of arrivals. When the weather deteriorates due the specified minima in Figure 1 each pair of runways is used as the single runway for both arrivals and departures (West Plan for Runways 28R/L and Southeast Plan for Runways 1L/R). Such bad weather prevails on average for about 20% of time during the year (Cotton et al., 20011). In addition to geometry of runways, the additional inputs for the model are as follows: The arrivals are realized on the runways 28R/L or 1L/R with the length of final approach path, i.e., the distance between FAG and landing threshold(s), $E_{L/1}$ and $E_{H/2}$ and the runway thresholds $T_{L/1}$ and $T_{H/2}$ of $\gamma_{H/1} = \gamma_{L/2} = 12$ *nm* (see Figure 5). If the standard GS angle $\theta_l = 3^0$ is used the aircraft altitude at the gate $E_{1/2}$ will be 4000 ft; if the steeper GS angle $\theta_H = 5.5^0$ is used, this altitude will be about 7000 ft. The difference is greater than the ATC minimum vertical separation rules (1000ft) thus enabling safe pairing of aircraft of particular wake vortex/speed combinations approximately above each other at the entry gates $E_{L/1}$ and $E_{H/2}$, respectively (FAA, 2006).
The aircraft fleet in terms of the weight and wake vortex categories is as follows: Small (7%). Large (52%), B757 (19%), and Heavy (22%). The average approach speeds of particular aircraft categories are as follows: Small 120kts, Large 130kts, B757 140kts, and Heavy 150kts. The

average runway landing occupancy time is 40s for Small and 50s for Large, B757 and Heavy. The average departure runway occupancy time is 30s for Small, and 40s for Large, B757 and Heavy aircraft categories (LMI, 2004).
The ATC is supposed to apply the minimum longitudinal and horizontal-diagonal radar-based separation rules between arriving aircraft similarly as given in Table 1. The radar-based minimum horizontal-diagonal separation rules are: $\rho = 2.5nm$. The minimum vertical separation rules are: $H = 1000ft$. The separation between the arrival and departure on the same runway is ${}_{d}\delta_{(.)} = 2nm$ (FAA, 2006; NASA, 1998).
Assignment of the approach procedures (CNAP or SEAP) to particular aircraft categories is carried out according to the two hypothetical scenarios: Scenario 1 implies that only Small aircraft can perform SEAP. Scenario 2 implies that Small, Large and B757 aircraft can perform SEAP. In both Scenarios Heavy aircraft do not perform SEAP. Comparing to the present situation the former Scenario looks more realistic than the latter.

4.3.1.2 Results

Using the above-mentioned inputs has enabled calculation of the "ultimate" landing capacity of the closely-spaced parallel runways for eth case airport - SFO. In addition, the "ultimate" capacities for take-offs and mixed operations are calculated in order synthesize the capacity coverage curve(s). The results are shown in Figure 8.

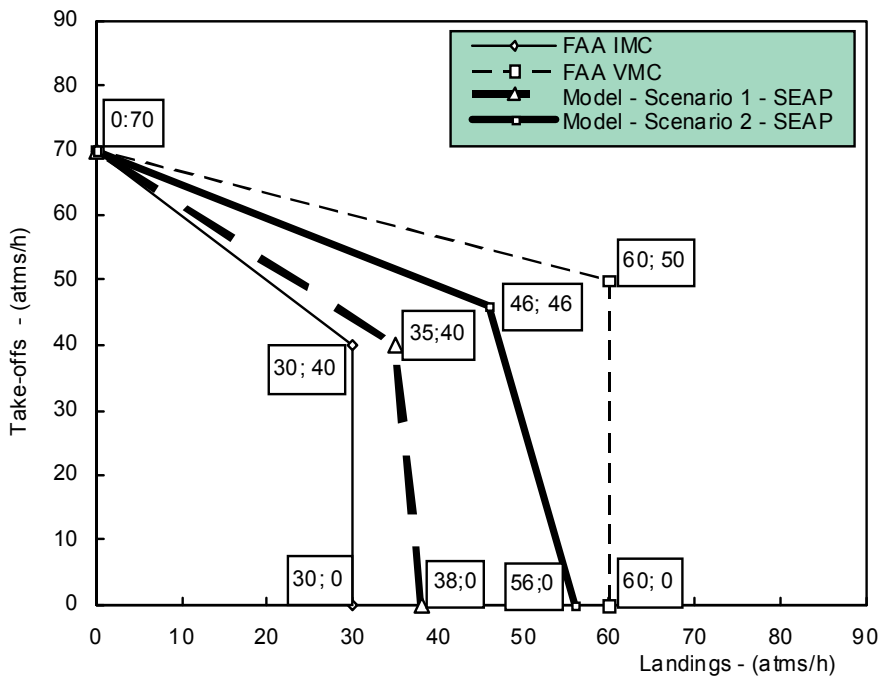

Fig. 8. The capacity of San Francisco International Airport achieved by different approach procedures (Compiled from Janic, 2008a)

The VMC and IMC capacity curves for the current situation are synthesized from the FAA airport capacity benchmark calculations (FAA, 2004a). As can be seen, according to Scenario 1 in which only Small aircraft performed SEAP, the arrival capacity would be 38 arr/h, the mixed capacity 35 arr/h and 35 dep/h, and the departure capacity 70 dep/h. This is higher than the corresponding current benchmarking capacities for about 27%, 17/5% and 0%, respectively. According to Scenario 2 when all except Heavy aircraft performed SEAP, the arrival capacity would be 56 arr/h, the mixed capacity 46 arr/h and 46 dep/h, and the departure capacity 70 dep/h. These are for about 83%, 53%/13%, and 0%, respectively, higher than the current corresponding IMC capacities when CNAP is performed. As well, these capacities are for about 7%, 30/9%, and 0% lower than the current corresponding VMC capacities, respectively. This indicates that in given case, the SEAP could have the potential to rather substantively increase the "ultimate" (landing) capacity of the given system of closely-spaced parallel runways under IMC and IFR (FAA, 2004a; Janic, 2008a).

5. Conclusions

This Chapter has presented the potential of some innovative procedures for increasing the airport runway landing capacity. These have included: i) the ATC tine-based separation rules between landing aircraft on a single runway and ii) the SEAP (Steeper Approach Procedure) to the closely-spaced parallel runways. The methodology consisting of the dedicated models of the "ultimate" runway capacity under the above-mentioned conditions has been developed and applied.

In particular, the model of the landing capacity based on the ATC time-based separation rules has been applied to a busy landing runway with the given geometry of the "wake reference airspace" serving the four aircraft FAA/ICAO categories. These have been characterized by the wake vortex parameters (the approach speed, the wing span, and weight), and the runway landing occupancy time under given atmospheric (crosswind) conditions. The results have indicated that the ATC time-based separation rules, based exclusively on the wake vortices decaying to the typical atmospheric circulation, have produced the lowest runway landing capacity. The dynamically selected ATC time-based separation rules based on the current ATC VFR and the influence of the crosswind on the wake vortices have produced the highest runway landing capacity. The ATC time separations based on the wake vortex self-induced descent speed have produced a landing capacity slightly lower than the capacity achieved under the current ATC IFR. Finally, the ATC time-based separation rules based on the impact of the crosswind on the wake vortices have produced a capacity, which is somewhere between the capacities achieved under the current distance-based VFR and the IFR. In all cases, the landing capacity has generally decreased with increasing of the heterogeneity of the aircraft fleet mix and particularly with increasing of the proportion of Heavy aircraft in the fleet mix.

The model for the landing capacity of the closely-spaced parallel runways when both CNAP (Conventional Approach Procedure) and SEAP (Steeper Approach Procedure) are simultaneously used has been applied to the traffic scenario of San Francisco International (SFO) airport (US). The results have indicated that SEAP as compared to CNAP has possessed the potential for increasing the IMC landing capacity of given parallel runways for about 27% when only the small aircraft could perform SEAP, and for about 83% when all except Heavy aircraft could perform SEAP. Consequently a gap between the current VMC and IMC landing capacity could be narrowed to about 7%.

In general, the SEAP has shown advantages in comparison to the current CNAP as follows: i) significant increase in the IMC runway landing capacity; ii) substantive filling in existing gap between VMC and IMC landing capacity; and iii) diminished sensitivity of the landing capacity to the weather conditions, thus making the airport and airline operations more reliable and predictable.

6. References

Andreatta, G., Romanin-Jacur, G., (1987), "Aircraft Flow Management under Congestion", Transportation Science, Vol. 21, No. 4, 249-253

Bianco, L. Bielli, M., (1992), "Air Traffic Management: Optimization Models and Algorithms", Journal of Advanced Transportation, Vol. 26, No. 2, 1992, 131-167

Blumstein, A., (1959), "The Landing Capacity of a Runway", Operations Research, Vol. 7, No.1, 1959, pp. 752-763

Burnham, D. C., Hallock, J. N., Greene, G. C., (2002), "Wake Turbulence Limits on Paired Approaches to Parallel Runways", Journal of Aircraft, Vol. 39, No. 4, pp 630-637

Choroba, P., (2003), "A Vision of Wake Vortex Research for Next 20 Years", Working paper, EUROCONTROL, Bretigny sur de Orge, Paris, France

Cotton, W., Foggin, J., Gosling, G. D., (2001), Potential Future Contribution of Air Traffic Management Technology to the Capacity of San Francisco International Airport, Report on the Independent Technology Panel, Federal Aviation Administration EIR/EIS–Emerging & New Technologies, San Francisco, California, USA

CRS, (2007), Aviation Congestion and Delay: System-Wide and New York Area Issues, CRS Report for Congress, Congressional Research Service, RL 34284, Washington DC, USA

Czerny, A. I., Forsyth, P., Gillen, D., Niemeier, H. M., (2008), Airport Slots: International Experiences and Options for Reform, Ashgate Publishing Limited, Aldershot, UK

Donohue, G. L., (1999), "A Simplified Air Transportation Capacity Model", Journal of ATC, April-June, pp. 8-15

Donohue, G. L., Rutishauser, D. K., (2001) "The Effect of Aircraft Wake Vortex Separation on Air Transportation Capacity", 4th FAA/Eurocontrol R&D Conference, Santa Fe, new Mexico, USA

Donahue, G. L., Shorttle, J., Jeddi, B., (2008), "Looking for the Capacity in NGATS", on Transportation Research Board (TRB) Annual Meeting, January 14, Washington DC, USA

EEC, (2005), Optimal Procedures and Techniques for the Improvement of Approach and Landing – OPTIMA, Sixth Framework Program, FP6-2002-Aero 1502880, Deliverable 1.2, European commission, Brussels, Belgium

FAA, (2004), Summary Results from Long-Term Wake Turbulence Measurement at San Francisco International Airport, U.S. Department of Transportation, Federal Aviation Administration, DOT-VNTSC-FA27-PM-04-13, Washington, DC, USA

FAA, (2004a), Airport Capacity Benchmark Report, Federal Aviation Administration, U.S. Department of Transportation, The MITRE Corporation, Washington DC, USA,

FAA, (2006), Aeronautical Information Manual: Official Guide to Basic Flight Information and ATC Procedures", Federal Aviation Administration, Washington D. C., USA

Fraport, (2004), EDDF-SOP – Standard Operating Manual- Frankfurt Main Airport, Virtual Frankfurt Airport SOP V9.6, http://www.vacc-sag.org, Accessed April 15, 2004

Gilbo, E. P., (1993), "Airport Capacity: Representation Estimation, Optimization", IEEE Transactions on Control System Technology, Vol. 1, No. 3, 1993, pp. 144-153

Hammer, J., (2000), "A Case Study of Paired Approach Procedure to Closely Spaced Parallel Runways", Air Traffic Control Quarterly, Vol. 8, No. 3, 2000, pp. 223-252

Harris, R. M., (1972), Models for Runway Capacity Analysis, The MITRE Corporation Technical Report, MTR-4102, Rev. 2, Langley, Virginia, USA

Hockaday, S. L. M., Kanafani, A., (1974), "Development in Airport Capacity Analysis", Transportation Research, Vol. 8, No. 3, 171-180

ICAO, (1996), Rules of the air and air Traffic Services: Procedures for Air Navigation Services, Doc. 4444 –RAC/501, 13-th Edition, International Civil Aviation Organization. Montreal, Canada

Ignaccolo, M., (2003), "A Simulation Model for Airport Capacity and Delay Analysis", Transportation Planning and Technology, Vol. 26, No. 2, pp. 135-170

Janic, M., Tosic, V., (1982), "Terminal Airspace Capacity Model", Transportation Research, Vol. 16A, No. 4, pp. 253-260

Janic, M., (2001), Air Transport System Analysis and Modeling: Capacity, Quality of Service and Economics, Transport Series Books Vol. 16, Taylor and Francis, UK

Janic, M., (2006), "Model of Ultimate Capacity of Dual-Dependent Parallel Runways", Transportation Research Record 1951, pp. 76-85

Janic, M, (2008), "A Model of Runway Landing Capacity Based on the ATC Time-Based Separation Rules", Transportation Research Record (TRB), No. 2052 Aviation, pp. 79-89

Janic, M., (2008a), "Modelling the Capacity of Closely-Spaced Parallel Runways Using Innovative Approach Procedures, Transportation Research C, Vol. 16, No. 6, pp. 704-730

LMI, (2004), "Business Case for NASA Wake Vortex Technology", Power-Point

Presentation, Logistics Management Institute, Governmental Consulting, Washington D.C., USA

Newell, G. F., (1979), "Airport Capacity and Delays", Transportation Science, Vol. 13, No. 3, pp. 201-241

NASA, (1998), Air Traffic and Operational Data on Selected U.S. Airports With Parallel Runways, National Aeronautic and Space Administration, NASA/CR-1998-207675, Langley, Virginia, USA

NASA, (1999), Benefit Estimates of Terminal Area Productivity Program Technologies, NASA/CR – 1999 208989, National Aeronautics and Space Administration, Virginia, USA

NASA, (2001), Enhancement Airport Capacity through Safe Dynamic Reduction of Aircraft Separation: NASA's Aircraft Vortex Spacing System (AVOSS), National Aeronautical and Space Administration, Hampton, Virginia. USA.

ONERA/DOTA, (2005), WV Separation Technology Case: Preparation of Wake Detection Technology Case, EUROCONTROL EEC TRSC42/2004, Public Summary Report Version 1.1, Palaiseau, Cedex, France

Odoni, A. R., Bowman, J., (1997), Existing and Required Modelling Capabilities for Evaluating ATM Systems and Concepts, Final Report No. NAG2-997, International Centre for Air Transportation, Massachusetts Institute of Technology, Massachusetts, Boston, USA

Richetta, O., Odoni, A. R. (1993), "Solving Optimally the Static Ground Holding Policy Problem in Air Traffic Control", Transportation Science, Vol. 27, No. 3, 1993, pp. 228-238

Richetta, O., Odoni, A. R., (1994), "Dynamic Solution to the Ground –holding Problem in air Traffic Control", Transportation Research A, Vol. 28A, No. 3, pp. 167-185

Richetta, O., (1995), "Optimal Algorithms and a Remarkable Efficient Heuristic for the Ground Holding Problem in Air Traffic Control", Operations Research, Vol. 43, No. 5, pp. 758-770

Robinson III, J. E., Davis, T. J., Isaacson, D. R., (1997), "Fuzzy Reasoning Based Sequencing of Arrival Aircraft in the Terminal Area", The American Institute of Aeronautics and Astronautics (AIAA) Guidance, Navigation, and Control Conference, New Orleans, USA, p. 11, 1997

Sarpkaya, T, (2000), "New Model for Vortex Decay in the Atmosphere", Journal of Aircraft, Vol. 37, No. 1, pp. 53-61

Shortle, J. F., Jeddi, B. G., (2007), "Probabilistic Analysis of Wake Vortex Hazards for Landing Aircraft Using Multilateration Data, 86th TRB Conference, Transportation Research Board, Washington D.C., USA

Swedish, W. J/. (1981), Upgraded Airfield Capacity Model, The MITRE Corporation Technical Report, MTR-81W16, Vols 1 and 2, Langley, Virginia, USA

TC, (2004), Approval of Steep Approach Landing Capability of Transport Category Aircraft, Aircraft Certification, Civil Aviation, Transport Canada

Terrab, M., Odoni, A. R. (1993), "Strategic Flow Management in Air Traffic Control", Operations Research, Vol. 41, No. 1, pp. 138-152

Winckelmans, G., Desenfans, D., (2006), "Probabilistic Prediction of Wake Position and Strength", Specialist's Report – Final Part II, Research Needs, WakeNet2, Europe

Wu Cheng-Lung, Caves R., (2002), "Research Review of Air Traffic Management." Transport Reviews, Vol. 22, No. 1, pp. 115-132

5

Time-based Spaced Continuous Descent Approaches in busy Terminal Manoeuvring Areas

L. K. Meijer[1], N. de Gelder[1], M. M. van Paassen[2] and M. Mulder[2]
[1]*Training, Human Factors and Cockpit Operations*
Air Transport Division
National Aerospace Laboratory
The Netherlands
[2]*Control and Simulation Division*
Faculty of Aerospace Engineering
Delft University of Technology
The Netherlands

1. Introduction

Mitigation of aircraft noise for approaching aircraft is an area where considerable improvements are still possible through the introduction of noise abatement procedures, such as the Continuous Descent Approach (CDA) (Erkelens, 2000). One of the main issues when implementing CDAs is their negative effect on runway throughput, especially during busy operations in daytime. A reduction in landing time intervals might be achieved through precise inter arrival spacing. The combination of aircraft performing the CDA controlled by precise spacing algorithms is seen as one of the solutions to safely increase runway throughput, reduce delay times for arriving aircraft, and reducing fuel burn, emissions and noise impact (De Gaay Fortman et al., 2007; De Leege et al., 2009; De Prins et al., 2007).
The main algorithms used in these researches are all based on the Flap/Gear Scheduler (*FGS*) developed by Koeslag (2001) and improved by In 't Veld et al. (2009). The *FGS* is evaluated in these researches to investigate the effects of different flight path angles, different types of aircraft, different aircraft weight configurations and different wind conditions on *FGS* performance. The *FGS* is also combined with time and distance based spacing algorithms to ensure proper spacing between aircraft in arrival streams.
There are more spacing algorithms developed to control the Time-based Spaced CDA (TSCDA), such as the Thrust Controller (*TC*) by De Muynck et al. (2008) and the Speed Constraint Deviation controller (*SCD*), both developed at the National Aerospace Laboratory (NLR). The performances of these three controllers are evaluated in this chapter. Fast-time Monte Carlo Simulations (MCS) are performed using a realistic simulation environment and a realistic scenario. The effects of different wind conditions, aircraft weight configuration, arrival stream setup and the position of the aircraft in the arrival stream on the performance of the controllers are also evaluated.
In Section 2 the definition of the TSCDA is elaborated by discussing the goals of this concept and by giving the description of the approach used in this research. In Section 3 the working principles of the controllers are discussed. The results of the initial simulations performed to prove the working principles and to investigate the performance of the controllers in nominal conditions are also evaluated here. The experiment is described in Section 4, by discussing the independent variables and the simulation disturbances. The hypotheses of this research are

also given. The results of the MCS are listed in Section 5. The hypotheses are compared with the results and discussed in Section 6. The chapter ends with conclusions and recommendations.

2. Time-based Spaced Continuous Descent Approaches

2.1 Requirements

To perform the evaluation of the controllers thoroughly, first the main requirements for the controllers are elaborated. The origins of these requirements follow from the main purposes of the TSCDA controllers, reduce fuel, reduce noise and maintain the throughput at the Runway Threshold (RWT):

- The algorithms should strive for a minimisation of noise and emissions produced by approaching aircraft in the Terminal Manoeuvring Area (TMA). The amount of noise at ground level is mainly determined by the altitude, thrust setting and configuration of passing aircraft. Reducing noise can thus be achieved by delaying the descent as much as possible (steep and continuous descent), by choosing "idle" thrust-setting and maintaining the cleanest configuration as long as possible. The CDA developed by Koeslag (2001) is based on this criterion.
- The algorithm should strive for a maximum throughput at the runway threshold. Maximum throughput at the RWT can be achieved by reducing the variability of the time space between landing aircraft. The minimum separation criteria are defined by the wake-vortex criteria which are set by the weight class of the landing aircraft.
- To avoid the development of an expensive concept, an integration of the algorithm in today's or near future's Air Traffic Management (ATM) systems should be easily possible without major changes in those ATM systems. Therefore, the assumption that other systems must be adapted to make use of the new algorithms should be avoided as much as possible. An implication of this requirement is that the aircraft should perform their approaches, while knowing as little as possible about the other aircraft in the arriving stream.
- The algorithm must be easily accepted by all who are involved. Pilots and Air Traffic Control (ATC) must be willing to use this new technique. The consequence of this requirement is for example that the algorithms should work properly with speed limitations set by ATC to improve the predictability of the aircraft movements in the TMA.
- The maximum possible difference between the slowest and fastest CDA at a certain moment in the approach is indicated by the *control space*. The last requirement is that this control space for each aircraft in the arrival stream should be as high as possible. The control of each aircraft should then be independent on the behaviour of other aircraft in the arrival stream and thus the need of knowing information about the other aircraft should again be limited as much as possible.

To meet the requirements related to noise and emissions, aircraft should perform a CDA in the TMA. The other requirements demand a simple and efficient algorithm that ensures proper spacing between aircraft in the arrival stream, which can easily be implemented in today's aircraft and ATC systems.

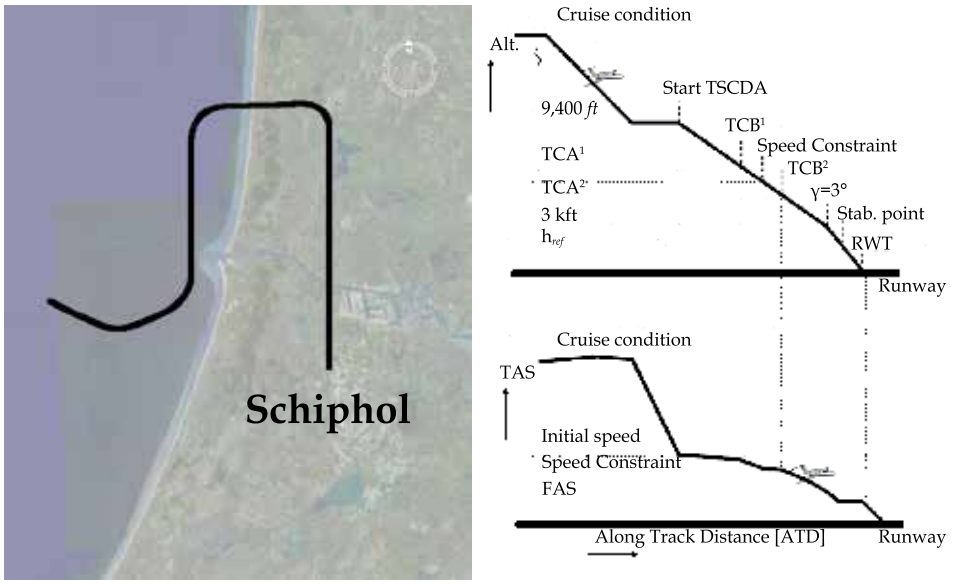

(a) Lateral path (b) Vertical path and speed profile

Fig. 1. Schematic presentation of the flight path. Characteristics according to Table 1 are based on (Meijer, 2008, A-3). In this illustration only one speed constraint is active.

2.2 Approach description

The CDA procedure used in this research is based on the same procedure as used in the *OPTIMAL* project (De Muynck et al., 2008). The characteristics of the approach are given in Table 1 and the schematic presentation of the approach is given in Figure 1.

2.2.1 Start altitude

The start altitude of the CDA is in this research set at 9,400 ft. The largest part of the noise is produced by aircraft flying below 10,000 ft. Therefore this research focuses on the last part of the descent from cruise altitude. The airspace below 10,000 ft is very crowded and it is worth to invest possible spacing issues. Merging aircraft into an arrival stream is another issue in the descent between cruise altitude and 10,000 ft, it is considered outside the scope of this research however.

2.2.2 Reference altitude

The Reference Altitude (h_{ref}) is the point where aircraft must be stabilised, in this scenario it is set at 1,000 ft. Stabilised means that the aircraft speed is equal to the Final Approach Speed (FAS), and the aircraft is in landing configuration, i.e., flaps and slats at maximum angle and gear down.

3. Algorithms

The algorithms used in this research are elaborated, first stating the main principle of time-based spacing CDAs, yielding the TSCDA. Then the three controllers are elaborated by discussing the basic principles and showing results of some initial simulations. These initial

Start altitude	9,400 ft
Initial speed	240 kts IAS
h_{ref}	1,000 ft
Speed constraint	250 kts IAS for $h < 10{,}000$ ft 220 kts IAS for $h < 5{,}500$ ft 180 kts IAS for $h < 3{,}400$ ft 160 kts IAS for $h < 1.500$ ft
Vertical path	$\gamma = 2^\circ$ for $h > 3{,}000$ ft $\gamma = 3^\circ$ for $h < 3{,}000$ ft
Lateral path	according to path illustrated in Figure 1(a)
End of simulation	at the RWT which is 50 ft above the begin of the runway 18R Schiphol airport

Table 1. Scenario characteristics.

simulations are performed for one type of aircraft, the Airbus A330-200, using a high-fidelity model.

3.1 Main principle

3.1.1 Required Time of Arrival

The combination of TBS with the CDA is based on a dynamically calculated Required Time of Arrival (RTA). During the TSCDA the Estimated Time of Arrival (ETA) is calculated by the Flight Management System (FMS) using the Trajectory Predictor (TP). It is assumed that this ETA can be send to the following aircraft in the arrival stream using ADS-B. The following aircraft in the arrival stream uses this ETA to calculate its RTA. Using:

$$RTA = ETA_{lead} + T_{space}, \tag{1}$$

where T_{space} is the required spacing interval between aircraft pairs in the arrival stream at the RWT, assumed to be 120 s (*Website: Single European Sky ATM Research [SESAR]*, n.d.).

3.1.2 Trajectory predictor

The ETA is calculated by the TP of the FMS. In this research the NLR's Research FMS (RFMS) is used, see (Meijer, 2008, A-1-2). The TP uses the actual state of the aircraft, the flight plan stored in the RFMS and a simplified aircraft model to integrate the trajectory backwards from the end situation, which is zero altitude at the runway, to the actual state of the aircraft.
The output of the TP is the speed profile, altitude profile, the lateral profile, thrust profile and configuration profile. It is used for guidance purposes of the aircraft and also to control the aircraft performing the TSCDA. Using the speed, altitude and lateral profiles the ETA is calculated. This ETA is then corrected for the difference in actual position and predicted position of the aircraft. This means that the ETA is dependent on the calculation of the trajectory profiles and the actual state of the aircraft. So even if the TP is not triggered to calculate a new prediction, the ETA is updated during the approach.

3.1.3 Time-based spacing

Using the calculated RTA and the ETA calculated by the TP the spacing error (T_{err}) can be calculated:

$$T_{err} = RTA - ETA \tag{2}$$

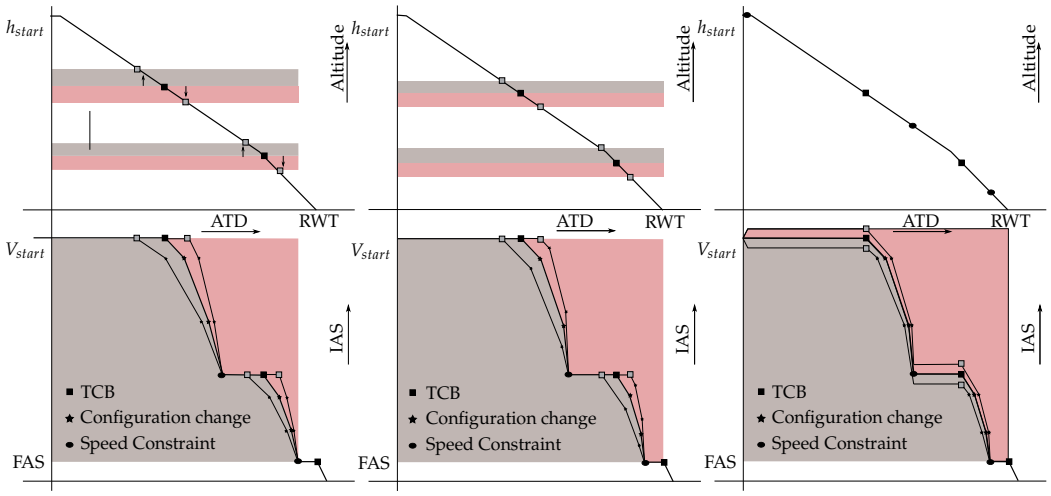

(a) Thrust Controller (*TC*) (b) Flap/Gear Scheduler (*FGS*) (c) Speed Constraint Deviation controller (*SCD*)

Fig. 2. Schematic illustrations of the principles of the three TSCDA-controllers.

Every second during the approach T_{err} is calculated. If $|T_{err}| > 1.5$ s then the controllers are triggered to control the approach and the TP is triggered to calculate the profiles because the controllers changed the approach with respect to the speed, thrust and configuration profiles. The objective is to control the aircraft during the TSCDA so that T_{err} is zero at the RWT. Three different controllers have been evaluated: the *TC*, the *FGS* and the *SCD*, which are able to control the average airspeed during the TSCDA. If $T_{err} > 0$ then $RTA > ETA$ and the aircraft will arrive earlier than required at the RWT, the aircraft must fly the TSCDA at a lower average speed than the nominal situation. It must perform the TSCDA at a higher average speed in case $ETA > RTA$, see Figures 2(a), 2(b) and 2(c).

3.2 TSCDA controllers

3.2.1 Thrust Controller (*TC*)

3.2.1.1 Principle

The standard speed profile shown in Figure 1 indicates that the TSCDA can be divided in several parts. Due to the presence of speed constraints there are three parts where the aircraft decelerates to a new speed constraint and a fourth part where the aircraft decelerates to the Final Approach Speed (FAS). The noise reduction requirement demands idle thrust at these deceleration parts of the approach. These small differences in added thrust compared to idle thrust during the deceleration parts of the approach can have a negative effect on the produced noise and emissions. However, these differences in added thrust can be used to control the aircraft ETA, required to maintain the throughput at the RWT.

Now consider a nominal thrust setting of $N_{nominal} = N_{idle} + 10\%$ then $N_{min} = N_{nominal} - 10\% = N_{idle}$ and $N_{max} = N_{nominal} + 10\%$. The difference in the amount of thrust added can be used to control the average speed indirectly during deceleration and therefore can control the ETA and thus the spacing error T_{err}, see Figure 2(a). The *TC* uses the calculated T_{err} as input and it decides to increase or decrease the thrust for the decelerating parts of the TSCDA. This

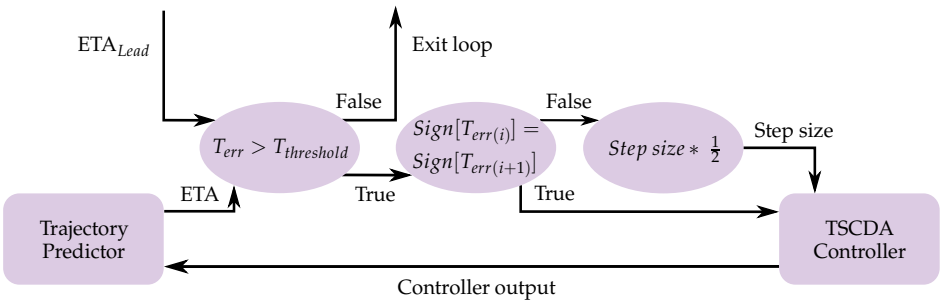

Fig. 3. Illustration of the main loop used by the TSCDA controllers. Stabilisation is derived using the reduction of the step size, each time the value of T_{err} crosses zero, where $T_{threshold}$ is set to 1.5 s.

Altitude [ft]	0	1,000	7,000	10,000	20,000	30,000	40,000	50,000
Speed [kts]	20	25	40	50	60	70	80	80
Direction [deg]	210	220	240	240	240	240	240	240

Table 2. Wind speeds, South West (SW) used in this research.

new thrust setting will be used by the TP to calculate the new speed profile for the rest of the TSCDA. This will be done until T_{err} <1 s or $N_{calc} = N_{min}$ or $N_{calc} = N_{max}$. This principle has been implemented in the RFMS and has been used in the *OPTIMAL* project (De Muynck et al., 2008), where it was investigated whether this method can be used to control the ETA while performing a TSCDA. An illustration of the main algorithm is given in Figure 3. This principle can only be used if the FMS is capable of giving any required N_1-command to control thrust instead of the normally used speed commands for this phase of flight. The NLR's RFMS in combination with NLR's *GRACE* based aircraft model is able to do that.

3.2.1.2 Initial simulations

Initial simulations have been performed to prove the working of the controller. These simulations are performed using the simulation environment described in (Meijer, 2008, A). The scenario as described in Table 1 has been simulated in combination with two wind conditions and two different weight configurations of the Airbus A330-200, see Table 3. For these four conditions the controller has been triggered to perform the slowest, nominal and longest TSCDA possible. The results of the initial simulation (no wind and lightweight configuration) are given in Figures 4(a) and 4(b) and Table 4. With these results the working of the *TC* is proven. The difference between the speed profiles given in Figure 4(a), indicates that the *TC* enables a control space to slow down or speed up the TSCDA. The *TC* shows a better performance in slowing down the TSCDA than in speeding up the approach, Table 4. Figure 4(b)

parameter	research ID	mass · 1,000 kg
Light Weight (75% MLW)	LW	135.2
Heavy Weight (92% MLW)	HW	165.2

Table 3. Airbus A330-200 mass specification as percentage of the Maximum Landing Weight (MLW).

wind	mass	T_{nom}	T_{max}	$\Delta+$	T_{min}	$\Delta-$
Zero	HW	666.1	738.0	71.9	656.0	-10.1
SW	HW	671.1	760.9	96.9	664.0	-7.1
Zero	LW	697.1	801.1	104.0	671.9	-25.2
SW	LW	699.0	761.1	62.1	678.0	-21.0

Table 4. Method: *TC*, TSCDA duration in seconds.

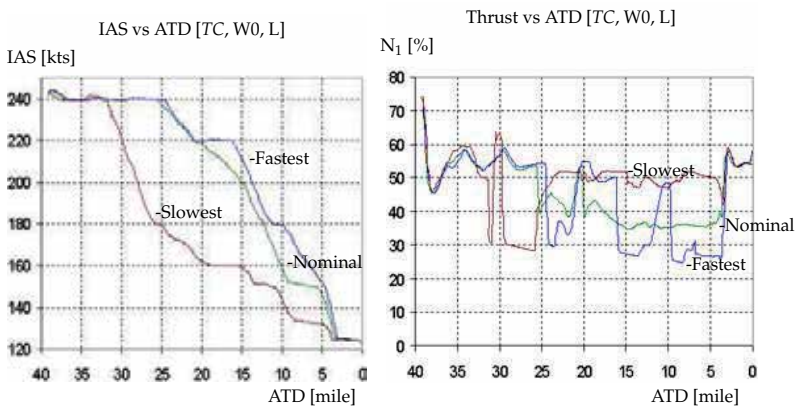

(a) *TC* Speed profile (b) *TC* Output profile

Fig. 4. *TC*, one of the initial simulations of the basic scenario (zero Wind and LW).

shows an earlier Thrust Cutback (TCB) when performing a slow approach. The decelerating parts of the TSCDA are at a higher than nominal thrust setting, which results in a smaller deceleration possible and resulting in a lower average speed and therefore a longer duration of the approach. Table 4 shows the difference in TSCDA duration between heavyweight and lightweight aircraft. The FAS is lower for the LW configuration and this lower speed results in a lower average approach speed and thus in a longer duration of the TSCDA. A longer nominal duration of the TSCDA yields a larger control margin.

3.2.2 Flap/Gear scheduler (*FGS*)

3.2.2.1 Principle

In the *FGS* (In 't Veld et al., 2009; Koeslag, 2001) the basic principle of controlling the ETA is based on optimising the moments of drag increase. Increasing the drag by selecting a next flap position or by deployment of the gear and holding the thrust constant at idle level decreases the speed of the aircraft. As for the other methods, this method uses the T_{err} as input. It calculates the next configuration speed till $T_{err} < 1s$ or $V_{config(i)} = V_{min(i)}$ or $V_{config(i)} = V_{max(i)}$. $V_{min(i)}$ and $V_{max(i)}$ according to Table 5.

3.2.2.2 Initial simulations

The same simulations have been performed with the *FGS* as those performed with the *TC* controller. Looking at the distances between the nominal, fast and slow graphs displayed in Figure 5(a) there is a small margin between the lines, this means a little control margin to control the duration of the TSCDA. This can also be seen in Table 6. Only a few seconds

	Condition:	FULL	3	GEAR	2	1	0
HW	$V_{FlapNom}$	152.2	167.0	167.0	174.4	209.3	-
	$V_{FlapMin}$	136.0	149.0	155.0	158.0	195.0	-
	$V_{FlapMax}$	179.0	185.0	195.0	204.0	235.0	-
LW	$V_{FlapNom}$	138.0	145.0	150.0	177.0	195.0	-
	$V_{FlapMin}$	130.0	140.0	150.0	160.0	170.0	-
	$V_{FlapMax}$	177.0	185.0	190.0	200.0	230.0	-

Table 5. Configuration speeds of the Airbus A330-200 [kts IAS], for HW and LW weight configurations.

wind	mass	T_{nom}	T_{max}	$\Delta+$	T_{min}	$\Delta-$
Zero	HW	657.0	658.2	1.2	655.0	-2.0
SW	HW	666.0	668.0	2.0	661.2	-4.8
Zero	LW	676.0	685.1	9.1	668.0	-8.0
SW	LW	682.1	694.0	11.9	674.0	-8.1

Table 6. Method: *FGS*, TSCDA duration in seconds.

of control margin is available. The lightweight configuration has a positive influence on the control margin, however it is still not the result which was expected by earlier researches (De Gaay Fortman et al., 2007; De Leege et al., 2009). The cause for this might be that the performance of the *FGS* is highly dependent on the type of aircraft used. The Airbus A330-200 used in this research is not the best type to show the working principle of the *FGS*. Figure 5(a) shows clearly the differences in TCB Altitude (TCA) resulting from the presence of speed constraints in the scenario. An earlier TCB in the slow case and a relative late TCB for the fast TSCDA. The controller output, the IAS at which a next configuration must be selected is given in Figure 5(b). Selecting the next configuration at a higher IAS results in a relative faster deceleration, so the moment of selecting idle thrust can be delayed and thus a longer period of the TSCDA the aircraft can fly at higher speed resulting in a higher average approach speed.

3.2.3 Speed Constraint Deviation controller (*SCD*)

3.2.3.1 Principle

The presence of speed constraints in the TSCDA procedure makes another principle of controlling possible, the *SCD*. The procedural speed constraints (see Table 1) introduce parts of the TSCDA where the aircraft is flying at constant IAS. A deviation of the speed constraint affects the average approach speed and thus the ETA, see Figure 2(c). The input is again the T_{err}. The output is a speed command for the autopilot. This $V_{command} = V_{constraint(i)} \pm V_{offset}$, where $V_{offset_{Max}}$ is 10 kts. This value is chosen to prove the working of this method. Implementing this controller in the FMS is done by integrating the controller in the speed controller of the autopilot. The working of the main algorithm, which is the same as used by the *TC* is illustrated in Figure 3.

3.2.3.2 Initial simulations

The principle illustrated in Figure 2(c) is shown in Figure 6(a). In contrast to the other methods there is no difference in the TCA. The control margin is only dependent on the selection of a higher or lower IAS compared to the original speed constraint. The output of the controller, Figure 6(b) shows that the commanded speed is according to the theory. Due to practical

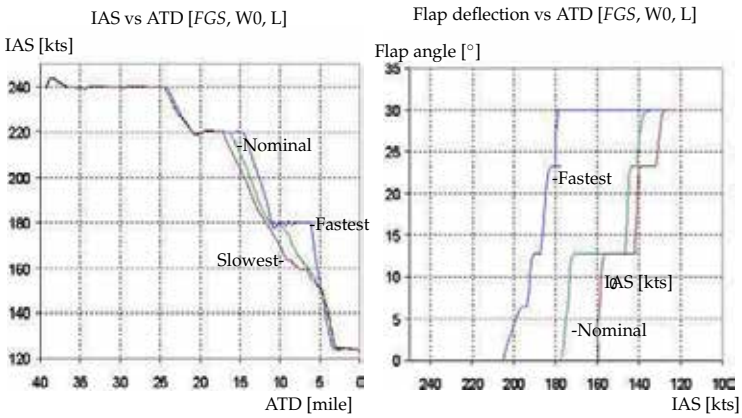

(a) *FGS* Speed profile (b) *FGS* Output profile

Fig. 5. *FGS*, initial simulations of the basic scenario (zero Wind and LW).

wind	mass	T_{nom}	T_{max}	$\Delta+$	T_{min}	$\Delta-$
Zero	HW	657.2	687.1	29.9	640.2	-17.0
SW	HW	666.1	696.0	29.9	634.0	-32.1
Zero	LW	676.1	698.1	22.0	656.0	-20.1
SW	LW	682.0	703.1	21.1	657.0	-25.0

Table 7. Method: *SCD*, TSCDA duration in seconds.

reasons the last speed constraint of 160 kts at 1,500 ft is not used to control the ETA in this research, so the *SCD* is inactive at that specific speed constraint. The commanded speed is then equal for the three conditions. This affects the control margin gained by the deviation at the speed constraint of 180 kts. In fact, the control margin gained by a specific speed constraint would be higher if that speed constraint is followed by another.

3.3 Controller performance

A comparison in TSCDA-duration, Tables 4, 6 and 7, and illustrated also in Figure 7, shows quite some difference in control margin between the three controllers. Also the influence of wind and mass on the performance of each controller is different. Even in these initial simulations without disturbances the differences between the performance are significant and therefore it is worth to investigate and evaluate the controllers performance more thoroughly.

4. Monte Carlo Simulation Experiment

The main question in this research is which of the three controllers shows the best performance in controlling the TSCDA. Considering the main purpose of the TSCDA: *reduce fuel use*, *reduce noise impact* while maintaining the *throughput at the RWT*, the performances of the controllers must be measured in performance metrics set by the objectives. It is not possible to answer the main question using the results of the initial simulations given in Section 2 only. It is necessary to perform Monte Carlo Simulations (MCS) to evaluate the controllers in a realistic test environment.

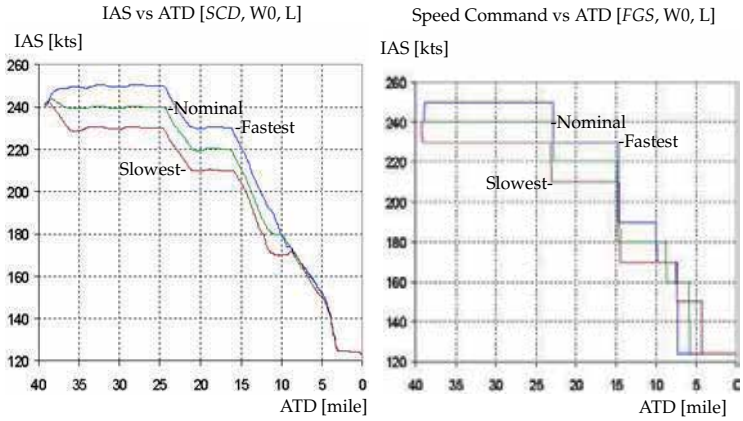

(a) *SCD* Speed profile (b) *SCD* Output profile

Fig. 6. *SCD*, initial simulations of the basic scenario (zero Wind and LW).

4.1 Monte Carlo Simulations

The MCS has three independent variables: the *type of controller*, the *wind condition* and the *setup of the arrival stream in terms of different aircraft mass*. The influence of these variables on the performance of the three different controllers must be derived from the results of the simulations. Besides those independent variables the simulations are performed in a realistic environment. The same scenario as used in the initial simulations of Section 2 has been used for the MCS. Two disturbances, a *Pilot Delay* at every change of configuration and an *Initial Spacing Error* are modelled in the simulation environment to improve the level of realism of this set of simulations. A combination of NLR's research simulators; *TMX*, *PC-Host* and *RFMS* is used as the simulation platform for the MCS (Meijer, 2008, A-1,3).

4.1.1 Independent variables

4.1.1.1 Controller

The three controllers; *TC*, *FGS* and *SCD*.

4.1.1.2 Wind condition

The influence of the wind will be evaluated by performing simulations without wind and with a South-Western wind, see Table 2 (as used in the *OPTIMAL* project (De Muynck et al., 2008)). During the TSCDA following the lateral path given in Figure 1(a) the controllers have to deal with cross wind, tailwind and a headwind with a strong cross component during final phase of the approach. This South-Western wind is also the most common wind direction in the TMA of Schiphol Airport.

4.1.1.3 Aircraft mass

The simulations used to evaluate the effect of a mass on the performance of the TSCDA controllers is combined with the simulations to evaluate the influence of the position of the aircraft in the arrival stream. In this research two different weight conditions are used. Lightweight LW and Heavyweight HW defined in Table 3. The difference in mass should be large enough to show possible effects.

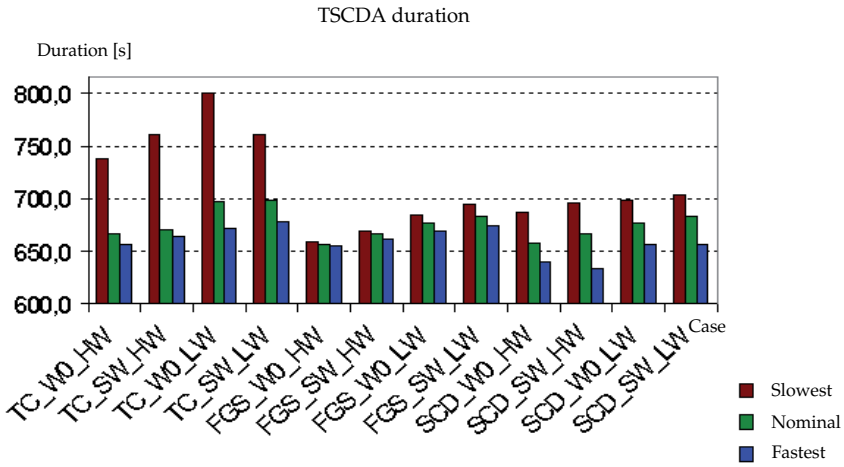

Fig. 7. TSCDA duration of all initial simulations.

stream	lead	pos. 2	pos. 3	pos. 4	trail
1, Full HW	HW	HW	HW	HW	HW
2, Full LW	LW	LW	LW	LW	LW
3, Mixed HW	HW	LW	HW	HW	HW
4, Mixed LW	LW	HW	LW	LW	LW

Table 8. The four types of arrival streams.

4.1.1.4 Arrival stream setup

The arrival streams consist of five aircraft, all the same Airbus A330-200 type. There are four different types of arrival streams, see Table 8. The mixed streams, three and four are used to evaluate the disturbance of a different deceleration profile induced by the different masses of aircraft in these streams. The first aircraft in the arrival stream performing the TSCDA according to the nominal speed profile, without the presence of a RTA at the RWT.

4.1.2 Simulation matrix

The combination of three different controllers, two types of wind and four types of arrival streams forms a set of 24 basic conditions for the MCS, see Figure 8. To test significance at a meaningful level, each basic condition has been simulated 50 times. Each simulation of a basic condition uses another set of disturbances, discussed below.

4.1.3 Disturbances

Two types of disturbances are used to make the simulations more realistic and to test the performance of the controllers in a more realistic environment. These two types are the modelled Pilot Delay on configuration changes. The second type of disturbance is the Initial Spacing Error. It is assumed that aircraft are properly merged but not perfectly spaced at the beginning of the approach. The induced time error at the begin of the TSCDA must be reduced to zero at the RWT.

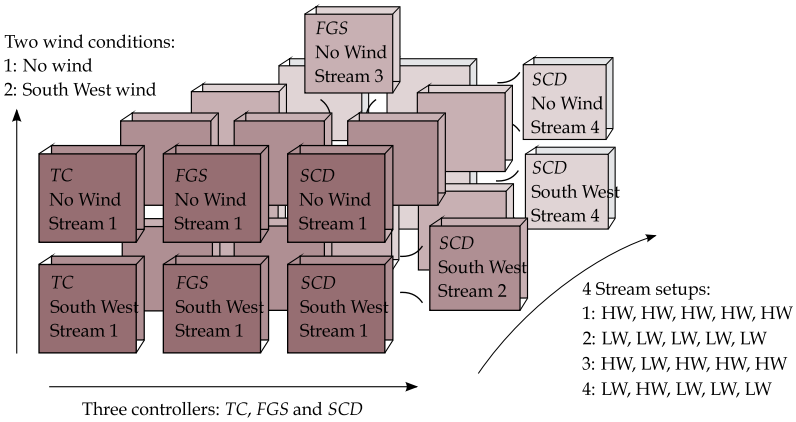

Fig. 8. Simulation matrix, 24 basic conditions.

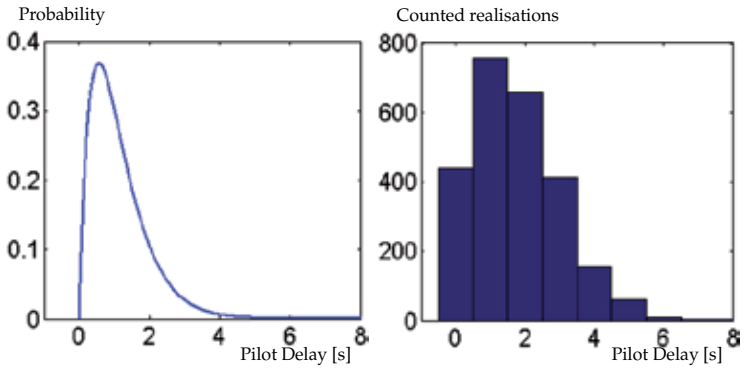

(a) Poisson Distribution (b) Histogram of the generated data

Fig. 9. Pilot Response Delay Model, Poisson distribution, mean = 1.75 s.

4.1.3.1 Pilot Response Delay Model

Configuration changes are the only pilot actions during the TSCDA. Thrust adjustment, vertical and lateral guidance are the other actions, which are performed by the autopilot. The delay between next configuration cues given by the FMS and the response of the pilot to these cues is modelled by the *Pilot Response Delay Model [PRDM]*. The delays are based on a Poisson distribution (De Prins et al., 2007). Each basic condition is simulated 50 times in this research. To get significant data from these runs, the data used by the disturbance models must be chosen carefully. A realisation of the Poisson distribution has been chosen for which the histogram of the generated data shows an equal distribution as compared with the theoretical distribution, see Figure 9.

4.1.3.2 Initial Spacing Error

To trigger the TSCDA-controllers, an Initial Spacing Error (ISE) has been modelled in the simulation environment. At the start point of the TSCDA, it is expected that the aircraft are properly merged in the arrival streams. However, the time space between aircraft at the start of

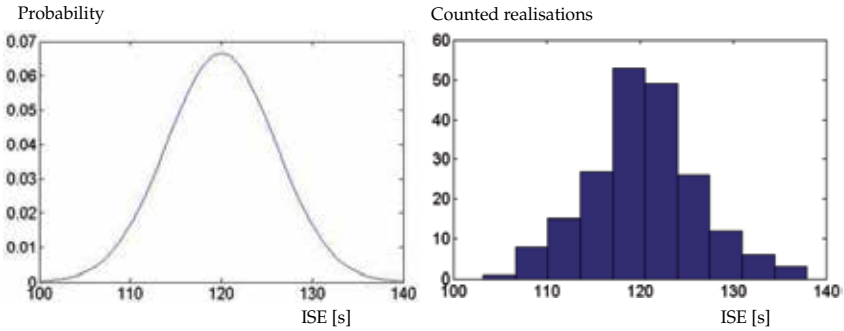

(a) Normal Distribution (b) Histogram of the generated data

Fig. 10. Overview of the Initial Spacing Errors in seconds, generated by a normal distribution with mean equal to 120 s and σ = 6 s.

the TSCDA is not expected to be equal to the required time space of 120 s at the RWT. The ISE is different between all aircraft in each of the 50 different arrival streams. The ISE sets are generated according to a normal distribution. The mean is chosen as the required time space between aircraft at the RWT and is equal to 120 s. The value for the standard deviation σ has been chosen so that the three controllers are tested to their limit derived in the initial simulations and set to σ = 6 s. To be sure that the generated data are according to the required normal distribution, the generated data has been evaluated by comparing the histogram of the generated data with the theoretical normal distribution, see Figure 10.

4.2 Hypotheses

From the definitions of the MCS described in the previous subsections, the following can be expected. The statements are related to the objectives for which the controllers are developed. The parameters which are derived from the MCS to evaluate these hypotheses are elaborated below.

4.2.1 Fuel use

The thrust is set to minimum when the TSCDA is controlled by the *FGS*. The other controllers use a higher thrust-setting and therefore it is hypothesised that the fuel use is minimum when using the *FGS*.

4.2.2 Noise reduction

Avoiding high thrust at low altitudes is the main method to reduce the noise impact on the ground. The most common reason to add thrust at low altitude is when the FAS is reached at a higher altitude than the reference altitude. A better controlled TSCDA reduces therefore the noise impact at ground level. It is hypothesised that there is a relation between the control margin and the accuracy of the controllers, see Figure 7, and therefore it is hypothesised that the *SCD* shows the best performance with respect to the accuracy. Since it is assumed that a better controlled TSCDA reduces the noise impact, it is hypothesised that the *SCD* shows the best performance with respect to noise reduction.

4.2.3 Spacing at RWT

Looking at the results given in Section 3.3, the control margin in a scenario without disturbances is the highest when using the *SCD* controller. However, the controller principle of the *SCD* is based on the presence of speed constraints. The lowest active speed constraint in this research is 180 kts if $h < 3{,}400$ ft. No active control is possible below this altitude, but below this altitude one kind of the disturbances are the pilot delay errors, which are activated during configuration changes. The *SCD* is not capable to control the TSCDA to compensate for those induced errors. The *FGS* and the *TC* are controllers which can compensate for errors induced during the last part of the TSCDA. It is hypothesised that the large control margin of the *SCD* affects the spacing at the RWT more than the reduced accuracy induced by the pilot delay errors effects the spacing at the RWT. Therefore it is hypothesised that the *SCD* will be the best controller to use to get the best time-based spacing between pairs of aircraft at the RWT.

4.2.4 Error accumulation in the arrival stream

Better controller performance will decrease the time-based spacing error between aircraft at the RWT. Better timing at the RWT of the leading aircraft will have a positive effect on the timing of the other aircraft in the arrival stream. Therefore it is hypothesised that a better control performance of a controller increases the performance of the other aircraft in the arrival stream.

4.2.5 Wind effects

The SW wind in combination with the scenario used in this research results in a headwind during the final part of the approach. This headwind reduces the ground speed and therefore increases the flight time of this final part. This can have a positive effect on the control space of the controllers. The effect of a larger control space will be the smallest on the *SCD*, because the control space of the *SCD* is the largest of the three controllers. So the effect of wind on the performance of the controllers will be smallest in the *SCD* case. However the Trajectory Predictor of the RFMS predicts the wind by interpolating the wind given in Table 2. The actual wind will be different because the aircraft model uses another algorithm to compute the actual wind. This difference between predicted wind and actual wind is used as variance in the predicted wind. It is hypothesised that these prediction errors have a negative influence on the accuracy of the controllers and therefore the performance of the controllers.

4.2.6 Effect of varying aircraft mass

A lower aircraft mass will decrease the FAS. A lower FAS will increase the duration of the deceleration to this FAS. A longer flight time has a positive effect on the control margin of the *TC* and *FGS* controller and a negative effect on the control margin of the *SCD*. The influence of the longer flight time on the accuracy of the controllers is the smallest in case of the *SCD*, because the *SCD* has the largest control space and therefore the possible impact on the control space is relative small.

4.2.7 Effect of disturbance early in the arrival stream

The differences in flight times between HW and LW are relatively large compared to the control space of the controllers, see Tables 4, 6 and 7 and Figure 7. A different aircraft mass early in the stream means a large disturbance and it is expected that the controllers must work at their maximum performance. The spacing error at the RWT will be large for all second air-

craft in the arrival streams. It is expected that the effect of this disturbance on the *SCD* is the smallest of the three controllers.

4.3 Performance metrics

From the results of the MCS several performance metrics must be derived. These metrics are chosen so that the hypotheses can be evaluated and so that the main question in this research can be answered. Looking at the three main objectives for which the TSCDA is developed: *reduce fuel use during the approach*, *reduce noise impact at ground level in the TMA* and *maintain throughput at the RWT*, the main performance metrics are:

- The *fuel use* during the TSCDA. This parameter shows directly the capability of the controller to reduce fuel during the approach.
- The *spacing at the RWT*. This parameter indicates the accuracy of the controller and it also indicates the possible control margin of the controller. It therefore gives an indication if the *minimum time space between aircraft at the RWT* objective can be met. The ISE is distributed with σ = 6 s. This σ is also chosen to set the reference values of the spacing times at the RWT. The upper and lower bound of the spacing times are set by 120 s $\pm$ 6σ.
- The *stabilisation altitude h_{stab}, where V reaches the FAS*. If h_{stab} is above h_{ref} = 1,000 ft then thrust must be added earlier in the approach to maintain the speed, this will result in a higher noise impact. If the value of this performance metric is below 1,000 ft then safety issues occur, because the aircraft is not in a stabilised landing configuration below h_{ref}. A σ = 80 ft for h_{stab} is expected (De Leege et al., 2009). The upper and lower bound is set as 1,000 ft $\pm$ 3σ.
- The *controller efficiency* is also a factor to compute. The specific maximum controller output is recorded during the simulation. The actual controller output at h_{ref} is divided by the maximum controller output at h_{ref}. This computed value indicates that spacing errors at the RWT are the result of disturbances where the controllers can not compensate for.

5. Results

5.1 Controllers compared

In this section the three controllers are evaluated by comparing the performance metrics derived from all the results of the simulations, these results are including the two wind conditions, four types of arrival streams and all the aircraft in the stream.

5.1.1 Stabilisation altitude

Figure 11 shows three diagrams which enable a visual comparison between the performance of the three controllers with respect to the performance metric: *the altitude where V reaches the FAS*, which is the stabilisation altitude (h_{stab}). The differences between the controllers are significant; *Analysis of Variance (ANOVA): F=78.876 , p <0.001*. The means, Figure 11(b), show the best performance of the *SCD* and the worst peformance of the *FGS*.
The *FGS* gives the most violations with respect to the lower bound of 760 ft. The distribution of h_{stab} in the *SCD* controlled case is the smallest of the three and the distribution in the *FGS* case is the largest. The three histograms, Figure 11(c), show distributions with two or three peaks. Further investigation of the influences of the other independent variables gives more insight in these distributions.

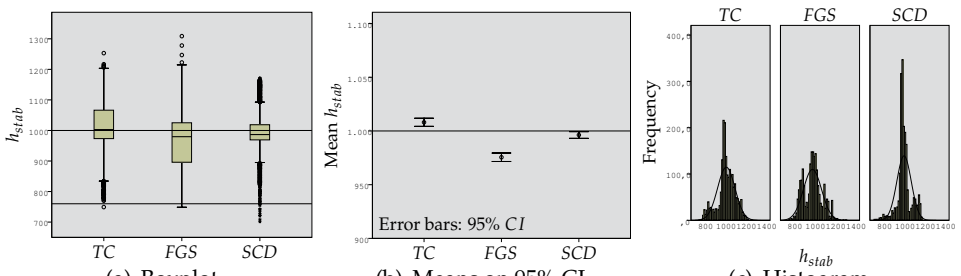

(a) Boxplot (b) Means on 95% CI (c) Histogram

Fig. 11. Altitude where V reaches the FAS (2,000 samples per controller).

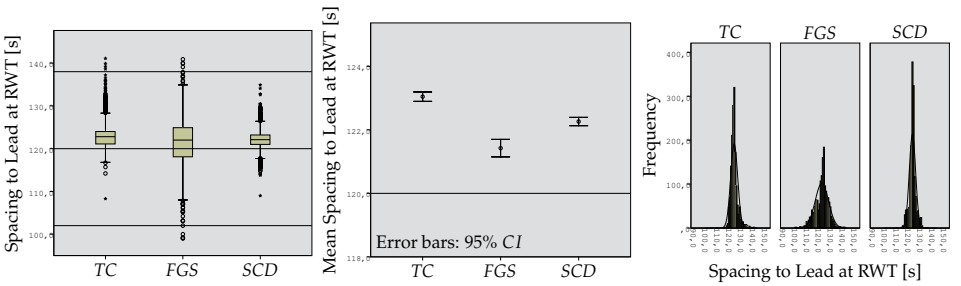

(a) Boxplot (b) Means on 95% CI (c) Histogram

Fig. 12. Spacing to Lead at RWT [s] (1,600 samples per controller).

5.1.2 Spacing at RWT

The differences between the controller performance with respect to the performance metric: spacing at the RWT as given in Figure 12 are significant; *ANOVA:* $F = 65.726$, $p < 0.001$. The means, Figure 12(b), show that the *FGS* controller performs best, the *TC* performs worst. The means of the three controllers lie all above the objective nominal value of 120 s. The *FGS* shows many violations on the lower limit set by 102 s. Using the *TC*, there are some violations on the upper limit only. The *SCD* gives no violations on the limits. The histograms in Figure 12(c) show all a normal distribution.

5.1.3 Fuel use

The performance metric 'fuel used' is shown in Figure 13. The differences between the controllers are partly significant *ANOVA: F=96.294 , p <0.001*. The *SCD* shows the lowest mean fuel use, on average 20 kg less fuel use per approach compared to the *TC* and *FGS*. The *FGS* gives a wide distribution compared to the other controllers and the *FGS* also gives the minimum and maximum values of the fuel use of all approaches. The *TC* and *SCD* show a more converged distribution than the *FGS*. The histograms of the *TC* and *FGS* results show a different distribution, although the means are equal.

5.1.4 Controller efficiency

Figure 14 shows the performance metric 'controller efficiency' per controller. Although the histograms show no normal distributions, the ANOVA gives a clear result; the differences are

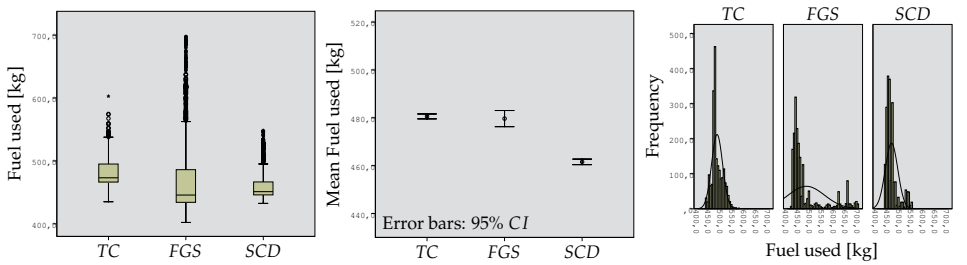

(a) Boxplot (b) Means on 95% CI (c) Histogram

Fig. 13. Fuel used during TSCDA [kg] (2,000 samples per controller).

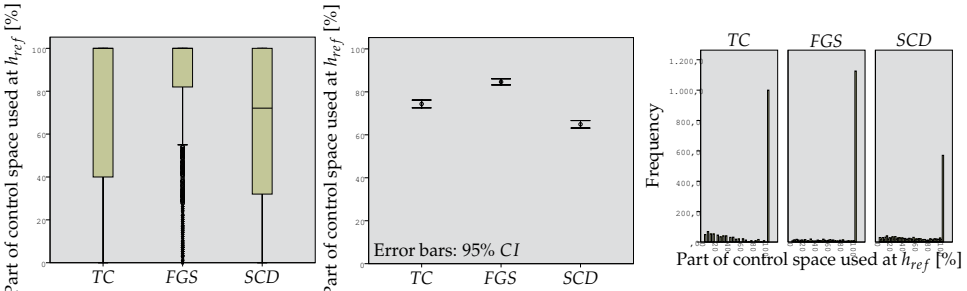

(a) Boxplot (b) Means on 95% CI (c) Histogram

Fig. 14. Part of control space used at h_{ref} [% of max. output] (1,600 samples per controller).

significant *ANOVA: F=135.528 , p <0.001*. Looking at the histograms, the *FGS* and the *TC* use their maximum control space most of the approaches, which is also indicated by the median which is equal to 100 for both cases. The mean of the *SCD* (65%) is low compared to the other means (*TC* 75% and *FGS* 85%).

5.2 Wind influence on controller performance

The wind influence on the performance of the three controllers is evaluated using the same performance metrics as used for the comparison of the three controllers for all the simulations. The results are split up by the controllers and by the wind conditions. Table 9 gives the results of the ANOVAs which are performed to evaluate the wind influence on the different controllers.

performance metric	general [F, p]	*TC* [F, p]	*FGS* [F, p]	*SCD* [F, p]
stabilisation altitude	151.2 , $\star\star$	1259 , $\star\star$	17.43 , $\star\star$	121.2 , $\star\star$
spacing at RWT	0.387 , 0.534	0.275 , 0.600	0.580 , 0.446	0.201 , 0.654
fuel use	138.3 , $\star\star$	52.60 , $\star\star$	64.82 , $\star\star$	189.0 , $\star\star$
control efficiency	2.920 , 0.088	4.349 , 0.037	2.510 , 0.113	0.388 , 0.533

Table 9. Overview of ANOVAs with respect to Wind influence; a significant difference occurs if p <0.05, and $\star\star$ indicates that $p < 0.001$.

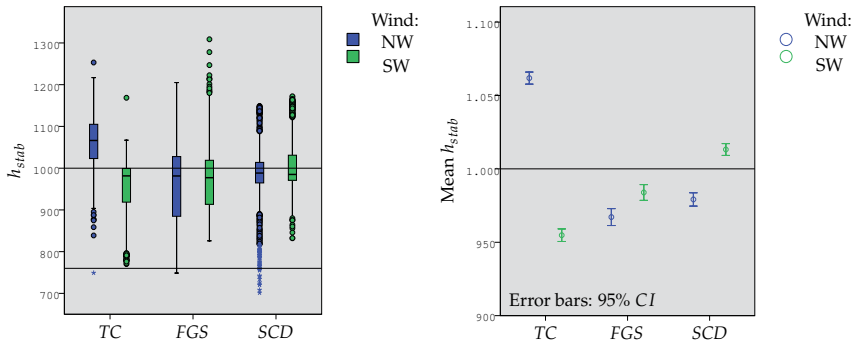

(a) Boxplot (b) Mean on 95% CI

Fig. 15. Wind influence on h_{stab} (1,000 samples per controller per wind condition).

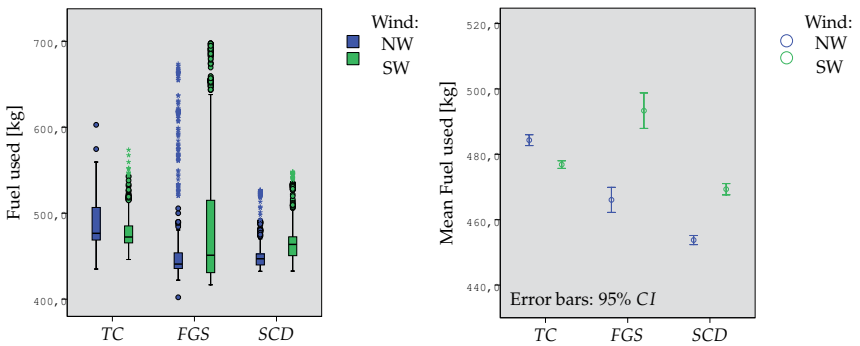

(a) Boxplot (b) Means on 95% CI

Fig. 16. Wind influence on fuel burn [kg] (1,000 samples per controller per wind condition).

5.2.1 Stabilisation altitude

There are significant differences between the stabilisation altitudes of the two wind conditions. The differences in wind influence on the different controllers are also significant, see Table 9. In all the three controller cases the wind influence has a positive effect on the means of h_{stab}. The absolute effect of wind on the means of the *TC* and *FGS* are opposite compared to the effect of wind on the *SCD*. The wind influence on the *SCD* is small as compared to the other controllers.

5.2.2 Spacing at RWT

There is no significant influence of the wind on the spacing performance at the RWT, Table 9. The spacing times out of limits appear in the wind case only.

5.2.3 Fuel use

Figure 16 and Table 9 show significant differences in fuel burn. The *TC* uses on average less fuel in the wind case, *FGS* and *SCD* use on average more fuel in case of wind. There is a wide distribution of fuel burn in the wind case in combination with the *FGS*.

performance metric	general [F, p]	TC [F, p]	FGS [F, p]	SCD [F, p]
stabilisation altitude	107.2 , $\star\star$	50.49 , $\star\star$	30.66 , $\star\star$	14.23 , $\star\star$
spacing at RWT	15.76 , $\star\star$	42.73 , $\star\star$	3.681 , 0.012	2.907 , 0.034
fuel use	163.0 , $\star\star$	18.86 , $\star\star$	70.19 , $\star\star$	52.79 , $\star\star$
control efficiency	21.33 , $\star\star$	14.75 , $\star\star$	13.50 , $\star\star$	15.97 , $\star\star$

Table 10. ANOVAs with respect to stream setup and aircraft mass; a significant difference occurs if p <0.05, and $\star\star$ indicates that $p < 0.001$.

5.2.4 Controller efficiency

Table 9 indicates no significant differences in the controller efficiency when analysing the wind influence on all simulation results and the wind influence on the *FGS* and *SCD* controllers. The wind influence on the *TC* controller is significant. A SW wind has a negative effect on the control efficiency.

5.3 Effect of aircraft mass and stream setup

5.3.1 Stabilisation altitude

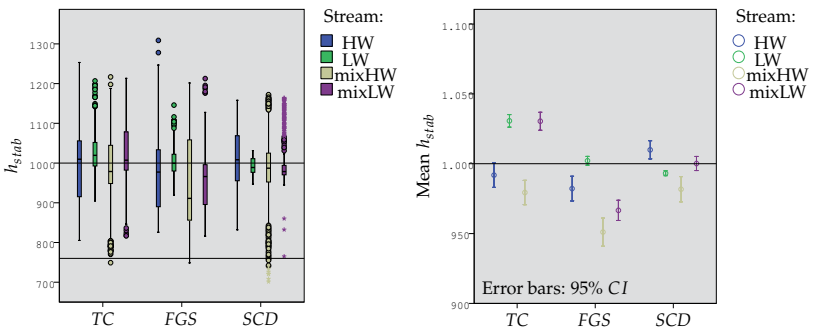

(a) Boxplot (b) Means on 95% CI

Fig. 17. Effects of aircraft mass and stream setup on h_{stab} (500 samples per controller/stream type).

Figure 17 and Table 10 show significant differences between the means of h_{stab}. The effect of the stream setup and aircraft mass is significantly different for each controller. This effect is smallest in the *SCD* case and largest in the *TC* case. The *Mixed HW* stream shows h_{stab} values below the lower limit only. The values of h_{stab} in case of mixed streams are wider distributed than the values of h_{stab} of the HW and LW streams and distribution of h_{stab} is wider for the HW stream compared to distribution of h_{stab} of the LW stream. The effect of a different stream setup is the smallest for the *SCD* controller.

5.3.2 Spacing at RWT

Figure 18 and Table 10 show significant differences between the spacing times at the RWT for all runs. Further analysing all data focused on the effect of the different streams gives no significant differences for spacing times. Table 10 shows significant different effects of the different streams in spacing times on the controllers specific. Spacing times below the lower limit only occur in the *mixedLW* stream.

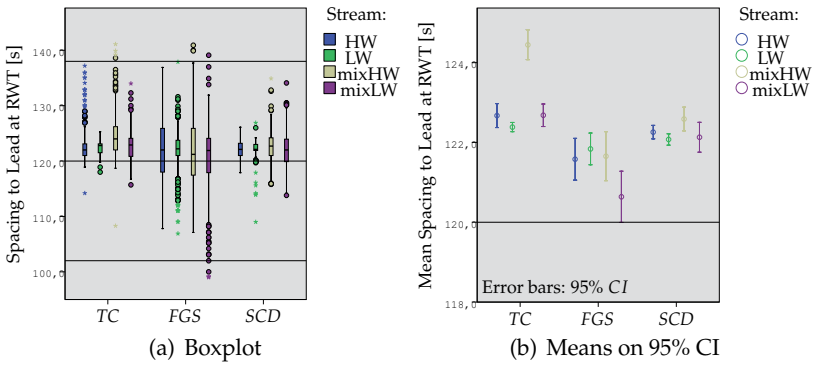

(a) Boxplot (b) Means on 95% CI

Fig. 18. Effects of aircraft mass and stream setup, spacing to Lead at RWT [s] (400 samples per controller/stream type).

The effects of the different streams on the spacing times is the smallest using the *SCD*. The mean of the spacing time in the *mixedLW* stream using the *TC* is large compared to the means of the other streams. The distribution of spacing times at the RWT is smallest for the LW stream for all controllers.

5.3.3 Fuel use

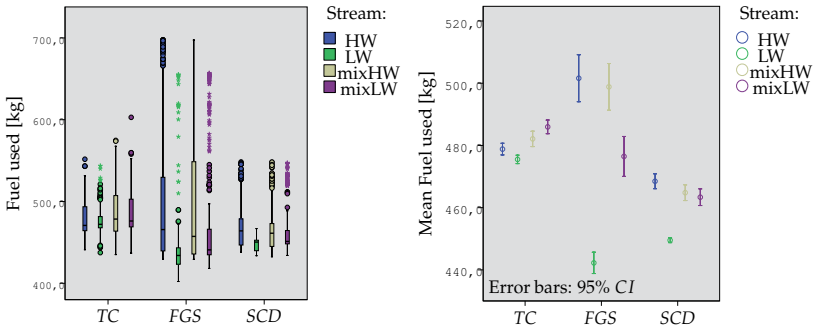

(a) Boxplot (b) Means on 95% CI

Fig. 19. Effect of aircraft mass and stream setup, fuel burn [kg] (500 samples per controller/stream type)

Figure 19 and Table 10 show significant differences in fuel burn between the arrival streams. The differences between the HW and *mixedHW* streams are not significant. Generally, LW aircraft consume less fuel. Figure 19(b) shows a large difference in fuel use of the LW stream in the *TC* and *SCD* cases. The effect of different arrival streams on the fuel use is the smallest for the *TC* and largest for the *FGS*.

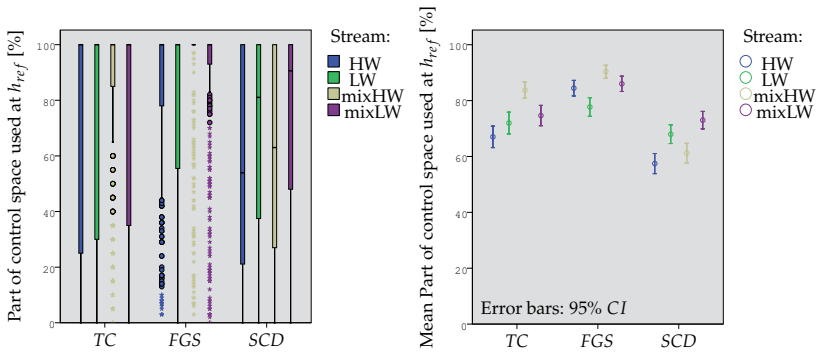

(a) Boxplot (b) Mean on 95% CI

Fig. 20. Effect of aircraft mass and stream setup, part of control space used at h_{ref} [% of max. controller output] (400 samples per controller/stream type).

5.3.4 Controller efficiency

Figure 20 and Table 10 show different controller efficiencies for the different arrival streams. The differences between the HW and LW streams are not significant, the differences between the *mixedHW* and *mixedLW* streams are also not significant. The position of the means for each stream in Figure 20(b) show different patterns for each controller.

5.4 Effect of the position in arrival stream

performance metric	general [F, p]	TC [F, p]	FGS [F, p]	SCD [F, p]
stabilisation altitude	61.31 , $\star\star$	26.76 , $\star\star$	4.883 , 0.001	29.59 , $\star\star$
spacing at RWT	26.23 , $\star\star$	37.51 , 0.600	0.513 , 0.673	28.38 , 0.654
fuel use	80.99 , $\star\star$	45.96 , $\star\star$	28.29 , $\star\star$	25.37 , $\star\star$
control efficiency	0.352 , 0.788	1.835 , 0.139	3.689 , 0.012	0.539 , 0.655

Table 11. Overview of ANOVAs with respect to the position in arrival stream; a significant difference occurs if p <0.05, and $\star\star$ indicates that $p < 0.001$.

5.4.1 Stabilisation altitude

Figure 21 and Table 11 give significant differences in the effect of the aircraft's position in the arrival stream with respect to h_{stab}. Further analysis shows that there are no significant differences between positions 2 to 5 in the stream. The influence of the position in the arrival stream on h_{stab} with respect to the three controllers is significant. The distribution of h_{stab} 'position 1' is largest compared to the other positions. The means of h_{stab} for 'position 2' are different compared to h_{stab} of the other positions.

The pattern of the means for the *FGS* in Figure 21(b) shows a decrease in h_{stab}, the *TC* and *SCD* shows an increase in h_{stab}. The distribution of h_{stab} for 'position 1' controlled by the *TC* shows a peak at 800 ft, see Figure 22(a), this is further analysed. Figure 22(b) shows the relative low means h_{stab} of the *TC* runs for position 1. All simulations of the first aircraft in the arrival stream are loaded by disturbances, those aircraft should perform the approach according to the nominal profiles of the controllers. So it is expected that there are no large differences between h_{stab} of the first aircraft in the different streams if the aircraft mass is equal.

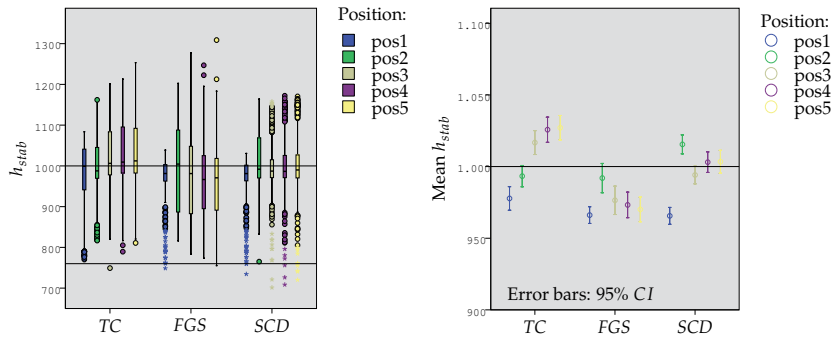

(a) Boxplot (b) Means on 95% CI

Fig. 21. Effect of the position in arrival stream on h_{stab} (400 samples per controller per position).

Figure 23 shows flight data of the second run of the HW and *mixedHW* streams controlled by the *TC* and with the SW wind condition. The data presented in this figure shows what happened during all the simulations in this specific case. Problems occurred in the flap deflection while descending from 1,850 ft to 1,700 ft. Output data of the Trajectory Predictor of the RFMS show normal behaviour for all the runs in this case, so the problem can be found in the aircraft model. More specific data of the flap deflection in the aircraft model is not available and therefore a further analysis of the problem which caused the wrong flap deflection in this specific case could not be performed.
The problem of the worse deceleration caused by problems in the flap deflection part of the aircraft model has no effect on the other aircraft in the arrival stream because there is no relation found between the spacing at the RWT and the stabilisation altitude and the input of the controllers is only the ETA of Lead in the arrival stream.

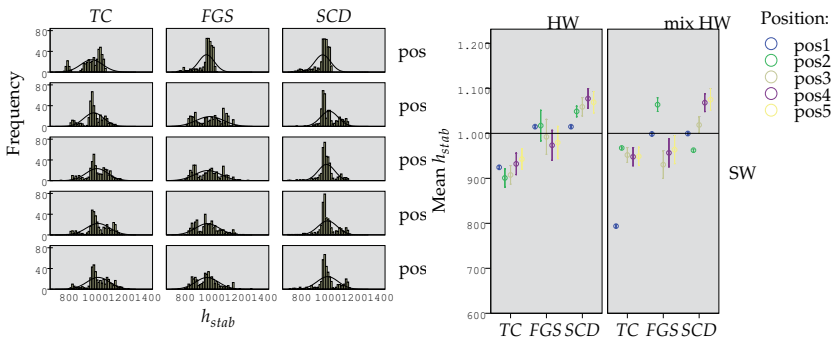

(a) Histograms

(b) Means on 95% CI, split up by type of stream, wind condition, position in arrival stream and controller, zoomed in on the HW and *mixedHW* streams

Fig. 22. Altitude where V reaches the FAS (400 samples per controller per position).

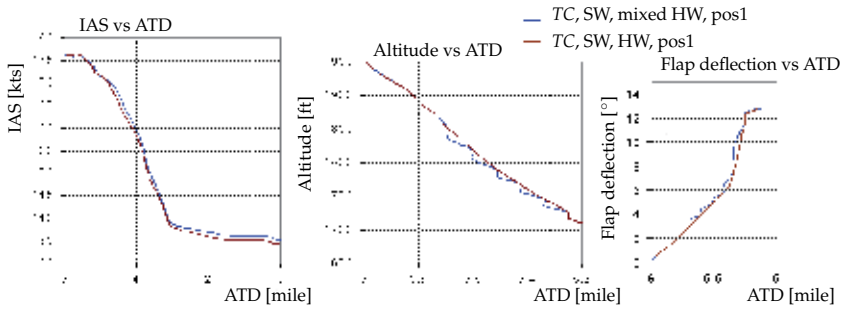

Fig. 23. Two particular approaches compared with respect to altitude, IAS and Flap deflection vs ATD. The data are derived from flight data of the first aircraft of the second stream.

5.4.2 Spacing at RWT

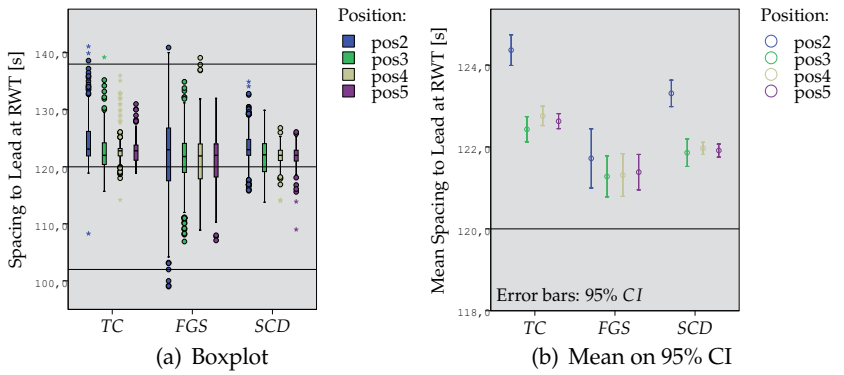

(a) Boxplot (b) Mean on 95% CI

Fig. 24. Effect of the position in arrival stream, spacing to Lead at RWT [s] (400 samples per controller per wind condition).

There are significant differences of the spacing times at the RWT between the positions in the arrival stream according to Table 11. This significant difference is not found for the positions 3, 4 and 5 in the arrival stream, however. Within the three controllers the differences in spacing times is not significant between the positions, according to Table 11. The only values out of the lower limit are in *Position 2* in the *FGS* case. The distribution of the spacing times at higher positions in the streams is smaller than the distribution of the spacing times of positions 1 and 2.

5.4.3 Fuel use

There are significant differences of fuel use between the positions in the arrival stream according to Table 11. This significant difference is not found for the positions 3, 4 and 5 in the arrival stream. Within the three controllers the differences in fuel use is significant between the positions, according to Table 11. Figure 25 shows the lowest fuel use at position 1. In the *TC* case, a higher position in the stream causes a higher fuel use. In the *FGS* case there is a lower fuel use at higher positions in the stream (after position 2). The *SCD* case shows the

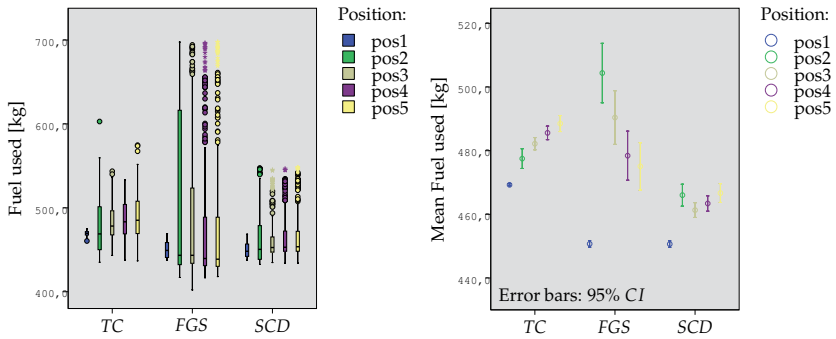

(a) Boxplot (b) Means on 95% CI

Fig. 25. Effect of the position in arrival stream, fuel used during TSCDA [kg] (400 samples per controller per wind condition).

smallest effect of the different positions of the three controllers. The fuel use of position 2 is different compared to the other positions.

5.4.4 Controller efficiency

Table 11 shows no significant differences between the controller efficiencies between the positions in the arrival stream. Within the controller cases there are no significant differences between the efficiencies of the *TC* and *SCD*. The differences are in the *FGS*, i.e., at higher positions performance is better.

5.5 Interaction effects

Interaction effects of the independent variables on the performance metrics are investigated. These effects are in most of the cases significant. The significant effects can be summarised as follows; the stream setup amplifies the influence of the other independent variables on the performance metrics significantly in all cases. Different positions and different wind conditions show the same effect, however these effects are not significant.

6. Discussion

6.1 Fuel use

It was hypothesised that the *FGS* uses on average the lowest amount of fuel for the approach. The results of the simulations show that the *SCD* uses on average the lowest amount of fuel. The meaning of an, on average, 20 kg less fuel use per approach is quite significant. However looking at the extreme values, the approach with the minimum fuel use is controlled by the *FGS* as hypothesised. The results show a relation between the control performance of the *FGS* controller and a larger standard deviation of the fuel use and on average larger amount of fuel per approach.

A SW wind condition results in a higher fuel use for the *FGS* and *SCD*, but reduces the fuel use of the *TC*. This might be caused by the fact that the *TC* uses thrust adjustments to control the TSCDA and therefore directly affects the fuel use during the approach. This statement combined with the fact that the SW wind condition affects the ground speed, and therefore the ETA of the aircraft, results in the good performance of the *TC* in the SW condition.

LW aircraft uses less fuel than HW aircraft. The effect of a different aircraft mass on the fuel use is largest for the *FGS* and smallest for the *TC*. It was hypothesised that the *SCD* should have the smallest deviations caused by differences in aircraft mass and stream setup. For the fuel use this hypotheses is rejected, because the *TC* controller performs best. The first aircraft in the arrival stream uses the lowest amount of fuel, these aircraft perform the approach at nominal profiles, the controllers are inactive. The *FGS* shows the largest difference in fuel use per position, as hypothesized.

6.2 Noise reduction and safety aspects

The controllers have to perform the approach so that the stabilisation altitude h_{stab} equals the h_{ref} = 1,000 ft. Higher stabilisation means that the FAS is reached at a higher altitude which results in an earlier moment of adding thrust to maintain the speed. Lower stabilisation is not preferred because safety aspects require a minimum stabilisation altitude of 1,000 ft. Looking at all results it can be concluded that the *SCD* controls the TSCDA the best of the three controllers. The mean stabilisation altitude of the *SCD* is almost equal to 1,000 ft and the standard deviation is small compared to those of the other controllers. The histograms show more than one peak in the distributions of h_{stab}. These peaks are related to the effect of the different arrival streams on h_{stab}.
The wind influence on the performance of the *TC* is large compared to the other controllers, the *SCD* gives the smallest differences in h_{stab} between the two wind conditions. Is was hypothesised that the influence of wind on the controller's performance is smallest in the *SCD* case. Different aircraft mass contributes to large differences in h_{stab}. Again this effect is smallest on the *SCD*. LW aircraft perform the approach better than the HW aircraft with respect to h_{stab}. The results of the *FGS* indicates many problems in the mixed aircraft streams. The disturbance induced by the second aircraft has a large negative effect on the performance of the *FGS*. The stabilisation altitudes at each position in the arrival stream are quite different for each controller. The *TC* and *SCD* give higher h_{stab} for higher positions in the arrival stream. The results of the *FGS* case show not this pattern. The second position in the arrival streams shows the largest differences compared to the other positions. The extra initial spacing error caused by the different flight times between HW and LW aircraft affects the controllers' performance.

6.3 Spacing at RWT

The average spacing times of the *FGS* are closest to the objective of 120 s. However, there were many runs in the *FGS* case where the spacing at the RWT was outside the limits set by 102 s and 138 s. This means that although the mean spacing error is smallest, the variability is the largest. The *SCD* gives the narrowest distribution and is therefore the best controller with respect to the performance metric 'spacing at the RWT', as was hypothesised. The assumption that the negative effect of the presence of an ISE on the spacing at the RWT is larger than the effect of the presence of pilot delay errors on the spacing at the RWT, is also justified.
The controller efficiencies of the three controllers gives the same result, the *SCD* is best capable of controlling the aircraft with respect to the spacing at the RWT. The maximum output value of the *SCD* is $\pm$ 10 kts. This value was arbitrary chosen. The controller efficiencies of the *SCD* show that the TSCDA concept is even possible with a smaller maximum *SCD* output value.
Earlier researches on the *FGS* show a better performance of this controller with respect to the spacing at the RWT (De Leege et al., 2009). The bad performance of the *FGS* in this research is related to the type of aircraft used, the Airbus A330. The *FGS* of the A330 controls 4 dif-

ferent flap positions, the *FGS* of a B747 controls 6 flap positions which increases the control space. The scenario used in this research is more realistic than the scenarios used by previous researches, however.
The wind influences on the spacing times at the RTW are not significant.
There are differences in spacing performance between the different arrival streams. First the mean spacing time is closer to the objective for LW aircraft compared to HW aircraft. This effect is smallest for the *SCD* as hypothesised. A disturbance in the arrival stream as in the mixed weight aircraft streams has a negative influence on the performance of the controllers. LW aircraft perform better in combination with all controllers, this was also hypothesised. The duration of the deceleration is longer for LW aircraft, this increases the control margin of the controllers resulting in better spacing performance.
The *SCD* controller is not capable to compensate for errors induces by the PRDM. It was hypothesised that this could have a bad influence on the performance of the *SCD*. The results also show this influence, because the mean spacing error of 2.5 s in the *SCD* case is large, although the controller is not performing at its maximum capacity. However, the *SCD* still performs properly, because the mean spacing time of the *SCD* is situated between the mean spacing times of the *FGS* and the *TC* and the standard deviation of the *SCD* is smallest of the three controllers.
The mean of the spacing error derived from all results is +3 s. The spacing error is derived from the ETA, which is calculated using the TP of the RFMS. A positive standard spacing error indicates that the calculation of the ETA is not performed properly. The code of the TP of the RFMS shows that the backwards calculation of the speed and altitude profiles starts at 0 ft above the runway. The end of the simulation is the RWT which is situated 50 ft above the runway. This difference of 50 ft introduces a standard error in the calculation of the ETA which results in the slow approaches.

7. Conclusions

This research showed significant differences in the performance of three different controllers *TC*, *FGS* and *SCD* capable of performing the TSCDA in arrival streams. The fuel use, noise impact and spacing performance of the three controllers are compared, and the *SCD* shows the best performance. Wind influence, different aircraft mass, arrival stream setup and position in the arrival streams affects the performance of the controllers. These effects are smallest for the *SCD*. Compared to the *FGS* used in previous researches the *FGS* performs less accurate at controlling the TSCDA. The more realistic scenario, the high-fidelity simulation environment and the specific type of aircraft used in this research give new insight in the performance of the *FGS*. With respect to fuel use the performances of the *TC* and *FGS* are equal. The *TC* performs between the *SCD* and *FGS* with respect to spacing criteria.

8. Recommendations

It is recommended that more types of aircraft are simulated. The specific aircraft deceleration performance has a large influence on the performance on the TSCDA controllers. The interaction between aircraft in arrival streams built up from applying more than one type of aircraft is worth to evaluate.
Disturbances such as a reduced accuracy of the ADS-B model, turbulence during the approach and a reduced navigation performance should be implemented as well to get a more realistic simulation environment. The influence of larger ISE's should also be investigated.

It is further recommended that the results of this research are analysed using a noise footprint tool to compute the absolute noise impact. The results could give a different conclusion about the best controller performance, because other important parameters, such as the configuration change moments, can have a different effect on the noise impact. Similarly, it is recommended that metrics regarding emissions during the approach are included in future research efforts.

9. References

De Gaay Fortman, W. F., Van Paassen, M. M., Mulder, M., In 't Veld, A. C. & Clarke, J.-P. B. (2007). Implementing Time-Based Spacing for Decelerating Approaches, *Journal of Aircraft* **44**(1): 106–118.

De Leege, A. M. P., In 't Veld, A. C., Mulder, M. & Van Paassen, M. M. (2009). Three-Degree Decelerating Approaches in High-Density Arrival Streams, *Journal of Aircraft* **46**(5): 1681–1691.

De Muynck, R. J., Verhoeff, L., Verhoeven, R. P. M. & De Gelder, N. (2008). Enabling technology evaluation for efficient continuous descent approaches, *26th International Congress of the Aeronautical Sciences, Anchorage (AL), USA, September 14-19* .

De Prins, J. L., Schippers, K. F. M., Mulder, M., Van Paassen, M. M., In 't Veld, A. C. & Clarke, J.-P. B. (2007). Enhanced Self-Spacing Algorithm for Three-Degree Decelerating Approaches, *Journal of Guidance, Control & Dynamics* **30**(2): 576–590.

Erkelens, L. J. J. (2000). Research into new noise abatement procedures for the 21st century, *Proceedings of the AIAA Guidance, Navigation and Control conference, Denver (CO), USA* (AIAA-2000-4474).

In 't Veld, A. C., Mulder, M., Van Paassen, M. M. & Clarke, J.-P. B. (2009). Pilot Support Interface for Three-degree Decelerating Approach Procedures, *International Journal of Aviation Psychology* **19**(3): 287–308.

Koeslag, M. F. (2001). Advanced continuous descent approaches, an algorithm design for the flight management system, *Technical Report NLR-TR-2001-359*, National Aerospace Laboratory NLR.

Meijer, L. K. (2008). Time based spaced continuous descent approaches in busy terminal manoeuvring areas, *Unpublished MSc thesis report*, National Aerospace Laboratory & Faculty of Aerospace Engineering.

Website: Single European Sky ATM Research [SESAR] (n.d.). www.eurocontrol.int/sesar.

6

Investigating requirements for the design of a 3D weather visualization environment for air traffic controllers

Dang Nguyen Thong
Institute of Movement Sciences, CNRS and University of Aix-Marseille II
France

1. Introduction

This chapter involves a long-term investigation into the applicability of three-dimensional (3D) interfaces for Air Traffic Control Officers (ATCOs). This investigation is part of collaboration between EUROCONTROL Experimental Centre (EEC) and the Norrköping Visualization and Interaction Studio (NVIS) of Linköping University in which a test-bed was developed in order to evaluate the different features of a 3D interface for ATCOs. This test-bed, known as the 3D-Air Traffic Control (3D-ATC) application, provides controllers with a detailed semi-immersive stereoscopic 3D representation of air traffic. Different aspects of the 3D-ATC application include 3D visualization and interactive resolution of potential conflict between flights (Lange et al., 2006), a voice command interface for visualizing air traffic (Lange et al., 2003), and interactive 3D weather images (Bourgois et al., 2005). Among these various features, the 3D weather visualization was chosen as a first case for carrying out a more accurate users' study.

Weather is considered as one of the major factors contributing to aviation accidents (Spirkovska and Lodha, 2002). As stated by Kauffmann and Pothanun (2000) "weather related accidents comprise 33% of commercial carrier accidents and 27% of General Aviation (GA) accidents". Moreover, adequate weather information (both for now-cast and forecast information) is often not available to pilots or controllers. The limitation in the way the weather information is represented in current weather displays has been also pointed out in several studies. Boyer and Wickens (1994) claimed that current presentation of weather information *is not easily understandable* and that it should be made more user-friendly. Lindholm (1999) argued that the *incomplete and imprecise weather* information currently displayed at the controllers' working position limits their job function. According to him, a better weather display could increase the controller weather situation awareness and possibly increase their strategic planning role. Boyer and Wickens (1994) reported the fact that the forecasts are generated from data that are collected only twice daily and that controllers require *weather forecasts that are updated on a more frequent basis*. Ahlstrom and Della Rocco (2003) claimed that pilots frequently chose enhanced real-time weather displays

for controllers when asked to rank different sources of important weather information. A similar opinion was collected from a study of Forman et al. (1999).
Providing suitable weather information could contribute in reducing the impact of adverse weather conditions both on delays and aviation accidents. However, weather-related research has mostly focused on the pilot side. Extensive research on controller weather information needs is largely lacking, although the importance of suitable weather information for controllers has increased considerably. In this respect, we can quote the Committee Chairman Albert J. Kaehn Jr., U.S. Air Force (NBAAD, 1995): "Although the primary role of air traffic controllers is to keep aircraft from colliding, accidents such as the 1994 crash of USAir Flight 1016 in Charlotte, North Carolina, demonstrate that air traffic controllers should exercise more caution about allowing aircraft to fly in or near hazardous weather". Hence, accurate and timely information about weather is essential for controllers, in order to support tactical and strategic planning for safe and judicious operations. However, what exactly do controllers need in order to rapidly gather the weather information necessary for carrying out their tasks?
To answer that question, we carried out a user study to understand controller weather information needs in order to define content requirements for weather support tools. In addition, we aimed to gather initial controller feedback on the applicability of 3D weather displays and on their potential benefits. This user study was carried out in two steps: a field observation of controllers' work at Stockholm Air Traffic Control Centre and an onsite survey with a demonstration of a prototype of 3D weather visualization in order to get controllers' feedback on weather information needs and 3D weather visualization.
This chapter presents the results of this user study and will be structured in 6 sections as follows. Section 2 summarizes related work concerning controller weather information needs, computer-human interface issues in the design of weather information display for controllers and 3D weather visualization for air traffic control. Section 3 presents the findings from the field observation on the daily work of controllers with weather information. Section 4 details the design of the onsite survey including both a demonstration of 3D weather presentation and the questionnaire. Section 5 presents the empirical results and main findings obtained from the survey, followed by the "Conclusions and Future Work" in Section 6.

2. Literature Review

The present study concerns both controllers' weather information needs and 3D weather information display. As a result, we will first examine previous studies addressing the controllers' weather information needs in this section. Then, we will outline results of research on 3D weather information display for controllers.

2.1 Related Work on Controllers' Weather Information Needs

Actually, little empirical research is available on controllers' weather information needs (Ahlstrom et al., 2001). In general, previous studies in literature agree not only on what weather data controllers need to gather, but also on how this data should be made available.

Regarding the nature of weather information controllers need to gather, the importance of having reliable weather information, especially concerning *adverse conditions*, is stressed in

literature. For instance, Lindholm (1999) reported that controllers' weather concerns include variations in wind speed and direction, clouds, visibility, turbulence, icing, and convective systems such as thunderstorms. The FAA Mission Need Statement (MNS) (FAA, 2002) suggested that phenomena that have impact on controller activities are adversities such as *t*hunderstorms, in-flight icing, obstruction to visibility (i.e. low ceilings and poor visibility), wind shear, severe non-convective turbulence, snow storms and surface icing. The *dynamic aspect of weather information* is also of particular concern to controllers (Chornoboy et al., 1994) especially with respect to weather trends, direction of movements, and intensity within a control sector (Ahlstrom, 2001).
Regarding the quality of weather information, Lindholm (1999) suggested that both en-route and approach controllers need a precise weather information picture that *requires little or no interpretation*, because controllers are not meteorologists. Similarly, Chornoboy et al. (1994) claimed that controllers want to have unambiguous weather tools that can be used without interpretation and coordination. In addition, controllers might also need *interactive, real-time weather inputs* because weather phenomena and trends frequently change (Whatley, 1999).
In short, the most prominent weather information needs for controllers consist in gathering reliable, real-time and updated weather information especially with respect to hazards. This information should be accurate but also simple and easy to understand. Moreover, it should be detailed, at least concerning position, intensity and trends. More in-depth research, especially empirical research, is needed to refine different user weather needs and the associated impact on operational services.

2.2 Related Work on 3D Weather Information Display for Controllers

According to Boyer and Wickens (1994), it is difficult to display all of the necessary information concerning a weather situation through one-dimensional (1D) display or even in two-dimensional (2D) graphical display. Many have been thinking about using 3D weather display; for example, Cechile et al. (1989) suggested that "*since the main purpose of the displays should be to support the development and updating of the mental models, a 3D display would be the most appropriate*". Because of the intuitive benefits of 3D in representing weather information, much research has explored the possible effects of representing weather information on 3D display. Such display formats could have good effects on weather situation awareness since a 3D weather presentation could show the spatial positions of the weather phenomena, which is difficult or even impossible to show in a 2D representation.
In literature, we can find a number of studies trying to assess and evaluate the utility and usability of 3D weather displays, like the work of Pruyn and Greenberg (1993) and Boyer and Wickens (1994) about weather displays for cockpits, the Aviation Weather Data Visualization Environment (AWE) which presents graphical displays of weather information to pilots (Spirkovska & Lodha, 2002), special displays designed for providing 3D support tools for meteorologists (Ziegeler et al., 2000). However, applications of 3D weather displays for air traffic controllers received less attention. One of the few academic works in the field was performed by Wickens et al. (1995). The study aimed to compare controller performances with a 3D perspective versus 2D plane view displays, for vectoring tasks in weather penetration scenarios. In brief, participants had to determine if the trajectory of an aircraft would intersect the graphically rendered hazardous weather system and, if so, issue headings so as to guide the aircraft in avoiding the weather structure; if not, they had to estimate the point of closest passage to the weather formation. The results did

not show any significant difference in terms of accuracy between the two displays types, although it was argued that some benefits could be implied in using a weather display that allows switching between 2D and 3D formats (Wickens et al., 1994). The 2D and 3D formats provide different weather information that is best suited for different controller tasks. St. John et al. (2001) found differences in display formats from their research on 2D and 3D displays for shape-understanding and relative-position tasks. 2D displays are superior for judging relative positions (e.g., positions between aircraft), whereas 3D displays are superior for shape understanding.
In summary, early efforts on using 3D graphics in weather displays have revealed both advantages and disadvantages of this kind of display. However, it is too early and there have not yet been enough empirical results to have a complete view on the potential of 3D in weather display in particular and in ATC in general. More empirical studies are required on this direction of research.

2.3 Approach

As stated above, the main objectives of this study are to discover what type of weather information is mostly necessary for controllers and initially to gather feedback about the potential of 3D weather visualization in ATC. In order to do so, we performed a field observation followed by an on-site survey at a Swedish air traffic control centre combined with a presentation to controllers of a prototype of our 3D-ATC weather support tool.

3. The Field Observation

3.1 Goal

The goal of this field observation was to understand the way the controller works with weather information in particular. The field observation was carried out during 2 days at Arlanda ATCC (Air Traffic Control Centre), one of the two main air traffic control centres in Sweden. During this informal study, we observed the daily work of both en route and approach controllers. We also had the opportunity to ask controllers about different ATC issues in situ. These instant questions and answers on different ATC issues were helpful for us in understanding the critical parts of air traffic control work. More importantly, the findings from the field observation were used for designing the questionnaire used in the onsite survey.

3.2 Weather Information Display at Arlanda ATCC

The Arlanda ATCC is divided into two parts. One part is called the ACC (Area Control Centre) and the second part is a TMC (Terminal Control Centre). En route controllers work in ACC and approach controllers work in TMC.

The controller sees briefing information from a special display to acquire an overview of weather information before a working session. This display shows the precipitation level of different zones in Sweden in general and more detailed precipitation information for the TMC sectors (cf. Figure 1). The weather information is updated every 5 minutes.

Fig. 1. Weather RADAR display

3.3 Findings

At the Swedish air traffic control centre we visited, both en route and approach controllers have two ways of obtaining weather information: the first one concerns routine or "general" weather information, and the second one concerns weather hazards.

- *Routine weather data* is reported to supervisors and air traffic managers by meteorologists. This information is usually provided both in graphical and textual forms. By graphical forms, we intend a dedicated display that shows the level of precipitations. Whereas each approach controller has his/her own separate "precipitation display", en route controllers might have access to this information only via an explicit request to the supervisor. Textual weather data, called "briefing", is directly sent to both en route and approach controllers can be displayed (on demand) on their RADAR displays. The briefing contains information on wind, clouds, RVR, visibility, air temperature and dew-point, pressure, weather trend, etc. Examples of briefings are the METAR (Meteorological Aerodrome Report; see Figure 2) and TAF (Terminal Aerodrome Forecast) standards for reporting weather forecast information.

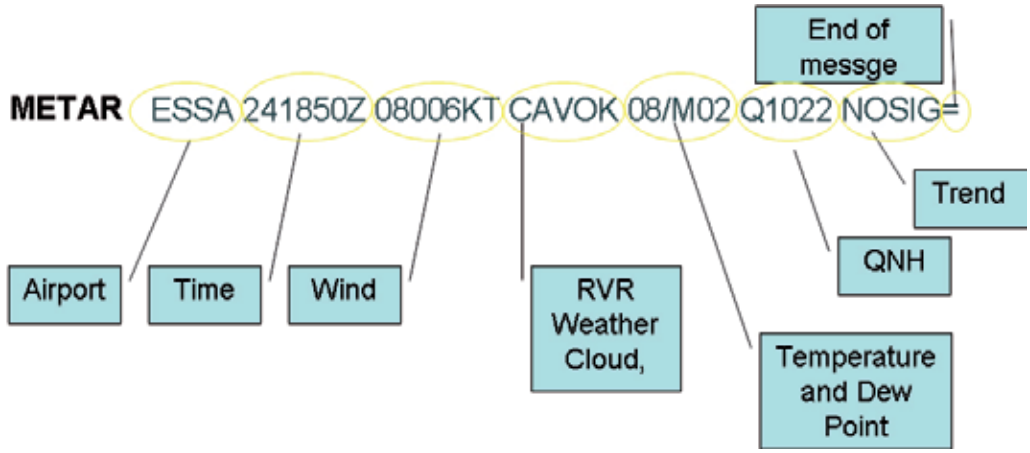

Fig. 2. A METAR Weather Briefing

- *Hazardous weather information* can be obtained both from pilots and from supervisors. Supervisors receive hazardous weather information from meteorologists: The supervisor, at her/his discretion, provides weather information to controllers. However, the most precious source of real-time hazardous whether data is the Pilot Report (PIREP), a report of conditions encountered by pilots during the flight. This information is usually relayed by radio to the nearest ground station. Weather PIREP may include information such as height of cloud layers, in-flight visibility, icing conditions or turbulence. Weather PIREPs have a double function: on the one hand, they simply confirm weather information that might already be available to controllers; on the other hand, they offer real-time and timely updated information about the development and progress of certain weather conditions. This makes the PIREP a unique and crucial source of information for a strategic weather factor in air traffic management: the presence of adversity and thunderstorms.

4. The Survey

The questionnaire we presented to controllers was composed of four main parts: *Controller demographics* (e.g. age, years of experience), *weather information needs*, *level of satisfaction* with available weather displays, and *potential use of 3D displays* for weather representation.

4.1 Questionnaire Design Details

In the weather information needs part, controllers were required to determine what weather information is needed for carrying out their activities by replying either YES or NO to each weather item provided in the questionnaire (i.e. a YES next to the item Wind, means that Wind information is needed for carrying out ATC tasks). The list of weather items was derived from the literature review and the field observation, and structured as follows:

- *Routine weather data*: Wind; Clouds; Visibility (the farthest distance at which an observer can distinguish objects, which is very important parameter in takeoff or

landing phases); Runway Visual Range (RVR) which means the visibility distance on the runway of an airport; Temperature (which is used for determining current meteorological conditions, calculating takeoff weight and providing information to passengers); Pressure (that is used to measure the altitude of a flight); Present Weather (including types and intensity of precipitation such as light rain or heavy snow, as well as the condition of the air environment such as foggy, hazy or blowing dust); Weather Trend informs about significant changes of reported weather conditions within short and long term; Weather Forecast.

- *Hazardous weather data*: Wind Shear (sudden change in wind direction or speed over a short distance); Turbulence; Thunderstorm; Low Ceiling and/or Low Visibility (which can severely reduce the capacity of an airport and lead to ground delays that result in diversions, cancellations and extra operational costs); CB (Cumulonimbus, that is the cloud forming in the final stage of a thunderstorm which is very dangerous and it usually avoided by flight); In-flight Icing (ice aircraft surfaces that increases the aircraft weight); Jet Stream (wind created at the border of two air masses with different temperature; and Mountain Waves (i.e. the rolling waves of wind caused by air blowing over mountains tops).

Controllers were also asked to rate the importance of each weather-related item (on a scale ranging from 1=very low importance, to 6=very high importance).

In the level of satisfaction part, controllers were demanded to express their level of satisfaction about hazardous weather data provided by current displays. The items presented in this part of the questionnaire were: Wind Shear, Turbulence, Thunderstorm, Low Ceiling, Low Visibility, CB, Icing, Jet Stream and Mountain Waves. Controllers were asked to rate the level of satisfaction of those weather items (on a scale ranging from 1=very poor to 6=very good).

The last part of the questionnaire concerned 3D weather visualization. Prior to filling the questionnaire, controllers were given a demonstration of our 3D-ATC prototype. Then they were asked to envision if 3D could more suitably provide weather information for supporting ATC tasks and to reply with a YES or NO answer to the questionnaire weather items (e.g. a YES next to the item Wind Shear, denote that 3D would be a useful option for displaying Wind Shear information). The choice was constrained, in that controllers had to indicate preferences considering the list of routine and hazardous weather items (presented in the previous section and consistently used throughout the questionnaire). In addition, ATCOs were asked to rate their level of interest in having a 3D representation with respect to any weather item of the questionnaire (a scale ranging from 1=very low interest, to 6=very high interest).

4.2 Demonstration of the 3D-ATC Prototype

The goal of the demonstration was to give controllers a basic understanding of the 3D representation of air space, air traffic (flight trajectory, waypoint and flight information (cf. Figure 3(a)) and in particular of weather visualization (wind and pressure, see Figure 3(b)) allowing them to envision potential applications of 3D displays for weather information.

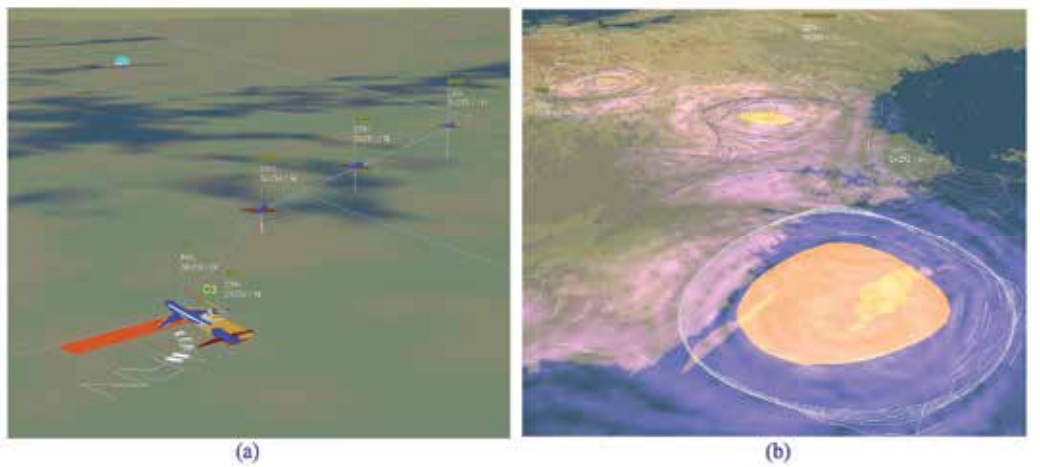

Fig. 3. (a) 3D presentation of flight, flight trajectory and flight information, (b) 3D Visualization of Wind and Pressure

The demonstration was run on a Linux based laptop (Dell Inspiron 9300 Pentium M 2GHz with a NVIDIA GeForce 6800 graphic card) and was shown to the controllers on a wall screen by using a projector. The 3D-ATC prototype was implemented using OpenGL.

4.3 Procedure

The survey was performed on-site. The questionnaires were given and the 3D Demo presented during controllers' rest time. In total we had four sessions spreading over one day. The total number of controllers involved in the study was 26 (ranging from 2 to 15 per session). An introduction script was written in advance and read at the beginning of each session. Then, the 3D demonstration had been shown for approximately 15 minutes, and it was kept running freely during the questionnaire filling phase.

Every controller filled in her/his own questionnaire independently and no verbal exchanges among controllers were allowed during this task. Controllers were allowed to ask questions and request explanations about the questionnaire from researcher. However, none did.

4.4 Participants

As stated above, 26 controllers participated in the survey. Among this sample, 10 were approach controllers and 16 en route controllers.

The age of the en route controllers ranged from 29 to 57 years (average 39.47 years) and their operational experience ranged from 4.33 to 23 years (average 11.83 years). Even though one in three had past experience in approach control, all the controllers assigned to the category of "en route" worked currently on en route positions, and has been since at least 4.33 years.

The age of the approach controllers ranged from 26 to 38 (average 33.10 years) and their operational experience ranged from 1.17 to 14 years (average 8.57 years).

5. Results

5.1 Routine Weather Information Needs

The results concerning routine weather information needs are summarized in Figure 4. Figure 4(a) shows the percentage of controllers who gave a "YES answer" for expressing their need to receive information about each given weather item. Figure 4(b) shows the median values of the importance ratings assigned by controllers to each weather item.

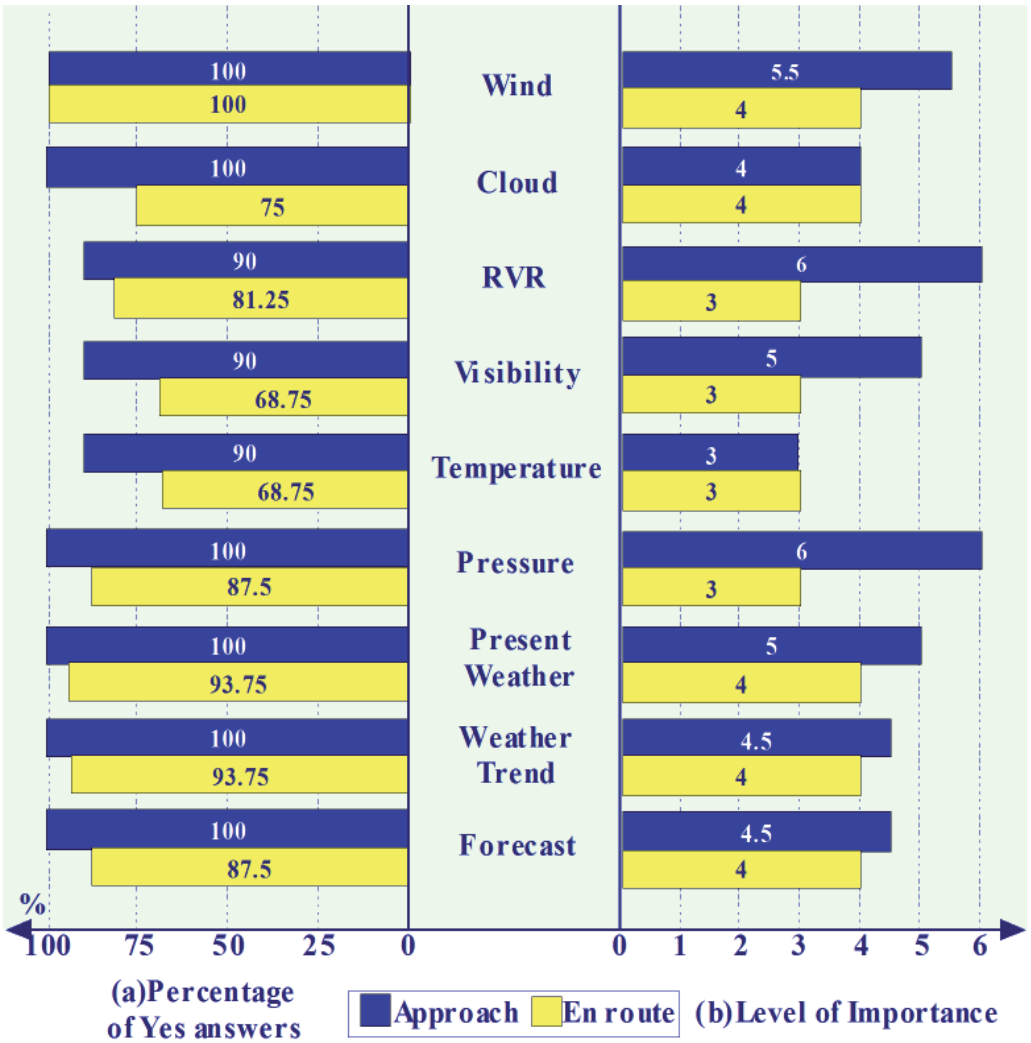

Fig. 4. Summary of Results for Routine Weather Information

As for the percentage values of "YES answers" - for each weather item - we can observe a somewhat different pattern of responses between approach and en route controllers. The percentage of "YES" given by approach controllers ranges from 90% to 100%; whereas those given by en route controllers range from 68.75% to 100%. The same pattern can be also

observed for the median values (see Figure 4(b)). Hence, we decided to find out whether any significant differences between the response patterns exist.
Because of the ordinal scales used in the questionnaire, the non-parametric test Mann-Whitney U test was used to compare the importance ratings given by en route and approach controllers for each weather item separately. As we did not have any specific hypothesis, we performed a two-tailed test. A $\propto$-level of .05 was chosen as decision criterion.
We found a significant difference between the importance ratings of Wind (Mann Whitney U=42.5, p=0.042, two-tailed test), RVR (U=9.0, p=0.000, two-tailed test), Visibility (U=15.0, p=0.007, two-tailed test), Pressure (U=21.0, p=0.003, two-tailed test), Present Weather (U=35.0, p=0.019, two-tailed test). A brief summary of these results is given in Table 1. No significant differences were found between the ratings given by approach and en route controllers for the items Cloud, Weather Trend, Forecast and Temperature.

	Median (Approach controller)	Median (En route controller)	P-value
Wind	5.5	4	0.042
RVR	6	3	0.000
Visibility	5	3	0.007
Pressure	6	3	0.003
Present Weather	5	4	0.019
Cloud	4	4	Non-significant
Weather Trend	4.5	4	Non-significant
Forecast	4.5	4	Non-significant
Temperature	3	3	Non-significant

Table 1. Routine Weather Importance Ratings Medians for Approach and En Route

These results are not surprising; it is quite evident that approach and en route controllers have different routine weather information needs that correspond to different operational requirements. And these differences were well captured by the questionnaire and revealed by the analysis. For instance, approach controllers assigned to the items RVR, Pressure, Wind, Visibility, and Present Weather ratings, ranging from 5 to 6 (i.e. high and very high importance). It is rather obvious that this type of weather data is not only useful, but also necessary for the management of inbound and outbound air traffic. Thus, for example, if weather and visibility conditions of the final aerodrome destination are extremely adverse, approach controllers might decide to divert aircraft to nearby airports.

By way of contrast, overall en route controllers assigned lower importance ratings, ranging from 3 to 4 (i.e. from rather low to rather high). This is a clear indication that approach and aerodrome-related weather information (e.g. RVR, Visibility, etc.) is not a major concern for control in upper airspace. However, Weather Forecast and Trends seem to be important also to en route controllers, at least to the extent to which projections on hazards are enabled. Indeed this idea seems quite realistic, if we have a look at the data reported in the next section.

5.2 Hazardous Weather Information

Figure 5(a) shows the percentage of controllers who gave a "YES answer" on their need to receive information about each of the different hazardous weather item, whereas Figure 5(b) shows the medians of importance ratings assigned by controllers to each item.

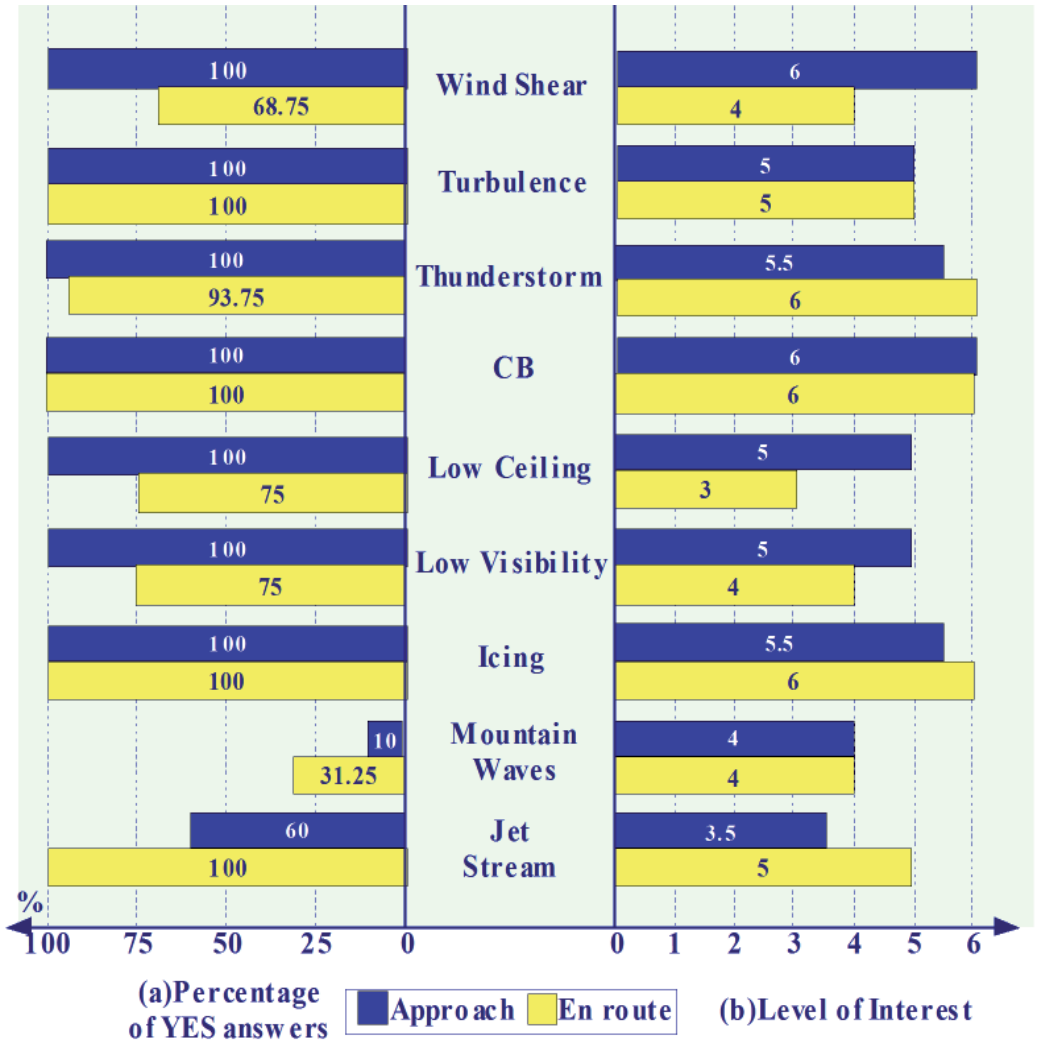

Fig. 5. Summary of Results for Hazardous Weather Information

Note that the item Mountain Waves was rated by a small percentage of controllers (10% approach and 31.25% en route). This weather occurrence is a phenomenon typical of mountain regions, which does not involve the airspace of Swedish centre that we visited. Also note that there is a clear disparity between the percentages of "YES answers" given by approach and en route with respect to the item "Jet stream". This is easily justified by the fact that the Jet stream is characteristic to high altitudes, and thus only relevant in en route.

Besides those two items, the remainder of responses shows a homogeneous pattern between the two groups. Nevertheless, we performed a comparison between the importance ratings assigned by approach and en route controllers.

We found a significant difference between the importance ratings of Wind Shear (Mann Whitney U=13.0, p=0.002, two-tailed test), Low Ceiling (U=28.5, p=0.032, two-tailed test), and Low Visibility (U=24.5, p=0.016, two-tailed test). This is summarized in Table 2. No significant differences were found between the ratings given by approach and en route controllers for the items Turbulence, Thunderstorm, CB, Icing, Mountain Waves and Jet Stream.

	Median (Approach controller)	Median (En route controller)	P-value
Wind Shear	6	4	0.002
Low Ceiling	5	3	0.032
Low Visibility	5	4	0.016

Table 2. Hazardous Weather Importance Ratings Medians for Approach and En Route

Coherently with the results discussed in the previous section, specific information related to weather hazards entailing the approach (i.e. Low Visibility, Low Ceiling and Wind Shear) was rated significantly higher by approach controllers. However, when we consider hazards like Turbulence, Thunderstorm, Icing and CB we notice two things. First, both en route and approach controllers gave fairly high ratings to these items. Second, for these items no differences exist between the ratings given by the two groups of controllers. Hence, these weather phenomena have a relevant impact on control activities independently from the specific working context, and may represent a factor contributing to the complexity of ATC tasks (Pawlak et al., 1996). We therefore hypothesize that complexity could be reduced by an adequate representation of those hazardous weather phenomena, as well as a suitable projection of the forth-coming hazards. In order to gain insights on this issue, the questionnaire requested controllers to express their level of satisfaction concerning the way weather hazards are currently displayed and represented.

5.3 Satisfaction with Available Displays

Figure 6 shows the medians of satisfaction ratings assigned by controllers to the display of each hazardous weather item.

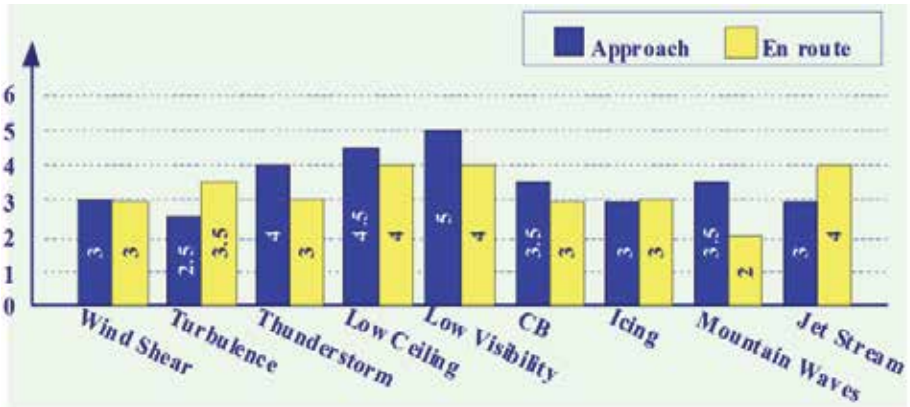

Fig. 6. Summary of Results for Satisfaction Ratings about Current Displays for Hazardous Weather Information

The way Low Ceiling and Low Visibility information is currently represented in the displays available at the Swedish control centre, was judged as being quite adequate and show median ratings of 4.5 and 5 respectively. Jet Stream, at least with respect to en route controllers, has a median satisfaction rating of 4 and the median for Thunderstorm (for approach controllers) is 4.

	Approach controller		En route controller	
	Need	Satisfaction	Need	Satisfaction
CB	6	3.5	6	3
Thunderstorm	5.5	4	6	3
Turbulence	5	2.5	5	3.5
Icing	5.5	3	6	3
Wind Shear	6	3	4	3
Jet Stream	3.5	3	5	4

Table 3. Comparable Results between Need and Satisfaction on Different Hazardous Weather Information

The interesting result here is that critical weather items that are both highly and equally important for approach and en route controllers (i.e. Wind Shear, Turbulence, CB, and Icing), are not suitably represented in current displays and median satisfaction ratings for these items range from 2.5 to 3.5. Such poor ratings were given by both controllers groups, and no statistically significant differences were found between the ratings given to those items.

Table 3 shows clearly the contrast between the weather information needs and the level of satisfaction of current displays on CB, Thunderstorm, Turbulence, Icing, Wind Shear and Jet Stream.

Informal discussions with controllers, especially during the 3D demonstrations, and comments written by controllers, helped us to gain some insights on how to improve the visualization of critical weather information.

5.4 3D for Hazardous Weather: A Suitable Option?

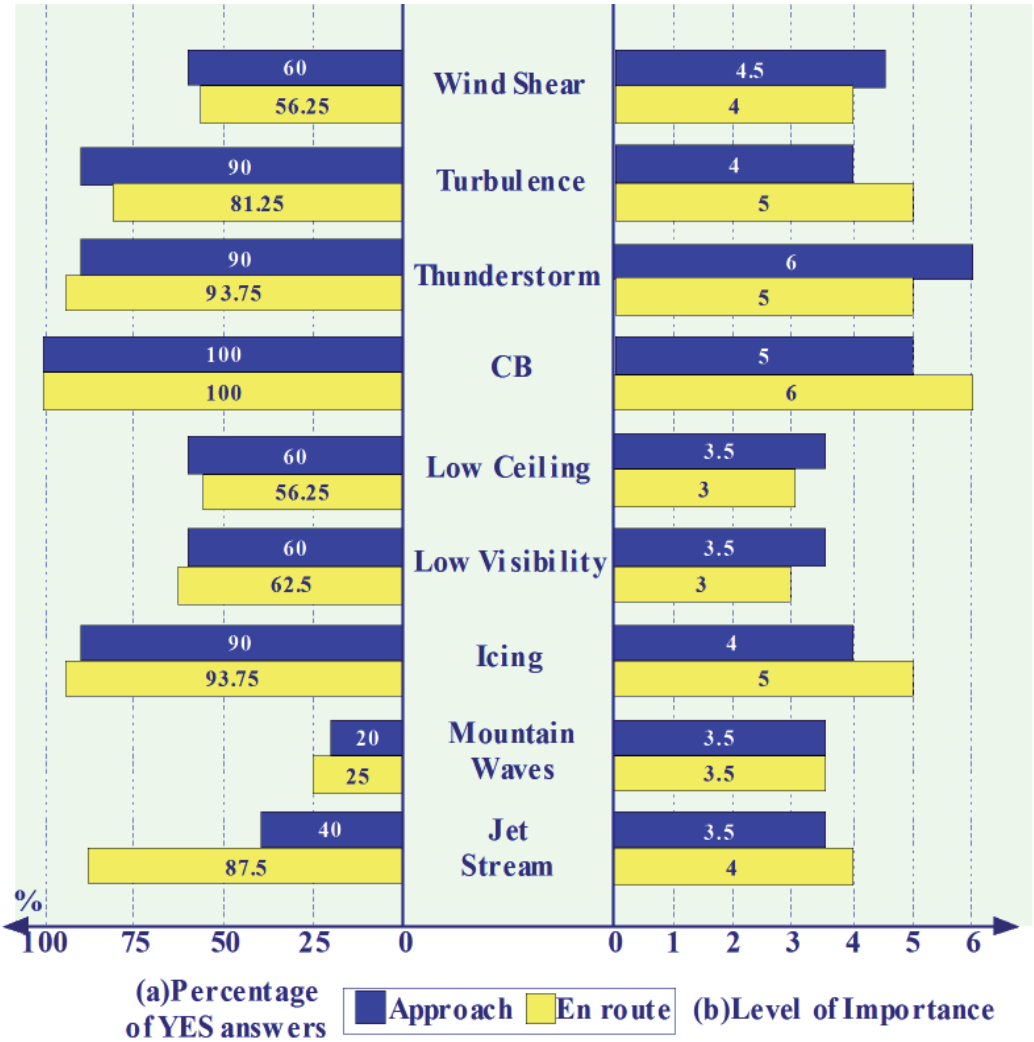

Fig. 7. Summary of Results for 3D Visualization of Hazardous Weather Information

As stated above, a part of the questionnaire was dedicated to collecting controllers' opinions about their interest in having weather information displayed in 3D. Overall, controllers (both en route and approach) expressed high interest in 3D representations of weather phenomena, especially with respect to the critical weather items that are not adequately supported by current displays.

Figure 7(a) shows the percentage of controllers who provided a "YES answer" for having 3D visualizations for any of the hazardous weather items. Whereas Figure 7(b) shows the medians of importance ratings assigned by controllers to each hazardous weather item that should be displayed in 3D.

CB formation, Thunderstorm, Turbulence, Icing, Wind Shear and Jet Stream show median ratings ranging from 4 to 6 and the data reported in Table 4 gives useful insights for focusing the research on 3D weather visualization for ATC, both for en route and for approach.

	Approach controller			En route controller		
	Need	Satisfaction	3D	Need	Satisfaction	3D
CB	6	3.5	5	6	3	6
Thunderstorm	5.5	4	6	6	3	5
Turbulence	5	2.5	4	5	3.5	5
Icing	5.5	3	4	6	3	5
Wind Shear	6	3	4.5	4	3	4
Jet Stream	3.5	3	3.5	5	4	4

Table 4. Comparable Results among Need, Satisfaction and 3D Option for Different Hazardous Weather Information

Controllers were quite curious about the possibility of visualizing 3D weather information, and provided numerous comments and suggestions, both written (in the questionnaire) and verbal, during the 3D demonstration. This additional information can be summarized as follow.

Controllers clearly stated that, not only cumulonimbus but also towering cumulus (TCU) has a three-dimensional nature. Directing aircraft so as to avoid these weather formations could be enhanced by providing a representation that highlights certain 3D features such as volume extension, location with a spatially coherent configuration. In addition, both approach and en route controllers stated that these weather phenomena are early stages of thunderstorms. According to controllers, dynamic and anticipated projections of such 3D weather images would be quite beneficial for promptly defining re-routing strategies for directing flights out of thunderstorm zones.

Another interesting result is that controllers stated that having a 3D representation of the out-of- cockpit view, at any given moment, would be quite useful. According to ATCOs, if pilots and controllers could have a common and shared understanding of the same information, then elaborating effective plans and providing appropriate instructions would be enhanced.

In general, controllers do not seem satisfied with interfaces that show too many widgets, windows, and features, but a problem with 3D displays is visual information clutter. Some controllers declared that having a detailed 3D view of air traffic (as the one shown during the demonstration, with visible trajectories, waypoints, and other flight information) would look “too crowded”. And yet, controllers suggested that 3D weather visualization could support weather-related tasks, if the possibility of displaying 3D images is provided upon demand. This would allow having a more detailed depiction of 3D weather data only under the conditions specified by the end-users themselves.

6. Conclusions and Future Work

The present work aimed to discover controllers weather information needs and assess if 3D weather visualization could provide added benefits to controllers. The results of the survey can be summarized as follows.

There are several differences in the weather information needs between en route and approach controllers, which logically reflect the different focus of activities carried out by each group of controllers. For example, approach controllers need very specific knowledge such as Wind, RVR, Visibility, etc. that is not normally required to en route controllers (at least, in the light of the results that we obtained). This fact has to be considered for the design of ATC weather interfaces, for example, by conceiving dedicated and customized weather representations that are suitable for the tasks that controllers actually perform. By this, we do not mean that information should be hidden from controllers; more simply, we claim that interfaces should avoid displaying unnecessary data and, eventually, providing extra information only upon request.

Moreover, according to the results of this study, both en route and approach controllers seem to value and use critical weather information such as CB, Thunderstorm, Turbulence and Icing. As we stated in the previous sections, hazardous weather information has direct impact on the safety and efficiency of air traffic. Devising visual techniques for allowing controllers to perform "ahead assessments" about weather hazards, could support controllers in identifying in advance strategic solutions for responding to the restrictions imposed by weather on upper space sectors, terminal areas and aerodromes.

Controllers declared having a quite low degree of satisfaction about the displays currently used for hazardous weather information. In particular, both en route and approach controllers gave low scores to very critical weather data such as Wind Shear, Turbulence, CB and Icing. Suitable representations as well as projections of adverse weather events seem missing. We suppose that the solely textual representation largely contributes to this result and, perhaps, graphical information could better suit controllers´ needs, independently from the interface style (either 2D or 3D). But, controllers' comments gave promising insights on the use of 3D as a more intuitive representation of hazardous weather.

However, at this stage of the study, we can only accept controllers' comments as they are, hence, these ideas remain hypotheses that need further investigation.

Short-term plans for continuing this research entail the implementation of a small mock-up of CB formation embedded into a sector with a realistic traffic flow. The choice of CB is justified by the fact that controllers expressed a high interest for having 3D representations of cumulonimbus and further stressed this interest in an explicit manner, adding comments in the questionnaire and during informal talks.

We intend to perform additional demonstration sessions showing this new implementation and carrying out in-depth interviews with controllers, in order to understand what the supposed benefits of 3D weather images would be. Perhaps there are some specific visual properties of 3D weather representations that could indeed enhance controllers' tasks. Understanding what these visual properties are, would give us sufficient information for defining the functional requirements of a more refined 3D prototype.

7. Acknowledgment

The author would like to thank Monica Tavanti, Matt Copper, and Marc Bourgois for providing corrections, precious comments, and useful suggestion. The author wishes to thank Team Manager Adam Lassen, ACC controller Christopher Vozmediano, TMC controller Lena Palmqvist who helped him to conduct this study and all the controllers at Air Traffic Control Centre STOCKHOLM who participated in the survey. This work was supported by the Strategic Research Center MOVIII, funded by the Swedish Foundation for Strategic Research (SSF) and by the EUROCONTROL Experimental Centre.

8. References

Ahlstrom, U., Rubinstein, J., Siegel, S., Mogford, R., Manning, C. (2001). *Display concepts for en route air traffic control* (DOT/FAA/CT-TN01/06). Atlantic City International Airport: Federal Aviation Administration William J. Hughes Technical Center.

Ahlstrom, U. & P. Della Rocco (2003). *TRACON controller weather information needs: I. Literature review* (DOT/FAA/CT-TN03/18). Atlantic City International Airport: Federal Aviation Administration Technical Center.

Ahlstrom, U., & Arend, L. (2005). Color usability on air traffic control displays. *Proceedings of the Human Factors and Ergonomics Society 49th Annual Meeting* (pp. 93-97). Santa Monica, CA: Human Factors and Ergonomics Society.

FAA (2002). *Mission need statement for aviation weather (MNS #339)*. Washington, DC: Office of Research and Requirements Development.

Bourgois, M., Cooper, M., Duong, V., Hjalmarsson, J., Lange, M., Ynnerman, A. (2005). Interactive and Immersive 3D Visualization for ATC. *Proceedings of ATM R&D 2005*.

Boyer, B.S. & Wickens, C.D. (1994). *3D weather displays for aircraft cockpit*, ARL-94-11/NASA-94-4. Aviation Research Laboratory, Savoy, IL.

Cechile, R.A., Eggleston, R.G., Fleishman, R.N., & Sasseville, A.M. (1989). Modeling the cognitive content of displays. *Human Factors*, 31, 31-43.

Chornoboy, E. S., Matlin, A. M., and Morgan, J. P. 1995. Automated storm tracking for terminal air traffic control. *Lincoln Lab*. J. 7, 2 (Sep. 1995), 427-448

Forman, B. E., Wolfson, M. M., Hallowell, R. G., & Moore, M. P. (1999). Aviation user needs for convective weather forecast. *American Meteorological Society 79th Annual Conference* (14.4). Dallas, TX.

John, M.S., Cowen, M. B., Smallman, H. S., & Oonk, H. M. (2001). The use of 2-D and 3-D displays for shape-understanding versus relative-position tasks. *Human Factors*, 43(1), 79-98.

Kauffmann, P., and Pothanun, K. (2000). *GAA17 - Estimating the Rate of Technology Adoption for Cockpit Weather Information Systems*. Old Dominion University. Society of Automotive Engineers, Inc.

Lange M., Hjalmarsson J., Cooper M., Ynnerman A., and Duong V. (2003). 3D Visualization and 3D Voice Interaction in Air Traffic Management. *Proceedings of the Annual SIGRAD Conference*, special theme Real Time Simulations, 17-22.

Lange, M., Dang, N.T., Cooper, M. (2006). Interactive Resolution of Conflicts in a 3D stereoscopic Environment for Air Traffic Control. *Proceedings of the 4th IEEE International Conference on Computer Sciences*- RIVF'06.

Lindholm, T. A. (1999). Weather information presentation. In D. J. Garland, J. A. Wise, & V. D. Hopkin (Eds.), *Handbook of aviation human factors* (pp. 567-589). Mahwah, NJ: Erlbaum.

NBAAD (1995). Weather reports should be higher priority for air traffic control. *National Business Aviation Association Digest*, 8(11). Retrieved January 21, 2007 from http://www.nbaa.org/digest/1995/11/atc.htm

Pawlak, W. S., Brinton, C. R., Crouch, K. & Lancaster, K. M. (1996). "A Framework for the Evaluation of Air Traffic Control Complexity", *Proceedings of the AIAA Guidance Navigation and Control Conference*, San Diego, CA.

Pruyn, P.W. & Greenberg, D.P. (1993). Exploring 3D Computer Graphics in Cockpit Avionics, *IEEE Computer Graphics and Applications*, Vol. 13, No. 3, May/June 1993, pp. 28-35.

Spirkovska, L. & Lodha, S.K. (2002). Awe: Aviation weather data visualization environment. *Computers and Graphics*, 26(1).

Whatley, D. (1999) *Decision-Based Weather Needs for the Air Route Traffic Control Center Traffic Management Unit*. Accessible at www.srh.noaa.gov/srh/cwwd/msd/sram/pace/TMUneeds.pdf

Wickens, C. D., Campbell, M., Liang, C. C., & Merwin, D. H. (1995). *Weather displays for Air Traffic Control: The effect of 3D perspective* (DTFA01-91-C-00045). Washington, DC: Office of Systems Operations and Engineering.

Wickens, C.D., Merwin, D.H., & Lin, E. (1994). The human factors implications of graphic enhancements for the visualization of scientific data: Dimensional integrality, stereopsis, motion, and mesh. *Human Factors*, 36, 44-61.

Wickens, C.D. (1984). *Engineering psychology and human performance*. Columbus, OH: Charles E. Merrill.

Ziegeler, S., Moorhead, R. J., Croft, P. J., and Lu, D. (2001). The MetVR case study: meteorological visualization in an immersive virtual environment, *Proceedings of the Conference on Visualization '01* (San Diego, California, October 21 - 26, 2001). VISUALIZATION. IEEE Computer Society, Washington, DC, 489-492.

7

Development of a Time-Space Diagram to Assist ATC in Monitoring Continuous Descent Approaches

M. Tielrooij, A. C. In 't Veld, M. M. van Paassen and M. Mulder
Control and Simulation Division
Faculty of Aerospace Engineering
Delft University of Technology
The Netherlands

1. Introduction

Continuous Descent Approaches (CDA) have shown to result in considerable reductions of aircraft noise during the approach phase of the flight (Erkelens, 2002). Due to uncertainties in aircraft behaviour, Air Traffic Control (ATC) tends to increase the minimum spacing interval in these approaches, leading to considerable reductions of runway capacity (Clarke, 2000). To enable the application of such procedures in higher traffic volumes, research has advanced in the creation of airborne tools and 4-dimensional prediction algorithms.
Little research has addressed the problem of sequencing and merging aircraft in such an approach, however. In this chapter we present the Time-Space Diagram (TSD) display that shows the aircraft along-track distance to the runway versus the time. On this display, the in-trail separation is presented as the horizontal distance between two predictions. It is hypothesised that this display will enable the air traffic controller to meter, sequence and merge aircraft flying a CDA at higher traffic volumes. In this chapter, the TSD will be introduced and the effects of various common separation techniques on the predictions of the display are discussed in detail. The display is currently being evaluated by actual air traffic controllers in a simulated traffic scenario to provide an initial validation of the design.

2. Problem statement

Aircraft noise is considered to be the most important cause of resistance to increases of flight operations and the expansions of airports (Dutch Ministry of Transport, Public works and Water Management, 2006; UK Dept. for Transport White Paper, 2003). CDA's such as the Three-Degree Decelerated Approach (TDDA) have shown to considerably reduce the aircraft noise footprint during approach (Clarke et al., 2004). In this particular procedure, aircraft descend along a continuous 3° glide slope at idle thrust (Clarke, 2000; De Prins et al., 2007).
The speed profiles of the descending and decelerating aircraft, however, are highly influenced by the aircraft types involved, the atmospheric conditions (wind in particular), and crew responses. The nature of the procedure, combined with the uncertainties in predicting the air-

craft trajectories, currently require air traffic controllers to increase initial spacing to assure separation throughout the approach (Clarke, 2000; Erkelens, 2002).
The 3° glide slope further requires the aircraft to fly a fixed lateral route from the top of descent (TOD). After this point, ATC can no longer give lateral instructions without compromising the TDDA. Once idle thrust is selected, the aircraft will not be able to change its speed profile without increasing thrust, or changing its configuration, and speed instructions from air traffic controllers are highly undesirable. In the example of a TDDA procedure starting from 7,000 ft (Clarke, 2000; De Gaay Fortman et al., 2007), this prevents ATC instructions from 22.1 nm to the threshold. Therefore, ATC has to space aircraft accurately beforehand, in such a way than the separation will not fall below the minimum required throughout the remainder of the approach. In order to do so accurately, controllers must be able to predict the future spacing over the remaining aircraft trajectory from the current aircraft position to the runway, and work on these predictions. Without some automated support, however, this is an impossible task.
The objective of this chapter is to discuss the potential benefits of a novel display for air traffic controllers. The Time-Space Diagram (TSD), as it is called, provides the aircraft 4-dimensional trajectory information to the controller. To this end, these predictions will be assumed available, and the means nor the accuracy of such predictions will be addressed within the scope of this work. It will be shown that when the aircraft trajectory predictions are available, the problem is reduced to one of obtaining a meaningful graphical representation.
The chapter is structured as follows. Section 3 will explain the task of ATC and the current availability and use of 4-dimensional trajectory information. Section 4 describes how, by reducing the 4-dimensional problem to a two dimensional one, the controller can be provided with the predicted separation on a two-dimensional display. The effect of instructions given by ATC to aircraft can now be translated to changes of the representation of the trajectory. The implementation of the display would require some adjustments to current procedures. As this display can only show trajectories to one runway, separation from other traffic needs to be ensured by other means.

3. ATC in CDA procedures

According to Annex 11 to the Convention on Civil Aviation (ICAO, 2003), the primary goal of ATC is to provide service for the purpose of safe, orderly and expeditious flow of traffic. In approach control, this task can be described as minimising delays while maintaining sufficient separation between the aircraft. During the TDDA, the in-trail distance between two approaching aircraft should therefore reach, but not go below, the minimal distance required. To achieve this, the primary tool common to all approach controllers is the two-dimensional Plan View Display (PVD). This screen shows the, mostly radar-derived, planar positions of the aircraft combined with numeric data on their velocity and altitude. Using this data, the Air Traffic Controller (ATCo) builds a mental model of the traffic scenario, commonly referred to as the "picture" (Nunes & Mogford, 2003). By mentally predicting the trajectories of the aircraft on the screen, the controllers can anticipate on the future spacing and select the appropriate actions to adjust spacing if necessary. The certainty of predicting the aircraft future positions depends on the skill of the controller, the behaviour of the aircraft involved and the length of the interval over which the prediction is made (Reynolds et al., 2005).

3.1 Controller prediction accuracy in TDDA

In a TDDA, aircraft will decelerate at different rates. Research with actual controllers has shown that humans perform rather poorly in estimating separation in such scenarios (Reynolds et al., 2005). Furthermore, it is likely that approach routes merge within a distance of 22nm from the runway threshold. Two aircraft that land in sequence might not need to be in trail at their TOD. The actual spacing may therefore not be observable from the conventional PVD.
Implementation of continuous descent procedures requires controllers to predict spacing over a longer horizon with a reduced certainty of aircraft behaviour. In implemented CDA procedures at Amsterdam Schiphol airport, ATC was required to increase the landing interval from 1.8 to 4 minutes (Erkelens, 2002). Currently, the resulting 50 percent reduction of capacity prevents the use of the procedure outside night hours, as the required daytime capacity can not be met (Hullah, 2005).

3.2 4D Navigation technologies

Developments in aircraft Flight Management Systems, communications and prediction algorithms enable new procedures which are based on four-dimensional trajectory predictions. In flight trials at Amsterdam (Wat et al., 2006) and San Francisco (Coppenbarger et al., 2007), long term predictions have shown to achieve accuracies in the order of seconds when predicted at cruise level. In those trials, ATC provided CDA-clearances based on those predictions. The availability of 4D trajectory predictions and the ways to communicate them, have proven to be technologically feasible.
Research at Delft University of Technology has shown promising results in maintaining separation during CDA procedures using airborne trajectory prediction. In these trials, pilots were provided with the predicted spacing with the aircraft in front of them (In 't Veld et al., 2009). Using this information, the pilots could adjust their speed profile to achieve but not go below minimal separation.
However, research has also shown that such procedures will only achieve optimal spacing when the initial spacing is already close to that optimum (De Leege et al., 2009). Furthermore, these scenarios have assumed all aircraft on a single approach path, not requiring merging of different streams. If ATC is to assist such procedures, it will have to establish this optimum spacing by metering and merging all aircraft from all routes.

3.3 4D Information available to ATC

The current approach control systems use – ground-based – 4D predictions. These predictions mostly provide controllers with Estimated Time of Arrival (ETA) at the runway threshold. Using the prediction at the threshold, the controller can then establish the required spacing.
Spacing using these tools implicitly requires that minimal separation is achieved at the threshold. Analysis of different aircraft in TDDA scenarios has shown that minimal separation might occur at an earlier point in the approach (De Leege et al., 2009). When the tools indicate a predicted separation violation, the controller is not aware of the moment at which this violation occurs for the first time. Therefore, controllers can not apply an appropriate technique to adjust spacing as one has no indication of the available time and distance.

4. Providing predicted spacing information to ATC

The current ATC system relies on flexible routing of aircraft in the final stages of the approach. In this segment, ATC uses procedures which are often only defined the local ATC manuals.

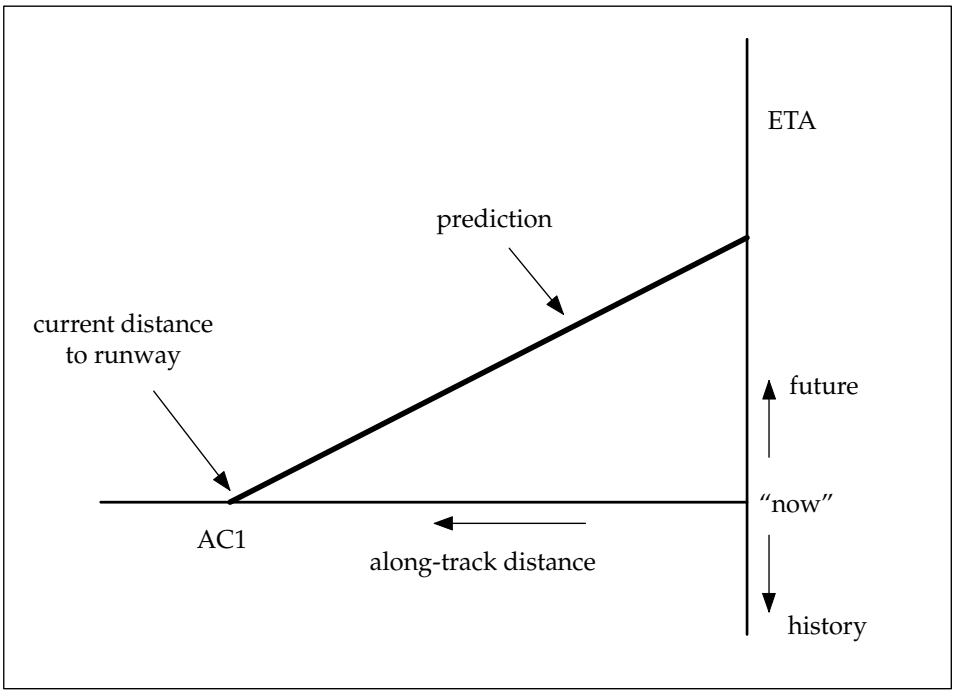

Fig. 1. The basic elements of the Time-Space Diagram (TSD).

Using these procedures, the approach controller is capable of metering, sequencing and merging the inbound flows of aircraft while maintaining separation.
The need for more consistent routing has prompted a move toward more rigid trajectories (EUROCONTROL, 1999). By 2006, over 1,500 aircraft in the European airspace were compliant to this navigation standard, which included 95% of the flights at airports like Amsterdam Schiphol and London Heathrow (Roelandt, 2006). With the advent and progressive implementation of Precision-Area Navigation (P-RNAV), and hence predictable and feasible lateral trajectories, more complex procedures like the TDDA may be realised (Erkelens, 2002).

4.1 Time-Distance Diagram

As the TDDA has a known lateral and vertical trajectory, the position of the aircraft can be defined by its distance to the runway. For all aircraft, the TSD (De Jong, 2006) plots the aircraft's distance to the runway versus the expected time at that distance, see (Figure 1). The figure shows a situation where an aircraft flies at constant ground speed to the runway. Typically, aircraft decelerate during the approach which would mean that the trajectory prediction in time/space is not a straight line but curved. Flying faster means that the line becomes less steep, as more ground is covered in less time. Flying slower means that the curve becomes more steep, as here less ground is covered per unit of time. Note that although only straight lines are shown in the following figures, to illustrate the basic concepts, generally the time/space trajectories of decelerating aircraft will be curved more steeply when closer to the runway threshold.

When the time/space trajectory can be shown for one aircraft, based on the trajectory predictions, the same can be done for the other aircraft. Consequently, the required in-trail separation distance can be represented as an *area* between a particular aircraft pair. Figure 2(a) shows this area, created by offsetting the leading aircraft's prediction with the distance required between the two aircraft. The goal of the controller will now be to avoid any trajectory to fall within such a separation area of another trajectory.
When a prediction falls within the separation area, a separation violation occurs. However, this does assume that both aircraft are on the same trajectory. When two aircraft are on different, but merging, routes this assumption is not valid. The conflict occurs when both aircraft have joined the common remainder of their approach. To indicate this point, the different tracks are represented below the graph, see Figure 2(b), with an indication of the aircraft on the horizontal line representing its route. For a conflict that starts when two aircraft merge, the location of that merging point indicates the remaining time and distance to resolve a predicted conflict. Using this information, the controller can select an appropriate technique to adjust spacing.
The required in-trail separation between the approaching aircraft is mainly dependent on the aircraft wake turbulence categories. The size of this separation area depends on the types of aircraft involved. To enable an early assessment of changing the aircraft arrival sequence, all possible separation minima behind the aircraft are indicated. The target separation distance, based on the *current* sequence at the threshold, is indicated by a fill area (Figure 3).

5. ATC options on the TSD

When instructions from the ATCo are executed, the predictions change according to the new state of the aircraft. This state includes the aircraft positions and velocities, as well as the changed speed profile and lateral trajectory. The instructions can now be divided into three categories based on their effect on the 4-dimensional trajectory.

5.1 Speed instructions

An *increase* of speed is unlikely during the approach phase of the flight. A speed instruction during approach will therefore imply the reduction of the constant speed before the deceleration phase of the TDDA. The reduction of speed translates to the increase of the slope of a prediction. Figure 4 shows two possible scenarios in which merging traffic is predicted to conflict. A similar application of speed reduction in both situations only resolves the conflict in one of the two scenarios. The figure also demonstrates the advantage over an indication of the arrival time only. Both situations are resolved and identical at the threshold, but Figure 4(d) shows that a conflict is still predicted at the merging point. In this figure, note that in all cases the effect of the speed instruction was identical in arrival times and resolved the conflict at the runway threshold. An indication of the separation at only the runway threshold would not have indicated the existence of the last conflict.

5.2 Changes to the planned route

The use of P-RNAV trajectories does not prevent the use of lateral instructions. As long as those instructions are given before the TOD of the TDDA, they can be used for spacing purposes. Crucial in this technique is the direct inclusion of the new routing in the prediction.
The second set of conflict possibilities includes 'directs to' waypoints further down the route, effectively providing shortcuts, see Figures 5(a) and 5(b). This set also includes holding patterns that consist of a known lateral trajectory. In the first case, the predictions will instantly

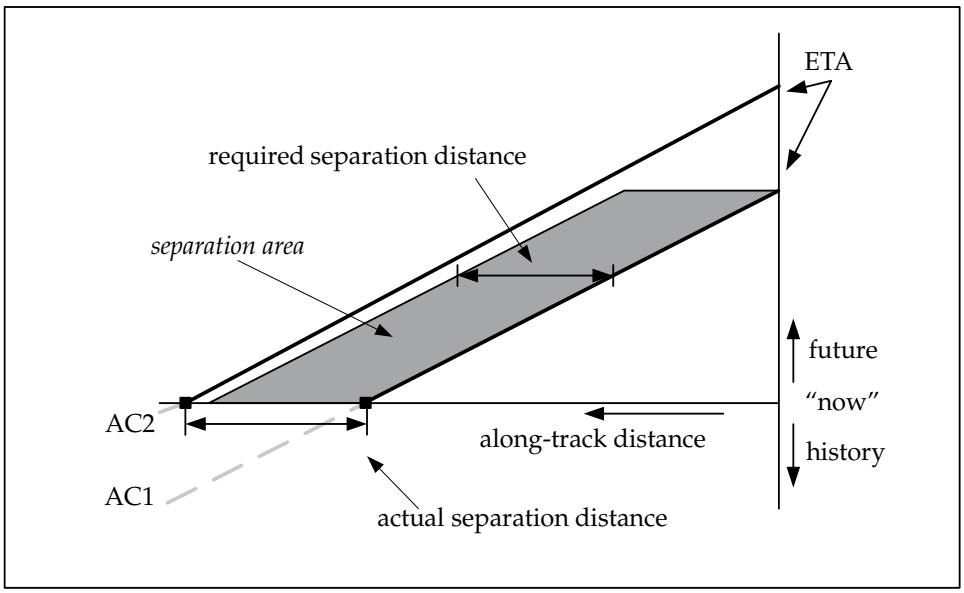

(a) The basic Time-Distance representation. Note that all predictions are drawn as straight lines for the sake of clarity.

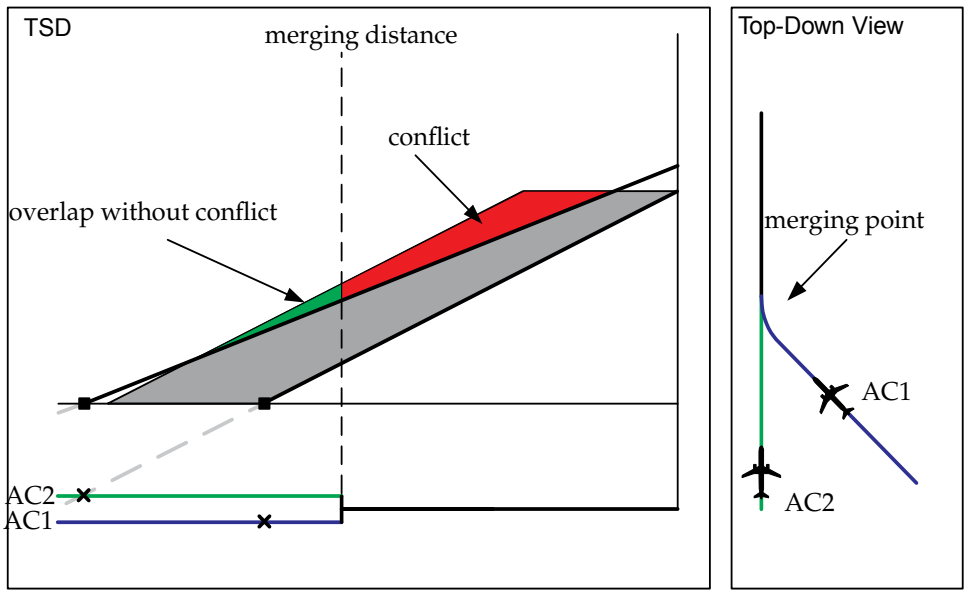

(b) Overlapping predictions that indicate a conflict once both aircraft have merged on the common remainder of the approach. The positions of the aircraft are indicated on the 'now'-axis as well as on the line representing their routes.

Fig. 2. The Time-Space Diagram concept, including separation minima. Note that here and in the following figures, the 'top-down' views are included for the sake of explanation, they are not included in the TSD.

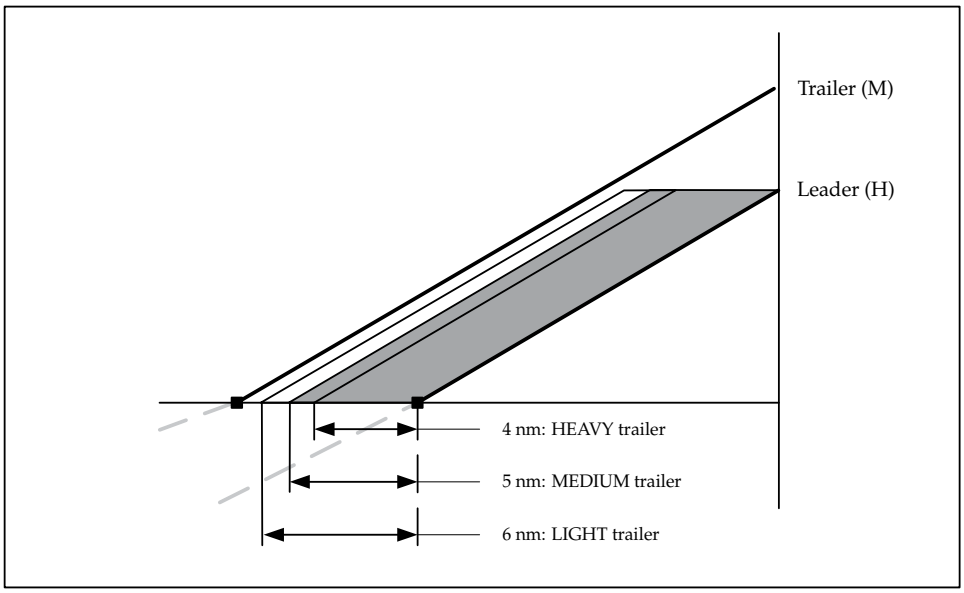

Fig. 3. The indication of separation minima based on wake turbulence categories. The current pair of aircraft (HEAVY (H) leader, MEDIUM (M) trailer) requires an in-trail separation of 5 nm according to ICAO Doc 4444 - PANS-ATM Section 8.7.4.

shift to the left on the TSD. In the latter, the prediction will instantly shift to the right, see Figures 5(c) and 5(d).

5.3 Temporarily abandoning the planned route

In current approach operations, many separation adjustments are done using vectors. The aircraft are issued a heading and will be returned to the planned route when the required spacing is attained. Although such heading instructions reduce the correlation between the distance to the runway and the location of the aircraft, they can be used in combination with the display. These instructions require the aircraft to predict the lateral trajectory starting at their present position and heading. The initial segment of the trajectory then includes a return to the route and the continuation of the route at that point, see (Figure 6). The advantage of this technique is that the separation is adjusted smoothly and the controller does not need to estimate the size of the shifts made in the speed and routing instructions.

6. Safety issues

The TSD only shows the in-trail spacing between aircraft that fly toward the same runway. It is not possible to provide a meaningful representation of other aircraft on the display. Furthermore, sufficient in-trail separation does not imply that the aircraft are actually separated. The latter can be demonstrated by two examples. Figure 7 shows a geometry that might provide sufficient along-track separation while the aircraft are actually flying head-on. A second problem occurs when the ground track intersects itself. This might be needed in confined airspace such as when in the vicinity of mountainous terrain. In such procedures, vertical separation is

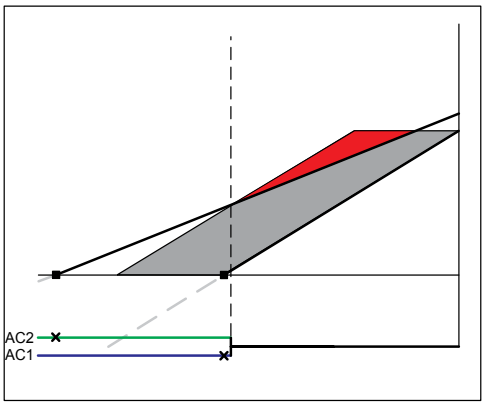

(a) Conflict 1: Aircraft 2 flies faster than aircraft 1.

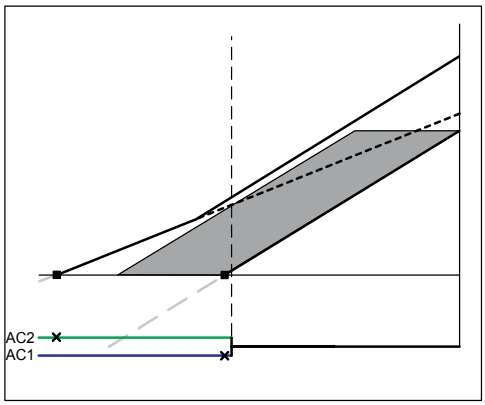

(b) Resolution 1: By reducing the speed of aircraft 2, the conflict is resolved.

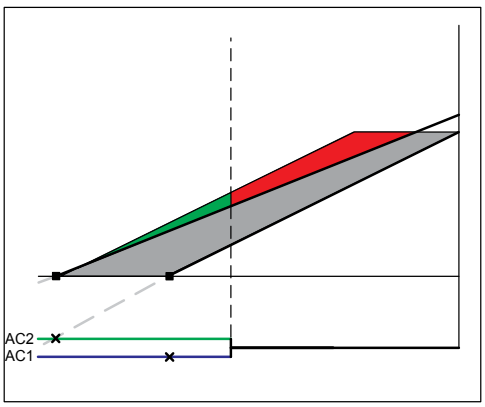

(c) Conflict 2: Similar to conflict 1, but now aircraft 1 is flying a little faster and the initial separation is smaller. A conflict occurs when both aircraft merge on the remaining track.

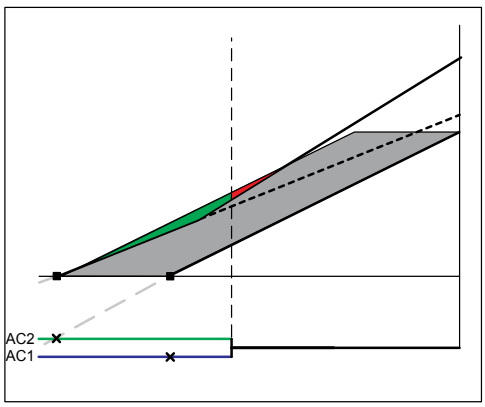

(d) Resolution 2: A separation violation still occurs after the aircraft have merged.

Fig. 4. Conflicts' resolution through a speed reduction. The slanted dashed lines in the right hand figures represent the original aircraft trajectories.

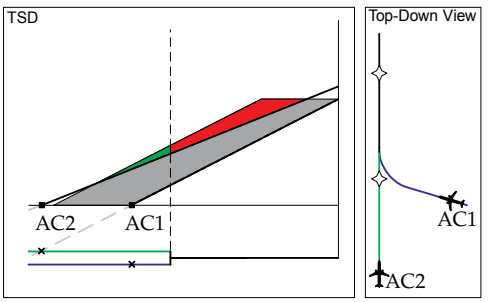

(a) Conflict 3: aircraft 2 flies faster than aircraft 1, and a conflict occurs when both aircraft merge on the remaining track.

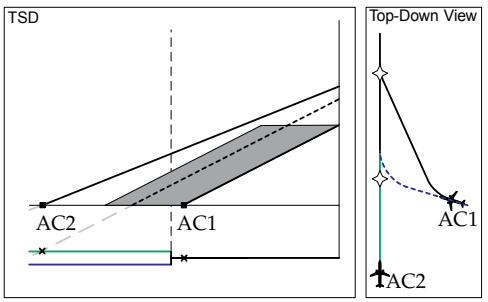

(b) Resolution 3: aircraft 1 is directed to the next waypoint and shortens its route to the runway.

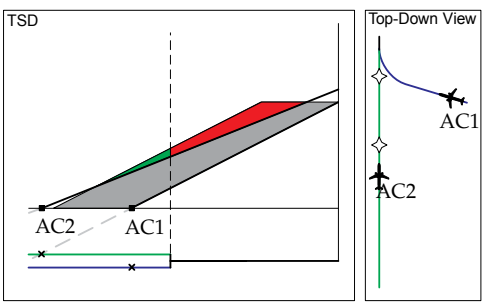

(c) Conflict 4: a situation identical to conflict 3.

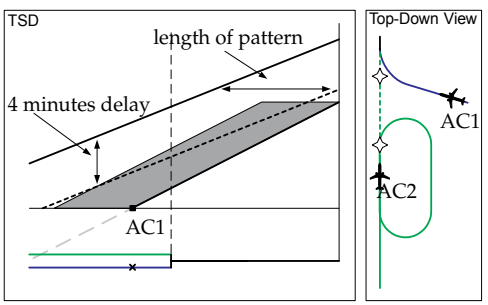

(d) Resolution 4: aircraft 2 is instructed to enter the holding pattern, delaying it by 4 minutes. The delay is indicated by a shift upward of 4 minutes (or, equivalently, a shift to the left by the path length of the holding pattern).

Fig. 5. Conflicts' resolution through lateral instructions. The first resolution provides a solution without causing a delay and would be preferred. The slanted dashed lines on the resolutions indicate the original trajectories of both aircraft.

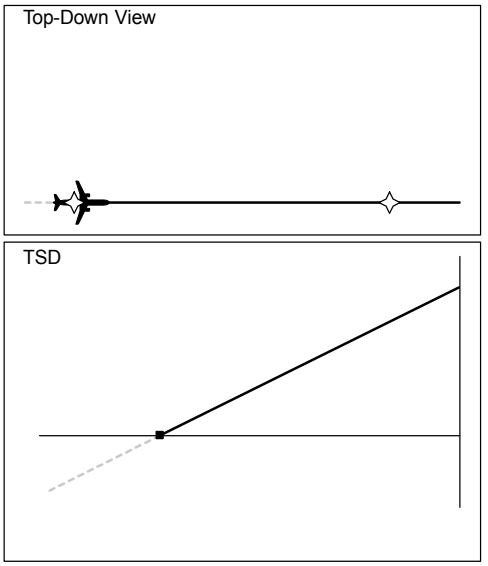

(a) The aircraft is on the route.

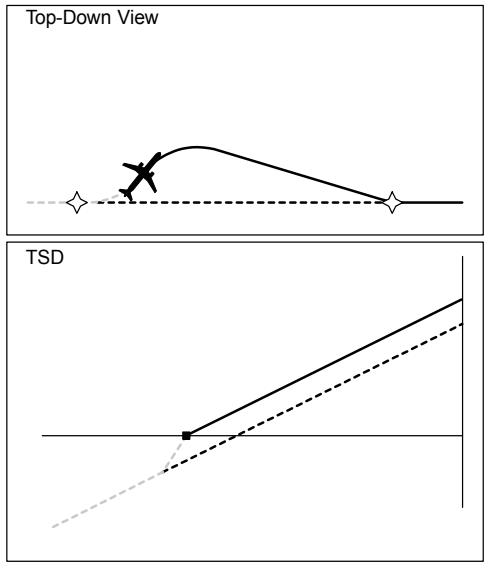

(b) A new heading is selected, a turn is required to return to the route. The distance to the runway reduces less than predicted.

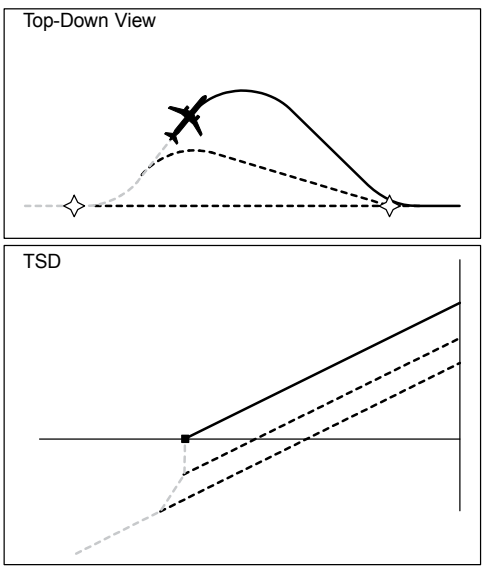

(c) The distance to the runway no longer changes.

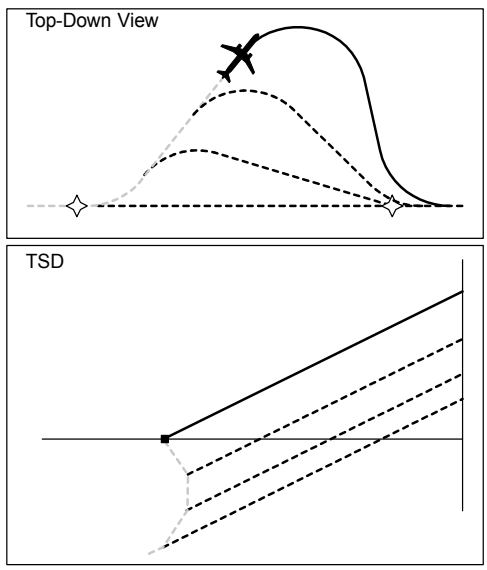

(d) The distance to the runway starts increasing.

Fig. 6. The effects of a heading instruction and the timing of the return to the planned route. The older predictions have been indicated by dotted lines to illustrate the motion of the predictions on the screen.

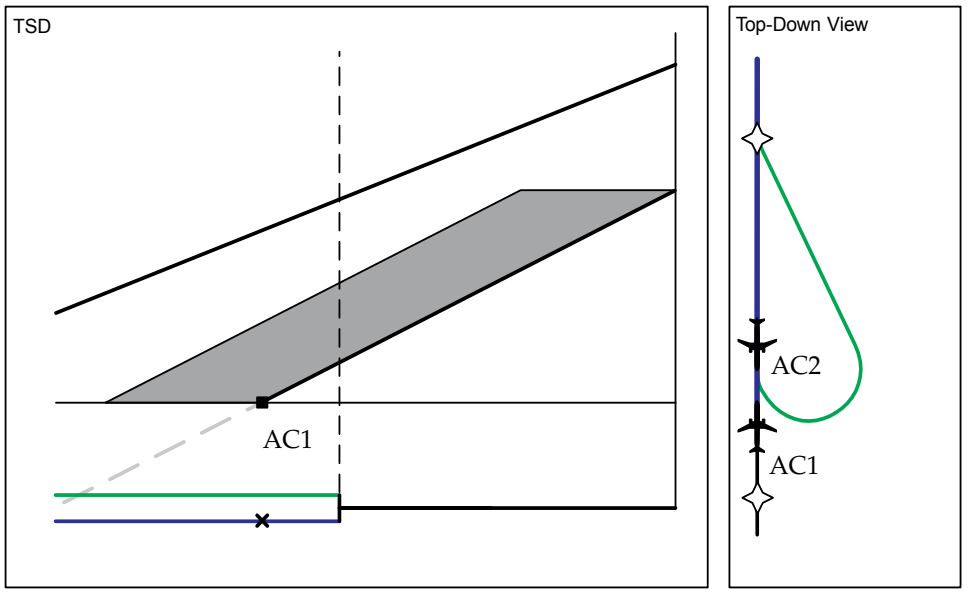

Fig. 7. A conflict geometry in which aircraft fly head-on while having sufficient along-track separation.

applied between the intersecting segments. However, the TSD can not show violation of the vertical trajectory.
Both the risks of undetected conflicts within the participating traffic as well as conflicts with other traffic, imply that the TSD should not be used without the PVD as currently used by ATC. Even more so, the PVD should be used as the first tool to assure separation, whereas the TSD should be used to adjust spacing such that the use of the runway can be maximised while still executing TDDA.

7. Procedural consequences of the TSD

In current P-RNAV operations, the radius of the turns is not defined. This radius nowadays depends on the actual airspeed and ground speed, altitude and company policy. The TSD relies on the comparability of the along-track distance. The ground track should therefore be identical for all aircraft at the same point on the route. Therefore, the turn radius should be specified in the approach procedure.
The use of vectors to adjust spacing must allow aircraft to leave the known trajectory. To allow this, while still providing a useful prediction, the trajectory algorithm should assume that the aircraft will return to the next waypoint on the route.
The requirement that all trajectories must have the same endpoint implies that the display can only be used for a single runway. For airports with multiple runways, the approach controller should be either assigned to one runway or needs more than one TSD. Currently, a version of the TSD is being developed that supports the use of more than one runway.
As this procedure is based on the exact following of paths, the airspace that is needed for the approaching aircraft can be accurately defined. The safety and procedural consequences of

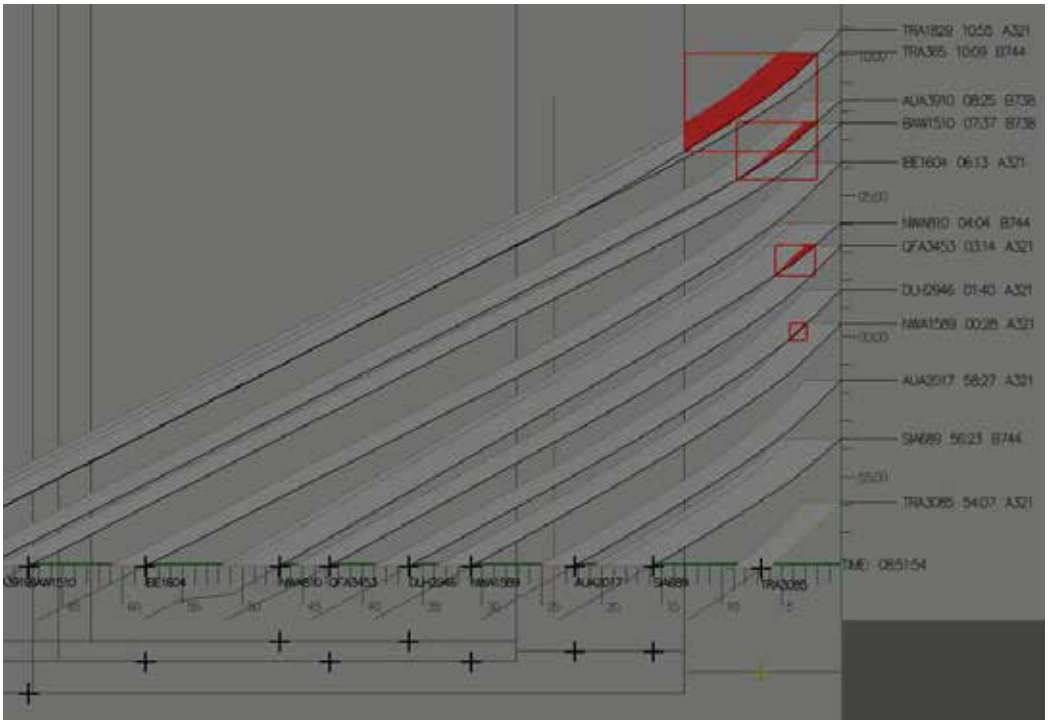

Fig. 8. The time space diagram displays as implemented in the simulator.

the display might be addressed through a restructuring of the airspace. Separation from other traffic could then be assured using airspace violation detection.

8. Future work

This chapter has presented the initial design of the Time-Space Diagram (TSD) display. It is hypothesized that the TSD, through the visual presentation of the 4D trajectory predictions of aircraft conducting a continuous descent approach, supports air traffic controllers in their task of safeguarding sufficient separation, while optimizing runway throughput.

The TSD has been implemented in DUT's real-time air traffic management simulator, and is currently being evaluated with experienced air traffic controllers. Figure 8 shows the Time-Space Diagram display as used in the evaluation.

The main questions that we hope to answer with the experimental evaluation are whether the work of the air traffic controller *changes* when operating with an additional display, and the user acceptance. It can be expected that, since the TSD provides information on the display that is currently not available with conventional plan view interfaces, the air traffic controllers will need to learn how to use the information correctly. Hence, different strategies may emerge from using the TSD. Second, it is important to investigate whether air traffic controllers will accept the introduction of a new interface in their workspace, and whether they will indeed appreciate and use the additional information that is provided.

9. References

Clarke, J.-P. B. (2000). Systems Analysis of Noise Abatement Procedures Enabled by Advanced Flight Guidance Technology, *Journal of Aircraft* **37**(2): 266–273.

Clarke, J.-P. B., Ho, N. T., Ren, L., Brown, J. A., Elmer, K. R., Tong, K.-O. & Wat, J. L. (2004). Continuous Decent Approach: Design and Flight Test for Louisville International Airport, *Journal of Aircraft* **41**(5): 1054–1066.

Coppenbarger, R. A., Mead, R. W. & Sweet, D. N. (2007). Field Evaluation of the Tailored Arrivals Concept for Datalink-Enabled Continuous Descent Approach, *7th AIAA Aviation Technology, Integration and Operations Conference (ATIO), September 18-20, Belfast (Northern Ireland)*, AIAA 2007-7778, pp. 1–14.

De Gaay Fortman, W. F., Van Paassen, M. M., Mulder, M., In 't Veld, A. C. & Clarke, J.-P. B. (2007). Implementing Time-Based Spacing for Decelerating Approaches, *Journal of Aircraft* **44**(1): 106–118.

De Jong, T. G. (2006). Principle of the Time-Space Diagram for ATCo, Unpublished Preliminary MSc. Thesis, Delft University of Technology, Delft, The Netherlands.

De Leege, A. M. P., In 't Veld, A. C., Mulder, M. & Van Paassen, M. M. (2009). Three-Degree Decelerating Approaches in High-Density Arrival Streams, *Journal of Aircraft* **46**(5): 1681–1691.

De Prins, J. L., Schippers, K. F. M., Mulder, M., Van Paassen, M. M., In 't Veld, A. C. & Clarke, J.-P. B. (2007). Enhanced Self-Spacing Algorithm for Three-Degree Decelerating Approaches, *Journal of Guidance, Control & Dynamics* **30**(2): 576–590.

Dutch Ministry of Transport, Public works and Water Management (2006). Evaluatie Schipholbeleid Eindrapport. (Report in Dutch).

Erkelens, L. J. J. (2002). Advanced Noise Abatement Procedures for Approach and Departure, *AIAA Guidance, Navigation, Control Conference and Exhibit, August 5-8, Monterey (CA)*, AIAA 2002-4671.

EUROCONTROL (1999). Navigation Strategy for ECAC, http://www.ecacnav.com.

Hullah, P. (2005). EUROCONTROL's "Basic" Continuous Descent Approach Programme, *Aircraft Noise and Emission Reduction Symposium, May 24-26, Monterey (CA)* .

ICAO (2003). Annex 11 to the Convention on Civil Aviation: Air Traffic Services.

In 't Veld, A. C., Mulder, M., Van Paassen, M. M. & Clarke, J.-P. B. (2009). Pilot Support Interface for Three-degree Decelerating Approach Procedures, *International Journal of Aviation Psychology* **19**(3): 287–308.

Nunes, A. & Mogford, R. H. (2003). Identifying Controller Strategies that Support the 'Picture', *47th Annual Meeting of the Human Factors and Ergonomics Society, October 13-17, Santa Monica (CA)*, pp. 71–75.

Reynolds, H. J. D., Reynolds, T. G. & Hansman, R. J. (2005). Human Factors Implications of Continuous Descent Approach Procedures for Noise Abatement in Air Traffic Control, *6rd USA/Europe Air Traffic Management R&D Seminar, June 25-27, Baltimore (MD)*, pp. 1–10.

Roelandt, M. (2006). Future Access to Airspace & Airports, Presentation at: EUROCONTROL EATM General & Business Aviation Day, March 26.

UK Dept. for Transport White Paper (2003). The Future of Air Transport: Summary, http://www.dft.gov.uk.

Wat, J., Follet, J., Mead, R., Brown, J., Kok, R., Dijkstra, F. & Vermeij, J. (2006). In Service Demonstration of Advanced Arrival Techniques at Schiphol Airport, *6th AIAA Avi-*

8

Legal aspects of Air traffic management based on satellite navigation[i]

A Mohamed Mustaque[ii]
Advocate at MK associates, Cochin
India

Satellite based navigation system have totally changed our concept of regulation in Air traffic Management as the legal regime or liability regime hitherto applicable for territorial service seems no longer support new global or at least regional ATM services offered by the various Providers. The legal issues related to satellite navigation vary and depend up on numerous factors including precise commercial application. The satellite navigation will be one of the key enabling technologies of future transportation and airspace management system. Thus this paper addresses the legal issues in air traffic management based on SATELLITE BASED AUGMENTED SYSTEM (SBAS).

This article will address issue of responsibility of state in the light of Liability convention 1972 and Chicago convention besides examining responsibility of service provider under private law (contract) to the extent of the application principle of CAVEAT EMPTOR as to the accuracy of positioning of aircraft based on the satellite signal.

The liability regime between service provider and beneficiary or passenger is either concluded under contract or under various Air law conventions like Warsaw conventions or Montreal conventions. However moot point arise as to the liability to third party on account of accident to the Aircraft caused by wrong signal from satellite or by other numerous reasons like interference with the satellite by a foreign state or by its subjects . Since issue is related to Space law and Air law, this article will examine it under Liability convention 1972 and under Rome Convention 1952. This article aims to achieve underlying importance for broader regulation by states for satellite based ATM as present regime continue to be vacuum in area resulted from outer space activities.

1. Introduction

"**Air** Traffic Control's primary objective is to ensure flight safety: pilots in their cockpit are to a large extent « blind » to the exterior world and, given the aircraft speed and trajectory complexity, it is necessary to control them from the ground in order to make sure that of course there are no accidents, but also to ensure the overall fluidity and efficiency of traffic flows. Air Traffic Control (ATC) is based on two main pillars: "surveillance", which enables ground operators to know precisely where the aircraft are, and the "controller", who

manages the safety of flights .Ever since the implementation of radars in the 70s-80s as surveillance means, air traffic control has not evolved much: ATC is essentially "craftsmanship", and relies entirely on the controllers' individual capability to handle always more traffic. Even though air transport has exceptionally good reliability and safety records, to a large extent thanks to the high quality of work performed by air traffic controllers, this craftsmanship is becoming anachronistic: in the information society era, communications between controllers and pilots are still using the voice-radio[iii]!"
The current Air Traffic Management (ATM) is based on ground navigational system such as radar and voice communications experience difficulty in meeting growing demand of air traffic. Despite economic recession ICAO[iv] expects moderate growth of air traffic of 3.3 percent to 5 percent during 2010-11[v].According to aircraft manufacturer Airbus, global air passenger traffic is set to increase by over 150% over the next 20 years, representing an annual growth of 4.7%. The size of the world's passenger aircraft fleet will double in number from 14,016 in 2008 to 28,111. The fastest growing regions will be India, China and Africa, driven by deregulation, economic growth, population growth and inter-regional trade. 2007, traffic slowed to a 2% growth in 2008 and this year will see an expected decline of 2%. By next year, a worst case scenario suggests zero growth and a best case of a return to growth of 4.6%. The plane-maker says the greatest demand for passenger aircraft will be from airlines in Asia-Pacific and emerging markets. The region that includes China and India will account for 31% of the total, followed by Europe (25%) and North America (23%). In terms of domestic passenger markets, India (10%) and China (7.9%) will have the fastest growth over the next 20 years. The largest by volume of traffic will remain domestic US.
Airbus says the main drivers of future traffic growth will be:

- growing Middle East passenger and cargo hubs;
- in Asia, more people able and wanting to fly everyday;
- low-cost carriers in Asia growing in number and traffic share;
- more potential through deregulation, particularly in Asia and Africa; and
- growing urbanization and a resulting increased demand between major cities

It is in this scenario global Air Traffic Management has to address to a system that provides a greater capacity for required surveillance in air space with assured safety. The introduction of satellite-based air navigation services to replace many of the existing line-of-sight systems represents a quantum step forward for civil aviation. Following comprehensive studies over several years, the global "communications, navigation and surveillance/air traffic management (CNS/ATM) systems" concept was endorsed by the ICAO Tenth Air Navigation Conference in 1991 and by the 29th Session of the ICAO Assembly in 1992.

The Global Navigation Satellite System[vi] is poised to be one of the most critical technologies in the 21st century and considered as an important element of the communications, navigations, surveillance etc, intended to provide worldwide coverage. At present the satellite navigation technologies like Internet is becoming a global means and is finding an application practically in all areas of the activities of a man.

Legal aspects of satellite based ATM is grappled mainly around lack of legislative will of world body like ICAO to regulate beyond air space as issues are surmounted on the interface of space law and air law.

The early stages of space activates only saw the participation of very few states. All the investment towards the space sector was purely from the government exchequer and because of this reason; all the space treaties only mention the rights, obligation and responsibilities of the state government. As stated above, all the international instruments governing outer-space were build-up and agreed before the high influx of commercial space activities and therefore, do not sufficiently take into account the implications and aftermath of the growing volume of commercial space activities.

ICAO is a global public international organization and its mandate originated from Chicago convention[vii]cannot go beyond mandate to regulate on non sovereign area of outer space. It is in this backdrop this paper addressing various legal aspects in the light of potential issues.

2. Satellite based ATM

Global Navigation Satellite Systems currently have two core constellations – Global Positioning System (GPS) of the United States and the Global Navigation Satellite System (GLONASS) of the Russian Federation. Other similar systems are the upcoming European Galileo positioning system; the proposed are COMPASS-Bediou Navigation System of China; Doppler Orbitography and Radio-positioning Integrated by Satellite (DORIS) of France and the Indian Regional Navigation Satellite System (IRNSS) of India. Almost all satellites are launched in order to provide service to people on earth. Satellites are routinely used to support sustainable development. Satellite is mainly used as source information for decision making or to transmit information.

Current and Planned System Providers[viii]

The United States: Global Positioning System (GPS)
GPS is a United States space-based radio-navigation system that provides reliable positioning, navigation, and timing services to users on a continuous worldwide basis– freely available to all. The outstanding performance of GPS over many years has earned the enduring confidence of millions of international users. With its ongoing modernization programme, GPS will continue to provide superb quality and performance in the future.

The Russian Federation: Global Navigation Satellite System (GLONASS)
The Russian navigation satellite system, GLONASS, is based on a constellation of active satellites which continuously transmit coded signals in two frequency bands, which can be received by users anywhere on the Earth's surface to identify their position and velocity in real time based on ranging measurements. In the future a third frequency for GLONASS signal transmission will be introduced. In some areas of application, the use of combined GPS, GLONASS and Galileo constellation appears to be preferable option.

The European Community: European Satellite Navigation System (GALILEO)
GALILEO, an initiative launched by the European Commission and the European Space Agency, will be a global navigation satellite system, owned by the European Community, providing highly accurate, guaranteed global positioning services under civilian control. The Galileo Open Services signal will be interoperable with the GPS civil signal, as well as with GLONASS.

China: COMPASS/BeiDou
The existing three-satellite COMPASS/BeiDou navigation system has played an important role in offering efficient positioning, timing, communication services and differential GPS information in surveying, telecommunications, transportation, meteorology, forest fi re prevention, disaster forecast and public security areas. On the basis of the COMPASS/BeiDou Navigation Test System, China has started to build a system with global coverage.

Current and planned augmentation system providers for ATM

A **satellite-based augmentation system** (SBAS) is a system that supports wide-area or regional augmentation through the use of additional satellite-broadcast messages. Such systems are commonly composed of multiple ground stations, located at accurately-surveyed points. The ground stations take measurements of one or more of the GNSS satellites, the satellite signals, or other environmental factors which may impact the signal received by the users. Using these measurements, information messages are created and sent to one or more satellites for broadcast to the end users.

In air traffic management SBAS provides signals from core constellations, GPS or GLONASS or from Interoperable systems through ground reference stations. Each station in network relays the data to master station where correction information for specific information is computed; corrected message is prepared and uplinked to a GEO stationary communication satellite via ground up link station. This message is broad casted to receivers onboard of aircraft flying within coverage area of system.

WAAS: The **Wide Area Augmentation System** (**WAAS**) is an air navigation aid developed by the Federal Aviation Administration(FAA) of US to augment the Global Positioning System (GPS), with the goal of improving its accuracy, integrity, and availability. Essentially, WAAS is intended to enable aircraft to rely on GPS for all phases of flight, including precision approaches to any airport within its coverage area.

EGNOS: The **European Geostationary Navigation Overlay Service** (EGNOS) is a satellite based augmentation system (SBAS) under development by the European Space Agency, the European Commission and EUROCONTROL[ix]. It is intended to supplement the GPS, GLONASS and Galileo systems by reporting on the reliability and accuracy of the signals

MSAS**: Multi-functional Satellite Augmentation System** (MSAS) i.e. a satellite navigation system which supports differential GPS (DGPS) designed to supplement the GPS system by reporting (then improving) on the reliability and accuracy of those signals. Tests had been

accomplished successfully; MSAS for aviation use was commissioned on September 27, 2007[x].

GAGAN: The **GPS Aided Geo Augmented Navigation** or **GPS and Geo Augmented Navigation** system (**GAGAN**) is a planned implementation of a regional Satellite Based Augmentation System (SBAS) by the Indian government. It is a system to improve the accuracy of a GNSS receiver by providing reference signals. The Rs. 7.74 billion (774 crore) project is being implemented in three phases through 2008 by the Airport Authority of India with the help of the Indian Space Research Organization's (ISRO) technology and space support. The goal is to provide navigation system for all phases of flight over the Indian airspace and in the adjoining area. It is applicable to safety-to-life operations, and meets the performance requirements of international civil aviation regulatory bodies. The final, operational phase of GAGAN is likely to be completed by May 2011. *Gagan* is the transliteration of a Hindi/Sanskrit word for the sky[xi].

3. Law of responsibility and liability

Law of responsibility is concerned with the determination of whether there is wrongful act for which the wrong doer is to be held responsible. Some time term "responsibility" interchangeably used with term "liability "which in common parlance understood obligation to pay compensation. In air law responsibility is on state to provide air navigation facilities to facilitate international air navigation[xii].In the context of space law, state shall bear international responsibility for national activities in outer space[xiii]. Law of liability is specific in air law as to claim of passengers and third parties as envisaged in Montreal Convention 1999 and Rome Convention 1952. In space law launching state shall be absolutely liable to pay compensation for damage caused by space object on the surface of the earth or to aircraft flight under Liability Convnetion1972[xiv].Nuances and intricacies of issues emanates from application of air navigation based SBAS could not contemplated while provisions in Air law and Space law were drafted. Therefore legal basis for "responsibility and liability" should be examined in the light potential claims on the interface of air and space law.

Essentially four types of claimants may be found in SBAS based ATM

1 Air carrier against ATM service provider
2 Passenger in aircraft
3 Third party
4 ATM service provider against Signal provider

Claim of Air carrier: It is not necessary for air carrier to have contractual obligation with the ATM service provider as later deemed to provide air navigation facilities to every contracting states under article 15 of Chicago convention on uniform conditions. Problem may arise as to application of law of in the claim of air carrier against ATM service provider especially for foreign air carrier for an accident in a country other than where ATM service provider is located. "Much of private air law however is not unified, substantially or as to conflict rules by international conventions. In these areas national private law will apply, the law of conflicts (in common law terminology) or private international law (in civil law terminology) serving to determinate which national laws will apply in a fact pattern with international elements. International elements are of course, dominant in the practice of air transport industry: these areas of non unified private air law are principally, but not

exclusively, product liability air traffic control and air port liability"[xv]... Actor sequitor forum rei –A pursuer follows the forum or court of defendant. Under Hague convention of private international law on traffic accidents [xvi] the applicable law is the internal law of the state where the accident occurred. It would be difficult to sustain tortuous claim in a country where sovereign immunity would apply. Thus jurisdiction can be either in country where accident occurs or in country where ATM service provider is located, however such claims have to be settled based on the broad principles of international responsibility of state. According to Prof. Brownlie

"One can regard responsibility as a general principle of international law , a concomitant of substantive rules and of the supposition that acts and omissions may be categorized as illegal by reference to the rules establishing rights and duties. Shortly, the law of responsibility is concerned with the incidence and consequence of illegal acts and particularly the payment of compensation caused"[xvii]

Liability of ATM service provider to carrier is part of non conventional private international law, as mentioned above claim has to be preferred in a jurisdiction where accident occurred or where ATM service provider is located. However law that would be applicable in such claim is of country where accident occurred. "ATC Liability will normally be extra-contractual (tortuous) in nature, governed by *lex loci defect*"[xviii] .

Claim by passenger: Claim by passenger is found base in Warsaw convention[xix] or Montreal Convention[xx] as such claims are related or arising from terrestrial cause of action, even though it may have origin from satellite or from augmented system, nevertheless, immediate tortfeasor being aircraft or ATC provider, their claim rest under relevant conventions."Air traffic control service providers maybe liable for damage to passengers (and their estates), shippers and third parties on the ground if, through wrong or faulty ATC instructions, they cause an aircraft to crash or collide"[xxi].However such claims is generally are non contractual and tortuous in nature. As mentioned earlier providing air navigation facilities rest with State, it may be difficult to sustain such claims in countries where sovereign immunity operates. Under United States Foreign Immunities Act of 1976 foreign state shall be immune from the jurisdiction of the courts of the United States except such in which the action is based up on a commercial activity carried on in the United States by the foreign state. Or up on an act performed in the United States in connection with a commercial activity of the foreign state elsewhere. Similarly United Kingdom State Immunity Act 1978 0r 1985 Foreign State Immunity Act of Australia affords immunity to States from the jurisdiction of courts in United Kingdom or Australia. In India under section 86 of Civil Procedure Code, a suit against foreign state is maintainable with consent of Central Government. Perhaps in the light of Article VI of Outer space treaty which mandate that State shall bear international responsibility for national activities, state immunity principle may be denuded for action in claims against ATC service provider for faulty or erroneous signal from satellite by applying Rule found in Article 27 of the Vienna Convention on the Law of Treaties which lays that' A party may not invoke the provisions of its internal law as justification for its failure to perform a treaty'.

Third party claims: The third party is having limited remedy against Air line carrier under Rome Convention 1952[xxii]. Signatories to the Rome Convention 1952 are only few countries (49 countries). In countries where Rome Convention is applicable, the third parties cannot resort for other remedies as Article 9 specifically excludes liability otherwise than through provisions of Rome Convention .In countries where Rome convention does not apply, law applicable to damage done by aircraft on the surface usually based up on fault or

negligence. Therefore the liability to be fastened is on proof negligence, when aircraft involves in an accident resulting damage to third party due to error of signal from satellite, on which liability could be fastened? Which law would apply? Are necessarily to be answered with reference to space law, as seemingly negligence originate from outer space. This issue dealt in next title under 'claims of ATM service provider against Signal provider'.

Claim of ATM service provider against signal service provider: There are many potential reasons for failure or erroneous signal from satellite which may result in accident. ATM service provider may have to resort to non contractual liabilities, but it may be a problem to establish for want of proof of negligence. It is in this backdrop legal position under space law has to be examined especially Liability Convention 1972. ArticleII of Liability Convention provide "A launching State shall be absolutely liable to pay compensation for damage caused by its space object on the surface of the earth or to aircraft flight". The liability is absolutely liability. Does Liability convention contemplate any liability emanates from signal from satellite? What is space object then? It may be recalled Liability Convention was drafted before influx of commercial activities in outer space. Like all other conventional navigation systems, the SBAS is subject to errors that can degrade the precision of the system. The errors are Ionospheric error, Troposheric error, Selective Availability, Satellite clock error, Receiver clock error, Multi path error, Receiver error, Satellites Ephemeris error and Geometrical error etc .It is not necessary that Satellite has caused any error on other hand signal error results in accident, since Liability Convention does not undertake any enquiry as to culpability of accident as accident itself speak about cause ,merely because of involvement of space object , it is difficult to say involvement of signal from satellite is contemplated under Liability Convention. Signal from satellite cannot be equated with space object, in this context space object means which can directly cause accident, as underlying principle of "absolute liability" in Article II of Liability Convention denote. To quote Dr Abeyrante "*Admittedly, neither the Outer Space Treaty nor Liability Convention explicitly provide remedies for damage caused by technology and communication provided through space objects*[xxiii]. *However the 'common interest' pricinciple and liability provisions of these two Conventions can impute culpability to states*". There is no provision under space law to sustain claim under relevant Convections or Treaties, nevertheless as argued by Dr Abeyrante international responsibility of state cannot be avoided under the principles of international law

4. Signal Precision and Product liability

"The most significant error occurs when the satellites signal goes through the earth atmosphere. This is a layer of electrically charged particles located approximately between 130 and 190 Km above the surface of the earth. As the GPS signal travels through the ionosphere, it is slowed down in a proportion that varies according to time of days, solar activity and series of the other elements. Ionospheric delays may be forecast and an average correction applied to the GPS position. Another error is caused by water vapour in the atmosphere which delays the GPS signal and also contributes to degrade the position of the system"[xxiv].Essentially most legal system recognize that the manufacturer of aeronautical products ,has triple duty; a duty to design safe product duty to manufacture a safe product and duty to warn against dangers in using product. Under article 1 of EC directive (87/374 EEC) on product Liability for European Union, the producer shall be liable for damage

caused by defect in his product. Product liability normally decided according to national laws and the principles of 'strict liability'. "Satellite based navigation system for ATM can be termed as a product. It employs various techniques in system design to correct ionospheric impact on signal. Though system is deployed after meeting ICAO SARP and Technology Demonstration System (TDS), the product liability would exist for inaccurate service due to design or defect in system[xxv]"However liability on Signal provider may not exist for error or for lack of precision due to atmospherical impact as every prudent man must know such impact likely to affect satellite signal..The error introduced by the ionosphere into GPS signal is highly variable and difficult to mode[xxvi].The influence of the ionosphere and strategies to isolate its effect are issues of major concern for GPS positioning and navigation application[xxvii] .The inaccuracy or degrading factors are not result of defect or design of the system. Infact system is designed taking into consideration of ionoshperic impact on signal, and therefore it would be justifiable defence for service provider to defend themselves relying principles of' Caveat emptor' which means 'let the buyer beware'. The technological constraints or barriers in atmosphere mitigate liability of signal provider on the above principle of law.

5. Interoperability

According to IEEExxviii definition interoperability is the ability of two or more systems or components to exchange information and to use the information that has been exchanged. In GNSS context ,interoperability can be understood such that individual GNSS components should be designed ,built and operated in such a way that they do not 'jam' each other and allow one to combine their signal in a navigation service of superior quality.ICG (International Committee on Global Navigation Satellite System) is a forum established on a voluntary basis as a informal body to promote cooperation, as appropriate ,on matters of mutual interest related to civil satellite based positioning, navigation ,timing and value added services, as well as the compatability and interoperability of global navigation satellite system while increasing their use to sustainable development. Within the ICG is the providers forum, consisting of those countries operating GNSS system or with plans to develop one .Providers forum adopted Definition of interoperability as follows

'Interoperability refers to the ability of global and regional navigation satellite systems and augmentations and service they provide to be used together to provide better capabilities at user level than would be achieved by relying solely on the open signal system'

Interoperability of GNSS poses innumerable issues to end user with regard to claim and jurisdiction[xxix]. .Certainly interoperability signifies involvement of multiple GNSS providers located indifferent jurisdiction having conflicting domestic laws. The task of claimant in such context is to identify appropriate jurisdiction and law applicable for such claim. ICAO identifies that substantive law may be reasonably adequate to determine or apportion liability from accidents involving failure or malfunction of GNSS systems, procedural rules and ,in particular, the applicable rules on jurisdiction may not be adequate to bring all parties to the court in order to ensure prompt and equitable compensation in these cases, in particular application of sovereign immunity and related principles may in many cases render court action against foreign states or foreign governmental entities providing ATC or

GNSS signals, facilities and services in countries other than their home states difficult or impossible[xxx].

[i] Copyright with author

[ii] A lawyer practicing at High Court of Kerala, India and having master from Paris XI in space and telecommunication law.

[iii] http://ec.europa.eu/transport/air_portal/traffic_management/sesame/index_en.htm viewed on12/04/2010

[iv] A specialized agency of UN created in 1944 to promote safe and orderly development international aviation throughout the world.

[v] ICAO news release PIO08/09

[vi] Global Navigation Satellite System (GNSS) is the standard generic term for satellite navigation systems that provide autonomous geo-spatial positioning with global coverage. A GNSS allows small electronic receivers to determine their location (longitude, latitude, and altitude) to within a few metres using time signals transmitted along a line of sight by radio from satellites. Receivers on the ground with a fixed position can also be used to calculate the precise time as a reference for scientific experiments.

[vii] Chicago Convention 1944, on international civil aviation signed at Chicago by contracting states.

[viii] Booklet published by international committee on Global navigation satellite system

[ix] Eurocontrol is the European Organisation for the Safety of Air Navigation. Founded in 1963, it is an international organisation working for seamless, pan-European air traffic management. Eurocontrol is a civil organisation and currently has 38 member states; its headquarters are in Brussels.

[x] Source http://en.wikipedia.org/wiki/Multi-functional_Satellite_Augmentation_System viewed on14/04/2010

[xi] Source http://en.wikipedia.org/wiki/GPS_Aided_Geo_Augmented_Navigation viewed on 14/04/2010

[xii] See art 28 of Chicago convention

[xiii] Art VI of Outer Space Treaty (a treaty on principles governing the activities of states in the exploration and use of outer space ,including the moon and other celestial bodies) .This treaty forms basis of international space law singed and came into force in the year 1967

[xiv] Convention on international liability for damage caused by space objects entered in the year 1972

[xvxv] Page 67 chapter Five The Law and policy of air space and outer space , A comparative approach By P.P.C Haanappel pub: Kluwer Law international

[xvi] Convention on the law applicable to traffic accidents (concluded4 may 1971,entered into force on June 1975

[xvii] Principles of public international law pub: Oxford Clarendon Press

[xviii] The Law and policy of Air space and outer space page.92 by Prof P.P.C Haanappel

[xix] The **Warsaw Convention** is an international convention which regulates liability for international carriage of persons, luggage or goods performed by aircraft for reward signed in 1929.

[xx] The **Montreal Convention**, formally the **Convention for the Unification of Certain Rules for International Carriage**, is a treaty adopted by a Diplomatic meeting of ICAO member states in 1999. It amended important provisions of the **Warsaw Convention**'s regime concerning compensation for the victims of air disasters.

[xxi] P.91 of The law and policy of air space and outer space by Prof P.P.C Haanappel

[xxii] Rome Convention applies only to damage caused by foreign civil aircraft ,for damage caused by national aircraft only local law would apply.

[xxiii] State responsibility in classical jurisprudence reflections on the GNSSS by Dr Abeyrante article pub:Annals of Air and Space Law V XXIII (1998)

[xxiv] Communication navigation and surveillance/ATM beyond 2012 by Arjun Sing Air port Authority of India ,source http://www.gisdevelopment.net/technology/gps/ma04082pf.htm

[xxv] Legal aspects relating to satellite navigation inair traffic management with specific reference to GAGAN in India copy right with IAF , presented in IAC 07author .A.Mohamed Mustaque

[xxvi] Assesment of ionosphereic impact on LAAS using WAAS super truth data by Ming Luo and other sStanford University

[xxvii] ibid

[xxviii] IEEE ,Institute of Electrical and Electronic Engineers , a nonprofit organization ,is the world`s leading professional association for the advancement of technology

[xxix] Interoperability of GNSS ,legal issues and implications under private international law ,presented at IAC 09 by A.MOHAMED MUSTAQUE copyright with IAF

[xxx] Report to the 35th session ICAO Assembly for consideration.

9

ATM systems and Wind Farms

Andrej Novak
University of Žilina
Slovakia

1. Introduction

Air safety includes all the rules and processes that enable commercial and cargo aeroplanes to fly safely across the European Union. It includes rules on aircraft construction and use, infrastructure safety, data management and analysis, flying operations, and cargo.

Air safety management aims to spot potential accidents and incidents before they occur. It is not the same as air security, which seeks to prevent voluntary illegal and harmful acts in the field of aviation. The wind is an increasingly important source of energy, but negative impact on air transport is in area of Air Traffic Services. Communication Navigation and Surveillance systems are endangered with big wind farms. Primary problem is in radar system and is detailed described in my text.

The potential impacts of wind farms on air traffic management include the cumulative effects on the Slovak republic airspace management and surveillance infrastructure and affect the following systems:

- Primary Radar,
- Secondary Surveillance Radar (SSR),
- Microwave links associated with a) and b),
- Navigation Aids

Background information on how these systems work and are used, together with the effects of wind turbines and mitigation techniques, is at next chapter. The remainder of this section concentrates on how the systems above can be affected by wind turbines and identifies, where known, mitigating measures that can be taken from a developer's perspective. However, many of the precise effects of wind turbines on these systems are not yet fully understood and the guidance issued in this section must therefore be considered as interim, based on the best knowledge currently available.

It should be borne in mind that it is not the effect that wind turbines have on technical systems in themselves that is important but the end effect that is caused to flight safety-critical air traffic management operations. Hence, if pragmatic solutions can be found (for example, by replacing the service provided by an affected SSR with a suitably located

replacement SSR), these may offer a way forward. On the other hand, if on aerodrome approach radar must be situated in one particular location in order to ensure safety of departing and arriving aircraft, any proposal for wind turbines that will cause detrimental effects to the radar is unlikely to be acceptable.

1.1 Radar Introduction

There are two types of radar used for air traffic control and air defence control and surveillance: Primary Surveillance Radar (PSR) and Secondary Surveillance Radar (SSR).

Primary radar operates by radiating electromagnetic energy and detecting the presence and character of the echo returned from reflecting objects. Comparison of the returned signal with that transmitted yields information about the target, such as location, size and whether it is in motion relative to the radar.

Primary radar cannot differentiate between types of object; its energy will bounce off any reflective surface in its path. Moreover, air traffic control primary radar has no means of determining the height of an object, whereas modern air defence radars do possess this capability, using electronic beam control techniques.

For SSR, the ground station emits 'interrogation' pulses of radio frequency (RF) energy via the directional beam of a rotating antenna system. When the antenna beam is pointing in the direction of an aircraft, airborne equipment, known as a transponder, transmits a reply to the interrogation (Gabriel & Hill, 2004). The reply is detected by the ground station and processed by a plot extractor.

The plot extractor measures the range and bearing of the aircraft and decodes the aircraft replies to determine the aircraft's flight level and identity (Mode C operation). In the Slovak Republic, all aircraft flying in controlled airspace must carry a SSR transponder. Some light aircraft do not, and aircraft that do carry them may not have them switched on, in which case they will not be visible to SSR. Most ATC units are equipped with both primary and SSR, but, increasingly, radar services are provided using SSR only.

From 2008 onwards, a new type of SSR called 'Mode S' will begin to be introduced in the SR airspace. Mode S is a development of classical SSR that overcomes many of the current limitations of the SSR system. It is proposed, subject to formal consultation, to introduce Mode S initially in 2008 with a second phase of regulatory changes in 2008. In addition, it is proposed that the requirements for the carriage and operation of transponders will be significantly extended in conjunction with the Mode S plans for 2009/2010.

2. Basic Radar Functions

Radar performs two functions for air traffic control:

a) Aerodrome surveillance radar allows air traffic controllers to provide air traffic services to aircraft in the vicinity of an airport. This service may include vectoring aircraft to land, providing a radar service to departing aircraft or providing a service to aircraft either transiting through the area or in the airfield circuit.

b) En route (or area) radars are used to provide services to traffic in transit. This includes commercial airliners and military traffic. Area radars have a longer range than aerodrome radars, particularly at high altitudes.

Fig. 1. Primary and secondary surveillance radar (picture source: author)

2.2 Air Defence

Air Defence radars are used in two ways. On the one hand, they perform a similar function to their ATC counterparts, in that they are used by air defence controllers to provide control services to military (usually air defence) traffic. However, they are also used to monitor all air traffic activity within the Slovak Republic and its approaches in order that a Recognised Air.

Recognised Air Picture can be produced, with the aim of preserving the integrity of the SR airspace through air policing. The Recognised Air Picture is produced by allocating Track Identities to each radar return (or "plot") of interest. Often, a radar plot can fade from a radar display for a period of time due to a number of factors, but the Track Identity will remain, indicating that the associated plot is still actually present (CAP 670, CAP 764).

2.3 Meteorological Radars

Meteorological Office weather radars use electromagnetic energy to monitor weather conditions (predominantly cloud and precipitation) at low altitudes, in order to assist weather forecasting. Wind profiling radars are used to measure wind speed at different altitudes.

There are 2 weather radar stations in the Slovakia (1 in Kojsova Hola and 1 in Maly Javornik) and they are used for monitoring weather conditions to assist in forecasting. A map of Meteorological Office radar sites is at Fig. 2. In simple terms, two types of radar are used:

- weather radar and
- wind profiling radar.

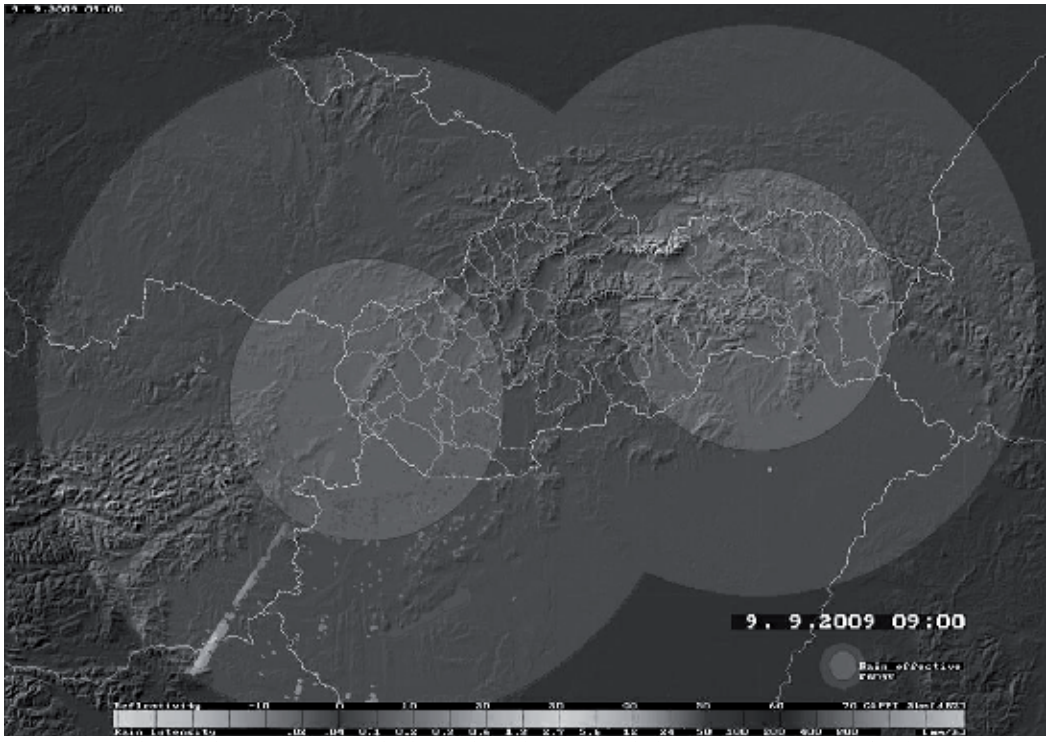

Fig. 2. Weather radar on Kojsova hola and Maly Javornik (picture source: author)

Weather radar is designed to look at a thin layer of the atmosphere, as close to the ground as possible, for accurate forecasting. For this reason, sites are situated on high ground and look out at a narrow band of airspace between 0 and 1° planning wind farms in close proximity to Meteorological Office wind profiling radars. As with all other issues, the key is to engage in dialogue with the Meteorological Office as early as possible if it is anticipated that there may be a conflict of elevation. Subsequently, there is potential for interference from wind turbines.

The easiest way to avoid disruption to weather radar is to ensure that the maximum height of the turbines (above mean sea level) is below the height of the radar. This will ensure that there is no interference. In addition, if terrain features lying between the turbine and the radar mask the turbines they will have no impact on the operation of the radar. Put simply, weather radar may still be able to operate with a few wind turbines within its line of sight, dependent upon range and other factors.

Accurate weather forecasting and reporting is highly important to aviation safety. One of the most important effects for aircraft is “wind shear”, where the winds at different altitudes may vary greatly in both direction and speed. Wind profiling radars are susceptible to spurious reflections and, for this reason, developers should avoid

2.4 Airborne Weather Radar

Airborne Weather Radar provides the pilot with a local (ahead only) weather picture in the cockpit and allows him to identify and avoid specific, undesirable weather formations. A maximum range of 180NM is common although the commonly used range (as selected by pilots) would normally be in the 30 to 80NM range.

3. The Nature of the Impacts of Wind Turbines

Masking

This is the main anticipated effect on air defence surveillance radars. Such radars work at high radio frequencies and therefore depend on a clear "line of sight" to the target object for successful detection. It follows that any geographical feature or structure which lies between the radar and the target will cause a shadowing or masking effect; indeed this phenomenon is readily exploited by military aircraft wishing to avoid detection. It is possible that, depending on their size, wind turbines may cause shadowing effects. Such effects may be expected to vary, depending upon the turbine dimensions, the type of transmitting radar and the aspect of the turbine relative to it.

The Meteorological Office is also concerned with the effect of masking on their sensors. Meteorological Office radars look at a relatively narrow altitude band, as near to the earth's surface as possible. Due to the sensitivity of the radars, wind turbines, if they are poorly sited, have the potential to significantly reduce weather radar performance.

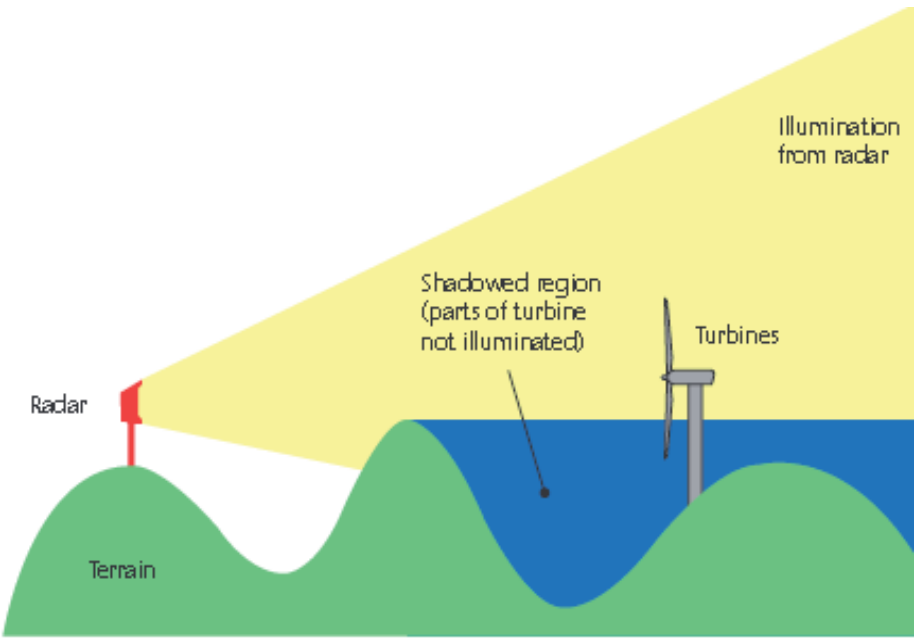

Fig. 3. General geometry of the problem – terrain shadowing (source: Greving, 2001)

Radar returns may be received from any radar-reflective surface. In certain geographical areas, or under particular meteorological conditions, radar performance may be adversely

affected by unwanted returns, which may mask those of interest. Such unwanted returns are known as radar clutter. Clutter is displayed to a controller as "interference" and is primarily to air defence in Slovakia and aerodrome radar operators, because it occurs more often at lower altitudes (Lewis, 2001).

For an aerodrome radar operator, a wind turbine or turbines in the vicinity of his airfield can present operational problems. If the turbine generates a return on his radar screen and the controller recognises it as such, he may choose to ignore it. However, such unwanted returns may obscure others that genuinely represent aircraft, thereby creating a potential hazard to flight safety. This may be of particular concern in poor weather.

A structure which permanently paints on the radar in the same position is preferable to one that only presents an intermittent return. This is because an intermittent return is more likely to represent a manoeuvring or unknown aircraft, obliging the controller to act accordingly. With this in mind, it is possible that aviators and radar operators could work safely with one or perhaps two turbines in the vicinity of an aerodrome. Of greater concern is the prospect of a proliferation of turbines, which could potentially saturate an airfield radar picture, making safe flying operations difficult to guarantee.

Several turbines in close proximity to each other, painting on radar, can present particular difficulties for long-range air surveillance radars. A rotating wind turbine is likely to appear on a radar display intermittently (studies suggest a working figure to be one paint, every six sweeps).

Multiple turbines, in proximity to each other, will present several returns during every radar sweep, causing a 'twinkling' effect. As these will appear at slightly different points in space, the radar system may interpret them as being one or more moving objects and a surveillance radar will then initiate a 'track' on the returns. This can confuse the system and may eventually overload it with too many tracks. Measures can be taken to mitigate this problem and they are amplified, but these too have their drawbacks.

The radar modelling study mentioned in Knill, 2001 includes some field measurements which will be used to validate the model. Figure 4 shows some data from these trials. It shows the Doppler signal against time recorded by a radar array from a single 1.5MW turbine. The turbine rotor was at an angle of 30° to the radar direction, with a rotor speed of 20.3RPM.

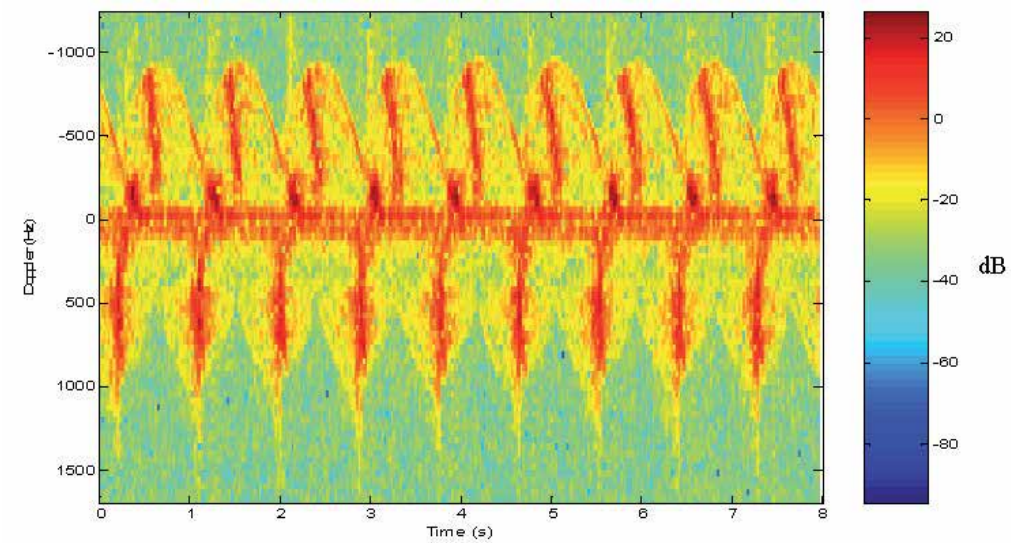

Fig. 4. Doppler radar signal from a single wind turbine

5. Radars Errors

It is important to clarify some of the common technical terms used throughout this document. Every effort has been made to use these terms consistently where their relevance has been discussed. The list comprises terms which are either felt to be sufficiently technical to warrant explanation, or it was felt that their use in the open literature was often ambiguous or confusing. Full technical treatments of these terms can be found in (Skolnik, 1962) and (Knott et al, 1993).

Diffraction
Diffraction is a special type of reflection, where energy is scattered by a discontinuity (e.g. the sharp edge of a wind turbine blade). Smooth objects will also diffract if the curvature is tight enough (compared to the wavelength of the EM wave). When an incoming EM wave hits an edge, energy is diffracted in all directions.

Multi-path
Multi-path refers to an EM wave travelling from one point to another via some intermediate object where it suffers a reflection. In this context, multi-path refers to a transmitted signal being reflected from a wind turbine before it reaches the receiver.

Reflection
This is a general "catch-all" term describing the fact that when an EM wave hits an object, it reflects/scatters energy in a number of directions. Radar reflections should be considered to be synonymous with "radar echoes" and "target scattering".

Refraction
Refraction is a phenomenon where the direction of a signal (an EM wave) changes as it passes through a medium whose refractive index (related to the density of the medium) changes. The

change can be abrupt (e.g. the bending of light entering a glass of water) or gradual (e.g. the bending of radio waves as they travel through the atmosphere). The amount of bending also depends on the frequency of the wave – this is why prisms split "white light" into a rainbow – because the different wavelengths are refracted by different amounts.

Shadowing
A shadow is a region of space where the strength of an electric field is reduced behind an object, compared to what the signal strength would have been without the object.

Signal / EM wave
All of the ATC systems in this report transfer information using RF signals. The "signal" is an electromagnetic (EM) wave which propagates at the speed of light, c. The frequency of an EM wave is inversely proportional to its wavelength, λ, by the equation $c = f \lambda$. The strength of an EM wave is measured in terms of its electric field-strength. The power carried by the wave is proportional to the square of the electric field-strength.

The relationship between the underlying physical mechanisms (causes) and the observed ATC impacts is illustrated in Figure 5 and Figure 6. Figure 6 considers generic ATC impacts while Figure 5 only considers those which are specific to PSR systems. In both figures it is assumed that the radar receiver has a threshold of P_{thresh} – i.e. only signals with a power greater or equal to P_{thresh} will be detected. The cause of each impact is related simply to the system's measured quantities – the time or arrival, the direction of arrival and the strength of the signal.

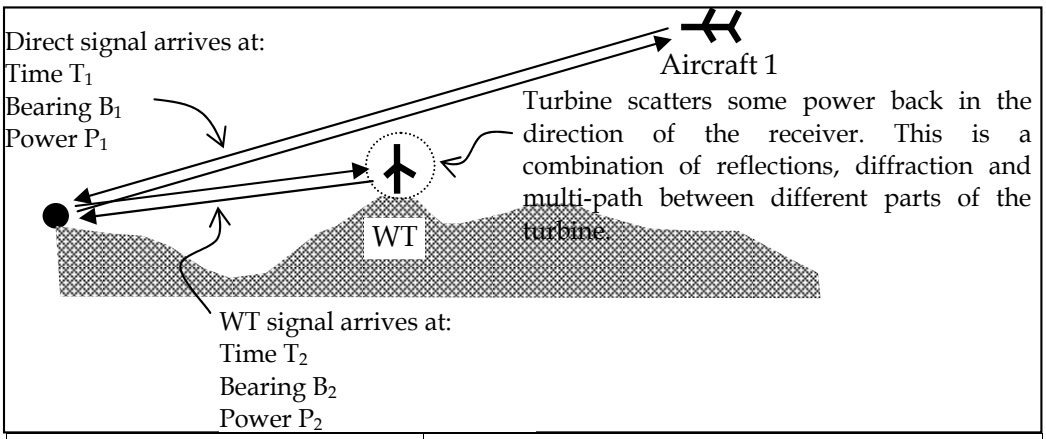

ATC impact	Technical Cause
Signal loss due to raised threshold settings	P_2 large enough to affect clutter map $P_1 < (P_2$ + cluttermap without wind turbine)
Clutter	$P_2 > P_{thresh}$
Failure to initiate an aircraft track	P_2 large enough to affect clutter map $P_1 > (P_2$ + cluttermap without wind turbine)
False track initiation	$P_2 > P_{thresh}$, and tracker affected
Loss of existing track	$P_1 < P_{thresh}$, and tracker affected
Receiver saturation	P_2 too large and saturates the receiver

Fig. 5. Illustration of the technical cause of PSR-specific ATC impacts

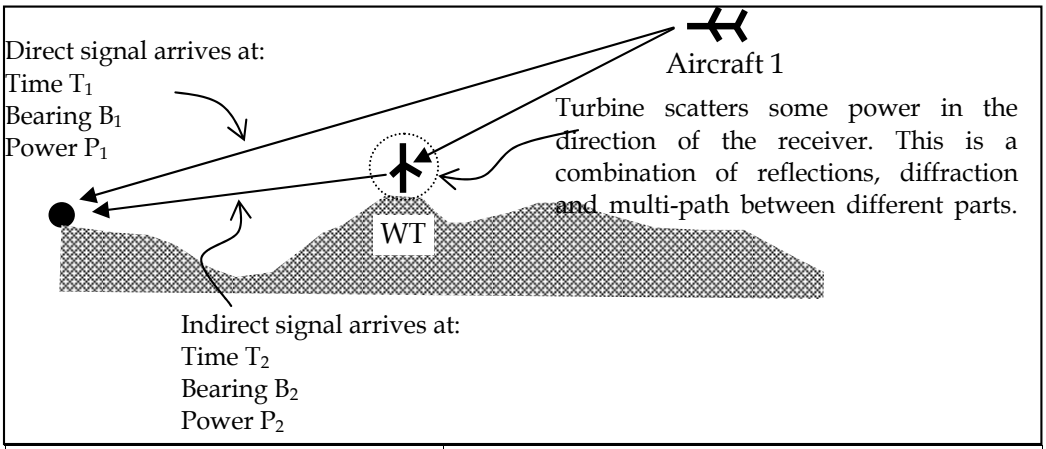

ATC Impact	Technical cause
Signal loss due to shadowing (fading)	P_1 & P_2 combine with net effect of reducing P1. T_1 & T_2 are very close
Signal corruption	P_1 & P_2 have similar strengths
Receiver saturation	P_2 too large and saturates the receiver
Error in bearing	B_1 and B_2 different, P_1 and P_2
Errors in height	P_2 too large and affects 3D PSR operation
Ghost / False target	$P_2 > P_{thresh}$ and T_2 separable from T_1

Fig. 6. Illustration of the technical cause of ATC impacts for non-PSR systems

6. Potential Mitigating Measures

6.1 Introduction

Wind turbines have a variety of impacts on ATC capability. Firstly, wind turbines present a physical obstruction which can modify or reduce a system's functionality. In this respect wind turbines are no different from any other object (e.g. a building, structure or terrain). Secondly, wind turbines have moving parts; their dynamic nature is the main reason that necessitates the development of specialised assessment methodologies.

A wind turbines motion has three distinct aspects worth noting here. These have different implications for the impact on ATC systems.

1. The reflections are time-varying. Because a wind turbine rotates on one or more axis, the way in which it will interfere with an EM system will vary. This means that impacts are more difficult to predict and more difficult to avoid. For instance, the strength of radar reflections from large wind turbines will vary from second to second (as the blades rotate). There may also be longer time-scale changes in the nature of the reflections, as the nacelle axis changes direction to face into the wind.
2. Doppler content. When EM waves reflect from a moving object, the frequency of the reflected energy is changed slightly as a result of the radial motion. This is analogous with the change in pitch of an ambulance siren as it passes – the change in pitch is caused by the change in wavelength of the reflected waves. Due to the

fact that the velocity of EM waves remains constant, the change in wavelength results in a small change in frequency. The shift in frequency is referred to as the Doppler shift. The Doppler content is used to remove echoes from stationary objects such as buildings and terrain. This does not work for wind turbines because of their moving parts.

3. Magnitude of reflections. The reflection magnitude of the moving parts of a typical HAWT, namely the rotor, can be very large. Although the magnitude can vary over several orders of magnitude, at some point in the rotation of the blades RCS levels of up to 40dBsm (10,000 square metres) are predicted and have been measured. Signals of this size can easily be detected by radar even when close to the ground where radar coverage may not be good. This makes it difficult to "shield" wind turbines from nearby radar sites. Also if the turbines are well illuminated by the radar, detecting small aircraft (circa 1 m2 RCS) close to the turbines, may be difficult due to limitations within the radar receiver or impacts to the radar clutter map.

Before progressing it is worthwhile to illustrate the second point further. Because the blades of a conventional HAWT have a spread of speeds (the tip travels faster than a point further down the blade) there is a spread of Doppler shifts in radar echoes. This is illustrated in Figure 7.

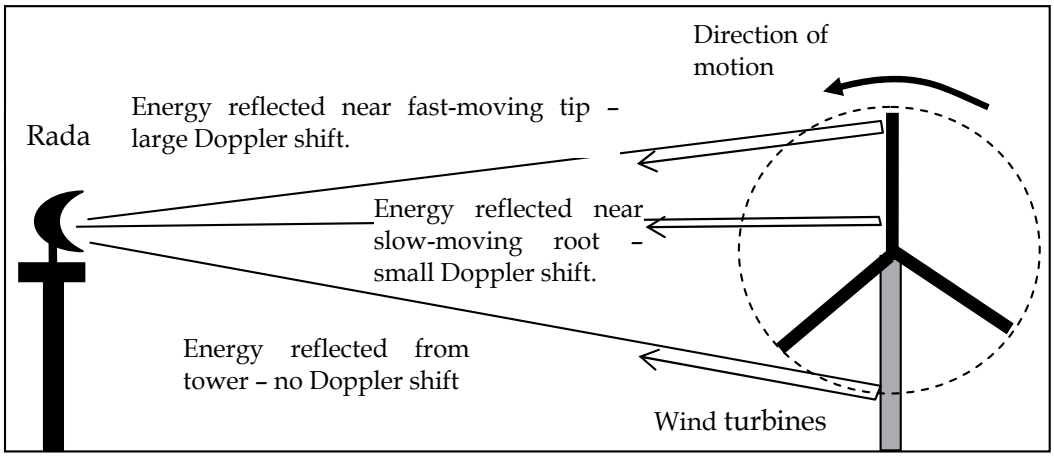

Fig. 7. Illustration of Doppler spread from a wind turbines

The Doppler content of targets is used by primary radars to discriminate between genuine targets (aircraft) and clutter (buildings, vehicles, trees, wind turbines, etc.). Moving Target (MTI) and Moving Target Detection (MTD) filters are employed to remove echoes from slow moving or stationary objects because these are unlikely to be aircraft. For example, a basic MTI filter will remove returns from stationary buildings and these returns will not be presented to the ATC display. Equally, a basic MTI filter will remove echoes from the slow-moving blade roots and the stationary tower on a horizontal axis wind turbines. More detailed discussions of Doppler from moving targets and MTI/MTD processing can be found in (Knil, 2002).

As the state-of-the-art of wind turbine design evolves it is possible that the nature of the Doppler content in wind turbine echoes will change, either increasing or diminishing the severity of the impacts on ATC systems. Although this possibility cannot be discounted, two points are made:

1. Maximum tip-speeds are fairly constant over all current designs, irrespective of turbine size. For example, with horizontal axis wind turbines, as the rotor diameter increases, the revolution speed drops. Small wind turbines typically have a higher rate of rotation. There is no evidence those maximum tip-speeds and hence the spread of Doppler content in wind turbine echoes will change substantially over the next ten years. There is of course a strong correlation between the size of the turbine and the magnitude of the echoes.
2. Constraints such as mechanical integrity and noise pollution mean maximum tip-speeds are unlikely to increase dramatically above existing values.

6.1 Technical measures

Moving Target Indicator Processing

Objects that are moving cause a shift in the frequency of the returned EM energy to the radar receiver; this is known as Doppler shift. Moving Target Indicator (MTI) processing removes from the display any returned pulses which indicate no movement or are within a specified range of Doppler shift. This removes unnecessary clutter, eliminates unwanted moving targets (such as road traffic) and makes moving targets above a certain velocity more visible.

Rotating wind turbine blades can impart Doppler shift to EM energy reflecting off the blades. Depending on the MTI thresholds set in the radar processor, this may be displayed as a moving target. Changes in wind direction at the turbine, the position of the blade in its rotation, the blade pitch, plus other factors, may cause the amount of energy returned to the radar on different sweeps to vary. At single turbine sites, a radar return will be repeatedly displayed in the same position and MTI processing can be deployed. However, multiple-turbine sites cause a different effect and MTI processing is much more difficult. On one return, blades from one (or more) turbine(s) may paint on the radar; on the next sweep, the blades of a different turbine may paint. This can create the appearance of radar returns moving around within the area of the wind farm.

On both aerodrome and air defence radar this can appear (depending on the type of radar and the processing thresholds in effect) as unknown aircraft manoeuvring unpredictably. On air defence radars such as those used in the air defence of the Slovak Republic, the overall system may well interpret the activity as an aircraft and automatically start tracking the activity.

Filters

It is technically possible with many types of radar to filter out returns from a given area to ensure they are not presented on operational displays. However, this is at the expense of detecting actual aircraft in the area concerned. In the case of radars that have the ability to discriminate returns in height, it may be possible to filter out only the affected height band.

On other radars, all returns in the given area will be lost and, in effect, no overall operational benefit is gained.

Non-Automatic Initiation
A measure that can be taken within the Command and Control system to mitigate the effects of spurious radar returns is to establish what is known as a Non-Automatic Initiation (NAI) area. Within this area the system does not perform its normal function of automatic track association and correlation. This would prevent the system attempting to correlate the returns from a large number of turbines in order to form what it perceives to be aircraft tracks. Instead, a human operator monitors the affected area to manually detect genuine aircraft tracks. Whilst this technique can help to avoid the problems both for surveillance and control of spurious tracks, it can be manpower intensive and requires operator expertise. Furthermore, it cannot help to overcome the effect on safety of clutter. Indeed, the use of clutter filters and NAIs may be operationally mutually exclusive.

6.2 Operational Measures

The type of operations being conducted and the type of airspace within which a controller is operating are both relevant factors if radar clutter is being experienced.

Controlled Airspace
Within controlled airspace, flight is only possible if approved by an ATC authority. Therefore, controllers should know of all aircraft within that controlled airspace. In this case, if radar clutter is experienced, whether from a wind turbine or other obstacle, the controller may assume that the return is not from an unknown aircraft and will not need to take any action. (There are exceptions to this rule, which do not need to be explored here.)

Outside Controlled Airspace
Outside controlled airspace (in the Slovak Republic, categorised as 'Class G' airspace), clutter and unknown radar returns present more of a problem. In such airspace, the radar returns of aircraft are the primary means on which the separation of aircraft is based; therefore, clutter must be avoided, as it is the only way of ensuring separation from unknown aircraft.

What may occur is that radar clutter from a wind turbine may be interpreted as being a return from an aircraft; or the clutter may be obscuring a genuine radar return from an actual aircraft operating in the vicinity of that clutter.

There are two ways a controller can deal with this problem; the safest option is to simply avoid the area of clutter, usually by a range of 5 nautical miles. Naturally, this is not always possible. Alternatively, the controller may 'limit' his radar service, whereby he informs the aircraft receiving the service that, due to being in an area of clutter, the pilot may receive late or no warning of other aircraft.

Controllers use both methods but each presents its own problem. The cumulative effects of clutter make vectoring to avoid clutter harder and harder. Controllers may be able to cope with one or two areas of clutter, but there is a difficult judgement as to how much

proliferation is acceptable. Alternatively, limiting the service is often a last resort, and to admit that clutter may well be obscuring returns from genuine aircraft is a clear indication that flight safety may be compromised.

The significance of unwanted radar returns from wind turbines will depend not only on what type of airspace they are in or underneath, but also on their proximity to traffic patterns and routes. Wind turbines on an extended centreline of a runway are more likely to present a significant problem to controllers at longer ranges due to aircraft lining up for approaches and on departure. Similarly, aerodromes have Standard Arrival Routes (STAR) and Standard Instrument Departure (SID) routes, which may also be considered problematic.

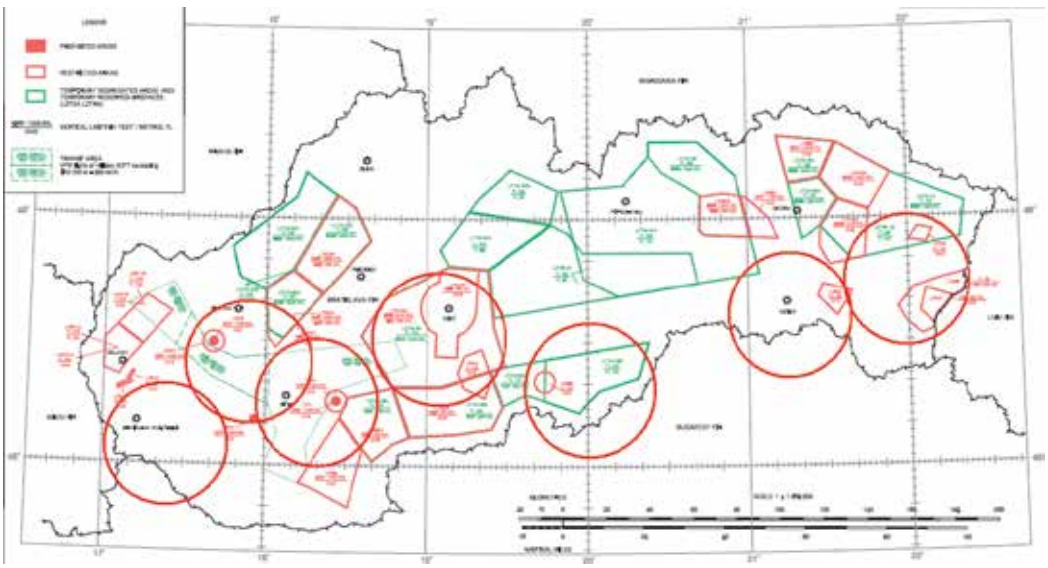

Fig. 7. Prohibited, Restricted, Temporary Segregated Areas in SR (source: Novak, 2009)

7. Conclusion

All radars are different (even if only due to the physical impacts of their operating locations) and creating a 'rule of thumb' for wind farm developments near all systems would require such a level of generalisation as to make it probably worthless.

Therefore, in considering the effect of wind turbines on radar, developers need to focus on individual radars in the vicinity of their planned development. It is important also that developers appreciate the nature and extent of any problem. (Novak, 2009) For example, studies into air defence radars that take no account of the associated Command and Control systems may be of very limited value.

Because both civil and military aviation communities have legitimate interests that must be protected; this includes protection against the adverse effects of wind turbines. However, there is scope for flexibility throughout the process of considering wind farm applications.

The effects of wind turbines on the physical element of the air domain (as obstructions) are well understood and the procedures for handling them are relatively straightforward. Certainly, a flexible approach to sitting of turbines can be expected to pay dividends. Developers must, however, bear in mind that there are some locations in which the presence of turbines is unlikely ever to be tolerated.

The effects of wind turbines on electronic systems and the measures that can be taken to overcome these effects are less clear-cut. The sitting of wind turbines will, potentially, affect the radar sensors belonging to both civil and military users in much the same ways, although the operational impact of these effects will probably not be the same. As further research is conducted and experience with existing (and currently approved) wind farms grows, all stakeholders will be able to determine more precisely what may be acceptable and what will not. No matter what, however, this is an area in which early dialogue with the relevant stakeholders is particularly recommended.

Acknowledgments
This research has been supported by the Scientific Grant Agency of the Ministry of Education of Slovak Republic and the Slovak Academy of Sciences (VEGA No: 1/0274/08).

8. References

CAP 670, (2009), *Air Traffic Services Safeguarding Policy*, *in* CAA, CAA document http://www.caa.co.uk/docs/33/cap670.pdf

CAP 764, (2009), *CAA Policy and Guidelines on Wind Turbines*, *in* CAA, CAA document www.caa.co.uk/docs/33/Cap764.pdf

Gabriel, M & Hill, W. (2004), *Investigation of the impact of wind turbines on the MSSR installations at Dooncarton*, QinetiQ Ireland, QinetiQ document http://www.sei.ie/index.asp?locID=325&docID=-1

Greving, G. (2001), *Numerical Analysis of the Effects by Scattering from Objects on ATC Radar and Various Methods for its Reduction - Theory*, EUROCONTROL, Paris

Knil, A. (2002), *Potential Effects of Wind Turbines on Navigational Systems*, CAA UK, London

Knil, A. (2001) *Wind Turbines and Radar: Operational Experience and Mitigation Measures*, CAA UK, London

Knott E. F., Shaeffer J. F. & Tuley M. T. (1993), *Radar Cross-Section*, Artech House Inc., 1993, Second Edition, ISBN 0-89006-618-3 pp. 90-92.

Lewis, R. (2001) *Information Paper – Radar Mitigations*, CAA SRG, available from CAA SRG web page.

Novak, A. (2009), Wind farm impact on CNS interests, *in 8th international technical systems degradation seminar* - Liptovský Mikuláš, 15-18 April 2009, Lublin: Wydawnictwo-Drukarnia Liber Duo, ISBN 978-83-911726-5-0, pp. 126-131.

Novak, A. (2009), Wind farms and aviation, *in Aviation*, - ISSN 1648-7788, Vol. 13, no. 2 (2009), pp. 56-59.

Skolnik M.I. (1962), *Introduction to Radar Systems*, McGraw-Hill book company inc., pp. 48-51.

Edited by Max Mulder

Improving air traffic control and air traffic management is currently one of the top priorities of the global research and development agenda. Massive, multi-billion euro programs like SESAR (Single European Sky ATM Research) in Europe and NextGen (Next Generation Air Transportation System) in the United States are on their way to create an air transportation system that meets the demands of the future. Air traffic control is a multi-disciplinary field that attracts the attention of many researchers, ranging from pure mathematicians to human factors specialists, and even in the legal and financial domains the optimization and control of air transport is extensively studied. This book, by no means intended to be a basic, formal introduction to the field, for which other textbooks are available, includes nine chapters that demonstrate the multi-disciplinary character of the air traffic control domain.

ISBN 978-953-51-5944-5

Photo by yellowpaul / iStock

IntechOpen